# Exploring the upper temperature limit and biosignatures of archaea and bacteria involved in anaerobic hydrocarbon degradation

Dissertation
zur Erlangung des Doktorgrades
der Naturwissenschaften
- Dr. rer. nat. -

Dem Fachbereich 5 - Geowissenschaften -
der Universität Bremen
vorgelegt von

**Hanna Stephanie Zehnle**

Bremen, August 2023

Die vorliegende Doktorarbeit wurde in der Zeit von Mai 2019 bis August 2023 im Rahmen des Programms „International Max Planck Research School of Marine Microbiology - MarMic“ in der HGF MPG Brückengruppe für Tiefsee-Ökologie und -Technologie am Max-Planck-Institut für Marine Mikrobiologie in Bremen angefertigt.

**Authorin:**
Hanna Stephanie Zehnle
ORCID: 0000-0001-9643-6420
Max-Planck-Institut für Marine Mikrobiologie, Bremen
MARUM – Zentrum für Marine Umweltwissenschaften der Universität Bremen, Bremen
Fachbereich Geowissenschaften, Universität Bremen, Bremen

**Erste Gutachterin:**
Prof. Dr. Antje Boetius
Fachbereich Geowissenschaften, Universität Bremen
Alfred-Wegener-Institut, Helmholtz-Zentrum für Polar- und Meeresforschung, Bremerhaven
Max-Planck-Institut für Marine Mikrobiologie, Bremen

**Zweiter Gutachter:**
Asst. Prof. Dr. Silvan Scheller
Department of Bioproducts and Biosystems, Aalto University, Espoo, Finland

**Erstprüfer:** Prof. Dr. Wolfgang Bach

**Zweitprüfer:** Dr. Gunter Wegener

**Datum des Promotionskolloquiums**: 20.10.2023

*"Our task now is to resynthesize biology*
*Put the organism back into its environment*
*Connect it again to its evolutionary past*
*And let us feel that complex flow that is organism, evolution, and environment united.*
*The time has come for biology to enter the nonlinear world."*
– Carl Woese

# Table of contents

## Summary

The Guaymas Basin in the Gulf of California is a deep-sea hydrothermal vent area. There, the combination of high pressure and heat transforms complex organic compounds into natural gas and petroleum. These thermocatalytic processes resemble processes taking place in petroleum reservoirs that are deeply buried in the subsurface. Because of the easier accessibility on the seafloor, such processes can be examined much easier in the Guaymas Basin. In sediment close to the seafloor surface, the produced hydrocarbons become available to anaerobic microorganisms as energy and carbon sources. The aim of my dissertation was to culture novel hydrocarbon-degrading microorganisms from Guaymas Basin sediment which are active at high temperatures. I also examined the membrane lipids of alkane-degrading cultures to determine the influence of different factors on membrane lipid composition.

In **chapter 2** I examined the anaerobic degradation of mid-chain linear alkanes. I was able to enrich two archaea of the novel genus *Candidatus* Alkanophaga, which degrade alkanes between pentane ($C_5$ alkane) and tetradecane ($C_{14}$) at 70 °C. These archaea activate the alkanes with highly transcribed alkyl-coenzyme M reductases. They form syntrophic relationships with the previously unknown sulfate-reducing bacterium *Ca.* Thermodesulfobacterium syntrophicum.

In **chapter 3** I established anaerobic cultures, in which the unsubstituted small aromatic hydrocarbons benzene and naphthalene were degraded at 50 °C and 70 °C. In these cultures, different microorganisms became enriched with different substrate and temperature combinations. Of particular interest are two new species of the sulfate-reducing bacterial order Desulfatiglandales, which were highly abundant and dispose of almost complete metabolic pathways for the degradation of the aromatic hydrocarbons.

In **chapter 4** I studied the core membrane lipids of twelve anaerobic cultures consisting of alkane-oxidizing archaea and sulfate-reducing bacteria. The cultures grew between 20-70 °C. The lipid composition depended on the incubation temperature, the growth substrate, and the prevalent archaeon and bacterium. Several lipids with peculiar modifications were identified, and especially at 70 °C the lipid composition was considerably different compared to the compositions at other incubation temperatures.

The enriched microorganisms might be involved in hydrocarbon degradation in heated petroleum reservoirs, and contribute to reservoir souring through sulfide formation. Especially the growth temperature of 70 °C approaches the upper limit of the temperature range in which hydrocarbon degradation in reservoirs was reported.

# Zusammenfassung

Das Guaymas-Becken im Golf von Kalifornien ist ein Gebiet hydrothermaler Tiefseequellen. Dort werden komplexe organische Verbindungen durch hohen Druck und Hitze in Erdöl und Erdgas umgewandelt. Diese thermokatalytischen Prozesse ähneln tief unter der Erdoberfläche stattfindenden Prozessen in und um Erdölspeichern. Aufgrund der besseren Erreichbarkeit an der Oberfläche des Meeresbodens können diese Vorgänge im Guaymas-Becken jedoch viel einfacher untersucht werden. Die gebildeten Kohlenwasserstoffe stehen in Sedimenten nahe der Oberfläche anaeroben Mikroorganismen als Kohlenstoff- und Energiequelle zu Verfügung. Das Ziel meiner Dissertation war es, neuartige Kohlenwasserstoff-abbauende Mikroorganismen aus Guaymas-Becken-Sediment zu kultivieren, die bei hohen Temperaturen aktiv sind. Zusätzlich habe ich die Membranlipide von alkan-abbauenden Kulturen untersucht, um den Einfluss verschiedener Faktoren auf die Lipidzusammensetzung zu untersuchen.

In **Kapitel 2** untersuchte ich den anaeroben Abbau von mittelkettigen linearen Alkanen. Ich konnte zwei Archaeen der neuen Gattung *Candidatus* Alkanophaga anreichern, die Alkane zwischen Pentan ($C_5$ Alkan) und Tetradekan ($C_{14}$) bei 70 °C abbauen. Diese Archaeen aktivieren die Alkane mit hoch transkribierten Alkyl-coenzym M Reduktasen. Sie bilden syntrophische Partnerschaften mit dem zuvor unbekannten sulfat-reduzierenden Bakterium *Ca.* Thermodesulfobacterium syntrophicum.

In **Kapitel 3** konnte ich anaerobe Kulturen gewinnen, in denen die unsubstituierten kleinen aromatischen Kohlenwasserstoffe Benzol und Naphthalen bei 50 °C und 70 °C abgebaut werden. In diesen Kulturen waren je nach Substrat und Temperature verschiedene Mikroorganismen angereichert. Von besonderem Interesse sind zwei neue Arten der sulfat-reduzierenden bakteriellen Ordnung Desulfatiglandales, die sehr abundant waren und über nahezu vollständige Stoffwechselwege für den Abbau der aromatischen Kohlenwasserstoffe verfügen.

In **Kapitel 4** untersuchte ich die Kernmembranlipide von zwölf anaeroben Kulturen, die aus alkan-oxidierenden Archaeen und sulfat-reduzierenden Bakterien bestanden. Die Kulturen wuchsen zwischen 20-70 °C. Die Lipidzusammensetzung war abhängig von der Inkubationstemperatur, dem Wachstumssubstrat, und den vorherrschenden Archaeen und Bakterien. Es wurden einige besonders modifizierte Lipide identifiziert, und besonders bei 70 °C war die Lipidzusammensetzung deutlich verschieden von den Zusammensetzungen bei anderen Inkubationstemperaturen.

Die angereicherten Mikroorganismen könnten in geheizten Erdölspeichern an Kohlenwasserstoffabbau beteiligt sein, und durch Sulfidbildung zur Säuerung dieser beitragen. Besonders die Wachstumstemperatur von 70 °C befindet sich an der Obergrenze des Temperaturbereichs, in dem Kohlenwasserstoffabbau in Erdölspeichern beschrieben wurde.

## Abbreviations

| | |
|---|---|
| **16S** | Small ribosomal subunit |
| **1Me-GMGT** | Monomethylated glycerol monoalkyl glycerol tetraether |
| **2Me-GMGT** | Dimethylated glycerol monoalkyl glycerol tetraether |
| **Abc** | Anaerobic benzene carboxylase |
| **Acr** | Alkyl-coenzyme M reductase |
| **ADP** | Adenosine diphosphate |
| **AH** | Aromatic hydrocarbon |
| **AlkB** | Alkane monooxygenase |
| **ANKA** | Anaerobic multi-carbon alkane-oxidizing archaea |
| **ANME** | Anaerobic methanotrophic archaea |
| **AOM** | Anaerobic oxidation of methane |
| **Apr** | APS-reductase |
| **AR** | Archaeol |
| **Ass** | Alkylsuccinate synthase |
| **ATP** | Adenosine triphosphate |
| **Bad** | *bcr* Type class I benzoyl-CoA reductase |
| **Bam** | Class II benzoyl-CoA reductase |
| **BamY** | Benzoate-CoA ligase |
| **BCoA** | Benzoyl-CoA |
| **BCR** | Benzoyl-CoA reductase |
| **Bcr** | *bcr* Type class I benzoyl-CoA reductase |
| **brGDGT** | Branched glycerol dialkyl glycerol tetraether |
| **Bss** | Benzylsuccinate synthase |
| **Bzd** | *bzd* Type class I benzoyl-CoA reductase |
| **$CH_4$** | Methane |
| **CL** | Core lipid |
| **$CO_2$** | Carbon dioxide |
| **CoA** | Coenzyme A |
| **CoB** | Coenzyme B |
| **CODH/ACS** | Carbon monoxide dehydrogenase/acetyl-CoA synthase |
| **CoM** | Coenzyme M |
| **DHNCR** | 5,6-Dihydro-2-naphthoyl-CoA reductase |

| | |
|---|---|
| **DIET** | Direct interspecies electron transfer |
| **DNA** | Deoxyribonucleic acid |
| **Dsr** | Dissimilatory sulfite reductase |
| **DSR** | Dissimilatory sulfate reduction |
| **EPS** | Extracellular polymeric substance |
| **Fe(III)** | Iron(III) |
| **G1P** | *sn*-Glycerol-1-phosphate |
| **G3P** | *sn*-Glycerol-3-phosphate |
| **GB** | Guaymas Basin |
| **GDD** | Glycerol dialkyl diether |
| **GDGT** | Glycerol dialkyl glycerol tetraether |
| **GMGT** | Glycerol monoalkyl glycerol tetraether |
| **GTDB** | Genome Taxonomy Database |
| **$H_2$** | Molecular hydrogen |
| **$H_4F$** | Tetrahydrofolate |
| **$H_4MPT$** | Tetrahydromethanopterin |
| **HC** | Hydrocarbon |
| **HGT** | Horizontal gene transfer |
| **HMW** | High molecular weight |
| **IB-GDGT** | Hybrid isoprenoidal/branched glycerol dialkyl glycerol tetraether |
| **MAG** | Metagenome-assembled genome |
| **MAR** | Macrocyclic archaeol |
| **Mas** | (1-Methylalkyl)succinate synthase |
| **Mcr** | Methyl-coenzyme M reductase |
| **Mer** | Methylenetetrahydromethanopterin reductase |
| **MetF** | Methylenetetrahydrofolate reductase |
| **MHC** | Multi-heme *c*-type cytochrome |
| **ML** | Membrane lipid |
| **Mn(IV)** | Manganese(IV) |
| **NCL** | 2-Naphthoyl-CoA ligase |
| **NCR** | 2-Naphthoyl-CoA reductase |
| **Nms** | Naphthyl-2-methyl-succinate synthase |
| **$NO_3^-$** | Nitrate |
| **OB-GDGT** | Overly branched glycerol dialkyl glycerol tetraether |

| | |
|---|---|
| **OH-AR** | Hydroxylated archaeol |
| **Pfl** | Pyruvate formate lyase |
| **Pps** | Phenylphosphate synthase |
| **prFMN** | Prenylated flavin mononucleotide |
| **RNA** | Ribonucleic acid |
| **rRNA** | Ribosomal RNA |
| **RV** | Research vessel |
| **SAM** | S-adenosylmethionine |
| **Sat** | ATP-sulfurylase |
| **SB-GDGT** | Sparsely branched glycerol dialkyl glycerol tetraether |
| **SMTZ** | Sulfate-methane transition zone |
| **$SO_4^{2-}$** | Sulfate |
| **SRB** | Sulfate-reducing bacterium/bacteria |
| **TACK** | Thaumarchaeota, Aigarchaeota, Crenarchaeota, Korarchaeota |
| **TCA** | Tricarboxylic acid |
| **THNCR** | 5,6,7,8-Tetrahydro-2-naphthoyl-CoA reductase |
| **UAH** | Unsubstituted aromatic hydrocarbon |
| **WHOI** | Woods Hole Oceanographic Institution |
| **WL** | Wood-Ljungdahl |

# Introduction

## 1.1 Anaerobic metabolism: how to thrive at the energetic limit of life

Anaerobic microorganisms face the challenge of generating sufficient energy to maintain basic cellular functions, and ideally sustain growth through the building of biomass, in a severely energy-limited environment (Valentine, 2001). Yet, microorganisms have evolved metabolic strategies to survive and thrive under these harsh conditions. For instance, autotrophic acetogenic bacteria and methanogenic archaea were presumably the first and prevalent life forms on anoxic early Earth (Berg et al., 2010; Martin and Sousa, 2016). In the current day and age, Earth's oxygen-rich atmosphere excludes anaerobes from superficial and surface-near air-ventilated environments. Because molecular oxygen diffuses much slower in water compared to air, anaerobes dwell in oxygen-depleted aquatic or water-permeated environments like swamps and marshes, wastewater remains like sewage sludge, and marine anoxic zones (Megonigal et al., 2004). While anaerobic microorganisms can be considered extremophiles in today's highly oxic Earth, they are crucially involved in global biological processes and biogeochemical cycles. For instance, microorganisms remove contaminants while producing energy in form of biogas in the anaerobic digestion of sewage sludge, a process more energetically feasible than aerobic digestion (Tomei et al., 2009; Abdelgadir et al., 2014). Further, denitrifying bacteria in soil use nitrate or nitrite as electron acceptors in the absence of oxygen, thereby returning nitrogen gas to the atmosphere (Firestone, 1982). Anaerobic microorganisms are also essential symbionts of many animals, aiding digestion and providing their hosts with vital nutrients and vitamins (Fernandez and Collins, 1987; Moore and Warren, 2012; Xu et al., 2021).

The largest anoxic habitat on Earth is formed by sediments of the deep seafloor, which cover 67% of Earth's surface and harbor a particularly high microbial cell density (Jørgensen and Boetius, 2007; Jørgensen et al., 2022). Oxygen supply from seawater in surface sediments varies depending on a multitude of factors like sediment porosity and bioturbation, water turbulence, organic matter input, and proximity to coastlines (Glud, 2008; D'Hondt et al., 2015). While oxygen occasionally diffuses up to tens of meters into the sediment, for instance in sediment underlying ocean gyres, most commonly it is depleted within the upper few millimeters to centimeters of the sediment (Glud, 2008; Jørgensen et al., 2022). Thus, anoxic marine sediments are considered the "greatest anaerobic bioreactor" on Earth (Jørgensen et al., 2022). This bioreactor is fueled by the input of organic matter originating from primary production in the photic zone and from terrestrial river runoff (Dunne et al., 2007; Regnier et al., 2013; Jørgensen et al., 2022). In combination, the seafloor is considered the largest organic carbon storage on Earth (Jørgensen et al., 2022).

While most of the organic matter that reaches the seafloor will be mineralized in the upper sediment layers by fast-acting aerobic microbes, a small fraction is buried to deeper layers

where it becomes subject to anaerobic degradation (Jørgensen et al., 2022). Anaerobic heterotrophic microorganisms degrade organic matter coupled to the reduction of the alternative electron acceptors nitrate ($NO_3^-$), manganese (Mn(IV)), iron (Fe(III)), sulfate ($SO_4^{2-}$), and carbon dioxide ($CO_2$) in a sequential vertical order according to availability (Figure 1) (Jørgensen et al., 2022). In contrast to aerobic microorganisms, which can directly degrade organic polymers, no anaerobic microorganism capable of completely degrading complex organic matter is known (Fenchel and Finlay, 1995). This is because of the much lower energy yield obtained from the usage of alternative electron acceptors compared to oxygen, which is the "fundamental difference between aerobic and anaerobic metabolism" (Megonigal et al., 2004). The energy yield constantly decreases within the redox cascade of alternative electron acceptors (Jørgensen *et al.*, 2022), and electron acceptors with higher thermodynamic energy yield are consumed first (Megonigal et al., 2004). Methanogenesis from $CO_2$ yields the least free energy in this series, and is operating very close to the theoretical thermodynamic limit of life of −20 kJ $mol^{-1}$ (−4.8 kcal $mol^{-1}$), a third of the energy required to convert phosphate and adenosine diphosphate (ADP) to cell's primary energy carrier adenosine triphosphate (ATP) (Valentine, 2001; Deppenmeier and Müller, 2008) (Table 1). Therefore, complex organic matter needs to be broken down into smaller fragments, such as monomers of sugars and nucleic and amino acids, by secreted enzymes first. These fragments then become fermented to smaller, bioaccessible molecules, which anaerobic microorganisms can utilize as electron donors (Figure 1) (Megonigal et al., 2004; Jørgensen et al., 2022).

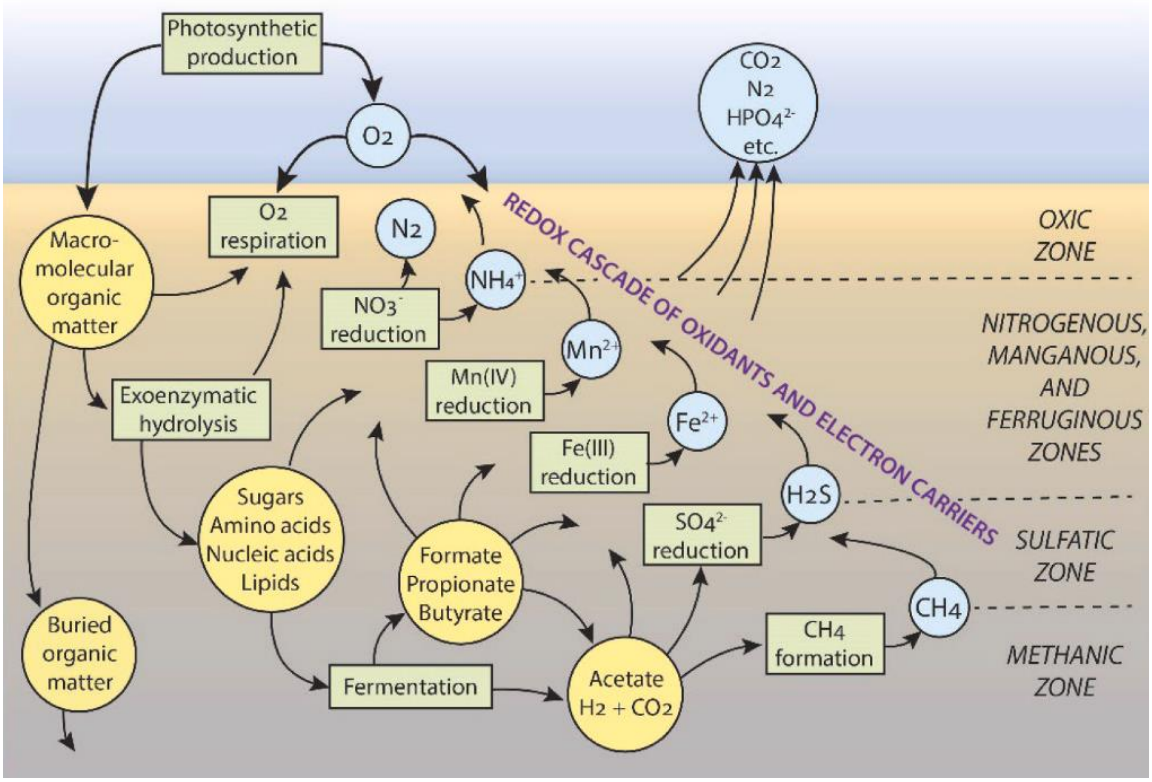


**Figure 1** | Vertical cascade of electron accepting processes in marine sediment. From Jørgensen et al. (2022)

**Table 1** | Redox potential and free energy yield from reduction of electron acceptors coupled to the oxidation of organic matter. Theoretical oxidation reaction: $\frac{1}{4}$ $CH_2O$ + $\frac{1}{4}$ $H_2O$ → $\frac{1}{4}$ $CO_2$ + $H^+$ + $e^-$ and ΔG = -RT ln (*K*) with pH 7.0 and T = 25 °C. $E_h$: redox potential; V: volt; ΔG: Gibbs free energy; R: gas constant; T: temperature (Kelvin); K: equilibrium constant.

| Reduction | $E_h$ (V) | ΔG (kcal $mol^{-1}$ $e^{-1}$) |
|---|---|---|
| $O_2 + 4H^+ + 4e^- \rightleftharpoons 2H_2O$ | 0.812 | -29.9 |
| $NO_3^- + 6H^+ + 6e^- \rightleftharpoons N_2 + 3H_2O$ | 0.747 | -28.4 |
| $MnO_2 + 4H^+ + 2e^- \rightleftharpoons Mn^{2+} + 2H_2O$ | 0.526 | -23.3 |
| $Fe(OH)_3 + 3H^+ + e^- \rightleftharpoons Fe^{2+} + 3H_2O$ | -0.047 | -10.1 |
| $SO_4^{2-} + 10H^+ + 8e^- \rightleftharpoons H_2S + 4H_2O$ | -0.221 | -5.9 |
| $CO_2 + 8H^+ + 8e^- \rightleftharpoons CH_4 + 2H_2O$ | -0.244 | -5.6 |

From Schlesinger (1997); Megonigal et al. (2004)

The anaerobic degradation of organic compounds is less understood than aerobic degradation because of the increased difficulty to culture the respective, often very slowly growing microbes. In this thesis, I will aim to contribute to the understanding of heterotrophic anaerobic microorganisms from the seafloor, focusing on one group of organic compounds as substrates, the naturally abundant, widely distributed hydrocarbons.

## 1.2 Hydrocarbons: a widespread carbon and energy source

Hydrocarbons (HCs) are among the most abundant small organic molecules on Earth, and are particularly found in anoxic environments like terrestrial soils, marine sediments, and the deep subsurface (Wilkes and Schwarzbauer, 2010; Rabus et al., 2016; Kleindienst and Joye, 2019). They are the simplest organic compounds, consisting of only carbon and hydrogen, and are conventionally classified based on their bond properties as saturated, unsaturated and aromatic HCs (Meinschein, 1969; Wilkes, 2020). Fully saturated HCs contain only single, apolar bonds (σ-bonds) and are called alkanes, whereas unsaturated HCs, which contain one or more C-C double or triple bonds (π-bonds), are designated alkenes and alkynes, respectively (Wilkes, 2020). Saturated and unsaturated HCs occur in linear (*n*-), branched (iso-), or cyclic (cyclo-) form (Wilkes, 2020). Because π-bonds increase the polarity of a molecule, unsaturated HCs are more reactive than saturated HCs, which are often considered chemically inert (McMillen and Golden, 1982; Wilkes, 2020). Aromatic HCs (AHs) consist of one or more six-carbon-atom ring system, in which the six π-electrons are delocalized; i.e. they are not confined to a specific location and instead form an electron cloud above and below the planar six-membered ring (Aihara, 1992; Wilkes, 2020). Delocalized electrons create resonance stability, making the molecule extremely unreactive (McMillen and Golden, 1982). The aromatic ring system(s) may be substituted with alkyl groups, which destabilize the ring and make it more reactive (McMillen and Golden, 1982; Wilkes and Schwarzbauer, 2010).

In nature, HCs occur in many sizes, from one-carbon compounds like the simplest alkane methane ($CH_4$), to large molecules like the AH ovalene ($C_{32}H_{14}$). The molecular weight and thus surface area of a HC strongly affects its physical properties, because the larger the molecule, the higher the intermolecular van der Waals forces become, thus the boiling point of HCs increases with molecular weight (Israelachvili, 1974; Morrison and Boyd, 1992). In general, small HCs like methane are gaseous, mid-sized HCs like benzene (one-ring AH) or nonane ($C_9$ alkane) are liquid, and large HCs like pyrene (four-ring AH) and icosene ($C_{20}$ alkene) are solid at standard conditions.

HCs in the environment originate from biological and abiotic sources. Plants and insects synthesize a wide range of long-chain linear alkanes, alkenes, and methyl-branched HCs, which in combination form a waxy substance which serves as a physical cuticle barrier to prevent desiccation and for communication purposes (Wilkes, 2020; Würf et al., 2020; Holze et al., 2021). Various HCs, among others alkanes, alkenes, and cyclic non-aromatic and aromatic HCs are also produced by many aerobic and anaerobic eukaryotic and prokaryotic microorganisms, e.g. filamentous fungi, algae, bacteria, and methanogenic archaea (Fehler and Light, 1970; Spakowicz and Strobel, 2015; Wackett and Wilmot, 2015). However, the major source of HCs are natural gas and petroleum. These fossil fuels are predominantly formed over geological timescales in the deep subsurface through the combination of organic matter, high pressure, and heat (Tissot and Welte, 1984; Schobert, 2013).

## 1.3 The geological formation of natural gas and petroleum

The formation of fossil fuel requires organic-rich mud as source material. The vast majority of this biomass (98-99%) is subject to fast aerobic bacterial degradation and eventually formation of $CO_2$ (Schobert, 2013). A prerequisite of fossil fuel formation is the almost complete exclusion of molecular oxygen through e.g. coverage of the mud with stagnant water, which prevents this decomposition of organic matter (Schobert, 2013). Then, degradation processes mediated by slower anaerobic microorganisms, including hydrolysis of macromolecules like polysaccharides, glycosides, and proteins become prevalent (Schobert, 2013). Once organic matter has been buried to a depth about 10 meters, these degradation processes have, for the most part, been completed. At this point, the components produced from this anaerobic microbial degradation, like humic acids, plus recalcitrant molecules that have evaded degradation, like fats, oils, and resins, start to assemble into kerogen. Kerogen is a dark solid consisting of high molecular weight (HMW) organic molecules, which is insoluble in organic solvents (Vandenbroucke and Largeau, 2007; Schobert, 2013). Three types of kerogens have been described, and named after the origin of the dominant organic matter from which they were formed: type I-algal (algae), type II-liptinitic (plankton), and type III-humic (woody plants) (Schobert, 2013). A vast amount of carbon on Earth, an estimated $10^{16}$ tonnes, is stored in the form of kerogen. Therewith, the organic matter of kerogen surpasses the organic matter of living

organisms about 10,000-fold (Horsfield et al., 2018). The formation of kerogen continues concomitantly with the compaction and cementation of sediment to sedimentary rock (Boggs, 2006), up to a depth of about 1,000 m, where temperatures reach up to 50 °C (Schobert, 2013). Here, the first phase of fossil fuel formation ends. The processes that have taken place starting from the burial of organic matter up to and including the formation of kerogen are described as the "biochemical phase of fossil fuel formation" and summarized under the term diagenesis, meaning "transformation of material through dissolution and redistribution" of its components (Tissot and Welte, 1984; Brand et al., 1998; Schobert, 2013).

The next phase is referred to as the "geochemical phase of fossil fuel formation" or catagenesis (Schobert, 2013). Catagenesis begins with a deeper burial of kerogen, where higher temperatures, the main driver of this phase, are reached (Schobert, 2013). The increasing heat with depth (~10-30 °C per km) originates predominantly from radioactive decay, particularly of the isotopes potassium-40 ($^{40}$K), thorium-232 ($^{232}$Th), uranium-235 ($^{235}$U), and uranium-238 ($^{238}$U) in Earth's crust (Schobert, 2013). Reactions in catagenesis take a long time, with timespans ranging from thousands to millions of years (Schobert, 2013). During catagenesis, the differing hydrogen to carbon (H/C) ratios of the three types of kerogen come into effect. Natural gas and petroleum are produced mainly from types I and II kerogens, which are rich in lipids and have high hydrogen to carbon (H/C) ratios. In contrast, type III kerogen has a low H/C ratio, and is mostly transformed into peat and carbon-rich products like coal (Tissot and Welte, 1984; Schobert, 2013). Kerogen-containing sedimentary rock, from which natural gas and/or petroleum may be released, is called source rock (Schobert, 2013). Sedimentary rocks occur in large amounts in sedimentary basins, many of which cover tens of thousands of km$^2$ (Selley and Sonnenberg, 2015). Sedimentary basins can be continental and form part of a mountain chain like the Himalaya or the Andes, or they may occur in nearshore or offshore marine environments, e.g. in the Gulf of Mexico or in the Laptev Sea (Solomon, 2007; Selley and Sonnenberg, 2015; Abdullayev, 2020).

Typical source rock, e.g. limestone or shale, consists to ~99% of inorganic matter, and only to ≤1% of organic matter (Gehman, 1962; Schobert, 2013). About 10% of the carbon stored in the organic fraction goes into solution in organic solvents (McNally, 2011; Schobert, 2013). This highly viscous fraction, termed bitumen, contains four classes of compounds: naphthalene AHs, polar AHs, saturated HCs, and asphaltenes (Schobert, 2013; Redelius and Soenen, 2015; Pevneva et al., 2017). Bitumen has been used by humans for construction purposes for over 5,000 years because of its waterproofing and bonding properties (Abraham, 1945). The remaining 90% of the organic fraction in the source rock is kerogen (Schobert, 2013). Some source rock contains significantly more than 1% organic matter, and is thus of higher interest for commercial exploitation, e.g. oil shale, with 2-50% kerogen, and coal, with >50% kerogen (Schobert, 2013; Horsfield et al., 2018).

To cleave gaseous and petroleum HC products from type I and II kerogen, the breaking of stable intramolecular C-C bonds is required. This process is called thermal cracking, as it is catalyzed by high temperatures (Schobert, 2013). This step is where the large diversity of HCs in petroleum is generated, as the thermal cracking of the large molecules present in kerogen, e.g. large alkanes like triacontane ($C_{30}H_{62}$), at different points within the molecules yields many different radical products, which in turn combine with other radicals to form new stable molecules (Schobert, 2013). The higher the temperature, the more C-C bonds are broken (Schobert, 2013). With greater burial depth, and therewith increasing temperatures, molecules produced by thermal cracking become smaller and more saturated, while boiling temperatures and viscosity of the molecule mixtures decrease (Schobert, 2013). Between 60-170 °C, predominantly liquid HCs are generated, with a minor contribution of gaseous HCs, of which production starts at 110 °C and then constantly increases. At temperatures ≥170 °C up to 225 °C, exclusively gaseous HCs are formed (Schobert, 2013). The phase of catagenesis in which predominantly liquid HCs are formed are referred to as the oil window, while the phase in which predominantly gaseous HCs are formed is called gas window (Figure 2) (Schobert, 2013). In the lower part of the gas window, produced gas is almost exclusively methane, i.e. “dry gas”. This part is designated metagenesis (Tissot and Welte, 1984; Seewald, 2003; Schobert, 2013).

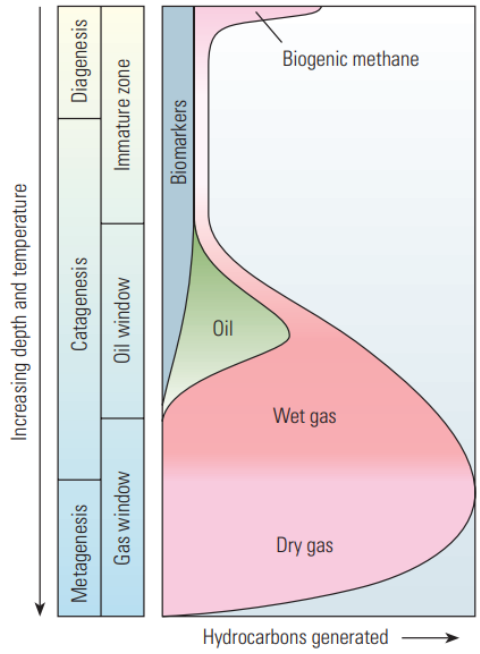


**Figure 2** | Phases of fossil fuel formation.
From Tissot et al. (1974) and McCarthy et al. (2011)

In order to form saturated, small HCs, i.e. HCs with high H/C ratio, at high temperatures, a lot of hydrogen is required. This hydrogen becomes available through the formation of AHs, i.e. HCs with low H/C ratio, which coincides with increasing temperature (Schobert, 2013). Thus, one would expect to find a higher ratio of AHs in lighter oil fractions. However, as aromatic rings fuse together to liberate more hydrogen, these large, HMW molecules become less and less soluble, and at some point they start to form a separate phase called asphaltene (Schobert, 2013). After the closing of the gas window at ~225°C, where the driest gas is produced, a solid with a low H/C ratio rich in AHs remains (Schobert, 2013). Metagenesis is

considered the last stage of the thermal maturation of organic matter, and transitions into metamorphism, in which the structure of the remaining rock is heavily altered on a mineralogical and chemical level through temperature and pressure (Bucher and Frey, 1967; Tissot and Welte, 1984).

## 1.4 Petroleum reservoirs

After the organic matter in the source rock has been cracked to liquid and gaseous HCs, those HCs migrate upwards until they encounter a subsurface reservoir rock, which exhibits sufficient porosity and permeability to allow migration of HCs and at the same time concentrates and binds them (Alamooti and Malekabadi, 2018). Reservoir rocks are mostly sedimentary rocks, e.g. silicates like sandstone and carbonates like dolomite and limestone (Fatt, 1958; McLatchie et al., 1958; Shen et al., 2016). In conventional reservoirs, the HCs accumulated in the reservoir rock are prevented from migrating further upwards by an impermeable cap rock, usually an anticline, i.e. a folded rock structure with an arched shape (Figure 3) (Onajite, 2014). Cap rocks are commonly formed out of small-pored shale or evaporites like anhydrite or rock salt, and less frequently out of tightly packed carbonates, mudstones, or sandstones (Grunau, 1987; Norman J. Hyne, 2013). Cap rocks are usually tens to hundreds of meters thick (Grunau, 1987).

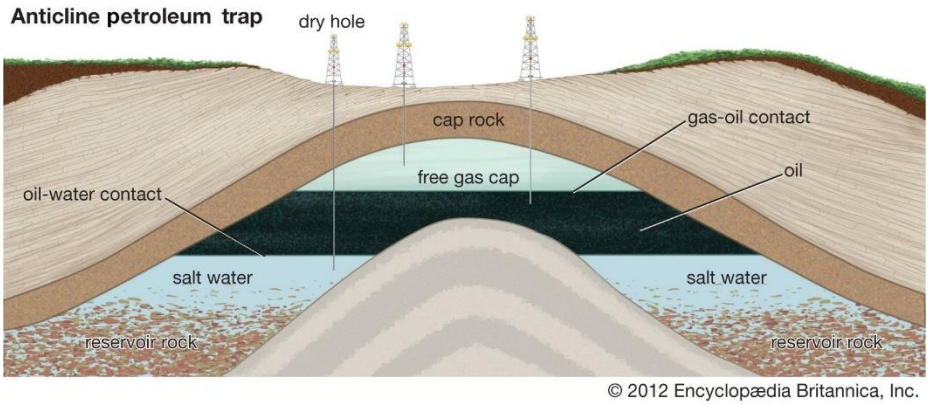


**Figure 3** | Oil and gas are trapped in petroleum reservoirs by a cap rock. From Encyclopædia Britannica

HCs are stored in the reservoir rock in predominantly liquid or gaseous form. Reservoirs containing mostly liquid HCs are called oil reservoirs, and reservoirs with mostly gaseous HCs are called gas reservoirs (Alamooti and Malekabadi, 2018). In most oil reservoirs, gaseous HCs are also present at low concentrations dissolved within the oil phase (Speight, 2011). If there are more gaseous HCs present than are necessary to saturate the oil, they form a separate layer on top of the oil phase (Onajite, 2014). Since all reservoir rocks are also infiltrated by water, a gas-oil-water configuration is often observed, with water being located on the bottom of the reservoir (Figure 3) (Onajite, 2014).

Multiple, potentially connected, oil and/or gas reservoirs located in the same area and related to the same geological structures are called field (API Executive Committee on

Standardization of Oilfield Equipment and Materials, 1988). Globally, more than 25,000 continental and offshore oil and gas fields have been recognized (Li, 2011; Speight, 2011). Notably, about 75% of oil is stored in only about 300 very large oil fields, so-called giants (Speight, 2011). Giant oil and gas fields are located predominantly (71%) in the Eastern hemisphere (Halbouty et al., 1970). The largest giant field is the Ghawar oil field in Saudi Arabia comprising an estimated ~200 billion barrel ultimately recoverable resources (URRs), followed by the Burgan oil field in Kuwait, with an estimated ~70 billion barrel URRs (Warren, 2016; Al-Hemoud et al., 2019; Berger et al., 2022).

Humans have explored and exploited oil and gas reservoirs intensely to recover fossil fuels for about 150 years. Large-scale reservoir exploration and fossil fuel recovery started around the 1850s with exploration at various sites, among others with the establishment of the first commercial oil well at Oil Creek in Pennsylvania (USA) in 1859, where drillings uncovered an extensive petroleum reservoir at only 21 m depth (Link, 1952; Hubbert, 1966). This event laid the technological groundwork for global reservoir exploration, which peaked in the 1960s to 1970s and then decreased to an undulating plateau (Hubbert, 1966; Caineng et al., 2010; Jackson and Smith, 2014). With the increasing depletion of surface-near reservoirs, recent exploration attempts were forced to focus more on deep (4,500-6,000 m) to ultra-deep (>6,000 m) located reservoirs, which comes with increased technological challenges (Guo et al., 2019).

Fossil fuel recovery is divided into three phases: primary recovery, secondary recovery, and enhanced or tertiary recovery (Wardlaw, 1996). During primary recovery, fossil fuels are driven out of the reservoir passively by release of internal pressure, i.e. by gas and oil expansion upon opening the reservoir (Wardlaw, 1996). Naturally, the internal reservoir pressure decreases with the continued withdrawal of oil and gas, at some point slowing down the revenue. At this point, secondary recovery methods are employed, the most common of which is seawater injection (McCune, 1982; Wardlaw, 1996). It is estimated that 20-50% of the reservoir resources can be recovered by primary and secondary recovery, leaving a large percentage untouched (Wardlaw, 1996; Alamooti and Malekabadi, 2018). The third phase, enhanced recovery, targets the large residual oil fraction, and consists of $CO_2$ and water injection in combination with thermal, chemical, and/or additional gas injection (Kantzas et al., 1988; Alamooti and Malekabadi, 2018; Berger et al., 2022). The recovered gas and oil are cleaned of contaminants like sand and water (Wei et al., 2014) and separated into groups of molecules with similar boiling point via fractional distillation (Kinsara and Demirbas, 2016). The economically most valuable fraction is gasoline, consisting of HCs of 5-10 carbon atoms, followed by the more viscous diesel, jet fuel, and heating oil (Kinsara and Demirbas, 2016).

Energy generated from the combustion of fossil fuels has enabled humanity a rapid advance in technology and industrialization, which may be considered necessary in order to provide for an exponentially increasing population. However, the cost for this progress was, and is high. Combustion of fossil fuels since the start of the industrial revolution has increased

atmospheric $CO_2$ concentrations from 277 ppm in 1760 to 411 ppm in 2019 (Joos and Spahni, 2008; Friedlingstein et al., 2019), with annual global $CO_2$ emissions exceeding $30 \times 10^9$ tonnes per year since 2006 (Friedlingstein et al., 2020). Without drastic changes in lifestyle and usage of energy sources, atmospheric $CO_2$ will keep increasing at a steady rate (Friedlingstein et al., 2019), driving global warming due to its strong greenhouse effect and causing irreversible changes in ecosystems (Solomon et al., 2009). Based on current estimates, currently accessible oil resources will become depleted within the next 50 years (Speight, 2011), highlighting the need for alternative energy sources.

## 1.5 Hydrothermal petroleum formation

Conventionally, fossil fuels are formed deep in the subsurface in sedimentary basins over geological timescales. Under certain circumstances, petroleum HCs are generated comparatively rapidly, in timespans of days to years, through the combination of hydrothermal heat (~60 to >400 °C) generated by tectonic plate activity and organic-rich sediments under high pressure (>150 atm) close to the seafloor surface (Hunt, 1979; Simoneit, 1990, 1993, 2018). Such systems are much more accessible than deeply buried reservoirs, and can thus serve as analogue environments where biological and geochemical processes involved in petroleum HC formation and transformation can be studied. Hydrothermal systems with considerable petroleum production have been found predominantly in marine environments. Examples include the Escanaba Trough at Gorda Ridge and Middle Valley in the Juan de Fuca Ridge, both situated in the northeast Pacific, the Bransfield Strait in Antarctica, and the Atlantis II Deep in the Red Sea (Simoneit et al., 1987, 1992; Kvenvolden et al., 1988; Whiticar and Suess, 1990). Like reservoir petroleum, hydrothermally generated petroleum contains natural gas and gasoline-range HCs, a full range of linear *n*-alkanes, plus branched and cyclic HCs (Table 2) (Simoneit and Lonsdale, 1982; Simoneit, 1984, 2018). In contrast to reservoir petroleum, hydrothermally generated petroleum contains higher portions of AHs, including HMW polycyclic AHs (Table 2) (Simoneit, 2018).

**Table 2 |** Comparison of hydrothermally generated petroleum to reservoir petroleum. Modified from Simoneit (2018)

| Similarities to reservoir petroleum | Differences from reservoir petroleum |
|---|---|
| • Natural gas and gasoline-range hydrocarbons<br>• Full range of linear *n*-alkanes (no carbon number predominance)<br>• Branched and cyclic hydrocarbons<br>• Isoprenoid hydrocarbons (e.g. phytane)<br>• Intact biomarkers (e.g. sterane)<br>• Alklylated aromatic hydrocarbons and asphaltenes | • High concentrations of polycyclic aromatic hydrocarbons (PAHs)<br>• Residual immature biomarkers and intermediates (e.g. sterenes)<br>• Degraded biomarkers (e.g. Diels' hydrocarbon)<br>• Significant heteroaromatic compounds (N and S)<br>• High sulfur content<br>• Alkene content in bitumen near "source rock" |

Hydrothermally formed petroleum does not accumulate to form reservoirs, and no trapping mechanisms are known (Didyk and Simoneit, 1989). Therefore, the generated HCs migrate to the surface and can interact with aerobic and anaerobic lifeforms. A prime example of a sedimentary hydrothermal system generating petroleum HCs is the Guaymas Basin (GB) located in the Gulf of California, which to this day is the most productive of such systems (Simoneit, 2018).

## 1.6 The Guaymas Basin - a surface analogue for petroleum reservoirs

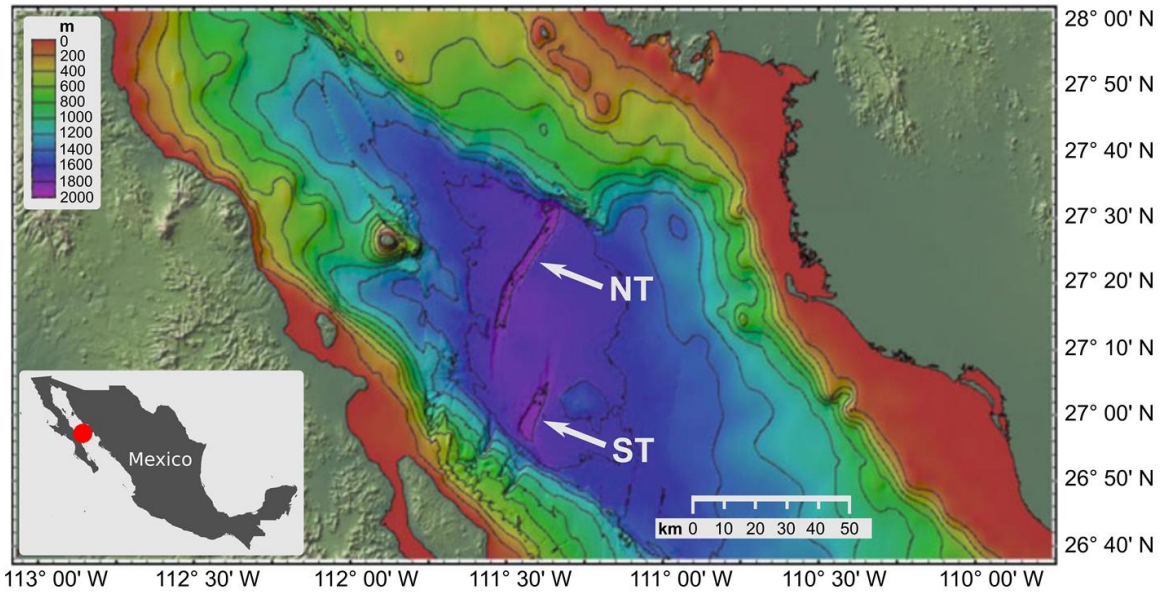


**Figure 4** | Bathymetry of the Guaymas Basin. The Northern Trough (NT) and Southern Trough (ST) are indicated by arrows. Modified from Teske (2020)

The GB is a young marginal rift basin created by two diverging tectonic plates, the North American and the Pacific plate, which connects the East Pacific Rise in the south to the San Andreas Fault in the north (Lonsdale, 1985). It is connected to the Carmen Fault in the north and to the Guaymas Fault in the south (Williams et al., 1979). The peninsula Baja California in the West of the GB and mainland Mexico in the East of the GB separate at a rapid rate of 5-6 cm per year (Lonsdale and Becker, 1985). The GB consists of two axial rift valleys located about 20 km apart, the Northern Trough (~40 km long, 2-3 km wide) and the Southern Trough (~30 km long, 2-4 km wide), each 50-200 m deeper than the surrounding seafloor (Figure 4) (Moore, 1973; Einsele et al., 1980; Lonsdale and Lawver, 1980; Lonsdale and Becker, 1985; Fisher and Becker, 1991). High primary productivity in surface waters and to a lower degree terrestrial runoff, transported among others by the Río Yaqui from the Mexican mainland, generate a high sedimentation rate of 0.2-1 mm per year into the basin (Lonsdale and Lawver, 1980; Merewether et al., 1985; Teske et al., 2019). Lonsdale and Lawver (1980) suggested that hydrothermal precipitation might further contribute to the rapid sedimentation in the GB, especially in the Northern Trough. The GB is comparatively young, having formed within the last 3.5 million years (Moore, 1973), which sets it apart from older mid-ocean spreading centers like Juan de

Fuca and Gorda Ridge and makes it a case study for early stages of rifting in combination with high sedimentation rates (Lonsdale and Lawver, 1980; Fisher and Becker, 1991). Understanding the geological processes in the GB can thereby help elucidate how more mature basins have developed (Lonsdale and Lawver, 1980).

On the seafloor, at approximately 2,000 m depth, the organic-rich sediments form thick layers of on average 100 meters, with a maximum thickness of about 500 meters (Einsele et al., 1980; Curray et al., 1982; Lonsdale and Becker, 1985). The sediment layer is in its upper, softer areas interspersed by characteristic intrusions of igneous doleritic sills and dikes (Einsele et al., 1980; Lonsdale and Becker, 1985). The GB features high conductive heat fluxes in both troughs. Those fluxes are to some degree attributed to the cooling of recent sill intrusions, but mainly to deep-seated magma chambers, which produce an upward flux of hydrothermally heated fluids with temperatures of up to 270-325 °C (Curray et al., 1982; Lonsdale and Becker, 1985; Von Damm et al., 1985; Fisher and Becker, 1991). The thick sediment cover prevents heat from escaping directly to the seafloor (Lawver et al., 1975; Lonsdale and Becker, 1985). This distinguishes the GB from more mature mid-ocean spreading centers with only a thin sediment cover, where heat escapes through porous surface rock (Lonsdale and Lawver, 1980). Heat flow values have been determined as ~660 to > 1,000 mW $m^{-2}$ inside the rift valleys, compared to 180 mW $m^{-2}$ outside of the valleys, and were assumed to generally be higher in the Southern compared to the Northern Trough (Fisher and Becker, 1991). However, a recent measurement of heat flow of 11,000 mW $m^{-2}$ in a recently discovered hydrothermal vent field in the Northern Trough proves that there are exceptions to this rule (Geilert et al., 2018). Overall, the Southern Trough seems hotter and more hydrothermally active than the Northern Trough, which is why some authors have hypothesized that the two troughs might be supplied by two distinct magma sources with differing activities (Lonsdale and Becker, 1985; Fisher and Becker, 1991). It was also proposed that hydrothermal activity in the Southern Trough temporally preceded the one in the Northern Trough (Geilert et al., 2018). In both troughs, heat fluxes reach their maxima in the trough center, where they manifest themselves as mounds and black smoker vents rising up to 20 m above the basin floor and emitting heated fluids with temperatures ≥300 °C (Lonsdale and Becker, 1985; Fisher and Becker, 1991; Teske et al., 2016). Those fluids produce thermal plumes containing finely suspended particulate matter which ascend up to 100-300 m above the basin floor (Campbell and Gieskes, 1984).

Especially near sills and above magmatic chambers, hydrothermal fluids transform organic macromolecules via thermal cracking into a plethora of smaller petroleum-range HCs (Simoneit and Lonsdale, 1982; Simoneit et al., 1986; Didyk and Simoneit, 1989; Simoneit, 1993). The so-generated HCs are quickly transported up through the sediment with the venting fluids, away from the site of their creation (Simoneit, 1993). This transport is aided by the liquid supercritical state of methane and $CO_2$, and the almost critical state of water, caused by the prevailing high temperatures and pressure (~260 atm) (Simoneit, 1984; Simoneit and Galimov,

1984; Von Damm et al., 1985; Karl et al., 1988; Simoneit et al., 1988; Budisa and Schulze-Makuch, 2014). Therewith, the hydrothermal fluids constitute a potent organic solvent for petroleum HCs (Budisa and Schulze-Makuch, 2014; Shibuya and Takai, 2022). Through this thermal alteration, the organic carbon content in deep sediment layers is reduced to 1-2wt% (Rullkötter et al., 1982; Simoneit and Bode, 1982) compared to 3-4wt% in younger surface sediments (De la Lanza-Espino and Soto, 1999). The temperatures that generate petroleum HCs hydrothermally can reach higher maxima (up to 400 °C) than those involved in reservoir petroleum HC formation (up to 225 °C) (Tissot and Welte, 1984; Simoneit, 1993; Schobert, 2013). It is believed that the rapid removal of petroleum HC products through hydrothermal venting most likely prevents a destruction of organic matter to a large extent (Simoneit, 1993).

Once HCs reach upper sediment layers, lighter HCs, predominantly methane, can diffuse into the seawater and form part of plumes that rise up to 1,000 m above the basin floor, as detected acoustically via sonar (Merewether et al., 1985). Heavier petroleum-range HCs condense and solidify at the sediment surface and become visible as oil globules that accumulate around hydrothermal mounds and chimneys (Simoneit and Lonsdale, 1982; Simoneit, 1984; Peter et al., 1990). This upper sediment exhibits a characteristic strong odor similar to diesel fuel, indicative of the high concentrations of petroleum HCs (Simoneit and Lonsdale, 1982). The composition of GB HC mixtures in general resembles that of conventional petroleum found in reservoirs, with compositional variations between sites (Simoneit and Lonsdale, 1982; Simoneit, 1983; Didyk and Simoneit, 1989).

Near the seafloor surface, where temperatures become habitable and sulfate is supplied, petroleum HCs become subject to degradation by anaerobic meso- to thermophilic microbial populations (Weber and Jørgensen, 2002; Teske et al., 2014; Simoneit, 2018; Edgcomb et al., 2022). This biodegradation is evidenced by decreased HC concentrations, particularly of alkanes, in certain surface sediments (Bazylinski et al., 1988). Microorganisms degrade HCs via oxidation to $CO_2$, which frees electrons that are shuttled into the reduction of sulfate, the dominant electron acceptor in the Guaymas Basin (Elsgaard et al., 1994; Rueter et al., 1994; Weber and Jørgensen, 2002; Teske et al., 2014; Teske, 2020). Sulfide then rises to the sediment surface, where it feeds populations of aerobic, large sulfide-oxidizing bacteria of the family *Beggiatoaceae* (Jannasch et al., 1989; Nelson et al., 1989). These bacteria form large microbial mats in areas with high hydrothermal venting and subsurface sulfide production rates, using energy from sulfide oxidation to generate biomass by chemoautotrophy (Figure 5) (Nelson and Jannasch, 1983; Gundersen et al., 1992; Weber and Jørgensen, 2002; McKay et al., 2012; Teske, 2020). Those mats often surround communities of the tube worm *Riftia pachyptila*, a keystone invertebrate species of eastern Pacific hydrothermal vents (Figure 5A,C) (Black et al., 1994; Teske, 2020). *Riftia* live together with aerobic symbiotic bacteria, which also require sulfide for energy generation (Felbeck, 1981). *Beggiatoaceae* mats exhibit a characteristic “fried-egg” morphology, with filaments of an orange, highly pigmented *Beggiatoaceae* clade in the center,

and another white, non-pigmented *Beggiatoaceae* clade in the periphery (Teske, 2020). Even though both prevalent *Beggiatoaceae* clades require temperatures of around 10 °C for optimal growth, the mat morphology mirrors steep vertical and horizontal thermal and geochemical gradients in the underlying sediments (Figure 5D) (McKay et al., 2012). The central, orange mat overlays the steepest gradients, characterized by high supply of carbon and energy sources and a strong temperature increase in the upper sediment layers (50-60 °C at 10-15 cm depth) (McKay et al., 2012, 2016). In the white mat area, gradients are smoother and reach lower temperatures at the same depth (20-30 °C) (McKay et al., 2012, 2016). The temperature in bare, brown sediment, uncovered by *Beggiatoaceae* mats, reaches only slightly higher temperatures than the ambient temperature at the seafloor surface (5-10 °C) (McKay et al., 2012, 2016).

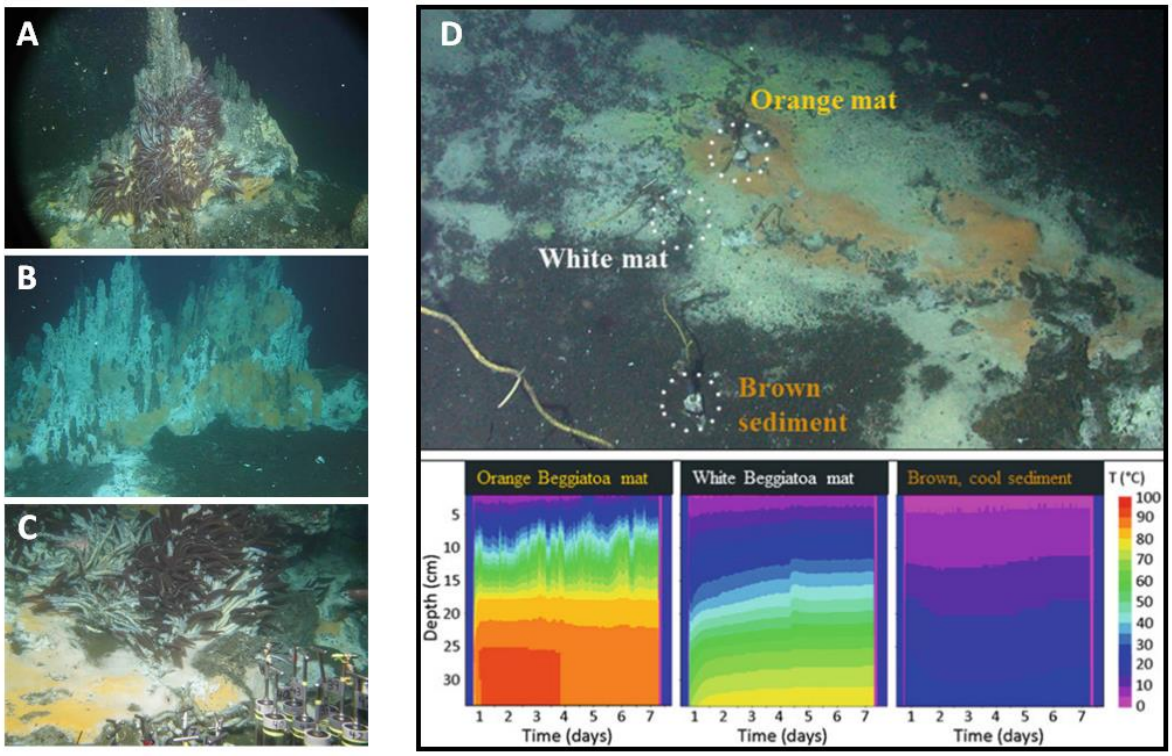


**Figure 5 | A-C:** Hydrothermal chimneys, microbial mats of *Beggiatoaceae*, and *Riftia pachyptila* in the Guaymas Basin. Image sources: **A:** Woods Hole Oceanographic Institution (WHOI) (*RV Atlantis* cruise AT42-05) **B:** Teske et al. (2016), WHOI (*RV Atlantis* cruise AT15-56) **C:** WHOI (*RV Atlantis* cruise AT42-05). **D**: Temperature gradients in the orange mat center, white peripheral mat, and brown sediment measured over a time period of seven days. From McKay et al. (2016); Teske (2020)

Thus, the petroleum HCs formed deep in the GB fuel microbial activity in upper sediment layers, which in turn supplies sulfide as energy source to simple and complex lifeforms on the seafloor surface. Many insights on anaerobic microorganisms mediating HC degradation and the mechanisms they employ to do so have been gained through enrichment cultures from the GB, e.g. (Phelps et al., 1996; Kniemeyer et al., 2007; Laso-Pérez et al., 2016). Thus, the GB constitutes a natural laboratory for the study of anaerobic petroleum HC degradation under a wide temperature range. In the next sections, microorganisms and the mechanisms they employ for HC degradation will be outlined both in general and in context to the GB specifically.

## 1.7 Sources and fate of petroleum HCs in the marine environment

HCs formed in the subsurface can enter the marine environment naturally through cracks and fissures on the seafloor. This seepage occurs as a result of over-filling of deeply-seated reservoirs, or of tectonic activity of geological formations like transform faults and fracture zones (Tveit et al., 2021). HC seeps are concentrated at continental margins, oceanic spreading centers, and subduction zones (Figure 6) (Le Bris et al., 2016; Teske and Carvalho, 2020). HCs can seep from both cold seeps and hydrothermal vents (Teske and Carvalho, 2020).

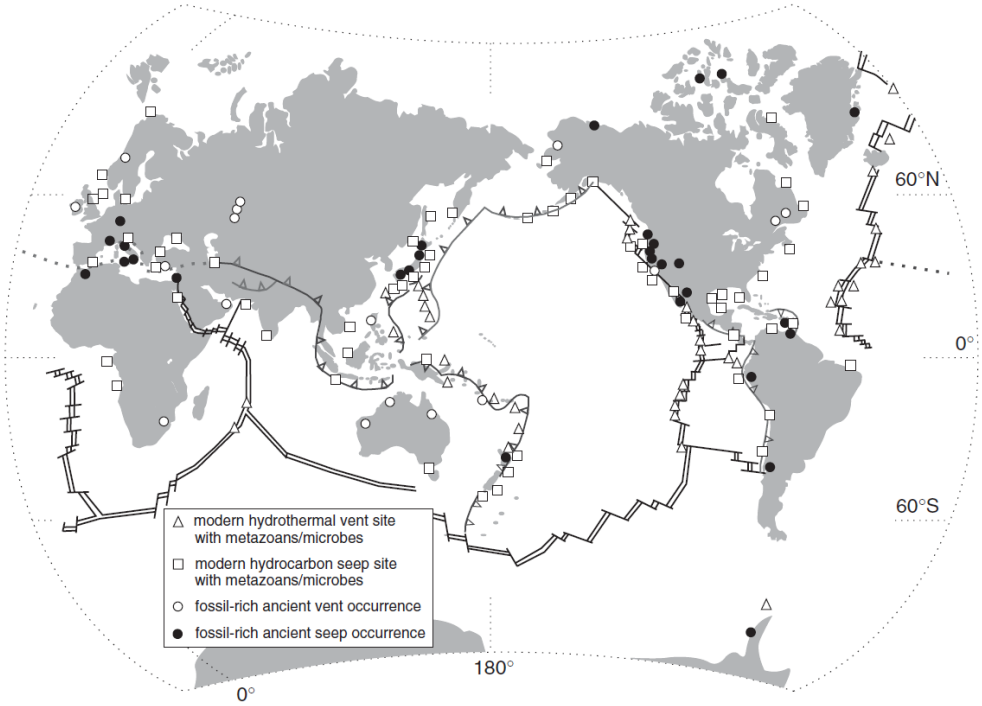


**Figure 6** | Global distribution of hydrocarbon seeps. From Campbell (2006)

Cold seeps emit HCs at temperatures slightly higher than ambient seawater temperature (Cordes et al., 2007; Åström et al., 2018; Ceramicola et al., 2018). Most cold seeps are located around continental margins (Ceramicola et al., 2018). Some cold seeps are associated with mud volcanism, pockmarks, and brine pool formation (Foucher et al., 2009). The largest continuous area of cold seeps is located at the continental slope of the northern Gulf of Mexico, where gaseous and liquid HCs emerge from large subsurface gas and oil reservoirs (Teske, 2019; Teske and Carvalho, 2020; Teske and Joye, 2020). Hydrothermal vents, like the GB, are located at mid-ocean ridges, volcanic arcs, and back-arc spreading centers (Le Bris et al., 2016). Other hydrothermal vents with HC seepage are located for instance at the Juan de Fuca Ridge in the in the northeast Pacific, in the Gulf of Aden, and in the Pescadero Basin in the southern Gulf of California (Hunt, 1975, 1979; Canadian American Seamount Expedition, 1985; Gamo et al., 2015; Paduan et al., 2018). Some environments like the GB comprise both cold seeps and hydrothermal vents depending on variations of geothermal circulation (Geilert et al., 2018). Seeps and vents are hotspots of reduced compounds and thereby sustain diverse life on the seafloor, which manifests itself as microbial mats and populations of symbiotic chemosynthetic

bacteria with their invertebrate hosts, *Riftia* tube worms and *Bathymodiolus* mussels (Campbell, 2006; Dubilier et al., 2008; Cordes et al., 2009; Le Bris et al., 2016).

HCs are also released into the marine environment through anthropogenic activities, e.g. accidents during reservoir exploration, petroleum transport, and refinement (NAS, 1975; Samiullah, 1985; Kvenvolden and Cooper, 2003). These spillages can be "point source pollution", i.e. release of large amounts of HCs on a short timescale from one source, e.g. accidents of oil tanker or pipeline spills, or "nonpoint source pollution", i.e. leakage of lower amounts of HCs from several sources over a longer time span (Kleindienst and Joye, 2019). An infamous example of a point source pollution is the Deepwater Horizon blowout in the Gulf of Mexico in 2010. which released an estimated 4.4 million barrel (~0.6 million tonnes) of liquid HCs and an estimated 0.5 million tonnes of gaseous HCs into the Gulf (Crone and Tolstoy, 2010; Joye et al., 2011). Because many HCs, particularly small volatile compounds like small AHs, have toxic and/or mutagenic effects on many lifeforms, which can be transported through trophic chains (Samiullah, 1985; An, 2004; Alonso-Alvarez et al., 2007; Paul et al., 2013), such spillages are environmentally concerning.

Natural seepage and anthropogenic-caused spillage each contribute about 50% to the total petroleum HC release into the marine environment (Kvenvolden and Cooper, 2003). This amounts to an estimated total of 1.2 million tonnes of petroleum per year (Kvenvolden and Cooper, 2003). Understanding the fate of petroleum HCs in the ocean is therefore of high interest to, first, better understand carbon cycling in deep-sea natural seepage areas, and second, allow estimations on processes of bioremediation of contaminated environments. Microorganisms capable of aerobic HC degradation, first identified through cultivation-based techniques, are ubiquitously present in the marine environment (Head et al., 2006; Kleindienst and Joye, 2019). At low HC concentrations, these microorganisms are often not particularly abundant, but their abundance and activity can be quickly stimulated through the input of large HC quantities (Syutsubo et al., 2001; Yakimov et al., 2007; Kimes et al., 2014; Kleindienst and Joye, 2019). Aerobic HC degraders consume HCs rapidly after activation via mono- and dioxygenase enzymes (Suzuki et al., 1991; Maeng et al., 1996; Sakai et al., 1996; Fritsche and Hofrichter, 2000; Rapp and Gabriel-Jürgens, 2003). Most of these organisms are bacteria of the class Gammaproteobacteria, for instance *Alcanivorax* spp., *Oleiphilus* spp. and *Oleispira* spp. (Yakimov et al., 1998, 2003; Golyshin et al., 2002; Liu and Shao, 2005; Wang et al., 2012) and of the class Alphaproteobacteria, e.g. *Roseobacter* and *Rhodospirillales* spp. (Lamendella et al., 2014; Dombrowski et al., 2016). Some halophilic aerobic HC-degrading archaea have also been isolated (e.g. *Haloferax*, *Halobacterium*, and *Halorubrum* spp.) (Tapilatu et al., 2010; Erdoğmuş et al., 2013). HC activation is followed by conversion to fatty acid intermediates and oxidation via the $\beta$-oxidation pathway and tricarboxylic acid (TCA) cycle to $CO_2$. Thereby, energy is liberated to sustain cell functions. Central intermediates like acetyl-coenzyme A (acetyl-CoA) are additionally used to generate biomass (Fritsche and Hofrichter, 2000; Park and Park, 2018;

Kleindienst and Joye, 2019). Aerobic microorganisms preferably degrade alkanes and small AHs, depleting petroleum of its lighter fractions and converting it into heavy oil (Head et al., 2006). When high activities of aerobic HC-oxidizing microorganisms have depleted all available oxygen, and in anoxic sediments, anaerobic degradation mechanisms need to be employed.

Because of their chemical stability and the high energy demand required for their degradation, HCs were initially believed to be recalcitrant under anoxic conditions (Widdel et al., 2010). The study of anaerobic HC-degrading microorganisms was substantially impaired by the often very slow growth rates of the respective microorganisms. Therefore, anaerobic HC degradation was confirmed only decades after the discovery of aerobic degradation (Widdel et al., 2010). Thanks to relentless isolation and enrichment efforts, it was learnt that the capacity for anaerobic HC degradation is scattered across diverse taxonomic groups (Widdel et al., 2010; Rabus et al., 2016). Widdel et al. (2010) suggested that this distribution could imply that HC degradation is an ancient trait and that HCs were likely available at an early stage of prokaryotic evolution. Most anaerobic HC degraders have a limited substrate range, specializing on one specific HC or group of HCs (Widdel et al., 2010). Anaerobic HC-degrading microorganisms have been enriched under sulfate-, nitrate-, manganese-, and iron-reducing and under methanogenic conditions e.g. (Phelps et al., 1998; Kniemeyer et al., 2007; Beal et al., 2009; Luo et al., 2014; Chen et al., 2020). For comprehensive overviews of pure and enriched anaerobic HC-degrading cultures up to 2016, the reader is referred to reviews by Widdel et al. (2010) and Rabus et al. (2016). The anaerobic degradation of linear alkanes (*n*-alkanes, hereafter referred to as alkanes) and aromatic HCs is of particularly high interest, as these compounds are abundant in petroleum and the most stable HCs (Tissot and Welte, 1984).

## 1.8 Anaerobic degradation of alkanes by bacteria

The first isolated alkane degrader operating under strictly anoxic conditions is the sulfate-reducing bacterium *Desulfosudis oleivorans* strain Hxd3 of the class Desulfobacteria, originating from an oil-water separator of an oil field near Hamburg (Germany) (Aeckersberg et al., 1991). Strain Hxd3 was enriched on hexadecane ($C_{16}$ alkane) and can degrade long-chain $C_{12}$-$C_{20}$ alkanes (Aeckersberg et al., 1991). Further sulfate-reducing bacteria (SRB) capable of alkane oxidation were described soon after that, including *Desulfothermus naphthae* strain TD3, the first anaerobic HC-degrader isolated from GB sediments, growing on $C_6$-$C_{16}$ alkanes (Rueter et al., 1994), and *Desulfatibacillum alkenivorans* strain AK-01 utilizing $C_{13}$-$C_{18}$ alkanes (So and Young, 1999b). Bacteria-mediated alkane oxidation was also demonstrated under nitrate-reducing and iron-reducing conditions (Ehrenreich et al., 2000; So and Young, 2001). Bacteria also form syntrophic consortia with methanogens, in which the bacteria oxidize long-chain alkanes and shuttle the freed electrons to the methane-forming archaea (Schink, 1997; Zengler et al., 1999; So and Young, 2001). Kniemeyer et al. (2007) extended the list of alkane-oxidizing bacteria into the realm of gaseous alkanes with the butane ($C_4$)- and propane ($C_3$)-oxidizing

culture BuS5 affiliated with *Desulfosarcina*/*Desulfococcus* and the propane-oxidizing *Desulfotomaculum* strain Propane60-GuB, both isolated from the GB. Thus, alkanes between $C_3$-$C_{20}$ are confirmed substrates of anaerobic bacteria (Widdel et al., 2010). Anaerobic alkane-oxidizing bacteria affiliate with the two phyla Proteobacteria (now reclassified by the Genome Taxonomy Database -GTDB- as several classes within the phylum Pseudomonata) (Parks et al., 2022) and Firmicutes (now several classes under the phylum Bacillota) (Widdel et al., 2010). In the marine environment, predominant bacterial alkane-oxidizers are SRB of the class Deltaproteobacteria (now reclassified as several classes within the phylum Desulfobacterota) (Davidova et al., 2018).

For the challenging initial activation of the unreactive alkanes, several mechanisms have been discussed, including hydroxylation and carboxylation (Heider, 2007; Callaghan, 2013). While strain Hxd3 seems to activate its substrates via hydroxylation and/or carboxylation, the best described and prevalent mechanism in bacteria is the fumarate addition pathway (Callaghan, 2013). First indications for this mechanism came from So and Young (1999a), who incubated strain AK-01 with stable-isotope labeled substrate to reveal the addition of an exogenous carbon compound at the subterminal (C2) position of $C_{16}$, followed by formation of a fatty acid. Kropp et al. (2000) and Callaghan et al. (2006) then supported this notion by detecting metabolites, including alkylsuccinates, in accordance with a fumarate-based activation mechanism. The enzyme catalyzing this activating reaction was revealed to belong to the pyruvate formate lyase (Pfl) family (Callaghan et al., 2008; Grundmann et al., 2008). Pfl is the central enzyme of anaerobic glucose metabolism (Abbe et al., 1982). The alkane-activating homologues can be distinguished from the ubiquitously present Pfl by differing numbers of conserved cysteine residues (Callaghan et al., 2008). They have been denoted (1-methylalkyl)succinate synthase (MasDEC) (Grundmann et al., 2008) or alkylsuccinate synthase (AssABC) (Callaghan et al., 2008; Callaghan, 2013). MasD and AssA constitute the catalytic subunit, respectively (Callaghan et al., 2008; Grundmann et al., 2008). MasD/AssA add fumarate to the alkanes through a glycyl radical mechanism (Heider et al., 2016). Fumarate is added predominantly to the C2 position of the alkane (Callaghan, 2013). Side reactions adding to the terminal (C1) (Kniemeyer et al., 2007) and C3 (Rabus et al., 2001) position have also been reported. The activated alkanes then undergo a carbon-skeleton rearrangement and subsequent decarboxylation (Wilkes et al., 2002). This process yields fatty acids that are shuttled into the $\beta$-oxidation pathway to produce acetyl-CoA, which is finally oxidized to $CO_2$ (Figure 7) (Wilkes et al., 2002).

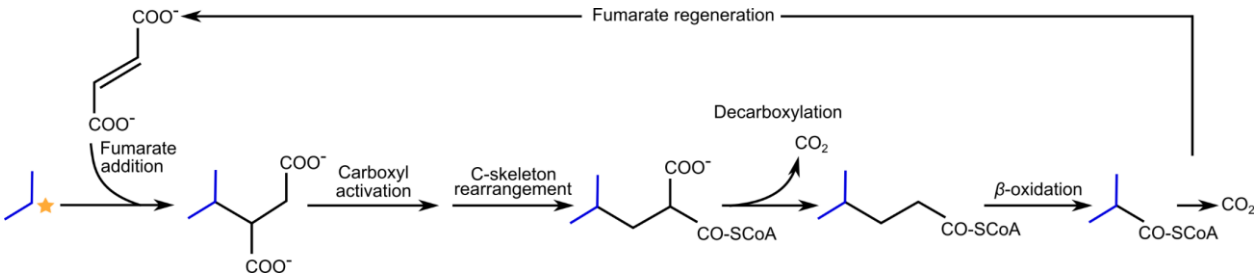


**Figure 7** | Anaerobic oxidation of propane via fumarate addition to the subterminal carbon atom. Modified from Singh et al. (2017)

Based on their essential role in anaerobic alkane activation, *masD*/*assA* sequences and the produced alkylsuccinate metabolites have been used as biomarkers to identify both the organisms mediating anaerobic alkane degradation and to detect petroleum contamination of pristine environments. For instance, Gittel et al. (2015) revealed that pristine areas of Danish coastal sediment showed a high diversity of *masD*/*assA* phylotypes, but a single cluster was prevalent in petroleum-rich sites. Gieg and Suflita (2002) detected $C_3$-$C_{10}$-alkylsuccinates in petroleum-contaminated aquifers and therefore proposed a prevalence of anaerobic HC degradation mechanisms. Stagars et al. (2016) examined the diversity of *masD* sequences in seven hydrothermal vents, including the GB, and cold seeps and found that sites with similar HC compositions contained similar *masD* sequence variants. In 2014, Khelifi et al. proposed that the sulfate-reducing archaeon *Archaeoglobus fulgidus* uses a homologue to AssA, which was likely acquired from a bacterium via horizontal gene transfer, to oxidize $C_{10}$-$C_{21}$ alkanes.

## 1.9 Anaerobic degradation of alkanes by archaea

Apart from *A. fulgidus*, another archaeon, *Thermococcus sibiricus*, grew on $C_{16}$ and encoded a MasD homologue (Mardanov et al., 2009). Aside from those two isolates, archaeal anaerobic alkane oxidizers were unknown. However, this dogma has changed in recent years, and a different alkane activation mechanism exclusively attributed to archaea was revealed. This mechanism was first described for archaea mediating the anaerobic oxidation of methane (AOM). AOM was first indicated by concomitant methane and sulfate depletion in marine sediments, creating sulfate-methane transition zones (SMTZs) (Iversen and Jørgensen, 1985; Borowski et al., 1999; D'Hondt et al., 2002). Stable carbon isotope compositional analyses, *in situ* hybridizations, and sequencing of the gene coding for the small subunit (16S) ribosomal RNA (rRNA) revealed that these reactions are orchestrated by anaerobic methanotrophic archaea (ANME) and partner SRB (Hinrichs et al., 1999; Boetius et al., 2000; Orphan et al., 2001b). ANME and SRB spatially assemble into syntrophic electron-exchanging consortia (Boetius et al., 2000; Orphan et al., 2001b). ANME-mediated AOM is an ecologically highly relevant process that removes 80-90% of methane, a strong greenhouse gas, in marine sediment before it can enter the atmosphere (Reeburgh, 1996, 2007; Lelieveld et al., 1998).

ANME are polyphyletic in the phylum Halobacterota and distribute into the three clades ANME-1 (subgroups a, b, and c) (Hinrichs et al., 1999; Orphan et al., 2001a; Benito Merino et al., 2022), ANME-2 (subgroups a, b, c, and d) (Orphan et al., 2001a; Raghoebarsing et al., 2006; Haroon et al., 2013; Benito Merino et al., 2022), and ANME-3 (Knittel et al., 2005; Niemann et al., 2006). The clades constitute different taxonomic levels; ANME-1 are classified as an order, ANME-2 consist of two families within the order Methanosarcinales, and ANME-3 form a genus within the family *Methanosarcinaceae* in the order Methanosarcinales (Orphan et al., 2001a; Knittel and Boetius, 2009; Chadwick et al., 2022; Parks et al., 2022). ANME-1 presumably dominate subsurface sediments, Black Sea chimneys and microbial mats, whereas ANME-2 are abundant at superficial cold seep sediments and in low-temperature SMTZs (Knittel et al., 2005; Knittel and Boetius, 2009). ANME-3 sequences have been recovered predominantly from mud volcanoes, e.g. the Håkon Mosby mud volcano in the Barents Sea (Niemann et al., 2006; Lösekann et al., 2007). ANME oxidize methane over a wide temperature range (Knittel and Boetius, 2009). AOM in the thermophilic range is currently only attributed to members of the ANME-1 clade (Holler et al., 2011; Benito Merino et al., 2022). Recently, the upper temperature limit of AOM was extended to 70 °C with the enrichment of thermophilic ANME-1c (Benito Merino et al., 2022). Most ANME lack reductive pathways and therefore require partner organisms that receive the electrons released during methane oxidation. An exception is the freshwater clade ANME-2d, which combines AOM with nitrate reduction independently of a partner organism (Haroon et al., 2013). Marine ANME partner with SRB of different clades within the phylum Desulfobacterota, including Seep-SRB1 (Schreiber et al., 2010), Seep-SRB2 (Ruff et al., 2016; Krukenberg et al., 2018), *Candidatus* Desulfofervidus auxilii of the HotSeep-1 clade (Holler et al., 2011; Krukenberg et al., 2016), and seepDBB of the *Desulfobulbaceae* (Green-Saxena et al., 2014). Recently, a novel thermophilic partner SRB was described, *Ca.* Thermodesulfobacterium torris, which partners with ANME-1c at 70 °C (Benito Merino et al., 2022).

ANME oxidize methane using the enzymes of the methanogenesis pathway in reverse direction (Hallam et al., 2003, 2004). Therein, variants of the key enzyme of methanogenesis, methyl-coenzyme M reductase (Mcr), catalyze the activation of methane to methyl-coenzyme M (methyl-CoM) (Hallam et al., 2003, 2004; Scheller et al., 2010). The Mcr is formed by three subunits: the catalytic α subunit encoded by *mcrA*, a β subunit encoded by *mcrB*, and a γ subunit encoded by *mcrG* (Gunsalus and Wolfe, 1980; Allmansberger et al., 1986; Hallam et al., 2003). The Mcr holoenzyme is a dimer of heterotrimers ($\alpha_2\beta_2\gamma_2$), and each heterotrimer contains an active site with a non-covalently bound nickel porphinoid coenzyme $F_{430}$, a tetrapyrrole compound (Figure 8A) (Ermler et al., 1997). In methanotrophy, the Mcr converts methane and the heterodisulfide of CoM and coenzyme B (CoM-S-S-CoB) to methyl-CoM and CoB (Figure 8B) (Scheller et al., 2010).

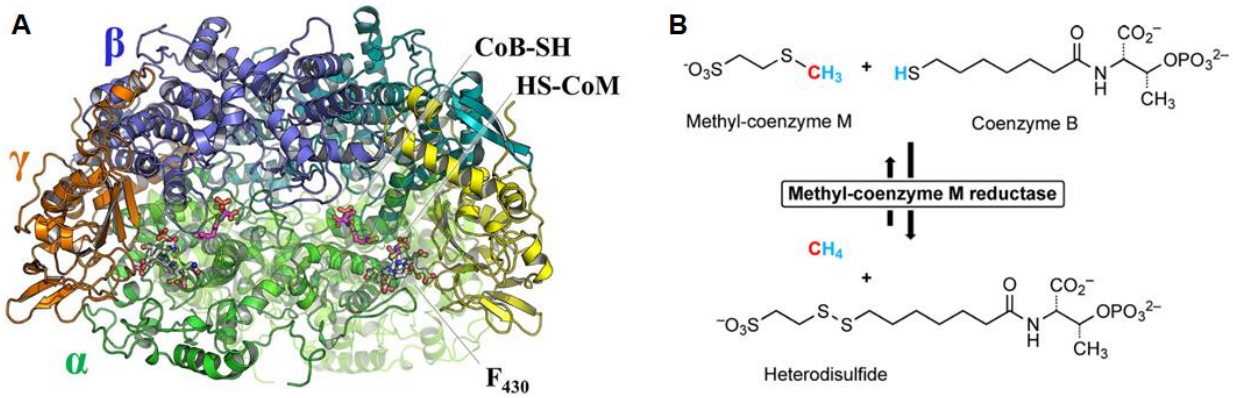


**Figure 8 | A:** Crystal structure of the methyl-coenyzme M reductase (Mcr) from the methanogen *Methanothermococcus thermolithotrophicus* with the bound cofactor $F_{430}$. From Wagner et al. (2017) **B:** Reaction catalyzed by the Mcr. The Mcr catalyzes the binding of methane to coenzyme M and the reverse reaction. From Scheller et al. (2013)

The activated methyl group is then transferred to the coenzyme tetrahydromethanopterin ($H_4$MPT) through the membrane-bound $Na^+$-translocating enzyme methyl-$H_4$MPT-CoM methyltransferase (Mtr) (Becher et al., 1992; Hallam et al., 2004). Methyl-$H_4$MPT is subsequently oxidized to $CO_2$ by the enzymes of the $H_4$MPT methyl branch of the Wood-Ljungdahl (WL) pathway (Hallam et al., 2004; Adam et al., 2019). Notably, ANME-1 lack the first enzyme of this pathway, methylene-$H_4$MPT reductase (Mer) (Hallam et al., 2004; Meyerdierks et al., 2010; Stokke et al., 2012; Chadwick et al., 2022), which they apparently replaced with methylene-tetrahydrofolate ($H_4$F) reductase (MetF) of the $H_4$F methyl branch of the WL pathway (Stokke et al., 2012; Timmers et al., 2017; Adam et al., 2019).

The exact mechanism of electron transport from ANME to partner SRB is a long-standing conundrum. While diffusion-based transfer via soluble small electron carriers like hydrogen and formate has been discussed, more evidence points toward direct interspecies electron transfer (DIET) via conductive cell-to-cell connections between archaea and bacteria (Chadwick et al., 2022). Dense structures of such "nanowires", likely consisting of multi-heme *c*-type cytochromes, archaeal flagellin and/or bacterial pilin, are visible in the intercellular space of consortia of ANME-1, ANME-2 and partner SRB (Wegener et al., 2015; Krukenberg et al., 2018). The partner SRB then channel the received electrons into the canonical dissimilatory sulfate reduction (DSR) pathway, consisting of ATP-sulfurylase (Sat), APS-reductase (Apr), and dissimilatory sulfite reductase (Dsr) (Rabus et al., 2013).

Structurally, Mcrs that activate methane are highly similar to those of methanogens (Shima et al., 2012; Chadwick et al., 2022). In 2016, Laso-Pérez et al. (2016) reported thermophilic propane ($C_3$)- and butane ($C_4$)-oxidizing consortia isolated from GB sediments. The consortia consisted of archaea of the novel genus *Ca.* Syntrophoarchaeum, partnering with *Ca.* D. auxilii, a known partner SRB of ANME (Krukenberg et al., 2016; Laso-Pérez et al., 2016). In these consortia, *Ca.* S. caldarius and *Ca.* S. butanivorans oxidize the gaseous alkanes after

activation to alkyl-CoMs via Mcrs. This induced a paradigm shift, as the Mcr was believed to be restricted to one-carbon compounds prior to that discovery. *Ca.* Syntrophoarchaeum spp. are closely related to ANME-1, together forming the class Syntrophoarchaeia. Both groups encode the *β*-oxidation pathway, which is necessary for the oxidation of alkanes longer than methane, but without a known purpose in ANME-1 (Laso-Pérez et al., 2016; Wang et al., 2021). *Ca.* Syntrophoarchaeum couple acetyl-CoA, the product of *β*-oxidation, to the WL pathway via the carbon monoxide dehydrogenase/acetyl-CoA synthase (CODH/ACS) (Laso-Pérez et al., 2016). The *mcrA* sequences of *Ca.* Syntrophoarchaeum were found to be highly divergent from sequences of methanogenic and methanotrophic archaea and clustered with sequences of other uncultured archaea, hinting at unexplored potential for non-methane alkane oxidation in the archaea (Laso-Pérez et al., 2016). In analyses based on environmental metagenomes, more and more divergent *mcrA* sequences were recovered, mostly from hydrothermal vent sites and hot springs (Wang et al., 2019b). Such sequences were detected in metagenome-assembled genomes (MAGs) of archaea within and outside the phylum Halobacterota, among others in the classes Bathyarchaeia (phylum Thermoproteota) (Evans et al., 2015) and Archaeoglobi (Boyd et al., 2019), in the phylum Thaumarchaeota (now reclassified as class Nitrosphaeria) (Hua et al., 2019) and in the order Helarchaeales within the Asgardarchaeota (Seitz et al., 2019) (Figure 9). Based on these discoveries, the more adequate name alkyl-coenzyme M reductase (Acr) was proposed for Mcr variants activating non-methane alkanes (Chen et al., 2019; Thauer, 2019). Another group of Mcrs affiliated with Verstraetearchaeota (now phylum Thermoproteota) was shown to mediate methylotrophic methanogenesis (Vanwonterghem et al., 2016; Wang et al., 2019b).

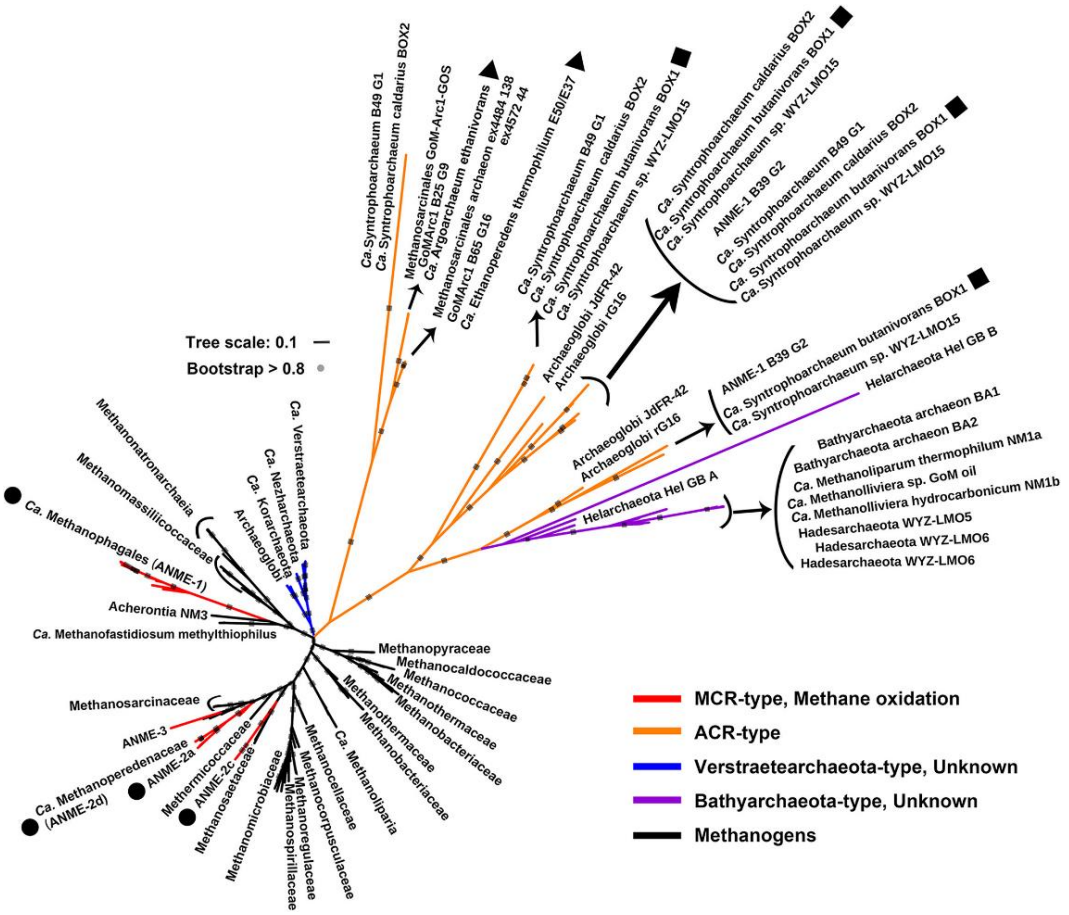


**Figure 9** | Phylogeny of *mcrA*/*acrA* sequences. Divergent sequences putatively used for multi-carbon alkane metabolism are located in the orange- and purple-colored branches. Modified from Wang et al. (2020)

Further cultivation-based evidence for a wider substrate range of the Mcr/Acr came from Chen et al. (2019) and Hahn et al. (2020), who enriched the psychrophilic ethane ($C_2$)-oxidizer *Ca.* Argoarchaeum ethanivorans from Gulf of Mexico sediment and the thermophilic $C_2$-oxidizer *Ca.* Ethanoperedens thermophilum from the GB, respectively. Both archaea are part of the taxonomic cluster GoM-Arc1, which is closely related to ANME-2d, use Acrs for $C_2$ activation, and form syntrophic consortia with partner SRB. Uncultured GoM-Arc1 members are all presumably $C_2$ oxidizers and have been detected in cold seep sediment from Hydrate Ridge in the northeastern Pacific and in samples from the Amon mud volcano in the eastern Mediterranean (Chen et al., 2019; Hahn et al., 2020). Zhou et al. (2022) extended the list of anaerobic multi-carbon alkane-oxidizing archaea -proposed to be referred to as ANKA- (Wang et al., 2020) by thermophilic *Ca.* Methanoliparum spp., isolated from the Shengli oil field in eastern China, which are capable of oxidizing most alkanes between $C_{13}$ and $C_{38}$. *Ca.* Methanoliparum additionally utilize *n*-alkylcyclohexanes and *n*-alkylbenzenes with long ($\geq C_{13}$) alkyl substituents (Zhou et al., 2022). Interestingly, *Ca.* Methanoliparum encode both an Acr and a Mcr, and shuttle electrons from long-chain alkane oxidation into methanogenesis in a single cell (Zhou et al., 2022). Sequences of the class Methanoliparia (previously known as the GoM-Arc2 clade) have also been recovered from the Gulf of Mexico (Orcutt et al., 2010; Laso-Pérez et al., 2019). With this recent isolation, archaea were confirmed to degrade $C_1$-$C_4$ alkanes and

alkanes ≥$C_{13}$ anaerobically through activation via Mcrs/Acrs, leaving a gap in the range of mid-chain alkanes (Figure 10).

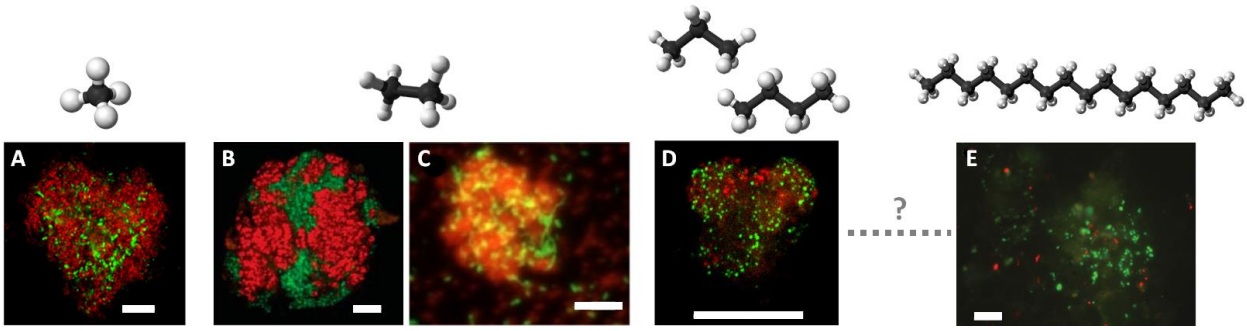


**Figure 10 |** Substrate range of cultured anaerobic alkane-oxidizing archaea. **A**: Consortia of ANME-1 (red) and *Ca.* Desulfofervidus auxilli (green) oxidize methane ($C_1$) (Wegener et al., 2016). **B & C**: Consortia of *Ca.* Ethanoperedens thermophilum (red) and *Ca.* D. auxilii (green) (Hahn et al., 2020) (**B**) and *Ca.* Argoarchaeum ethanivorans (red) and Eth-SRB bacteria (green) (Chen et al., 2019) (**C**) oxidize ethane ($C_2$). **D**: Consortia of *Ca.* Syntrophoarchaeum spp. (red) and *Ca.* D. auxilii (green) oxidize propane ($C_3$) and butane ($C_4$) (Laso-Pérez et al., 2016). **E**: *Ca.* Methanoliparum spp. (green) oxidize long-chain alkanes (≥$C_{13}$) independently of partner bacteria (Zhou et al., 2022). The scale bar is 10 µm in all images.

Efforts were undertaken to reveal the structural differences between canonical Mcrs and Acrs that enable ANKAs to activate larger alkanes. Hahn et al. (2021) were able to obtain a high-resolution crystal structure of the Acr of *Ca.* E. thermophilum. The enzyme exhibited the Mcr-typical $\alpha_2\beta_2\gamma_2$ organization but, compared to the canonical Mcr, displayed structural modifications to accommodate $C_2$, including insertions in all subunits, a larger catalytic chamber and formation of a hydrophobic tunnel. Lemaire and Wagner (2022) generated structural models of the Acrs of *Ca.* Syntrophoarchaeum and *Ca.* Methanoliparum, from which they inferred that Acrs activating alkanes larger than $C_2$ contain a catalytic open cleft instead of a tunnel. This cleft could accommodate alkanes up to $C_{13}$, with longer chains protruding out of the cleft. This is in accordance with the capacity of *Ca.* Methanoliparum to oxidize ≥$C_{13}$-substituted alkylcyclohexanes and alkylbenzenes (Zhou et al., 2022).

Environmental studies keep revealing more *acrA* sequences with unknown function, particularly in hydrothermal vent sediment including the GB (Wang et al., 2019a). To clarify the substrate range of these enzymes, and the taxonomy and physiology of archaea that utilize them, cultivation-based approaches are required. This is addressed in **chapter 2**.

## 1.10 Anaerobic degradation of AHs

Despite the toxicity and chemical stability of AHs, anaerobic microorganisms have developed ways to make use of these compounds as electron and energy sources. Like in anaerobic alkane degradation, the decisive step in anaerobic AH degradation is the activation of the stable compounds. A key learning from enrichment efforts is that the presence of functional groups facilitates faster AH degradation (Widdel et al., 2010). The inertness of unsubstituted AHs (UAHs) is illustrated by a sequential order of degradation of one-ringed AHs in anoxic environments. The substituted AHs toluene, xylene, and ethylbenzene are degraded first, while the UAH benzene is degraded last, if at all (Edwards and Grbić-Galić, 1992; Edwards et al., 1992). Toluene is the most readily degraded AH and numerous sulfate-, nitrate-, or iron-reducing degraders, plus methanogenic enrichments, have been established (Widdel et al., 2010). The key enzyme in anaerobic toluene degradation is benzylsuccinate synthase (BssABCD), which is closely related to Mas/Ass involved in bacterial anaerobic alkane activation. Equally, Bss activates toluene via fumarate addition (Beller et al., 1992; Evans et al., 1992; Beller and Edwards, 2000; Callaghan et al., 2008). Several bacteria of the phylum Pseudomonata, including *Thauera aromatica* and *Azoarcus* spp., are known toluene degraders (Heider et al., 1998; Heider, 2007).

Among the UAHs, benzene (one-ringed UAH) and naphthalene (two-ringed UAH) are the best-studied substrates. Despite slow growth, a few enrichment and some pure cultures, almost exclusively mesophilic bacteria, have been established from petroleum-contaminated sites under sulfate-, nitrate-, iron-, and manganese-reducing as well as under methanogenic conditions (Widdel et al., 2010). Direct fumarate addition to UAHs like in the case of toluene is not feasible. For benzene, three activation mechanism have been proposed instead: methylation to toluene, hydroxylation to phenol, and carboxylation to benzoate (Figure 11) (Abu Laban et al., 2010). All options activate benzene to a more reactive compound which can be processed via canonical pathways to the central intermediate benzoyl-CoA (BCoA) (Merkel et al., 1989; Kube et al., 2004; Schmeling et al., 2004; Schühle and Fuchs, 2004; Wischgoll et al., 2005). Evidence for all three activation mechanisms has been reported from different cultures. For instance, the iron-respiring bacterium *Geobacter metallireducens* produces trace amounts of phenol during benzene oxidation, and deletion of genes required for phenol degradation eliminated the capacity for benzene oxidation (Zhang et al., 2013). This observation indicated activation via hydroxylation. Chakraborty and Coates (2005) also reported transient phenol formation in cultures of the nitrate-reducing benzene-degrading *Dechloromonas* strain RCB and proposed a hydroxylation of benzene via hydroxyl free radicals (HO•). Ulrich et al. (2005) detected $^{13}$C-toluene and $^{13}$C-benzoate in nitrate-reducing and methanogenic enrichment cultures incubated with $^{13}$C-benzene, congruent with activation via methylation and carboxylation. However, enzymes catalyzing the direct hydroxylation or methylation of benzene remain unknown. For carboxylation, a two-subunit anaerobic benzene carboxylase, AbcAD, has been identified, which is highly expressed during benzene oxidation (Abu Laban et al., 2010; Luo et al., 2014). AbcAD

is an UbiD/UbiX-like carboxylase, in which the UbiD domain catalyzes the carboxylation itself, and the UbiX domain generates prenylated flavin mononucleotide (prFMN), the cofactor of UbiD (Abu Laban et al., 2010; Marshall et al., 2017). The currently only known archaeal UAH-oxidizer, the hyperthermophilic iron-reducer *Ferroglobus placidus*, likely uses a homologue of AbcAD for benzene carboxylation (Holmes et al., 2011).

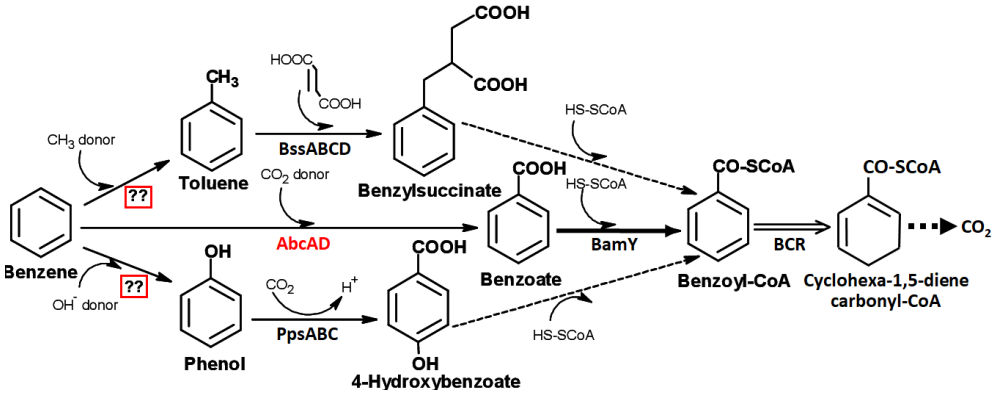


**Figure 11** | Pathways for anaerobic activation and degradation of benzene. Steps in red boxes are unresolved. Dashed arrows indicate multiple reactions. BssABCD: benzylsuccinate synthase, AbcAD: anaerobic benzene carboxylase, BamY: benzoate-CoA ligase, PpsABC: phenylphosphate synthase, BCR: benzoyl-CoA reductase, CoA: coenzyme A. Modified from Abu Laban (2010)

Next, BCoA is dearomatized by benzoyl-CoA reductase (BCR) (Boll et al., 1997, 2000), of which two classes are known. Class I BCR is ATP-dependent and was found mainly in facultative anaerobic bacteria (Carmona et al., 2009). Class I BCRs fall into two phylogenetic clusters: *bcr* type (BcrABCD/BadDEFG), isolated from *T. aromatica* and *Rhododpseudomonas palustris*, and *bzd* type (BzdNOPQ), isolated from *Azoarcus evansii* (Song and Ward, 2005; Porter and Young, 2014). Class II BCRs use an ATP-independent mechanism and are thus considered more feasible for obligate anaerobic microorganisms (Wischgoll et al., 2005). The best studied class II BCR is the membrane-associated BamBCDEFGHI protein complex of *G. metallireducens* (Huwiler et al., 2019). The product of the BCR, 1,5-dienoyl-CoA, is hydrolyzed in a modified *β*-oxidation pathway (Carmona et al., 2009). The key enzyme of this pathway is the ring-opening hydrolase, of which several homologues have been described, including Oah in *T. aromatica* (Breese et al., 1998), BzdY in *Azoarcus* sp. CIB (López Barragán et al., 2004), and BamA in *G. metallireducens* (Wischgoll et al., 2005). The product of the modified *β*-oxidation pathway, 3-hydroxypimelyl-CoA, is converted to other intermediates which are shuttled into the canonical *β*-oxidation pathway (Carmona et al., 2009). The produced acetyl-CoA enters central metabolic pathways for energy generation or biomass production.

For naphthalene, two potential activation pathways have been discussed: methylation and carboxylation (Meckenstock et al., 2016). In a sulfate-reducing enrichment culture of *Desulfobacterium* strain N47, first evidence pointed towards direct methylation to 2-methylnaphthalene (Figure 12). This was based on the capacity of N47 to metabolize 2-methylnaphthalene and the presence of required pathway genes in the genome, including naphthyl-2-methyl-succinate synthase (Nms), a homologue of Bss (Safinowski and

Meckenstock, 2006; Musat et al., 2009; Selesi et al., 2010). However, later results from other naphthalene-degrading *Desulfobacteraceae* closely related to N47 indicated that direct carboxylation at the C2 carbon forming 2-naphthoate is more likely (Kümmel et al., 2015). Recently, the gene cluster encoding a putative naphthalene carboxylase complex, which contains three UbiD-like carboxylases, and the reaction mechanism of this complex have been detailed (Kümmel et al., 2015; Koelschbach et al., 2019; Heker et al., 2023). In several other naphthalene-degraders, including the marine sulfate reducer NaphS2 (*Desulfatiglandaceae*) and the closely related strains NaphS3 and NaphS6, carboxylation is also the likely activation mechanism (Galushko et al., 1999; Musat et al., 2009). After carboxylation, 2-naphthoate is converted to 2-naphthoyl-CoA by a highly effective 2-naphthoyl-CoA ligase (NCL) (Heker et al., 2023). Candidate genes of NCL have been identified in N47 and NaphS2 (Bergmann et al., 2011; Meckenstock et al., 2016).

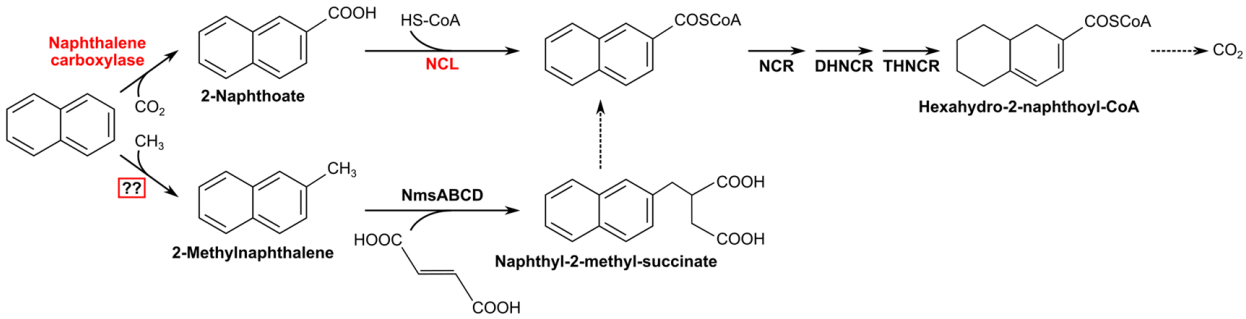


**Figure 12** | Pathways for anaerobic activation and degradation of naphthalene. Steps in red boxes are unresolved. Dashed arrows indicate multiple reactions. NCL: 2-naphthoyl-CoA ligase, NmsABCD: naphthyl-2-methyl-succinate synthase, NCR: 2-naphthoyl-CoA reductase, DHNCR: 5,6-dihydro-2-naphthoyl-CoA reductase, THNCR: 5,6-dihydro-2-naphthoyl-CoA reductase, CoA: coenzyme A. Modified from Meckenstock et al. (2016)

Then, the aromatic ring system becomes dearomatized in three consecutive two-electron reductions, mediated by 2-naphthoyl-CoA reductase (NCR), 5,6-dihydro-2-naphthoyl-CoA reductase (DHNCR), and 5,6,7,8-tetrahydro-2-naphthoyl-CoA reductase (THNCR) (Eberlein et al., 2013a, 2013b; Estelmann et al., 2015). NCR and DHNCR are both ATP-independent enzymes of the old yellow enzyme family, while THNCR is ATP-dependent and highly similar to class I BCR (Eberlein et al., 2013a, 2013b; Estelmann et al., 2015). Interestingly, metabolite analyses have revealed that the dearomatization occurs first on the unsubstituted ring (Meckenstock et al., 2000; Zhang et al., 2000). The product of THNCR, a hexahydro-2-naphthoyl-CoA isomer, is then stepwise oxidized to acetyl-CoA, presumably via proteins encoded by the 21-gene *thn* operon in N47 and NaphS2 (Eberlein et al., 2013b; Meckenstock et al., 2016).

Recently, several anaerobic cultures degrading UAHs larger than naphthalene have been established, which likely also activate their substrates via carboxylation. For instance, *Desulfatiglans* bacterium TRIP_1, *Desulfotomaculum* strain PheS1, and *Geobacter sulfurreducens* strain PheS2 degrade phenanthrene, a three-ringed UAH (Himmelberg et al.,

2018; Kraiselburd et al., 2019; Zhang et al., 2021a, 2021b). Other bacteria isolated from AH-contaminated sites, including *Castellaniella*, *Paracoccus*, and *Hydrogenophaga* spp. of the phylum Pseudomonata, degrade pyrene, a four-ringed UAH, under sulfate-, iron-, and nitrate-reducing conditions (Yang et al., 2013; Yan et al., 2017; Deng et al., 2021). Thus, the list of anaerobic UAH-degraders is growing; however, cultures established in the thermophilic temperature range are still scarce. This is addressed in **chapter 3**.

## 1.11 HC degradation in petroleum reservoirs

Petroleum reservoirs are extreme environments characterized by heat, high pressure and absence of molecular oxygen. Obtaining samples for microbial analyses from such reservoirs is logistically challenging, because they are often located kilometers deep in the subsurface (Marietou, 2021). Yet, previous studies have revealed that the subsurface is in no way sterile (Whitman et al., 1998), and that microbial transformation of oil compounds indeed takes place, particularly at the interface between oil and water phase (L'Haridon et al., 1995; Head et al., 2003; Gray et al., 2010; Pannekens et al., 2019). For instance, metabolites indicative of HC degradation, including 2-naphtoic acid indicative of naphthalene degradation, were detected in petroleum depleted of its lighter fraction, i.e. heavy oil, but were absent in non-degraded oil (Aitken et al., 2004). This biodegradation produces large deposits of heavy oil around the globe, which exceed those of conventional petroleum (Meyer, 1987). Sulfate reduction and methanogenesis are the predominant reductive processes in reservoirs (Jones et al., 2008; Magot, 2014). Sulfate in pristine reservoirs originates from sediment or rock, and is added in large amounts during secondary oil recovery through the injection of seawater (Sierra-Garcia and Oliveira, 2013; Tanji et al., 2014). Thus, secondary recovery often stimulates HC degradation processes, producing heavy oil and high levels of sulfide, which is called biological souring (Tanji et al., 2014). As methanogenesis is independent of external electron acceptors, it is the main reductive process when sulfate concentrations are low (Gray et al., 2010). *In vitro* studies with recovered petroleum or reservoir production water have shown that alkanes and AHs are subject to anaerobic microbial degradation (Zengler et al., 1999; Jones et al., 2008; Gray et al., 2010; Li et al., 2012). Because contaminations cannot be excluded during the challenging sampling process, the responsible microbes cannot be identified with certainty. Previously, sulfate-reducers like *Archaeoglobus* spp. and SRB, including Thermodesulfobacteria, and methanogenic archaea, including *Methanosaeta* and *Methanosarcina* spp., were frequently detected in samples from deep oil wells (Birkeland, 2004; Pannekens et al., 2019). These groups could perform reductive processes. While *masD*/*assA* and *mcrA* genes have been amplified from reservoir-based enrichments and production waters (Mbadinga et al., 2012; Berdugo-Clavijo and Gieg, 2014; Gao et al., 2015; Liu et al., 2016), the organisms responsible for HC degradation remain somewhat obscure.

The question which microorganisms might be responsible for biodegradation of HCs in reservoirs at its upper temperature limit is particularly intriguing. It was estimated that reservoirs become sterilized at temperatures around 80-90 °C (Wilhelms et al., 2001). Head et al. (2003) proposed that biodegradation in reservoirs virtually ceases at 80 °C, because the chance of finding heavily biodegraded oils in reservoirs heated to that temperature is almost zero. In contrast, at temperatures of 50 °C, 70 % of reservoirs would contain heavily degraded oil (Pepper and Santiago, 2001). The highest microbial diversity in reservoirs was observed at 55 °C (Lin et al., 2014). Yet, some microbial groups were more abundant at temperatures ≥50 °C. Those groups include Firmicutes, Thermotogae, and Thermodesulfobacteria among the bacteria, and Thermoproteales, Sulfolobales, and Halobacteriales among the archaea (Pannekens et al., 2019). Some archaeal groups were exclusively found in high temperature reservoirs (Li et al., 2017; Pannekens et al., 2019). Some of these thermophilic groups might perform HC degradation, but more cultivation-based studies at high temperatures are necessary for a better understanding of identities and metabolisms of such thermophilic HC-degrading microorganisms.

## 1.12 Membrane lipids of bacteria and archaea

Life at the seafloor, especially in anoxic, heated environments comes with energetic challenges that require cellular adaptations to minimize energy loss. The cellular membrane is a crucial site of such adaptations (Valentine, 2007). Functioning as a barrier between the cytoplasm and the environment, it gives shape and stability to all organisms (Albers et al., 2000; Lamparter and Galic, 2020). It is also the site where the electrochemical gradients that sustain life are generated through the translocation of ions between inside and outside of the cell (Henderson, 1971; Albers et al., 2000). Thus, the membrane constantly negotiates between two essential needs: sufficient rigidity and sufficient permeability for ion movement across the membranes at the prevailing environmental conditions. At the optimal growth temperature of an organism, the membrane is assumed to be in its liquid crystalline state (Jain et al., 2014). Membranes are composed of individual membrane lipids (MLs) that contain a hydrophobic core and a hydrophilic head which are linked via glycerol moieties (Goldfine, 1982). Those MLs usually organize to form an amphiphilic bilayer, with the hydrophobic tails oriented towards the interior and the hydrophilic heads oriented towards the aqueous exterior (Albers et al., 2000). The structure of MLs differs greatly between eukaryotes and bacteria on one side, and archaea on the other side. While the hydrophobic tails in eukaryotes and bacteria consist of fatty acids that are linked via ester bonds to *sn*-glycerol-3-phosphate (G3P), archaeal MLs are made up of isoprenoid tails ether-linked to *sn*-glycerol-1-phosphate (G1P) (Figure 13) (Koga et al., 1998; Koga and Morii, 2007; Lombard et al., 2012). This fundamental difference between the domains of life has been referred to as the "lipid divide" (Sojo, 2019).

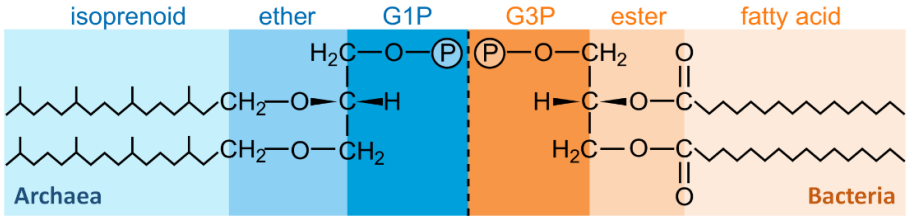


**Figure 13** | Structure of membrane lipids of bacteria and archaea. Archaeal lipids consist of isoprenoid tails connected via ether bonds to *sn*-glycerol-1-phosphate (G1P). In bacterial lipids, fatty acid chains are connected to *sn*-glycerol-3-phosphate (G3P). Modified from Sojo et al. (2014)

While the apolar core MLs differ strongly, phosphate-based (phospholipids) or sugar-based (glycolipids) (Yang et al., 2006; Yoshinaga et al., 2016) headgroups are universally shared across the domains of life (Koga and Morii, 2007). Specific variations exist in some microbial groups, often as a consequences of external factors, e.g. nutrient limitation. For instance, Cyanobacteria replace phospholipids with sulfoglycolipids upon phosphate limitation (Van Mooy et al., 2006). Some phosphorus-free headgroups, e.g. based on the amino acid ornithine or the triterpene hopane, are exclusively found in bacteria (Vences-Guzmán et al., 2012; Sohlenkamp and Geiger, 2016; Belin et al., 2018).

The different structure of archaeal MLs compared to bacterial and eukaryotic MLs has often been discussed as the main reason that enables archaea to occupy more extreme environments than bacteria (Van de Vossenberg et al., 1998; Albers et al., 2000; Valentine, 2007). Archaea additionally can fuse the carbon tails of their diether lipids to form membrane-spanning tetraether lipids, and thereby create a membrane monolayer (Van de Vossenberg et al., 1998; Albers et al., 2000). Liposomes consisting of archaeal tetraether MLs exhibit much lower proton permeability compared to liposomes of bacterial diester MLs, which was attributed to the bulky isoprenoid cores of archaeal MLs (Yamauchi et al., 1993; Elferink et al., 1994). This gives archaea an advantage in achieving high energy conservation, which is a major requirement for life in the hyperthermophilic range (Albers et al., 2000; Valentine, 2007). Valentine (2007) proposed on this basis that archaea specialized to live in low-energy environments, which comes with a decreased capacity to adapt their metabolism to environmental changes and maximize the usage of fluctuating resources, which is more attributed to bacteria. In recent years however, the boundaries between the lipid divide have become smaller, and archaea-type lipids have been reported in bacteria (Lorenzen et al., 2014; Sahonero-Canavesi et al., 2022).

Both archaea and bacteria modify the hydrophobic tails of their MLs in numerous ways under different environmental conditions. Temperature, pH, and pressure are important factors eliciting such modifications (Siliakus et al., 2017; Sollich et al., 2017). Oftentimes, specific modifications are connected to specific microbial groups (White et al., 1979; Sturt et al., 2004; Rossel et al., 2008). Because the hydrophobic cores of MLs can stay intact in sediments for a long time after cell decay, these modifications can serve as indicators of past microbial activities (Kuypers et al., 2001; Brocks et al., 2005; Summons et al., 2022). This is addressed in **chapter 4**.

## 1.13 Hypotheses and aims of this thesis

The GB in the Gulf of California has shown itself in the past as a natural laboratory for the study of anaerobic petroleum HC degradation, especially at high temperatures. More and more thermophilic microorganisms with sophisticated metabolic capacities have been isolated from its petroleum-rich sediments, such as the Acr-utilizing thermophilic gaseous alkane-oxidizing archaea *Ca.* E. thermophilum and *Ca.* Syntrophoarchaeum spp. (Laso-Pérez et al., 2016; Hahn et al., 2020). Recently, thermophilic ANME-1c thriving at 70 °C pushed the upper temperature limit of alkane oxidation (Benito Merino et al., 2022). Thus, I suspected that yet uncultured microorganisms from the GB are capable of degrading more HCs than previously known at higher temperatures.

The first two projects were therefore cultivation-based studies, which aimed to reveal the taxonomy and functioning of novel anaerobic microorganisms capable of degrading the most stable HCs, alkanes and UAHs, in combination with sulfate reduction, at temperatures approaching the predicted sterilization temperature of subsurface petroleum reservoirs of 80-90 °C (Wilhelms et al., 2001). First, I aimed to enrich novel archaea capable of oxidizing petroleum-range alkanes via Acrs. To minimize bacterial alkane oxidizers, which were previously more abundant at lower temperatures in GB sediment (McKay et al., 2016; Ramírez et al., 2021), I chose a comparatively high incubation temperature of 70 °C. This work yielded the first manuscript of the thesis (**chapter 2**). Aside from alkanes, GB sediments are also rich in AHs, and thermophilic anaerobic UAH degraders were scarce. Thus, in my second project, I aimed to enrich such microorganisms from GB sediment at temperatures of up to 70 °C. The result of this project is detailed in **chapter 3**. The third project was a collaboration with the Organic Geochemistry group, particularly Dr. Florence Schubotz, at the Center for Marine Environmental Sciences (MARUM) in Bremen. Here, we studied the core MLs of established anaerobic methane and non-methane alkane-oxidizing cultures. This study aimed to potentially detect MLs previously only known from environmental samples in cultures, and examine the suitability of such lipids as biosignatures for present and past activity of alkane-oxidizing consortia in marine sediments. This final study is summarized in **chapter 4**.

## 1.14 Overview over manuscripts included in this thesis

### Chapter 2: *Candidatus* Alkanophaga archaea from Guaymas Basin hydrothermal vent sediment oxidize petroleum alkanes

Hanna Zehnle, Rafael Laso-Pérez, Julius Lipp, Dietmar Riedel, David Benito Merino, Andreas Teske, and Gunter Wegener

Manuscript published in *Nature Microbiology* **8**, 1199–1212 (01.06.2023), doi: 10.1038/s41564-023-01400-3

In this study I obtained eight enrichment cultures degrading gasoline- and diesel-range alkanes between pentane ($C_5$) and tetradecane ($C_{14}$) at 70 °C. The cultures were analyzed via metagenomics, metatranscriptomics, metabolomics, physiological tests, and *in situ* hybridization. Analyses revealed that two archaea of the novel genus *Ca.* Alkanophaga mediate the anaerobic oxidation of the liquid alkanes via Acrs. *Ca.* Alkanophaga form syntrophic consortia with a novel species of sulfate-reducing *Thermodesulfobacterium*

**Contributions:** The study was designed by G.W. and H.Z., A.T. was the chief scientist of the cruise. H.Z. did 'omics analyses supported by R.L.-P. and D.B.M. D.B.M. and H.Z. designed specific CARD-FISH probes. J.L. was in charge of mass spectrometry and its analyses, D.R. carried out transmission electron microscopy of the culture samples. H.Z. did cultivations and molecular and laboratory experiments, and wrote the manuscript with contributions from all coauthors.

### Chapter 3: Anaerobic oxidation of benzene and naphthalene by thermophilic microorganisms from the Guaymas Basin

Hanna Zehnle, Carolin Otersen, David Benito Merino, and Gunter Wegener

Manuscript submitted to *Frontiers in Microbiology* (18.08.2023)

In this study, I established anaerobic benzene- and naphthalene-oxidizing cultures at 50 °C and 70 °C. I studied the microorganisms in the cultures and their capacity for UAH/AH oxidation based on short-read metagenomes. In two of the cultures, novel bacteria of the Desulfatiglandales were highly abundant. These bacteria encoded genes for UAH degradation via methylation and carboxylation and could combine UAH oxidation with sulfate reduction. In addition, I analyzed publicly available genomes of the prevalent bacterial groups, searching for UAH/AH degradation genes. Results indicated that genes for general anaerobic AH metabolism are relatively widespread, but the complete naphthalene degradation pathway is scarce in the examined groups. This study yielded a second manuscript, which was submitted to *Frontiers in Microbiology*.

**Contributions:** H.Z. designed the study, G.Z. was involved in recovering the sediment for cultivation. D.B.M., C.O. and H.Z. performed bioinformatical analyses. H.Z. wrote the manuscript.

### Chapter 4: The core lipidome of anaerobic alkane-oxidizing archaea and their sulfate-reducing partner bacteria

Hanna Zehnle, Christopher Klaembt, Qing-Zeng Zhu, Gunter Wegener, and Florence Schubotz

Manuscript in preparation

In this project, the core MLs of anaerobic cultures previously established in our working group were analyzed. In these cultures, archaea oxidize alkanes from methane ($C_1$) to hexadecane ($C_{16}$) via Mcrs/Acrs, coupled to sulfate reduction in partner SRB. Because the cultures grow at a wide range of temperatures, between 20 °C and 70 °C, they are well suited to study the factor of temperature in ML formation and modification. Statistical analyses revealed that temperature, substrate, and the archaeon and bacterium prevalent in the culture had a strong effect on ML composition. Further, the study identified several lipid groups in the cultures, including methylated GMGTs and branched GDGTs, of which the biological source was previously unclear, but which are frequently found in anoxic marine sediments.

**Contributions:** G.W., F.S., and H.Z. designed the study. H.Z. did bioinformatical analyses. C.K., Q.-Z.Z., and H.Z. extracted total lipids. F.S. performed mass spectrometry and analyzed the raw mass spectrometry data. F.S. and H.Z. performed further analyses. H.Z. wrote the manuscript with contributions from all coauthors.

### Additional contribution: Deep-branching ANME-1c archaea grow at the upper temperature limit of anaerobic oxidation of methane

David Benito Merino, Hanna Zehnle, Andreas Teske, and Gunter Wegener

Published in *Frontiers in Microbiology* **13** (23.09.2022), doi: 10.3389/fmicb.2022.988871

**Contributions:** D.B.M and G.W. designed the study. G.W. did sampling on board. A.T. planned and organized the cruise. D.B.M. and H.Z. did cultivation experiments. D.B.M. performed laboratory experiments and ‘omics analyses and wrote the manuscript with contributions from all coauthors.

*Please find the combined bibliography for this section and for the discussion after chapter 5*

## Manuscript 1

# *Candidatus* Alkanophaga archaea from Guaymas Basin hydrothermal vent sediment oxidize petroleum alkanes

Hanna Zehnle, Rafael Laso-Pérez, Julius Lipp, Dietmar Riedel, David Benito Merino, Andreas Teske, Gunter Wegener

Published in

*Nature Microbiology*

Received: 23 September 2022

Accepted: 28 April 2023

Published online: 01 June 2023

doi: 10.1038/s41564-023-01400-3

# *Candidatus* Alkanophaga archaea from Guaymas Basin hydrothermal vent sediment oxidize petroleum alkanes

Hanna Zehnle[1,2,3], Rafael Laso-Pérez[2,4,7], Julius Lipp[2], Dietmar Riedel[5], David Benito Merino[1,3], Andreas Teske[6], and Gunter Wegener[1,2]

1. Max Planck Institute for Marine Microbiology, Bremen, Germany
2. MARUM, Center for Marine Environmental Sciences, University of Bremen, Bremen, Germany
3. Faculty of Geosciences, University of Bremen, Bremen, Germany
4. Systems Biology Department, Centro Nacional de Biotecnología (CNB-CSIC), Madrid, Spain
5. Max Planck Institute for Multidisciplinary Sciences, Göttingen, Germany
6. Department of Earth, Marine and Environmental Sciences, University of North Carolina at Chapel Hill, Chapel Hill, NC, USA
7. Present address: Biogeochemistry and Microbial Ecology Department, Museo Nacional de Ciencias Naturales (MNCN-CSIC), Madrid, Spain

Correspondence: hzehnle@mpi-bremen.de; gwegener@marum.de

## Abstract

Methanogenic and methanotrophic archaea produce and consume the greenhouse gas methane, respectively, using the reversible enzyme methyl-coenzyme M reductase (Mcr). Recently, Mcr variants that can activate multi-carbon alkanes have been recovered from archaeal enrichment cultures. These enzymes, called alkyl-coenzyme M reductase (Acrs), are widespread in the environment but remain poorly understood. Here, we produced anoxic cultures degrading mid-chain petroleum *n*-alkanes between pentane ($C_5$) and tetradecane ($C_{14}$) at 70 °C using oil-rich Guaymas Basin sediments. In these cultures, archaea of the genus *Candidatus* Alkanophaga activate the alkanes with Acrs and completely oxidize the alkyl groups to $CO_2$. *Ca.* Alkanophaga form a deep-branching sister clade to the methanotrophs ANME-1 and are closely related to the short-chain alkane oxidizers *Ca.* Syntrophoarchaeum. Incapable of sulfate reduction, *Ca.* Alkanophaga shuttle electrons released from alkane oxidation to the sulfate-reducing *Ca.* Thermodesulfobacterium syntrophicum. These syntrophic consortia are potential key players in petroleum degradation in heated oil reservoirs.

## Introduction

In deep seafloor sediments, pressure and heat transform buried organic matter into complex hydrocarbon mixtures, forming natural gas and crude oil (Claypool and Kvenvolden, 1983; Simoneit, 1990). *n*-Alkanes (hereafter referred to as "alkanes") constitute a major fraction of these mixtures (Kissin, 1987) and become energy-rich substrates for microorganisms (Watkinson and Morgan, 1990) in habitable anoxic zones. Sulfate-reducing bacteria (SRB) oxidize alkanes ≥ propane ($C_3$ alkane) (Aeckersberg et al., 1991; Kniemeyer et al., 2007) after activation via fumarate addition through alkylsuccinate synthases (Rabus et al., 2001). Archaea possess a different mechanism for anaerobic alkane degradation based on reversal of the methanogenesis pathway. This mechanism was first revealed in anaerobic methanotrophic archaea (ANME) (Hinrichs et al., 1999; Boetius et al., 2000), which activate methane to methyl-coenzyme M (methyl-CoM) via the key enzyme of methanogenesis methyl-coenzyme M reductase (Mcr) (Scheller et al., 2010). Recently cultured archaea oxidize non-methane alkanes analogously to ANME, as a first step activating the alkanes to alkyl-CoMs via divergent variants of the Mcr, termed alkyl-CoM reductases (Acrs) (Wang et al., 2021). *Candidatus* Argoarchaeum ethanivorans (Chen et al., 2019), *Ca.* Ethanoperedens thermophilum (Hahn et al., 2020), and *Ca.* Syntrophoarchaeum spp. (Laso-Pérez et al., 2016) oxidize short-chain, gaseous alkanes ($C_2$-$C_4$), while *Ca.* Methanoliparum spp., enriched from oil-rich environments, oxidize long-chain alkanes (≥ $C_{16}$) (Zhou et al., 2022). Like most ANME, the short-chain alkane-oxidizing archaea lack respiratory pathways and shuttle the electrons from alkane oxidation to partner SRB (Holler et al., 2011; Krukenberg et al., 2016; Laso-Pérez et al., 2016; Hahn et al., 2020). In contrast, *Ca.* Methanoliparum encodes a canonical Mcr in addition to the Acr, with which it couples alkane oxidation to methanogenesis in a single cell (Zhou et al., 2022).

Anaerobic archaea capable of petroleum alkane ($C_5$-$C_{15}$) oxidation via Acrs were unknown. These alkanes are the major constituents of gasoline and kerosene (Johansen et al., 1983; Vishnoi et al., 1987), and of high ecological relevance because of their toxicity (Ono et al., 1981; Trac et al., 2018). Lately, many *acr* genes with unknown function have been recovered from environmental metagenomes, especially from hot springs (Hua et al., 2019; Wang et al., 2019; Lynes et al., 2023). We hypothesized that yet uncultured thermophilic archaea could activate petroleum alkanes via Acrs. We aimed to enrich such archaea from heated oil-rich sediment from the hydrothermal vent site Guaymas Basin (Gulf of California, Mexico) (Teske et al., 2016). We obtained eight enrichment cultures thriving at 70 °C, in which alkanes from $C_5$-$C_{14}$ were oxidized in combination with sulfate reduction. Analyses of these cultures via 'omics approaches and physiological tests revealed that a sister clade of ANME-1, *Ca.* Alkanophaga, was oxidizing the alkanes after activation via Acrs coupled to sulfate reduction by a partner *Thermodesulfobacterium*. Such consortia potentially contribute to souring in deeply buried, heated oil reservoirs.

## Methods

All chemicals were of analytical grade and obtained from Sigma Aldrich (Hamburg, Germany), if not otherwise stated. All incubations were done under gentle shaking (40 rpm) in the dark.

### *Cultivation of anaerobic thermophilic alkane degraders*

The push core used for anoxic cultivations was collected with submersible *Alvin* during *RV Atlantis* cruise AT42-05 in the Guaymas Basin (Gulf of California, Mexico) (dive 4991, core 15, 27° 00′ 41.1″ N, 111° 24′ 16.3″ W, 2,013 m water depth, November 17, 2018). On shipboard, the push core was transferred to a sealed glass bottle, purged with argon, and stored at 4 °C. In the home laboratory, an anoxic sediment slurry was prepared with synthetic sulfate-reducer medium (SRM) (Laso-Pérez et al., 2018), using a ratio of 10% sediment and 90% SRM (v:v), and distributed in 100 ml portions into culture bottles. Cultures were supplemented with 200 µl liquid alkane ($C_5$-$C_{15}$) in duplicates. For the $C_5$-$C_{10}$ alkanes, 4 ml 2,2,4,4,6,8,8-heptamethylnonane (HMN) were added to mitigate potential toxic effects of the substrate (Rabus and Widdel, 1995). A substrate-free culture served as a negative control. Headspaces were filled with $N_2$:$CO_2$ (90:10; 1 atm overpressure) and incubated at 70 °C.

Sulfide production was measured every 2-4 weeks using a copper sulfate assay (Cord-Ruwisch, 1985). Once sulfide concentrations reached 12-15 mM, cultures were diluted 1:3 with SRM and supplied with fresh substrate. Activity doubling times were determined from the development of sulfide concentrations during the first two dilutions. Sulfide concentrations over time were displayed using a logarithmic (base 2) y axis. An exponential trend line with the formula $y = n * e^{mx}$ was generated. Per definition, the doubling time equals $\frac{ln(2)}{m}$.

### *Quantitative substrate turnover experiment*

Triplicate 100 ml dilutions with 20 ml headspace were prepared from $C_6$- and $C_{14}$-oxidizing cultures, supplied with substrate and incubated at 70 °C, complemented by a substrate-free negative control. Sulfate and dissolved inorganic carbon (DIC) concentrations were measured from weekly subsamples until the cultures had reached sulfide concentrations of ≥15 mM. Samples were sterile filtered using a GTTP polycarbonate filter (0.2 µM pore size; Millipore, Darmstadt, Germany). For DIC measurements, 1 ml filtrate was transferred into synthetic-air purged 12 ml Exetainer vials (Labco, Lampeter, Wales, UK) filled with 100 µl phosphoric acid (45%). After 10 hours of equilibration, headspace DIC was measured by isotope ratio infrared spectroscopy (Thermo Fisher Scientific, Delta Ray IRIS with URI connect and Cetac ASX-7100 Autosampler) with standards of known concentration. To determine sulfate concentrations, 1 ml of the filtrate was fixed in 0.5 ml 100 mM zinc acetate. The sample was centrifuged and the clear supernatant was diluted 1:50 in deionized water. Sulfate was measured by ion chromatography (930 compact IC, Metrohm) against standards with known concentrations.

### *DNA extraction and short-read sequencing*

DNA was extracted from pellets of 25 ml culture samples collected after the third dilution using a modified SDS-based extraction method as previously described (Natarajan et al., 2016). Total DNA yield per sample, determined by fluorometric DNA concentration measurement, ranged from 0.9 µg to 3.6 µg. Samples were sequenced at the Max-Planck-Genome-Centre (Cologne, Germany). $C_6$-$C_{14}$ culture samples were sequenced as 2×250 paired-end reads on the Illumina HiSeq2500 sequencing platform. The $C_5$ culture sample was sequenced later because of slower growth together with a sample of the sediment slurry before incubation, by which time the sequencing facility had changed their settings to 2×150 bp paired-end reads on an Illumina HiSeq3000 platform. Between 4,140,953 and 4,234,808 raw reads were obtained per culture sample. From the original slurry, 3,130,329 reads were gained.

### *Short-read DNA data analysis*

Reads from short-read metagenome-sequencing were quality-trimmed using BBDuk (included in BBMap version 38.79; https://sourceforge.net/projects/bbmap/; minimum quality value: 20, minimum read length: 50). Reads of the $C_6$-$C_{14}$ samples were coassembled using SPAdes (version 3.14.0; https://github.com/ablab/spades) (Bankevich et al., 2012), running BayesHammer error correction and *k*-mer increments (21, 33, 55, 77, 99, and 121) with default settings. The output scaffolds were reformatted using anvi'o (version 7; https://github.com/merenlab/anvio/releases/) (Eren et al., 2015), simplifying names and removing contigs shorter than 3,000 bps. Trimmed reads were mapped back to the reformatted scaffolds using Bowtie2 (version 2.3.2; http://bowtie-bio.sourceforge.net/bowtie2/index.shtml) (Langmead and Salzberg, 2012) in the local read alignment setting. Sequence alignment map files were converted to binary alignment map (BAM) files with SAMtools (version 1.5; http://samtools.sourceforge.net/) (Danecek et al., 2021) and indexed with anvi'o. A contigs database was created from the reformatted scaffolds and profile databases were generated for each sample with anvi'o. Profile databases were merged, enforcing hierarchical clustering. Hidden Markov model (HMM) searches were run via anvi'o on the contigs database to detect genes encoding for Mcrs/Acrs, Wood-Ljungdahl pathway, and dissimilatory sulfate reduction (DSR). Taxonomies for open reading frames were imported into the contigs database using the Centrifuge classifier (version 1.0.2-beta; https://ccb.jhu.edu/software/centrifuge/) (Kim et al., 2016). The contigs database was inspected in the anvi'o interactive interface, which clusters the contigs hierarchically based on sequence composition and differential coverage, thereby indicating their relatedness to each other (Eren et al., 2015). Binning was performed manually in the interface by clicking branches of the dendrogram in the center of the interface, and using the GC content, mean coverage in the samples, gene taxonomy, and real-time statistics on completion and redundancy based on single-copy core genes as guides. The dendrogram branches were followed systematically in a counterclockwise direction to obtain the maximum number of bins. Bin quality was assessed again with CheckM (version 1.1.3; https://ecogenomics.github.io/CheckM/) (Parks et al., 2015) and only bins with completeness

>50% and redundancy <10% were kept. Taxonomies were assigned to these metagenome-assembles genomes (MAGs) using GTDB-Tk (version 1.5.1; https://github.com/Ecogenomics/GTDBTk) (Chaumeil et al., 2020). All manually generated MAGs were refined with anvi'o to minimize contamination. We identified MAGs 1 and 4 as the likely alkane oxidizers and MAG 24 as the likely sulfate reducer based on their mean coverages and HMM hits. To increase the completeness of these three MAGs, an iterative reassembly loop (https://github.com/zehanna/MCA70_analysis/targeted_reassembly_loop.sh) was performed. Therein, the trimmed reads were repeatedly mapped to the refined MAG using BBMap with a minimum alignment identity of 97%. Mapped reads were then assembled using SPAdes. The assembly was quality-checked with CheckM and used as a new reference file to map the trimmed reads to. After performing 25 iterations of this loop, the assembly with the highest quality (i.e. highest completeness, lowest contamination, and lowest strain heterogeneity) was selected for further analysis. Final MAGs were annotated with Prokka (version 1.14.6; https://github.com/tseemann/prokka) (Seemann, 2014) and the anvi'o-integrated databases NCBI clusters of orthologous genes (COGs) (Tatusov et al., 1997), Kyoto Encyclopedia of Genes and Genomes (KEGG) (Kanehisa et al., 2017), Protein Families (Pfams) (Mistry et al., 2021), and KEGG orthologues HMMs (KOfams) (Aramaki et al., 2020). A bash script (https://github.com/zehanna/MCA70_analysis/CxxCH_scan.sh) was run to search for the heme-binding CxxCH amino acid motif (Bertini et al., 2006) in the translated gene sequences of the three MAGs. Selected translated gene sequences were exported for gene calls from the contigs database with anvi'o and compared via the BLASTp (Altschul et al., 1990) web interface (http://www.ncbi.nlm.nih.gov/blast).

Relative abundances of the MAGs were calculated by mapping the trimmed reads to the manually curated and refined MAGs with CoverM (version 0.6.1; https://github.com/wwood/CoverM) in genome mode including the dereplication flag using the default aligner Minimap2 (version 2.21; https://docs.csc.fi/apps/minimap2/) in short-read mode, discarding unmapped reads. Final relative abundance of each MAG is percentage of the MAG in the mapped fraction of each sample. Average nucleotide identities (ANI) between MAGs were calculated with FastANI (version 1.32; https://github.com/ParBLiSS/FastANI).

Because of later sequencing, the original slurry and $C_5$ samples were treated separately from the previously sequenced samples, and assembled individually. We could not obtain quality MAGs for the original slurry sample, therefore we estimated the phylogenetic composition based on reconstructed small subunit ribosomal RNAs (SSU rRNAs) mapped against the SILVA SSU reference database (version 138.1) (Quast et al., 2013) with phyloFlash (version 3.4.1; https://github.com/HRGV/phyloFlash) (Gruber-Vodicka et al., 2022). For the $C_5$ sample, the same procedure was followed as for the previously sequenced culture samples. The identity (ANI ≥ 95%) (Jain et al., 2018) of the *Ca.* Alkanophaga volatiphilum and *Ca.* Thermodesulfobacterium syntrophicum MAGs from the $C_5$ sample, MAG 4_1 and MAG 24_1 respectively, to the previously reconstructed ones was confirmed via FastANI.

To estimate relative abundances of *Ca.* Alkanophaga and *Ca.* T. syntrophicum MAGs in the original slurry, the trimmed reads of the original slurry were mapped to the MAGs with CoverM.

### *Construction of phylogenomic trees for archaea and bacteria*

The archaeal tree was constructed using 98 publicly available Halobacteriota and Thermoproteota genomes (Supplementary Table 10) from NCBI plus the *Ca.* Alkanophaga MAGs from this study. For the bacterial tree, 121 publicly available Desulfobacterota and Bipolaricaulota genomes (Supplementary Table 10) and the *Thermodesulfobacterium* MAG from this study were included. Trees are based on the concatenated alignment of 76 single-copy core genes (SCG) for archaea and 71 SCGs for bacteria, respectively. Alignments were generated with anvi'o, which uses the multiple sequence alignment tool MUSCLE (version 5.1; https://github.com/rcedgar/muscle) (Edgar, 2004). Trees were calculated with RAxML (Randomized Accelerated Maximum Likelihood) (version 8.2.12; https://cme.h-its.org/exelixis/web/software/raxml/) (Stamatakis, 2014) using the PROTGAMMAAUTO model and autoMRE option, which required 50 iterations to reach a convergent tree for both alignments. Trees were visualized with the Interactive Tree of Life online tool (https://itol.embl.de/) (Letunic and Bork, 2011). To resolve taxonomic levels, the *Ca.* Alkanophaga MAGs were compared to the ANME-1 and *Ca.* Syntrophoarchaeales MAGs included in the tree by calculating average amino acid identities (AAIs) using the aai_wf feature of the CompareM software (version 0.1.2; https://github.com/dparks1134/CompareM) with default settings.

### In situ *hybridization and microscopy*

Culture samples were fixed in 1% formaldehyde for 1 h at room temperature (RT), washed twice in 1× PBS, and stored in 1× PBS-ethanol (1:1, v:v) at -20 °C. Aliquots were filtered onto GTTP polycarbonate filter (0.2 µM pore size; Millipore, Darmstadt, Germany). Filters were embedded in 0.2% agarose. For permeabilization, three consecutive treatments were performed: (1) lysozyme solution (0.05 M EDTA (pH 8.0), 0.1 M Tris-HCl (pH 7.5), and 10 mg $ml^{-1}$ lysozyme in MilliQ-grade deionized water) for 1 h at 37 °C (2) proteinase K solution (0.05 M EDTA (pH 8.0), 0.1 M Tris-HCl (pH 7.5), and 7.5 µg $ml^{-1}$ proteinase K in MilliQ) for 10 min at RT (3) 0.1 M HCl solution for 5 min at RT. Endogenous peroxidases were inactivated using 0.15% $H_2O_2$ in methanol for 30 min at RT.

A specific probe was designed to exclusively target the *Ca.* Alkanophagales clade. Therefore, the *Ca*. Alkanophaga 16S rRNA gene sequences were added to the SILVA SSU reference database (version 138.1) using the ARB software (version 7.1; http://www.arb-home.de/home.html) (Ludwig et al., 2004). A subtree containing all ANME-1 16S rRNA gene sequences, plus the two sequences from *Ca*. Alkanophaga, was calculated using RAxML (version 8; https://cme.h-its.org/exelixis/web/software/raxml/) with 100 bootstrap replicates, a 50% similarity filter, the GTRGAMMA model, and *Methanocella* as outgroup. The probe was

generated using the probe design feature with these parameters: length of probe: 19 nucleotides, temperature: 50-100 °C, GC content: 50-100%, *E. coli* position: any, max. nongroup hits: 5, min. group hits: 100%. Criteria for candidate probes were: GC content lower than 60%, lowest possible number of matches to non-group species with decreasing temperature, at least one mismatch to non-group species. We ordered a probe that fit these criteria (Aph183) with the sequence 5'-GCATTCCAGCACTCCATGG-3' from Biomers (Ulm, Germany). For bacteria, the general probe combination EUBI-III (I: 5-GCTGCCTCCCGTAGGAGT-3; II: 5-GCAGCCACCCGTAGGTGT-3; III: 5-GCTGCCACCCGTAGGTGT-3) (Daims et al., 1999) was applied. Probe working solution (50 ng $\mu l^{-1}$) was diluted 1:300 in hybridization buffer containing 30% formamide for Aph183 and 35% formamide for EUBI-III. Probes were hybridized at 46 °C for 3-4 hours. Signals were amplified with tyramides labelled with Alexa Fluor 488 for bacteria and Alexa Fluor 594 for *Ca.* Alkanophaga (Thermo Fisher Scientific, Bremen, Germany) for 45 min at 46 °C. For double hybridizations, peroxidases from the first hybridization were inactivated using 0.30% $H_2O_2$ in methanol for 30 min at RT before the second hybridization and amplification. Filters were analyzed via epifluorescence microscopy (Axiophot II imaging; Zeiss, Oberkochen, Germany). Images were captured with the AxioCamMR camera and the AxioVision software included in the microscope. Images were processed using ImageJ (version 1.49, https://imagej.nih.gov/ij/), where the color of Alexa488 was changed to cyan to improve accessibility.

### *Phylogenetic analysis of proteins involved in alkane oxidation in* Ca. *Alkanophaga*

For the *mcrA* tree, the six full-length *mcrA* sequences of *Ca.* Alkanophaga were aligned with 347 publicly available *mcrA* sequences. For the *mer* and the *metF* trees, *Ca.* Alkanophaga sequences were added to publicly available alignments by Chadwick et al. (2022) (*mer*: Fig04B; *metF*: Fig05C of Supplement S1). Sequences were aligned with MAFFT (Multiple Alignment using Fast Fourier Transform) (version 7.475; https://mafft.cbrc.jp/alignment/software/) (Katoh et al., 2009). Alignments were trimmed with SeaView (version 5; http://doua.prabi.fr/software/seaview) (Gouy et al., 2021). For the *mcrA* tree, sequences shorter than 450 amino acids were removed after trimming, after which 337 sequences remained (Supplementary Table 10). Trees were calculated with RAxML (version 8.2.4) using the PROTGAMMAAUTO model, which assigned LG with empirical base frequencies as amino acid model, and the autoMRE option for bootstraps, which required 300, 550, and 400 iterations to reach a consensus tree for the *mcrA*, *mer*, and *metF* alignments, respectively. Trees were visualized with the Interactive Tree of Life online tool (https://itol.embl.de/) (Letunic and Bork, 2011).

### *RNA extraction and short-read sequencing*

For total RNA extraction, 10 ml of culture material collected after the third dilution at the exponential growth stage were filtered through an RNAse-free cellulose nitrate filter (pore size 0.45 µm; Sartorius, Göttingen, Germany). Immediately after filtration, filters were incubated

with 5 ml RNAlater for 30 min. RNA was extracted from filters using the Quick-RNA miniprep kit (Zymo Research, Irvine, CA, USA). DNA was digested without RNase inhibitor. No rRNA depletion step was performed. Between 0.3 and 1.3 µg of total RNA were obtained per sample as determined by fluorometric RNA concentration measurement. Samples were sequenced as 2×250 ($C_5$: 2x150) paired-end reads at the Max-Planck-Genome-Centre (Cologne, Germany) on the Illumina HiSeq2500 ($C_5$: Illumina HiSeq3000) sequencing platform. Between 4,043,349 and 4,785,231 raw reads were obtained per sample.

### *Short-read RNA data analysis*

Reads from metatranscriptome sequencing were quality-trimmed using BBDuk (included in BBMap version 38.79). Trimmed reads were mapped to the concatenated *Ca.* Alkanophaga MAGs, to minimize unspecific mapping because of the high similarity of the two MAGs, and to the *Ca.* Thermodesulfobacterium syntrophicum MAG using BBMap (version 38.87) with minimal alignment identity of 98%. Mapped reads were counted with featureCounts (version 1.4.6-p5; http://subread.sourceforge.net/) (Liao et al., 2014) with minimum required number of overlapping bases and minimum mapping quality score of 10, counting fragments instead of reads.

Before normalization, rRNA reads were excluded. Fragments were first normalized to gene length, yielding fragments per kilobase (FPK).

$$\mathrm{FPK}_i = \frac{C_i}{L_i}$$

The centered-log ratio (CLR) was calculated as the base-10 logarithm of read count $C_i$ of gene $i$ normalized by gene length $L_i$ in kilobases and divided by the geometric mean of all read counts $C_1$ - $C_n$ normalized by their respective gene length $L_1$ - $L_n$.

$$CLR_i = log\left(\frac{\frac{C_i + 0.5}{L_i}}{\sqrt[n]{\frac{(C_1 + 0.5)}{L_1} \times \frac{(C_2 + 0.5)}{L_2} \times \ldots \times \frac{(C_n + 0.5)}{L_n}}}\right)$$

### *Test of a selective Mcr inhibitor on culture activity*

Duplicates of $C_6$- and $C_{14}$-oxidizing culture were supplied with substrate and 5 mM (final concentration) 2-bromoethanesulfonate (BES). A control culture was supplied with substrate but not with BES. Cultures were incubated at 70 °C and sulfide concentrations were measured until the control cultures had reached >15 mM sulfide.

### *Metabolite extraction*

Metabolite samples were collected at sulfide levels of 10-14 mM. An 80 ml culture sample of each substrate was pelleted via centrifugation (15 min, 3,100 × g, 4 °C). Supernatants were removed, pellets were resuspended in 1 ml of an acetonitrile:methanol:water (2:2:1, v:v:v)

and transferred to bead-beating tubes. Samples were agitated for 15 min on a rotor with vortex adapter at maximum speed. Samples were centrifuged for 20 min at 10,000 × g at 4 °C. Clear supernatants were stored at 4 °C.

### *Synthesis of authentic alkyl-CoM standards*

0.1 g of coenzyme M (sodium 2-mercaptoethanesulfonate) were dissolved in 2 ml 25% (v:v) ammonium hydroxide solution and twice the molar amount of bromoalkane was added. 2- And 3-bromohexane were acquired from Tokyo Chemical Industry (Tokyo, Japan), and 2-bromotetradecane was acquired from Alfa Aesar (Kandel, Germany). Vials were incubated for 6 hours at RT under gentle shaking on a rotor with vortex adapter. 1 ml of the clear upper phase was collected and stored at 4 °C.

### *Mass spectrometry of culture extracts and standards*

Culture extracts and standards were analyzed using high-resolution accurate-mass mass spectrometry on a Bruker maXis plus quadrupole time-of-flight (QTOF) mass spectrometer (Bruker Daltonics, Bremen, Germany) connected to a Thermo Dionex Ultimate 3000RS UHPLC system (Thermo Fisher Scientific, Bremen, Germany) via an electrospray ionization (ESI) ion source. Sample aliquots were evaporated under a nitrogen stream and re-dissolved in a methanol:water (1:1, v:v) mixture before injection. A 10 µl aliquot of the metabolites was injected and separated on an Acclaim C30 reversed phase column (Thermo Fisher Scientific; 3.0x250 mm, 3 µm particle size) set to 40 °C using a flow rate of 0.3 ml min-1 and the following gradient of eluent A (acetonitrile:water:formic acid, 5:95:0.1, v:v:v) and eluent B (2-propanol:acetonitrile:formic acid, 90:10:0.1, v:v:v): 0% B at 0 min, then ramp to 100% B at 30 min, hold at 100% B until 50 min, followed by re-equilibration at 0% B from 51 min to the end of the analysis at 60 min to prepare the column for the next analysis. The ESI source was set to the following parameters: capillary voltage 4500 V, end plate offset 500 V, nebulizer pressure 0.8 bar, dry gas flow 4 l min-1, dry gas heater 200 °C. The QTOF was set to acquire full scan spectra in a mass range of *m/z* 50-600 in negative ionization mode. The $C_{14}$ culture extract was additionally analyzed in tandem mass spectrometry mode and mass spectra of the fragmentation products of *m/z* 337.1877 isolated in a window of 3 Da and fragmented with 35 eV were acquired. Every analysis was mass-calibrated to reach mass accuracy of 1-3 ppm by loop injection of a calibration solution containing sodium formate cluster ions at the end of the analysis during the equilibration phase and using the high-precision calibration (HPC) algorithm. Data was processed using the Compass DataAnalysis software package version 5.0 (Bruker Daltonics, Bremen, Germany).

### *Substrate range tests*

Cultures originally grown with $C_6$ and $C_{14}$ were diluted 1:10 in fresh SRM. Dilutions were supplemented with alkanes between $C_5$ and $C_{14}$ for which growth had not been confirmed yet, and with shorter ($C_3$ and $C_4$) and longer ($C_{16}$-$C_{20}$) alkanes (Table 1).

**Table 1 |** Overview over substrate range test with *Candidatus* Alkanophaga cultures.

| Organism | Originally consumed $C_x$-*n*-alkanes | Culture used as inoculum | Tested $C_x$-*n*-alkanes |
|---|---|---|---|
| ***Candidatus* Alkanophaga volatiphilum** | $C_5$, $C_6$, $C_7$ | $C_6$ | $C_3$, $C_4$, $C_8$, $C_9$, $C_{10}$, $C_{11}$, $C_{12}$, $C_{13}$, $C_{14}$, $C_{15}$, $C_{16}$, $C_{18}$, $C_{20}$ |
| ***Candidatus* Alkanophaga liquidiphilum** | $C_8$, $C_9$, $C_{10}$, $C_{12}$, $C_{14}$ | $C_{14}$ | $C_3$, $C_4$, $C_{11}$, $C_{13}$, $C_{15}$, $C_{16}$, $C_{18}$, $C_{20}$ |

A negative (inoculated culture without substrate) and a positive (inoculated culture supplied with substrate with which the culture was originally grown) control were also set up. Cultures were incubated at 70 °C and activity was tracked via sulfide measurements. Once sulfide concentrations reached >10 mM, cultures were diluted 1:3 with SRM. The procedure was repeated and incubations that showed sustained activity over two dilutions were considered successful.

### *Hydrogen production measurements*

$C_6$ and $C_{14}$ cultures were divided into two 20 ml aliquots in 156 ml serum bottles. One aliquot was left untreated, the other one was treated with 10 mM (final concentration) sodium molybdate. Hydrogen was measured by injecting 1 ml of headspace sample into a Peak Performer 1 gas chromatograph (Peak Laboratories, Palo Alto, CA, USA). Measurements were taken in one hour intervals up to 8 hours after start of the experiment. A final measurement round was conducted from 24 hours to 30 hours in two hour intervals.

### *Test of the effect of addition of hydrogen and formate on culture activity*

Two replicates of $C_6$- and $C_{14}$-oxidizing cultures were supplied with substrate and with 10% $H_2$ in the headspace or 10 mM (final concentration) sodium formate in the medium. A control culture was supplied only with substrate. Cultures were incubated at 70 °C and sulfide concentrations were measured until the control cultures had reached ≥15 mM sulfide.

### *Transmission electron microscopy*

100 ml of $C_6$ and $C_{14}$ culture were harvested at 1,000 × g using a Stat Spin Microprep 2 table top centrifuge. Cells were transferred to aluminium platelets of 150 µm depth containing 1-hexadecene (Studer et al., 1989). Platelets were frozen using a Leica EM HPM100 high pressure freezer (Leica Mikrosysteme Vertrieb GmbH, Wetzlar,Germany). Frozen samples were transferred to an Automatic Freeze Substitution Unit Leica EM AFS2 and substituted at -90 °C in a solution containing anhydrous acetone, 0.1% tannic acid for 24 h and in anhydrous acetone, 2% $OsO_4$, 0.5% anhydrous glutaraldehyde (EMS Electron Microscopical Science, Ft. Washington, USA) for further 8h. After further incubation over 20 h at -20 °C, samples were warmed to +4 °C and washed with anhydrous acetone subsequently. Samples were embedded at RT in Agar 100 (Epon 812 equivalent) at 60 °C for 24 h. Thin sections (80 nm) were

counterstained using Reynolds Lead citrate solution for 7 s and examined using a Talos L120C microscope (Thermo Fisher Scientific Bremen, Germany).

### *Temperature range tests*

Aliquots of $C_6$- and $C_{14}$-oxidizing cultures were diluted 1:6, supplied with substrate, and incubated at 60-90 °C in 5 °C increments. Sulfide production was tracked until the 70 °C cultures had reached >10 mM sulfide.

### *Availability of biological materials*

Official culture collections do not accept syntrophic enrichment cultures, but G.W. will maintain the cultures. Non-profit organizations can obtain samples upon request.

## Data availability

The following databases were used in this study: SILVA SSU reference database (version 138.1; https://www.arb-silva.de/documentation/release-1381/), NCBI COGs (https://www.ncbi.nlm.nih.gov/research/cog-project/), KEGG (https://www.genome.jp/kegg/kegg1.html), Pfam (https://www.ebi.ac.uk/interpro/), KOfam (https://www.genome.jp/tools/kofamkoala/) plus alignments by Chadwick et al. (2022) (*mer*: Fig04B; *metF*: Fig05C of Supplement S1; https://doi.org/10.1371/journal.pbio.3001508.s017).

MAGs of *Ca.* Alkanophaga (*Ca.* A. volatiphilum: BioSample SAMN29995624, genome accession: JAPHEE000000000; *Ca.* A. liquidiphilum: SAMN29995625, JAPHEF000000000) and *Ca.* Thermodesulfobacterium syntrophicum (SAMN29995626, JAPHEG000000000), the raw reads from short-read metagenome and -transcriptome sequencing, the coassembly of the $C_6$-$C_{14}$ samples, and the single assemblies of the original slurry and the $C_5$ samples (SAMN30593190, Sequence Read Archive (SRA) accessions SRR22214785-SRR22214804) are accessible under BioProject PRJNA862876. The mass spectrometry runs for the detection of alkyl-CoMs have been deposited to the EMBL-EBI MetaboLights database (Haug et al., 2020) with the identifier MTBLS7727.

## Code availability

The workflow for metagenome- and transcriptome analysis and the scripts for targeted reassembly and for the search of CxxCH motifs are available under https://github.com/zehanna/MCA70_analysis. For further inquiries about bioinformatical analyses please contact the corresponding authors.

## Results

### *Thermophilic microorganisms thrive on petroleum alkanes*

Anoxic slurries produced from heated sediment collected at the hydrothermal vent complex Cathedral Hill in the Southern Trough of the Guaymas Basin (Extended Data Figure 1a-d) were amended with petroleum alkanes ($C_5$-$C_{14}$) as sole carbon and electron source and sulfate as electron acceptor and incubated at 70 °C. Within three to seven months, the slurries produced > 10 mM sulfide. Sulfide production was accompanied by dissolved inorganic carbon (DIC) production and sustained during dilution steps (Fig. 1, Extended Data Fig. 2), yielding effectively sediment-free cultures after the third dilution. Cultures, except the considerably slower $C_5$ culture, doubled within 13 to 40 days (Supplementary Table 1). According to the general formula

$$C_nH_{2n+2} + (0.75n+0.25)\ SO_4^{2-} \rightarrow nHCO_3^- + (0.75n+0.25)\ HS^- + H_2O + (0.25n-0.25)H^+$$

the ratio of DIC production to sulfate reduction is ~1.25-1.30 in case of complete alkane oxidation. In two representative cultures ($C_6$ and $C_{14}$), this ratio was slightly lower, with 1.21 (±0.22) in the $C_6$ culture, and 1.09 (±0.04) in the $C_{14}$ culture. These values suggest that around 10% ($C_6$) and 35% ($C_{14}$) of the carbon released from alkane oxidation is assimilated into biomass (Supplementary Table 2).

### Ca. *Alkanophagales archaea are abundant in the cultures*

We reconstructed two high-quality archaeal metagenome-assembled genomes (MAGs) from the cultures (Supplementary Table 3): MAG 4, abundant in the $C_5$-$C_7$ cultures, and MAG 1, abundant in the $C_8$-$C_{14}$ cultures (Fig. 2a, Supplementary Table 4). Both MAGs were rare (relative abundances ≤0.1%) in the original slurry (Extended Data Fig. 1e,f). The *in situ* temperatures of the studied sediment (Extended Data Fig. 1d), which captured only the upper sediment layer up to 30 cm depth, likely did not reach the optimal growth temperatures of the two organisms. Both MAGs recruited up to 39% (MAG 4) and 5% (MAG 1) of raw reads in deeper, hotter layers of the Guaymas Basin (McKay et al., 2016) (Supplementary Table 5). MAGs 1 and 4 represent two species within one genus (average nucleotide identity (ANI) 81.5%) and belong to the same genus as the previously published MAG ANME-1 B39_G2 reconstructed from Guaymas Basin sediments (ANIs: MAG 1-ANME-1 B39_G2 98.8% and MAG 4-ANME-1 B39_G2 80.8%) (Dombrowski et al., 2018). The name *Ca.* Alkanophagales was recently proposed for the clade represented by ANME-1 B39_G2 based on its genomic content which hinted at a capacity for multi-carbon alkane metabolism (Dombrowski et al., 2018; Wang et al., 2021). MAGs 1 and 4 form a clade diverging at the root of ANME-1 and next to *Ca.* Syntrophoarchaeum, together forming the class Syntrophoarchaeia (Fig. 2b).

Visualization of the organisms revealed mixed aggregates of archaea of the *Ca.* Alkanophagales clade and bacteria (Fig. 2c-f). These associations resemble those of short-chain alkane-oxidizing cultures (Holler et al., 2011; Laso-Pérez et al., 2016; Hahn et al., 2020), suggesting that archaea oxidize the alkanes and partner SRB perform sulfate reduction.

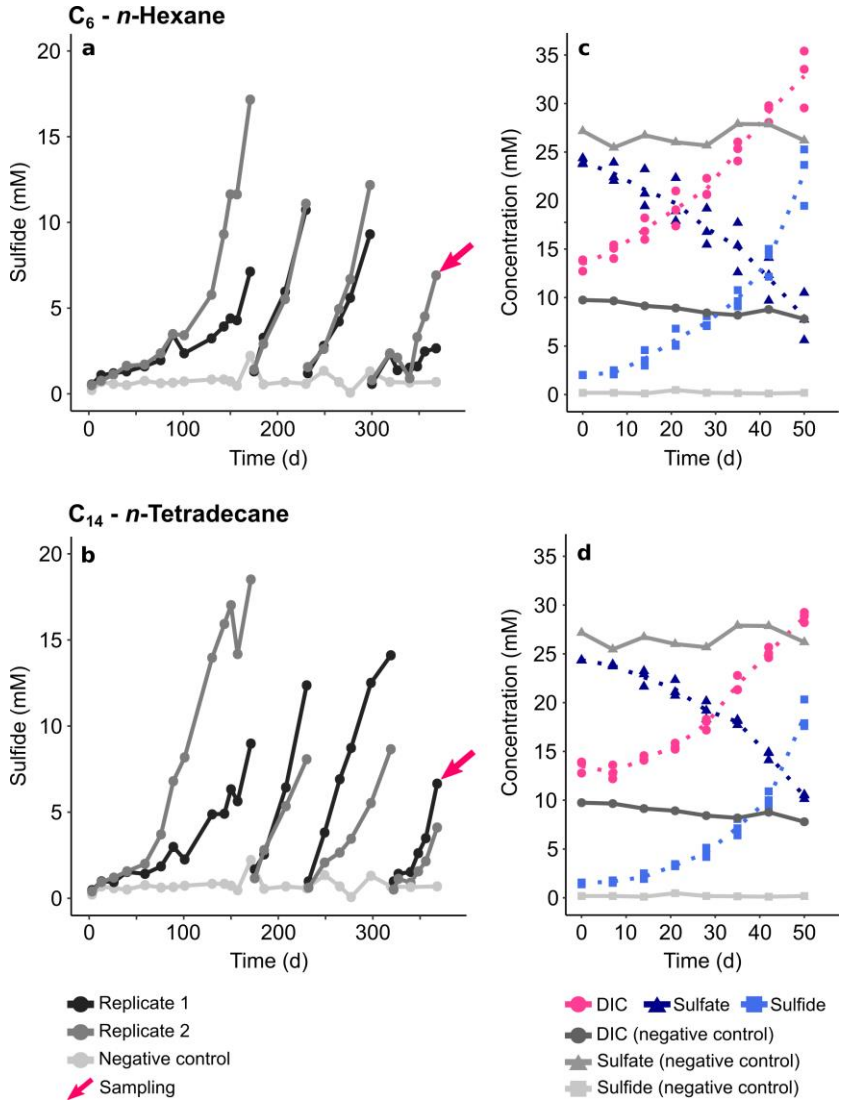


**Figure 1 | Metabolic activity in anaerobic petroleum alkane-oxidizing cultures at 70 °C. a,b,** Formation of sulfide over time in *n*-hexane ($C_6$) (**a**) and *n*-tetradecane ($C_{14}$) (**b**) cultures. Gaps in concentration profiles indicate dilution events. Arrows mark sampling for metagenomic and -transcriptomic analyses. **c,d,** Concentrations of dissolved inorganic carbon (DIC), sulfate, and sulfide in the $C_6$ (**c**) and $C_{14}$ (**d**) cultures, and in abiotic controls. For the cultures, three replicate samples were measured, of which the arithmetic mean is shown as a dotted line.

### *The enriched archaea activate alkanes with Acrs*

Both *Ca.* Alkanophagales MAGs encode three Acrs (*acrABG*) (Extended Data Fig. 3). Currently, only the sister group *Ca.* Syntrophoarchaeum encodes a higher number of Acrs with four copies (Laso-Pérez et al., 2016). The six *acrA* sequences, which code for the catalytic subunit (Hallam et al., 2003), form three clusters of two highly similar sequences, one of each species (≥ 89% identity) in the *acrA* clade (Fig. 3a, Supplementary Table 6) (Laso-Pérez et al., 2016; Chen et al., 2019; Hahn et al., 2020; Zhou et al., 2022). All clusters are highly similar to *acrAs* of *Ca.* Syntrophoarchaeum (Supplementary Table 6).

Both species highly expressed the *acrA* of the third cluster, placing it among the top 19 ($C_8$) to top 4 ($C_5$) expressed genes (Figure 3b, Supplementary Table 7). This cluster is phylogenetically closely related to *acrA*s that presumably activate long-chain alkanes, for

instance in *Ca.* Methanoliparum (Zhou et al., 2022). In both MAGs, this *acrA* is spatially separated from the *acrB* and *acrG* subunits (Extended Data Fig. 3), which has been previously reported for *Ca.* Syntrophoarchaeum (Laso-Pérez et al., 2016).

As in other Acr-dependent alkane-degrading cultures (Laso-Pérez et al., 2016; Hahn et al., 2021), a selective inhibitor of the Mcr/Acr, the CoM analogue 2-bromoethanosulfonate (BES) (Gunsalus et al., 1978), suppressed sulfide production (Extended Data Fig. 4a,b), consistent with an Acr-based activation mechanism. Further, metabolite extracts of all cultures contained peaks pertaining to the masses of the corresponding alkyl-CoMs as indicative activation product (Fig. 3c,d, Extended Data Fig. 5). While alkanes from $C_5$-$C_7$ were activated at the first and second carbon atom in similar ratios (Fig. 3c, Extended Data Fig. 5), we observed a shift to more subterminally activated alkanes with increasing alkane length ($\geq C_9$) (Fig. 3d, Extended Data Fig. 5). The longest alkanes $C_{12}$ and $C_{14}$ seemed to be activated predominantly to ≥3-alkyl-CoM (Fig. 3d, Extended Data Fig. 5). An activation at multiple positions was previously observed in *Ca.* Syntrophoarchaeum (Laso-Pérez et al., 2016). The comparatively high activation rate at the terminal position for shorter alkanes is unexpected, because particularly in short alkanes, C-H bonds are stronger at terminal positions compared to subterminal positions (Lemaire and Wagner, 2022). Further degradation of non-terminally activated alkanes likely requires a rearrangement to 1-alkyl-CoM similar as described for bacterial alkane degradation (Rojo, 2009).

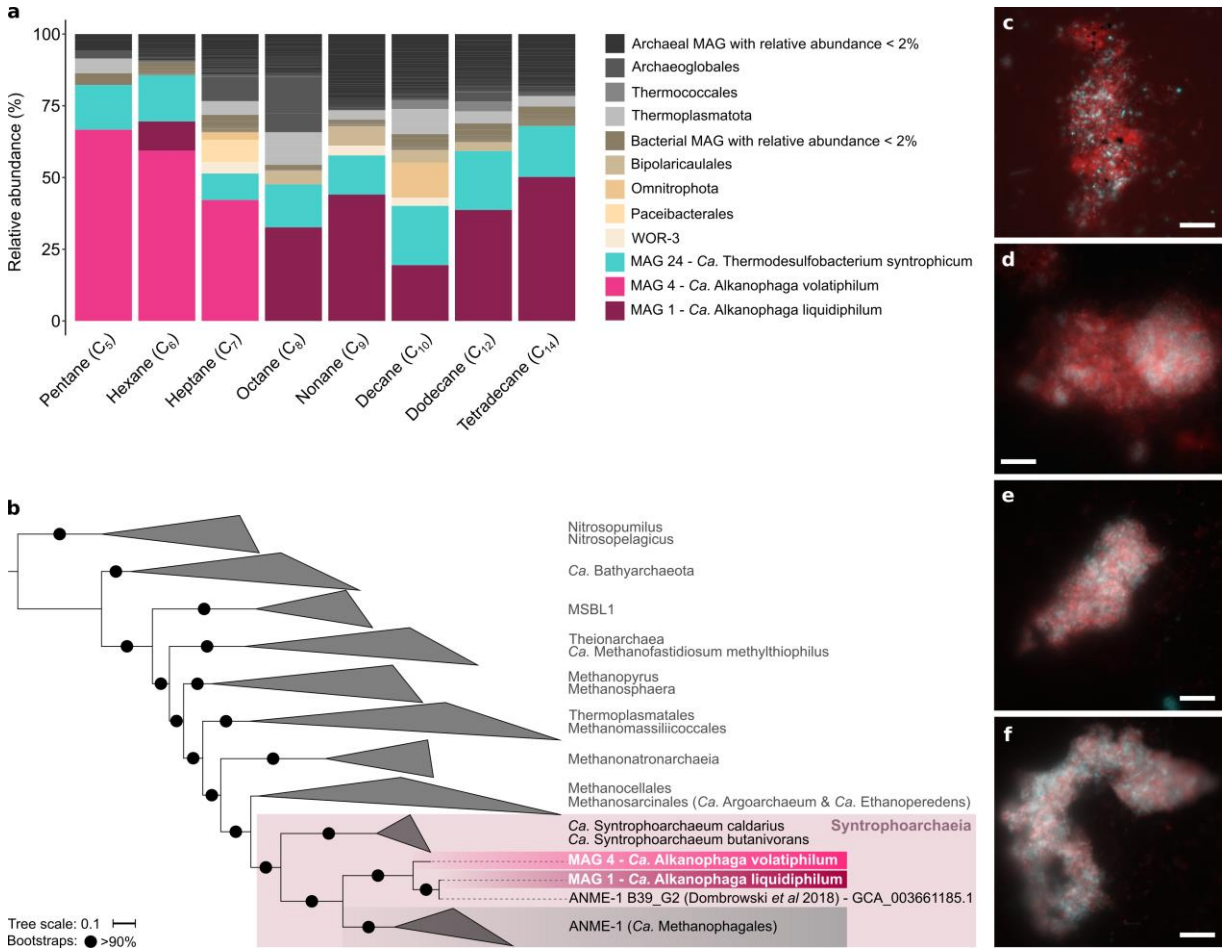


**Figure 2 | Two archaea of the genus *Candidatus* Alkanophaga are abundant in the cultures and closely related to ANME-1. a,** Relative abundances of metagenome-assembled genomes (MAGs) obtained from manual binning. *Ca.* Alkanophaga volatiphilum (MAG 4) is abundant in cultures oxidizing shorter, volatile alkanes between $C_5$-$C_7$, *Ca.* Alkanophaga liquidiphilum (MAG 1) is abundant in cultures oxidizing liquid alkanes between $C_8$-$C_{14}$. A *Thermodesulfobacterium* with the genomic capacities for dissimilatory sulfate reduction, *Ca.* Thermodesulfobacterium syntrophicum, is present in all cultures. Taxonomies of background MAGs are displayed at order level. Background archaea are shaded grey, background bacteria are shaded brown. **b,** Phylogenomic placement of *Ca.* Alkanophaga MAGs based on the concatenated alignment of 76 archaeal single copy core genes. *Ca.* Alkanophaga diverge at the root of ANME-1 (*Ca.* Methanophagales). The class Syntrophoarchaeia is highlighted with a rectangle. The outgroup consists of members of the Thermoproteota. The tree scale bar indicates 10% sequence divergence. **c,d,e,f,** Double hybridization of $C_6$ (**c,d**) and $C_{14}$ (**e,f**) culture samples with a specific probe targeting the *Ca.* Alkanophagales clade (Aph 183, red) and a general bacterial probe (EUBI-III, cyan). *Ca*. Alkanophaga cells are abundant in the aggregates where they co-occur with bacterial cells. The scale bar measures 10 µm.

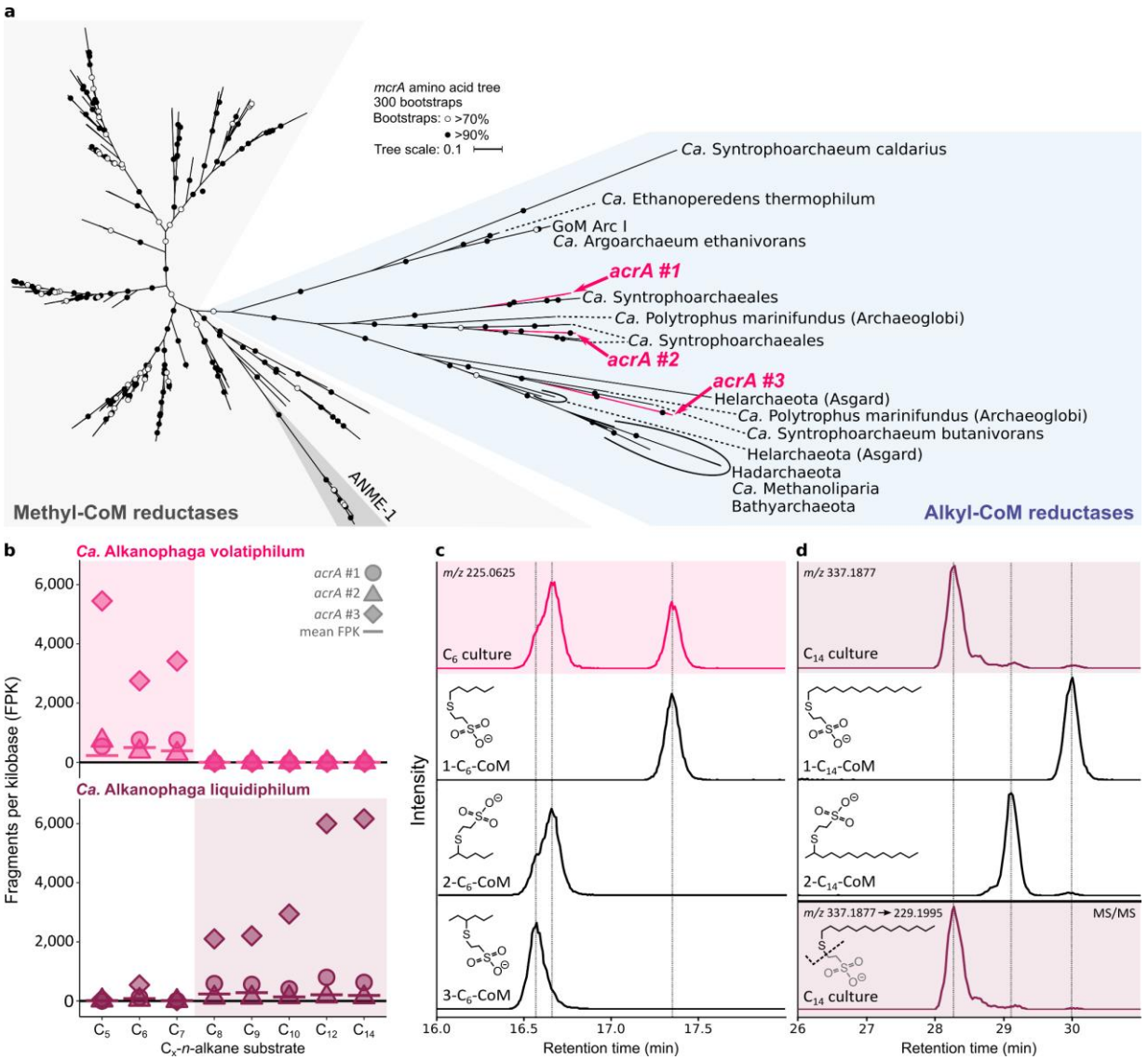


**Figure 3 | *Ca.* Alkanophaga use alkyl-coenzyme M reductases to activate alkanes to alkyl-CoMs. a,** Phylogenetic placement of translated *mcrA* sequences of *Ca.* Alkanophaga. Both *Ca.* Alkanophaga species contain three *mcrA* sequences, all of which fall into the divergent branch of *mcrA*s, encoding alkyl-CoM reductases (Acrs), highlighted in blue. The six *acrA* sequences form three clusters of two sequences, each cluster containing one sequence of each *Ca.* Alkanophaga species. The tree scale bar indicates 10% sequence divergence. **b,** Expression of *acrA* genes during growth on various alkanes for both *Ca.* Alkanophaga species. Cultures in which the respective species was prevalent in the metagenomes are highlighted by shaded boxes. The mean expression of all genes of the respective species is shown as a horizontal bar. The *acrA* of the third cluster was strongly expressed, irrespective of substrate length, by the species abundant in that culture. The expression of the other *acrA* genes was low. **c,d** Extracted ion chromatograms (EICs) based on exact mass and a window of ±10 mDa of deprotonated ions of variants of $C_6$-CoM (**c**) and $C_{14}$-CoM (**d**) detected via liquid chromatography-mass spectrometry. In both **c** and **d**, the upper panel shows the culture extract, with isomers of alkyl-CoM standards below. In **d**, the bottom panel shows the EIC produced with the exact mass of the $C_{14}$-thiolate, a fragmentation product derived in MS/MS experiments from the precursor $C_{14}$-CoM. Dashed vertical lines were added at retention times of peak maxima of standards (**c**) or standards and fragmentation products (**d**) for easier identification of peaks in the culture extracts. While $C_6$ is activated on the first and second carbon atom to a similar degree, $C_{14}$ is activated predominantly to ≥3-$C_{14}$-CoM.

We conclude that the archaea represented by MAGs 1 and 4 oxidize the petroleum alkanes. We propose the genus name *Candidatus* Alkanophaga, consistent with the previously suggested name *Candidatus* Alkanophagales (Wang et al., 2021), and analogous to the closely related methanotrophs *Ca.* Methanophagales (ANME-1) (Chadwick et al., 2022). The *Ca.* Alkanophaga MAGs share amino acid identities (AAIs) of 55-59% to ANME-1 MAGs (Supplementary Table 8), placing *Ca.* Alkanophaga within the ANME-1 family (Konstantinidis et al., 2017). Based on apparent substrate preference in our enrichment cultures, we propose the names *Ca*. Alkanophaga volatiphilum for the archaeon represented by MAG 4 and *Ca*. Alkanophaga liquidiphilum for the archaeon represented by MAG 1. Substrate tests corroborate that *Ca.* A. volatiphilum prefers shorter, volatile alkanes $<C_{10}$, while *Ca.* A. liquidiphilum readily degrades all alkanes between $C_6$ and $C_{15}$ (Extended Data Fig. 6).

### Ca. *Alkanophaga completely oxidize the alkanes to* $CO_2$

The oxidation of alkyl-CoMs generated by the Acr requires a conversion to acyl-CoA (Fig. 4a,b). The underlying reactions for this transformation are unknown, but for other alkane-degrading archaea some candidate enzymes have been proposed. The $C_2$-oxidizing *Ca.* Ethanoperedens thermophilum may catalyze this step with tungstate-containing aldehyde:ferredoxin reductases (Aors). This archaeon encodes three *aor* copies located closely to genes of the Wood-Ljungdahl (WL) pathway, and expresses them during ethane oxidation (Hahn et al., 2020). While both *Ca.* Alkanophaga encode complete *aor* gene sets, those genes were only moderately expressed (Supplementary Table 7), casting doubt on a crucial role of the Aor in this reaction in our cultures. A transfer of alkyl moieties to CoA via methyltransferases, as was hypothesized for *Ca.* Syntrophoarchaeum (Laso-Pérez et al., 2016), is equally unlikely because of the large alkanes consumed by *Ca.* Alkanophaga. In conclusion, the conversion of alkyl-CoM to acyl-CoA requires further investigation.

Like *Ca.* Syntrophoarchaeum (Laso-Pérez et al., 2016), *Ca.* Alkanophaga likely processes acyl-CoA to acetyl-CoA units via the *β*-oxidation pathway (Schulz, 1991) (Fig. 4b). *Ca*. Alkanophaga encode all genes for even-chain β-oxidation and expressed them during alkane oxidation (Figs. 4a and 5, Extended Data Fig. 7, Supplementary Table 7). For odd-chain alkanes, three additional genes are required to degrade the potentially toxic $C_3$-compound propionyl-CoA (Wongkittichote et al., 2017; Dolan et al., 2018), two of which are missing from *Ca.* Alkanophaga. We could not identify complete alternative pathways for the degradation of propionyl-CoA, e.g. the methylcitrate cycle (Dolan et al., 2018). Thus, the fate of the propionyl-CoA remains, for the moment, unclear.

Acetyl-CoA units from *β*-oxidation are shuttled into biomass production or completely oxidized. For the latter, the acetyl-CoA decarbonylase/synthase (ACDS) complex splits a methyl group from acetyl-CoA which is transferred to tetrahydromethanopterin ($H_4$MPT) (Fig. 4b). The enzymes of the $H_4$MPT methyl branch of the WL pathway then oxidize methyl-$H_4$MPT to $CO_2$ (Laso-Pérez et al., 2016; Hahn et al., 2020). Both *Ca.* Alkanophaga species encode and expressed

multiple ACDS and all enzymes of the WL pathway, except methylene-$H_4$MPT-deyhdrogenase (*mtd*) missing in *Ca.* A. volatiphilum (Figs. 4a and 5, Extended Data Fig. 7, Supplementary Table 7).

Unlike the closely related *Ca.* Syntrophoarchaeum and ANME-1, both *Ca.* Alkanophaga encode several 5,10-methylene-$H_4$MPT reductase (*mer*) genes. This enzyme catalyzes the oxidation of methyl-$H_4$MPT ($CH_3$-$H_4$MPT) to methylene-$H_4$MPT ($CH_2$=$H_4$MPT) in the first step of the oxidative WL pathway (Adam et al., 2019). Two of these genes, OD814_001315 in *Ca.* A. volatiphilum, and OD815_000385 in *Ca.* A. liquidiphilum, most likely code for a canonical *mer* because they are highly similar (>99%) to *mer* copies of Methanomicrobia. A phylogenetic analysis placed these two *mer* sequences next to each other and close to those of the hydrogenotrophic methanogens Methanocellales (Sakai et al., 2008) (Extended Data Fig. 8a). We therefore hypothesize that *Ca.* Alkanophaga inherited *mer* vertically from the methanogenic ancestor of Methanocellales. *Ca.* Syntrophoarchaeum and ANME-1 seem to have replaced *mer* with methylene-tetrahydrofolate ($H_4$F) reductase (*metF*) of the $H_4$F methyl branch of the WL pathway (Stokke et al., 2012; Laso-Pérez et al., 2016). Both *Ca.* Alkanophaga MAGs also encode *metF* copies, which are highly similar (70-80%) to those of *Ca.* Syntrophoarchaeum, and cluster next to *metF* sequences of Hadarchaeota from Jinze hot spring (China) and Yellowstone National Park (USA) (Extended Data Fig. 8b). While both *mer* and *metF* were transcribed, *mer* was especially expressed by *Ca.* A. liquidiphilum in cultures oxidizing longer alkanes ≥$C_{10}$ (Fig. 5b,d, Extended Data Figure 7e,f,k,l, and Supplementary Table 7).

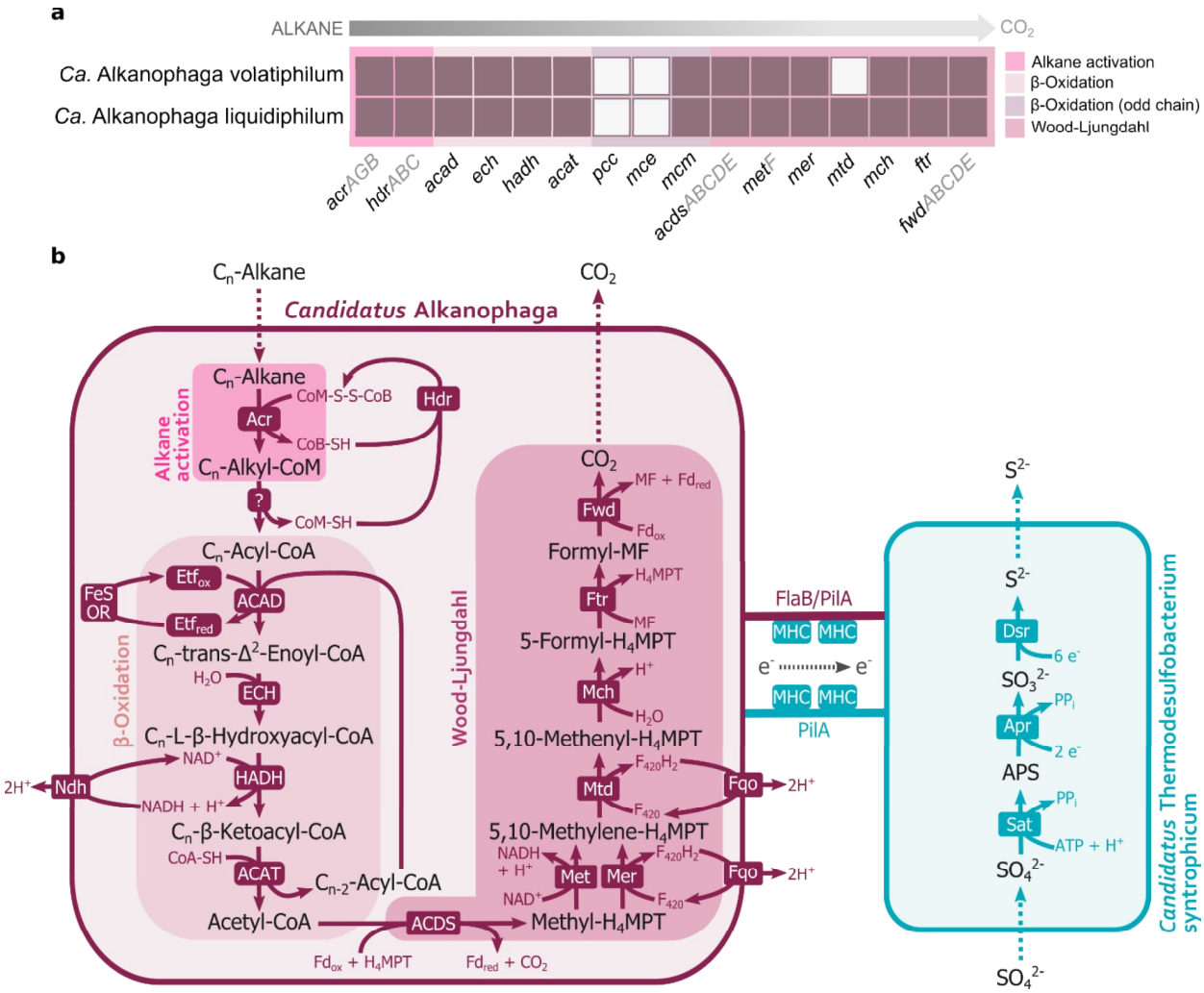


**Figure 4 | Mechanism of syntrophic petroleum alkane oxidation. a,** Genomic capacities for alkane oxidation in *Candidatus* Alkanophaga MAGs. Color-filled rectangles indicate presence of a gene; white rectangles indicate absence. For multiple-subunit proteins, at least one gene coding for each subunit was found in case of a filled rectangle. **b,** Metabolic model for syntrophic alkane oxidation. *Ca.* Alkanophaga activate alkanes via the alkyl-coenzyme M reductase (Acr). A yet unknown pathway transforms alkyl-CoM to acyl-CoA. The enzymes of the *β*-oxidation pathway (1) acyl-CoA dehydrogenase (ACAD) (2) enoyl-CoA hydratase (ECH) (3) hydroxyacyl-CoA dehydrogenase (HADH) and (4) acyl-CoA acetyltransferase (ACAT) cleave acyl-CoA into multiple acetyl-CoA units. The acetyl-CoA decarbonylase/synthase (ACDS) complex breaks the acetyl units into $CO_2$ and a tetrahydromethanopterin ($H_4$MPT)-bound methyl unit. The methyl branch of the Wood-Ljungdahl pathway, including (1) 5,10-methylene tetrahydrofolate reductase (MetF) and/or 5,10-methylene $H_4$MPT reductase (Mer) (2) methylene-$H_4$MPT dehydrogenase (Mtd) (3) methenyl-$H_4$MPT cyclohydrolase (Mch) (4) formylmethanofuran-$H_4$MPT formyltransferase (Ftr) and (5) tungsten-containing formylmethanofuran dehydrogenase (Fwd), oxidizes methyl-$H_4$MPT to $CO_2$. Most likely, an electron transfer flavoprotein (Etf) serves as electron acceptor in the first step of the *β*-oxidation pathway. Cofactor recycling is taken over by cytoplasmic heterodisulfide reductase (Hdr), [FeS]-oxidoreductase (FeS-OR), NADH dehydrogenase (Ndh), and $F_{420}H_2$:quinone oxidoreductase (Fqo). Electrons from alkane oxidation are transferred to *Ca.* Thermodesulfobacterium syntrophicum, most likely via direct interspecies electron transfer (DIET). DIET seems to rely on conductive filaments formed by type IV pilin (PilA) and/or flagellin B (FlaB) that are expressed by both partners and multi-heme *c*-type cytochromes (MHC) expressed solely by the bacterium. Sulfate reduction in *Ca.* T. syntrophicum follows the canonical dissimilatory sulfate pathway using the enzymes ATP-sulfurylase (Sat), APS-reductase (Apr), and dissimilatory sulfite reductase (Dsr). Other abbreviations: *pcc*: gene encoding propionyl-CoA decarboxylase; *mce*: gene encoding methylmalonyl-CoA epimerase; *mcm*: gene encoding methylmalonyl-CoA mutase.

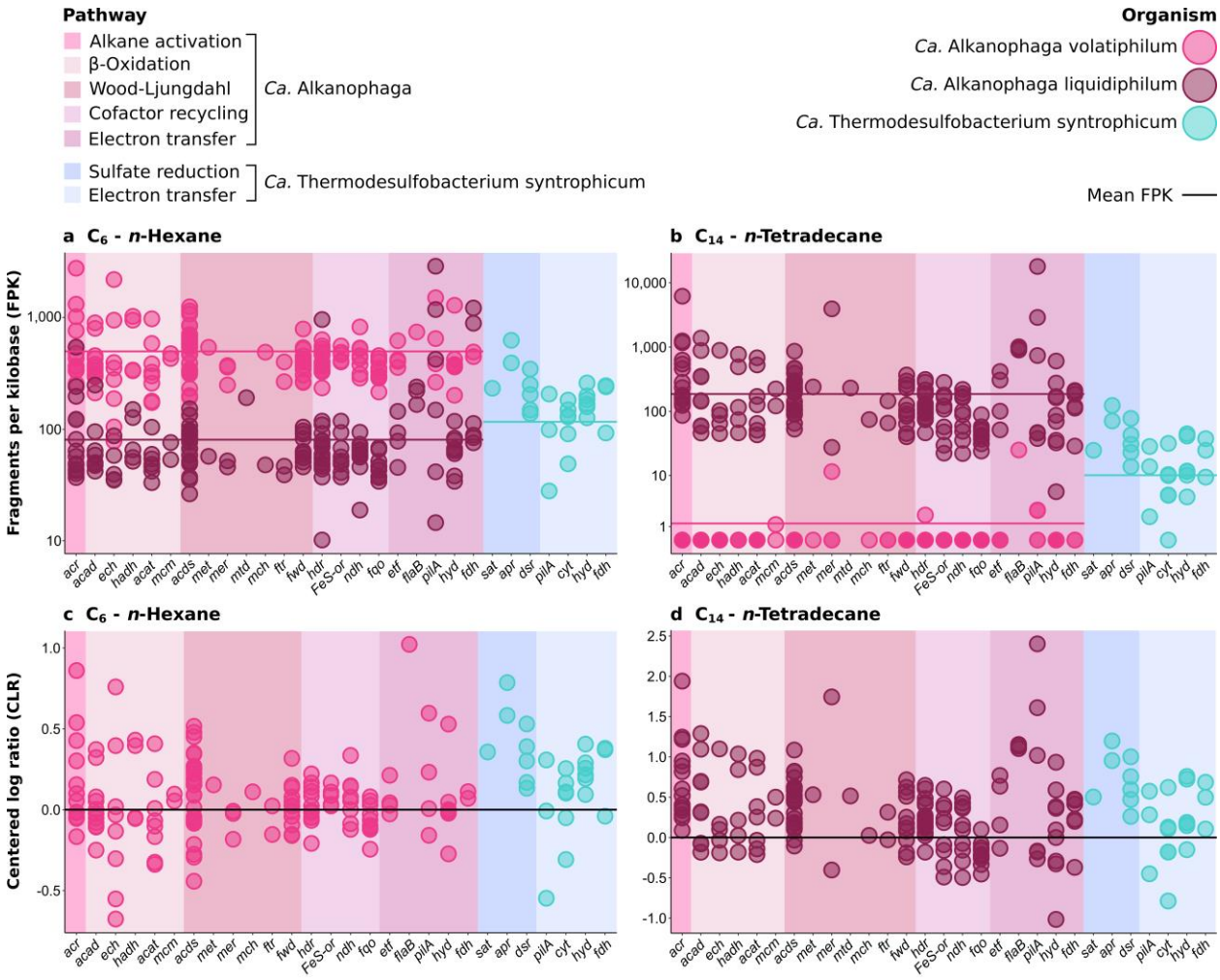


**Figure 5 | Gene expression profiles for syntrophic petroleum alkane oxidation. a**,**b,** Fragment counts normalized to gene length (fragments per kilobase - FPK) shown on a logarithmic y axis. The average gene expression of each organism is indicated as arithmetic mean (sum of all FPK values divided by number of genes) depicted as a horizontal line. **c,d,** Fragment counts normalized as centered log ratio (CLR). For simplicity, only the values of the more active *Ca.* Alkanophaga species are shown. For abbreviations see Figure 4, additional genes are encoding: *hyd*: [NiFe]-hydrogenase; *fdh*: gene encoding formate dehydrogenase, *cyt*: multi-heme cytochrome.

### Ca. *Alkanophaga partner with a* Thermodesulfobacterium

*Ca.* Alkanophaga lack the dissimilatory sulfate reduction (DSR) pathway and therefore require a partner organism. We identified a *Thermodesulfobacterium* represented by MAG 24, which was enriched in all cultures (Fig. 2a, Supplementary Table 4) and rare in the original slurry, as the most likely syntrophic sulfate reducer. MAG 24 encodes and expressed the three DSR proteins ATP-sulfurylase (Sat), APS-reductase (Apr), and dissimilatory sulfite reductase (Dsr) (Rabus et al., 2013) (Fig. 5, Extended Data Fig. 7, Supplementary Table 7). We propose the name *Candidatus* Thermodesulfobacterium syntrophicum for this bacterium, which is closely related to the hyperthermophilic, sulfate-reducing *Thermodesulfobacterium geofontis*, isolated from the Obsidian Pool in Yellowstone National Park (USA) (Hamilton-Brehm et al., 2013) (Extended Data Fig. 9).

**Etymology:** Alkanophaga: composite of *alkano* - (new Latin) pertaining to alkane and *phaga* - (Greek) eating; volatiphilum: composite of *volatilis* (Latin) - volatile and *-philum* (Greek) - preferring; liquidiphilum: composite of *liquidus* (Latin) - liquid and *-philum* (Greek) - preferring; syntrophicum: composite of *syn* - (Greek) together with, *trephein* - (Greek) nourish, and *icum* - (Latin) pertaining to

**Locality:** hydrothermally heated oil-rich deep-sea sediment in the Guaymas Basin, Gulf of California, Mexico

**Description:** *Candidatus* Alkanophaga volatiphilum and *Candidatus* Alkanophaga liquidiphilum: thermophilic, anaerobic, petroleum ($C_5$-$C_{14}$) *n*-alkane-oxidizing archaea, forming syntrophic consortia with the sulfate-reducing *Candidatus* Thermodesulfobacterium syntrophicum.

Syntrophic microorganisms trade electrons via molecular intermediates, like hydrogen or formate (Rotaru et al., 2012), or direct interspecies electron transfer (DIET) (Rotaru et al., 2014). Both *Ca.* Alkanophaga and *Ca.* T. syntrophicum encode membrane-bound [NiFe]-hydrogenases, including several hydrogenase maturation factors, enabling electron transfer via molecular hydrogen. Some hydrogenase genes were substantially expressed (Fig. 5, Extended Data Fig. 7, Supplementary Table 7). Formate dehydrogenases, necessary for electron transfer via formate, were also present in both partners, and moderately expressed (Fig. 5, Extended Data Fig. 7, Supplementary Table 7). However, the addition of hydrogen or formate did not accelerate sulfide production (Extended Data Fig. 4c,d). Moreover, cultures in which sulfate reduction was inhibited by the addition of sodium molybdate produced only miniscule fractions (max. 2.4% for $C_6$ and 0.9% for $C_{14}$) of the hydrogen concentrations that would be necessary were hydrogen the sole electron carrier (Supplementary Table 9). Thus, neither molecular hydrogen nor formate are likely primary electron carriers.

Alternatively, alkane oxidation and sulfate reduction are coupled through DIET, as suggested for other alkane-oxidizing consortia (Wegener et al., 2015; Laso-Pérez et al., 2016; Hahn et al., 2020). DIET likely involves cell appendages, like bacterial type IV pilin (PilA) or the archaeal flagellin B (FlaB), and multi-heme *c*-type cytochromes (MHCs), forming conductive nanowires enabling electron transport (Summers et al., 2010; Braun et al., 2016).

Both components are present and strongly expressed in previously established alkane-oxidizing consortia (Wegener et al., 2015; Laso-Pérez et al., 2016; Hahn et al., 2020). Surprisingly, neither our nor the previously published *Ca.* Alkanophaga MAGs encode any MHCs, while the closest relatives of *Ca.* Alkanophaga, ANME-1 and *Ca.* Syntrophoarchaeum, encode multiple MHCs (Laso-Pérez et al., 2016; Chadwick et al., 2022). *Ca.* T. syntrophicum encodes six MHCs, only one of which was slightly enriched in all cultures (Supplementary Table 7). This implies a minor role of MHCs in the interaction of both organisms.

Both *Ca.* Alkanophaga encode several copies of *pilA* and *flaB* for the formation of cell appendages for DIET. These genes were among the most highly expressed genes of *Ca.* Alkanophaga in all cultures. *Ca.* T. syntrophicum encodes several *pilA* genes as well, some of which were strongly enriched in the $C_{10}$-$C_{14}$ cultures (Supplementary Table 7). Transmission electron microscopy revealed diffuse filamentous structures in the intercellular space that might pertain to such nanowires (Extended Data Fig. 10), however further analyses are necessary to confirm the identity of these structures.

We predict that electron transfer in our cultures bases predominantly on DIET. The lack of MHCs in *Ca.* Alkanophaga might be compensated by MHC production in the partner bacterium similar to observations in syntrophic methane-oxidizing cultures, where only the bacterial partner expressed *pilA* genes (Wegener et al., 2015). Alternatively, DIET might be completely independent of MHCs, which has been observed before (Walker et al., 2019; Yee and Rotaru, 2020). It remains possible that a small fraction of electrons are transferred via soluble intermediates like hydrogen. Such a combination of DIET with diffusion-based electron transport was recently shown to be energetically favorable for syntrophic consortia (He et al., 2021).

## Discussion

Petroleum-rich anoxic environments like oil reservoirs, oily sludges, and polluted sediments harbor oil-degrading microorganisms. Isolates from these environments that couple petroleum alkane oxidation to sulfate reduction are mostly bacteria active at temperatures ≤60 °C (Mbadinga et al., 2011). With *Ca.* Alkanophaga, we enriched a thermophilic clade thriving on petroleum alkanes from $C_5$ to $C_{14}$ at temperatures between 65-75 °C (Extended Data Fig. 4e,f), which approach the suggested upper limit of microbial hydrocarbon degradation in petroleum reservoirs of around 80 °C (Wilhelms et al., 2001). This temperature optimum is reflected by the high relative abundance of *Ca.* Alkanophaga in deep, heated sediment layers of the Guaymas Basin, inferring a crucial role of these archaea in thermophilic hydrocarbon transformation.

*Ca.* Alkanophaga encode three Acrs for anaerobic alkane activation, one less than the closely related short-chain alkane oxidizer *Ca.* Syntrophoarchaeum (Laso-Pérez et al., 2016). Independent of alkane length, *Ca.* Alkanophaga strongly expressed only one of the Acrs, which is highly similar to the highest expressed Acr in *Ca.* Syntrophoarchaeum during $C_4$ oxidation (Laso-Pérez et al., 2016). Future studies may reveal functions or substrates of the other two lower expressed Acrs. *Ca.* Alkanophaga stand out among Acr-using archaea with their wide substrate range between $C_5$ and $C_{15}$. Therewith, all alkanes between $C_1$ and $C_{20}$ are confirmed substrates of alkane-oxidizing archaea (Laso-Pérez et al., 2016; Chen et al., 2019; Hahn et al., 2020; Zhou et al., 2022). Our study implies that substrate flexibility of the Acr increases with increasing alkane length, which is presumably enabled by a wider catalytic cleft in the Acrs activating $C_3$+ alkanes (Lemaire and Wagner, 2022) compared to the highly selective hydrophobic tunnel detected in the $C_2$-activating Acr (Hahn et al., 2021). Crystallization efforts may resolve molecular and structural modifications of these Acrs that make use of such a wide substrate spectrum.

The three clades of the class Syntrophoarchaeia (*Ca.* Alkanophaga, *Ca.* Syntrophoarchaeum, and ANME-1) share many metabolic features like obligate syntrophic growth with partner SRB and presence of the *β*-oxidation and WL pathways. At the same time, they exhibit remarkable metabolic and genomic differences. For instance, ANME-1 encode the canonical Mcr for methane metabolism, which is missing in *Ca.* Syntrophoarchaeum and *Ca.* Alkanophaga, preventing them from oxidizing and producing methane. Instead, the latter two possess multiple multi-carbon alkane-activating Acrs, which are in turn absent in ANME-1. Our study supports the previously established hypothesis that multi-carbon alkane metabolism likely preceded methanotrophy in the Syntrophoarchaeia (Wang et al., 2021; Wegener et al., 2022) because of the basal position of both multi-carbon alkane oxidizers (Fig. 2b) and their similar metabolisms. The presence of the *β*-oxidation pathway in ANME-1 (Wang et al., 2021) supports this notion, because this pathway is required for the oxidation of $C_3$+ alkanes, but serves no purpose in the oxidation of methane. We propose that the common ancestor of the Syntrophoarchaeia was a multi-carbon alkane-oxidizing archaeon with multiple Acrs. *Ca.* Syntrophoarchaeum and *Ca.* Alkanophaga emerged from this ancestor, preserving a similar

metabolism. Today, *Ca.* Syntrophoarchaeum thrives at much lower temperatures (50 °C) and seems incapable of oxidizing liquid alkanes (Laso-Pérez et al., 2016). Thus, adaptation to different temperatures and substrates might have enabled *Ca.* Syntrophoarchaeum and *Ca.* Alkanophaga to occupy different ecological niches. *Ca.* Alkanophaga and ANME-1 also shared a common ancestor, of which ANME-1 likely diverged after losing their Acrs (Laso-Pérez et al., 2023) and acquiring a Mcr, potentially from a methanogen, via lateral gene transfer (Borrel et al., 2019; Chadwick et al., 2022).

*Ca.* Alkanophaga differ from the two other groups of the Syntrophoarchaeia in two main aspects. First, *Ca.* Alkanophaga encode and expressed *mer*, an essential enzyme of the canonical methanogenesis pathway (Ma and Thauer, 1990). ANME-1, with the exception of a putative methanogenic ANME-1 member (Beulig et al., 2019), and *Ca.* Syntrophoarchaeum lack *mer* and instead code for the phylogenetically widely distributed *metF* (Maden and Edward, 1996; Laso-Pérez et al., 2016; Chadwick et al., 2022), which is also present and expressed in *Ca.* Alkanophaga. We hypothesize that *mer* in *Ca.* Alkanophaga is a remnant from a methanogenic ancestor. Second, *Ca.* Alkanophaga lack MHCs, which are often considered essential for DIET between syntrophic partners (Summers et al., 2010). All other syntrophic alkane-oxidizing archaea code for several MHCs (Wegener et al., 2022). However, an absence of MHCs in DIET-performing methanogens has been recognized before (Yee and Rotaru, 2020). It is thus conceivable that MHCs aid in but are not essential for DIET, and that MHCs were potentially lost by *Ca.* Alkanophaga without a substantial impact on the efficiency of electron transfer. The loss of all MHCs opens up questions as to the mechanisms that occurred. In a recent study, giant extrachromosomal elements named Borgs, many of which carried clusters of MHCs, were reconstructed from methane-oxidizing *Methanoperedens* (ANME-2d) archaea (Al-Shayeb et al., 2022). One could imagine that MHCs in the Syntrophoarchaeia ancestor were encoded on such a Borg, which was then lost by *Ca.* Alkanophaga. This could explain why all MHCs are absent in *Ca.* Alkanophaga. However, the presence of Borgs in other members of the Syntrophoarchaeia still needs to be examined.

*Ca.* Alkanophaga partner with the sulfate-reducing *Ca.* Thermodesulfobacterium syntrophicum. Previously enriched alkane-oxidizing archaea partner with a different bacterium, *Ca.* Desulfofervidus auxilii, which has an optimal growth temperature of 60 °C (Holler et al., 2011; Krukenberg et al., 2016; Laso-Pérez et al., 2016; Hahn et al., 2020). We suspect that the higher incubation temperature of our study selected for a more thermophilic partner organism. Recently, another *Thermodesulfobacterium* species, *Ca.* Thermodesulfobacterium torris (ANI 84.0%, Extended Data Fig. 9), has been reported as syntrophic sulfate reducer partnering with thermophilic ANME-1c at 70 °C (Benito Merino et al., 2022). Thus, Thermodesulfobacteria represent a new group of partner organisms for alkane-oxidizing archaea at high temperatures. In contrast to *Ca.* Alkanophaga, *Ca.* T. syntrophicum encodes and expressed several MHCs, which could support DIET for both partners.

All currently available *Ca.* Alkanophaga sequences originate from the Guaymas Basin, a thoroughly studied hydrothermal vent area hauling heated fluids rich in alkanes (Kawka and Simoneit, 1987). We suspect two main reasons for this apparent absence in other environments. First, until recently, microbial community studies have mostly focused on 16S rRNA gene (16S) amplification and sequencing, a method depending heavily on primer choice (Fischer et al., 2016). We discovered a mismatch of the commonly used archaeal primer Arch915 (5'-GTGCTCCCCCGCCAATTC**C**T-3' (Alm et al., 1996), mismatch in bold) to the 16S rRNA gene sequences of *Ca.* Alkanophaga, which likely produces an artificial underrepresentation of *Ca.* Alkanophaga in public databases. Second, sequencing data from other environments similar to the Guaymas Basin, i.e. heated oil reservoirs with sulfate supply, remains scarce. Many of these reservoirs, often buried kilometers deep within the subsurface, are extremely hard to access (Marietou, 2021). In addition, the risk of contamination from the upper biosphere during sampling increases with depth, which might conceal the native community (Marietou, 2021). Still, sampling technologies have greatly improved in recent years, and the focus has shifted from amplification-based 16S rRNA gene to shotgun metagenome studies, which should facilitate a more accurate molecular characterization of reservoir microorganisms. Thus, future studies may disclose the coexistence and activity of *Ca.* Alkanophaga and *Ca.* T. syntrophicum in other heated, petroleum-rich environments.

## Acknowledgements

This study was funded by the DFG under Germany's Excellence Initiative/Strategy through the Clusters of Excellence EXC 2077 "The Ocean Floor—Earth's Uncharted Interface" (project no. 390741603), the Andreas Rühl Foundation, and the Max Planck Society. R.L-P. was funded by a Juan de la Cierva grant (FJC2019-041362-I) from the Spanish Ministerio de Ciencia e Innovación. The Guaymas Basin expedition was supported by the National Science Foundation, Biological Oceanography grant no. 1357238 to A.T. (Collaborative Research: Microbial Carbon cycling and its interactions with Sulfur and Nitrogen transformations in Guaymas Basin hydrothermal sediments). We thank the captain and crew of *RV Atlantis* for their excellent work during the expedition AT42-05. Further, we thank Heidi Taubner and Martina Alisch for analytical measurements and Susanne Menger for technical support in the laboratory. We also thank Katrin Knittel and Andreas Ellrott for sharing their experience with CARD-FISH and microscopy. Finally, we thank Antje Boetius for fruitful scientific discussions.

## Author contributions

H.Z. and G.W. designed the study. G.W. conducted sampling on board. A.T. planned and organized the cruise. R.L.-P. and D.B.M. supported bioinformatical analyses. D.B.M. and H.Z. designed the specific CARD-FISH probe. J.L. conducted mass spectrometry measurements and analyses. D.R. carried out transmission electron microscopy. H.Z. did cultivation and laboratory experiments, 'omics analyses, and wrote the manuscript with contributions from all coauthors. All authors contributed to the article, agreed to all manuscript contents and to the author list and its order and approved the submitted version.

## Competing interests

The authors declare no competing interest

## Extended Data

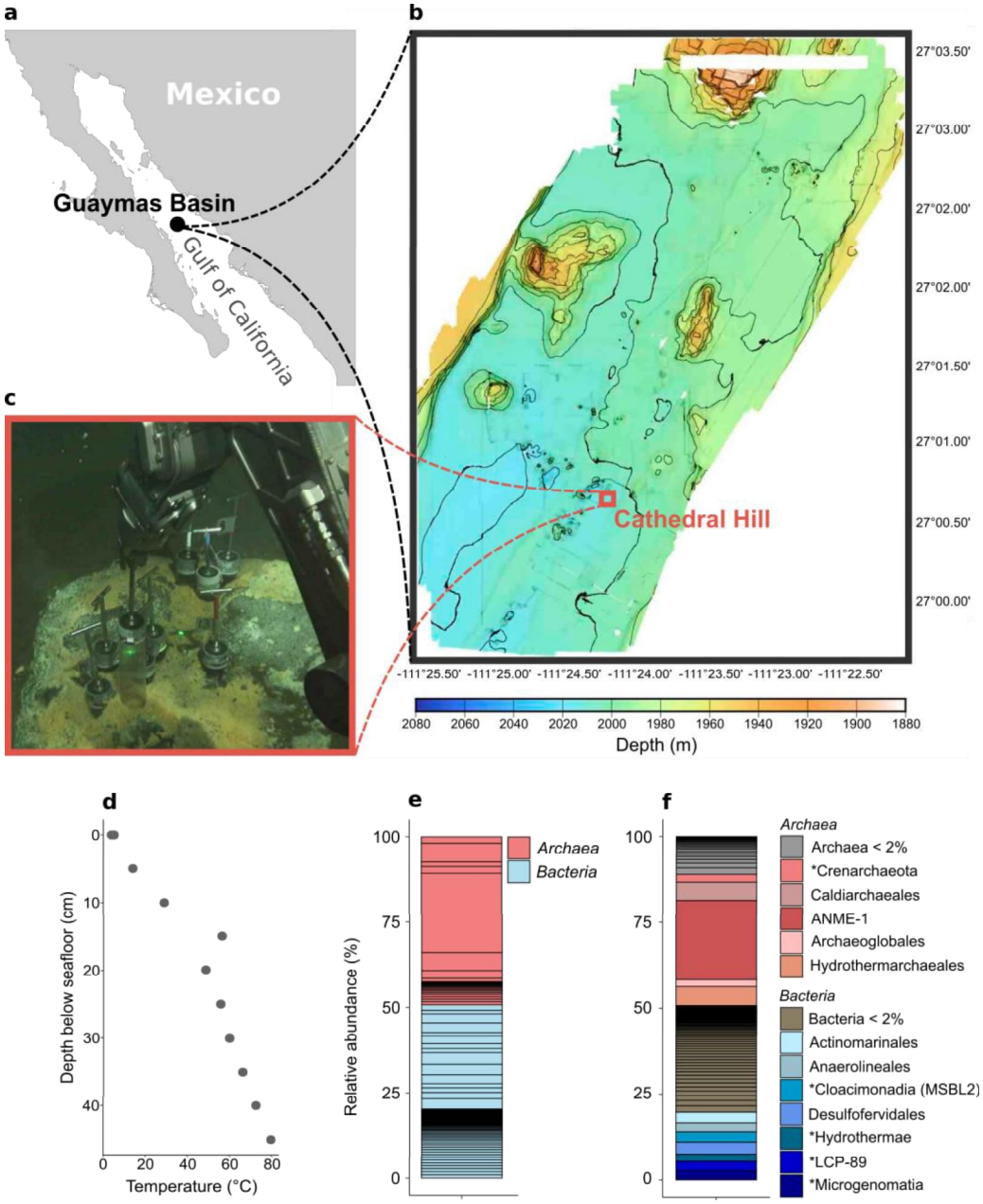


**Extended Data Figure 1 | Sampling site in the Guaymas Basin and microbial community in the original sediment. a,** Location of the Guaymas Basin in the Gulf of California. **b,** Bathymetry of the southern end of the Southern Trough of the Guaymas Basin with the location of the Cathedral Hill hydrothermal vent area. **c,** Sampling of the push core (4991-15) that was used for anoxic cultivations in an area densely covered by orange sulfur-oxidizing *Beggiatoa* mats. **d,** Depth-temperature profile in the sampling site. The temperature was measured using *Alvin*'s heatflow probe. Push cores reached about 30 cm into the sediment, where the temperature approached about 60 °C (sampling site photograph and temperature data courtesy of the Woods Hole Oceanographic Institution, from *RV Atlantis* cruise AT42-05). **e,f,** Microbial community in the anoxic sediment slurry prepared from core 4991-15 before starting anoxic incubations based on 16S rRNA gene fragments recruited from the metagenome**. e,** On the domain level, archaea and bacteria each make up around 50%. **f,** Taxonomic groups on order level. For groups with unknown order assignment marked with *, the next known higher taxonomic levels are indicated. An ANME-1 group is abundant within the archaeal fraction while the bacterial fraction is very diverse.

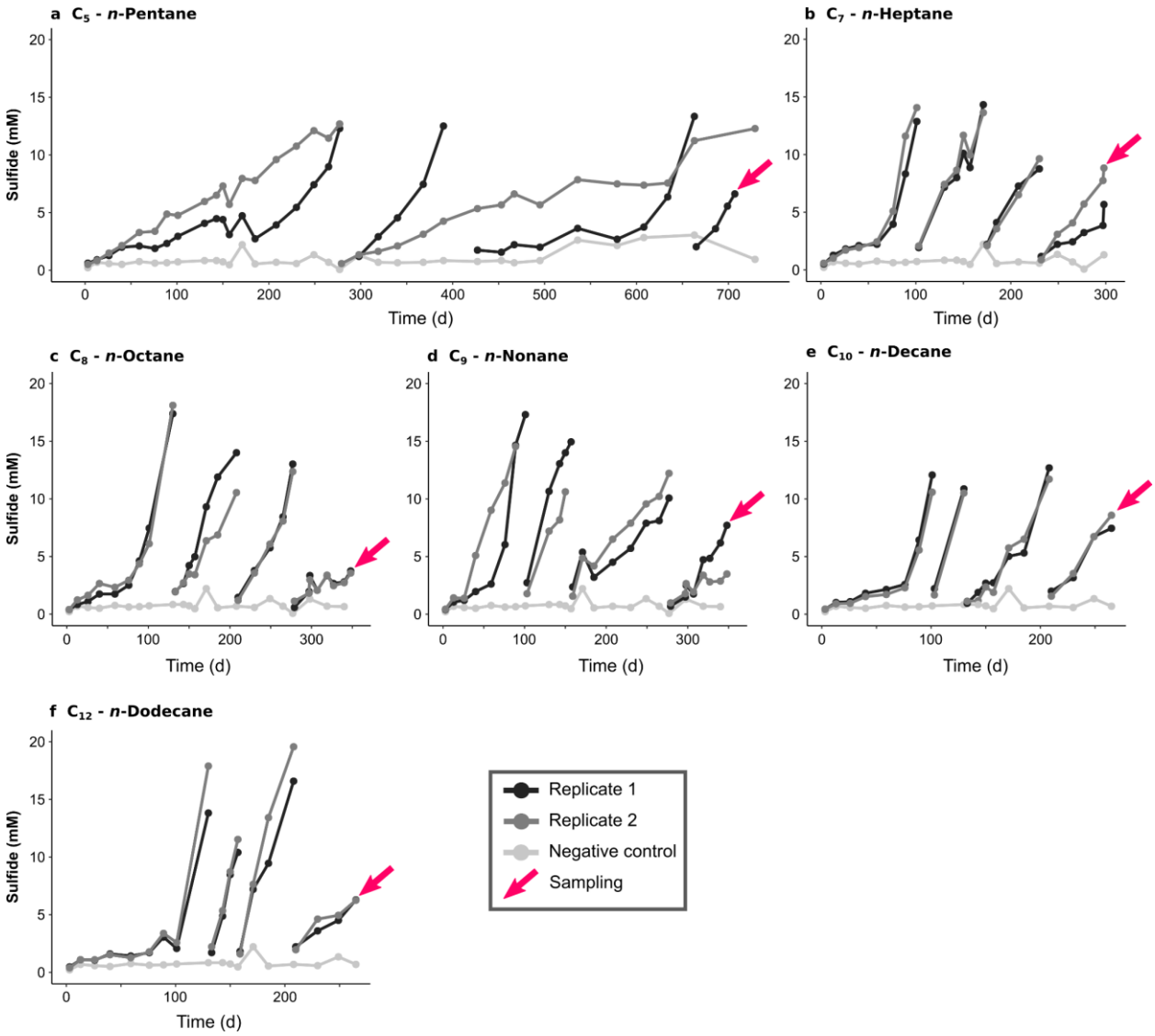


**Extended Data Figure 2 | Sulfide production in anoxic $C_5$-$C_{12}$ *n*-alkane-degrading cultures at 70 °C up to the third dilution.** Each culture was set up as a duplicate. Gaps in sulfide level indicate dilution steps. Pink arrows indicate the sampling points for metagenome and -transcriptome sequencing. The negative control consisted of a sediment slurry without added substrate.

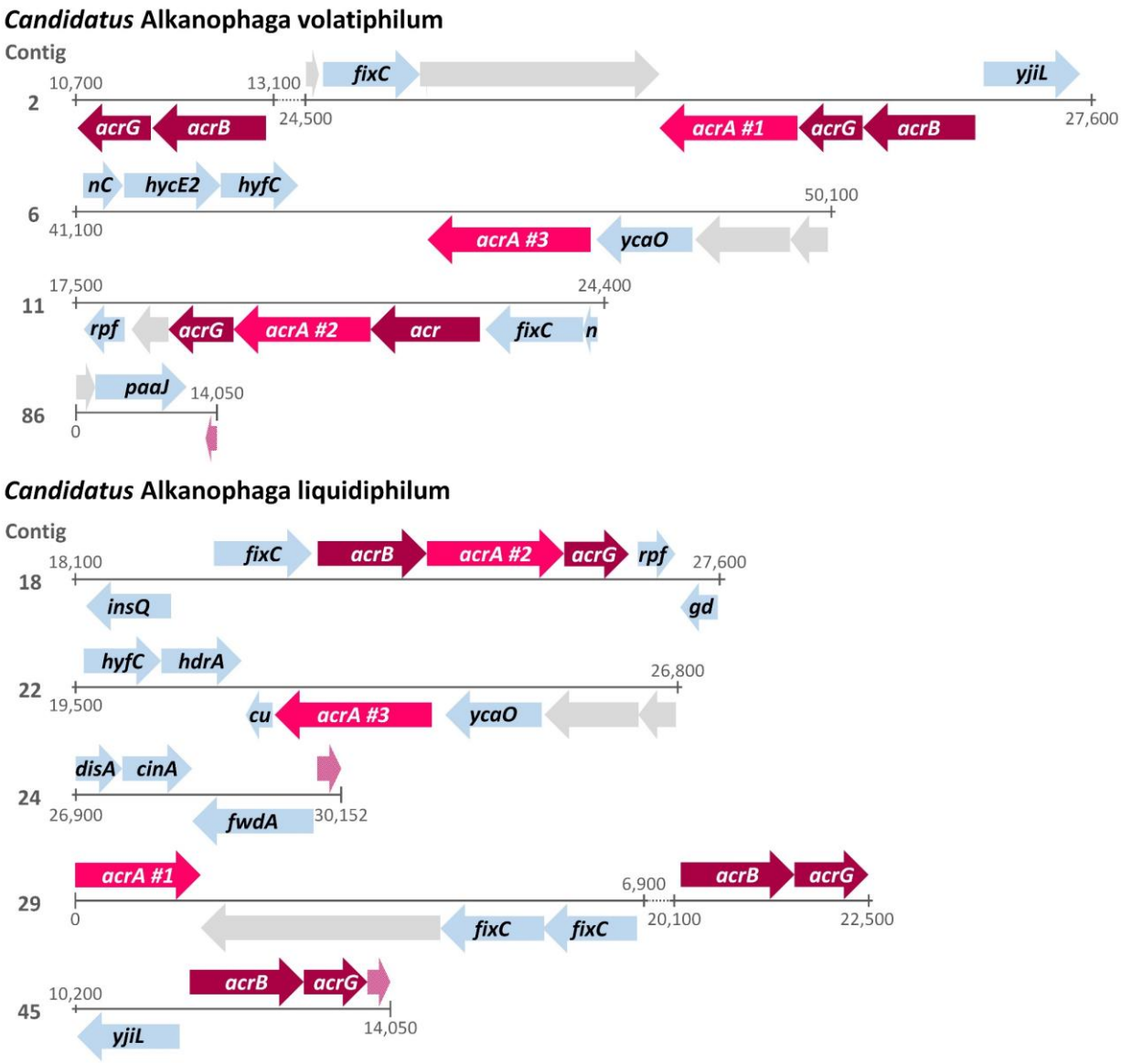


**Extended Data Figure 3 | Organization of *acr* genes in *Candidatus* Alkanophaga MAGs.** Partial *acrA* genes are shown in light pink, unannotated genes in light gray. Some gene names were shortened to fit the arrows. Genes code for: *acrA*: alkyl-coenzyme M reductase, alpha subunit; *acrB*: alkyl-coenzyme M reductase, beta subunit; *acrG*: alkyl-coenzyme M reductase, gamma subunit; *fixC*: flavoprotein dehydrogenase; *yjiL*: activator of 2-hydroxyglutaryl-CoA dehydratase; *nC*: *nuoC*-NADH:ubiquinone oxidoreductase; *hycE2*: [NiFe]-hydrogenase III large subunit; *hyfC*: formate hydrogenlyase; *ycaO*: ribosomal protein S12 methylthiotransferase accessory factor; *rpf*: *rpf1*-rRNA maturation protein; *n*: *nuoI*-formate hydrogenlyase subunit 6; *paaJ*: acetyl-CoA acetyltransferase; *insQ*: transposase; *gd*: *gdb1*-glycogen debranching enzyme; *hdrA*: heterodisulfide reductase, subunit A; *cu*: *cutA1*-divalent cation tolerance protein; *disA*: c-di-AMP synthetase; *cinA*: ADP-ribose pyrophosphatase domain of DNA damage- and competence-inducible protein CinA; *fwdA*: formylmethanofuran dehydrogenase subunit A.

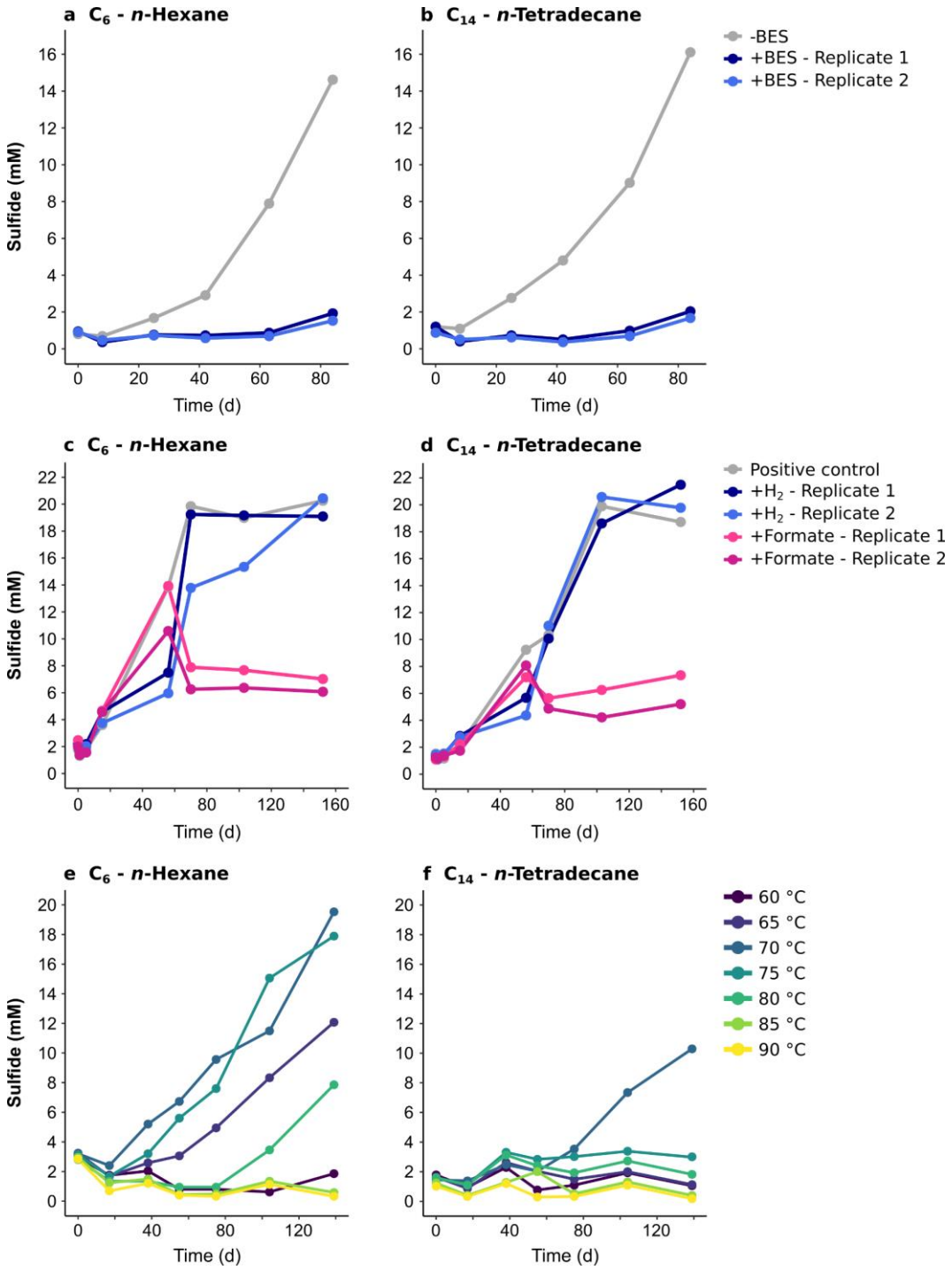


**Extended Data Figure 4 | Sulfide production in *n*-hexane ($C_6$)- and *n*-tetradecane ($C_{14}$)-degrading cultures under different conditions. a,b,** Treatment with 2-bromoethanosulfonate (BES). BES (5 mM final concentration) was added to duplicates of $C_6$ (**a**) and $C_{14}$ (**b**)-degrading cultures (+BES). A control culture (-BES) did not receive BES. The inhibition of alkane oxidation by BES corroborates an Acr-based substrate activation. **c,d,** Addition of hydrogen or formate to $C_6$ (**c**) and $C_{14}$ (**d**)-degrading cultures. All cultures were supplied with the original substrate. The addition of 10% $H_2$ into the headspace or 10 mM sodium formate into the medium did not accelerate sulfide production compared to positive controls. **e,f,** Incubation at temperatures between 60 °C and 90 °C. The $C_6$-degrading culture (**e**) grows optimally at 70 °C and 75 °C, while it still shows some activity at slightly lower (65 °C) and slightly higher (80 °C) temperatures. The activity of the $C_{14}$-degrading culture (**f**) seems to be limited to 70 °C.

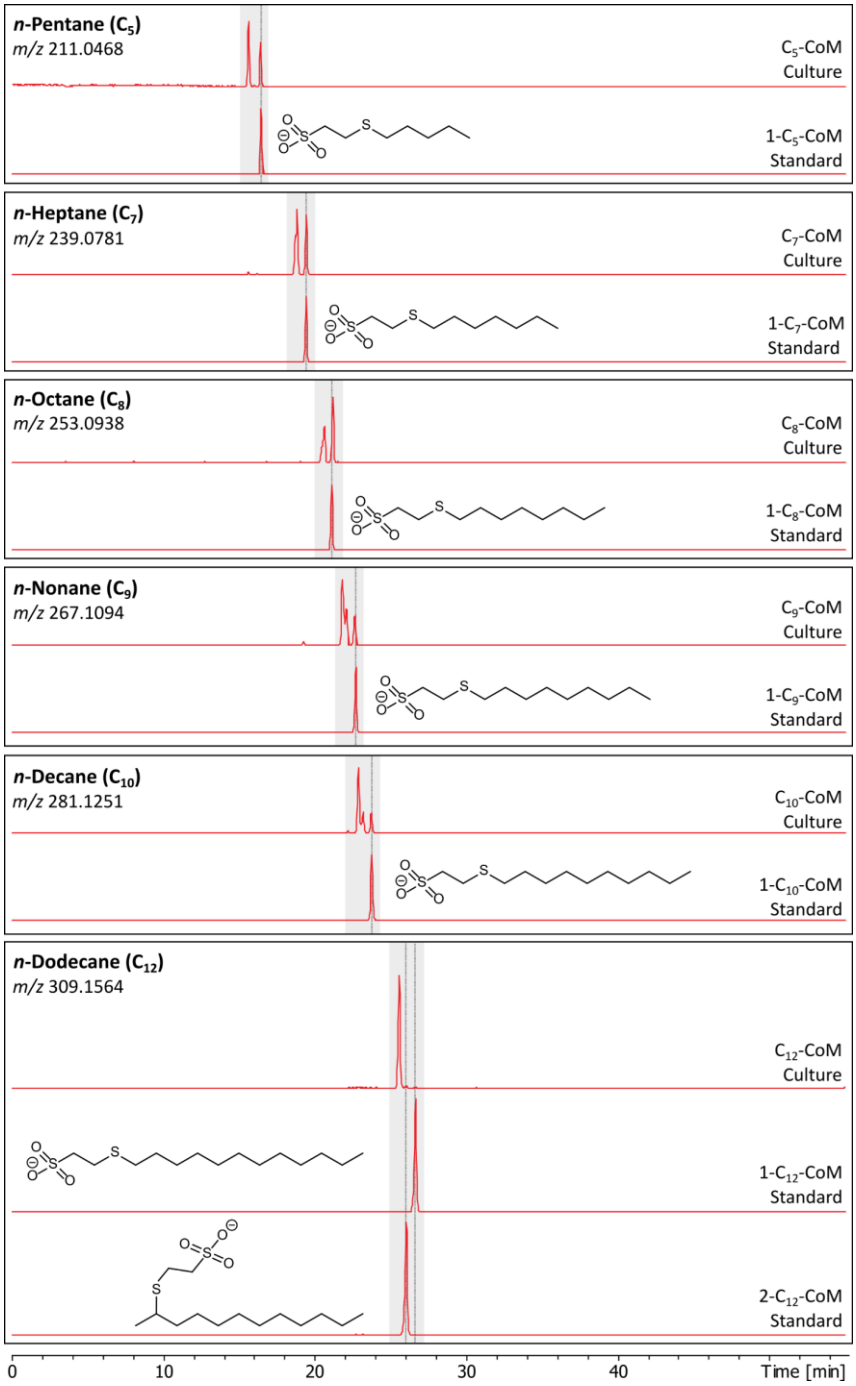


**Extended Data Figure 5 | Detection of alkyl-CoMs in $C_x$-*n*-alkane-degrading cultures.** Samples were separated by liquid chromatography and extracted ion chromatograms (EICs) based on the exact mass of deprotonated ions of the $C_x$-alkyl-CoMs with a window of ±10 mDa were created. Panels show the EICs of culture extracts together with synthetic standards. Dashed vertical lines were added at retention times of peak maxima of standards (**c**) or standards and fragmentation products (**d**) for easier identification of peaks in the culture extracts. Peaks with mass-to-charge ratios (*m/z*) of the respective alkyl-CoM were detected in all cultures. All culture extracts show several peaks, indicating an activation at different carbon atoms. While shorter alkanes are activated to a similar degree at subterminal and terminal positions, longer alkanes are predominantly activated at non-terminal carbon atoms.

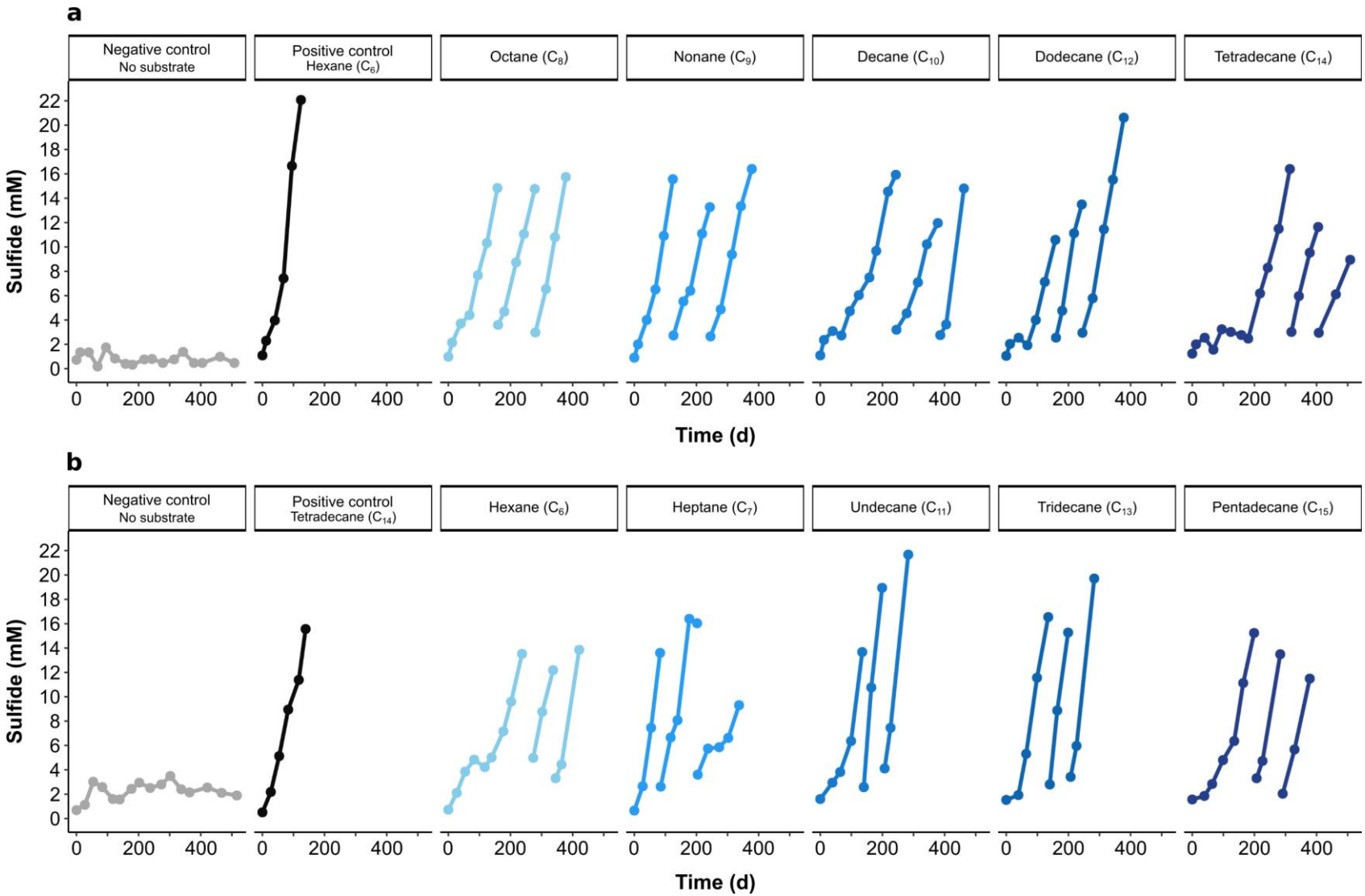


**Extended Data Figure 6 | Substrate spectra of originally (a) *n*-hexane- and (b) *n*-tetradecane-oxidizing enrichment cultures.** Cultures were diluted into fresh sulfate-reducer medium and supplemented with other *n*-alkanes between $C_3$ and $C_{20}$. Only active cultures are shown. No activity was observed for cultures supplied with $C_3$, $C_4$, $C_{16}$, $C_{18}$, or $C_{20}$.

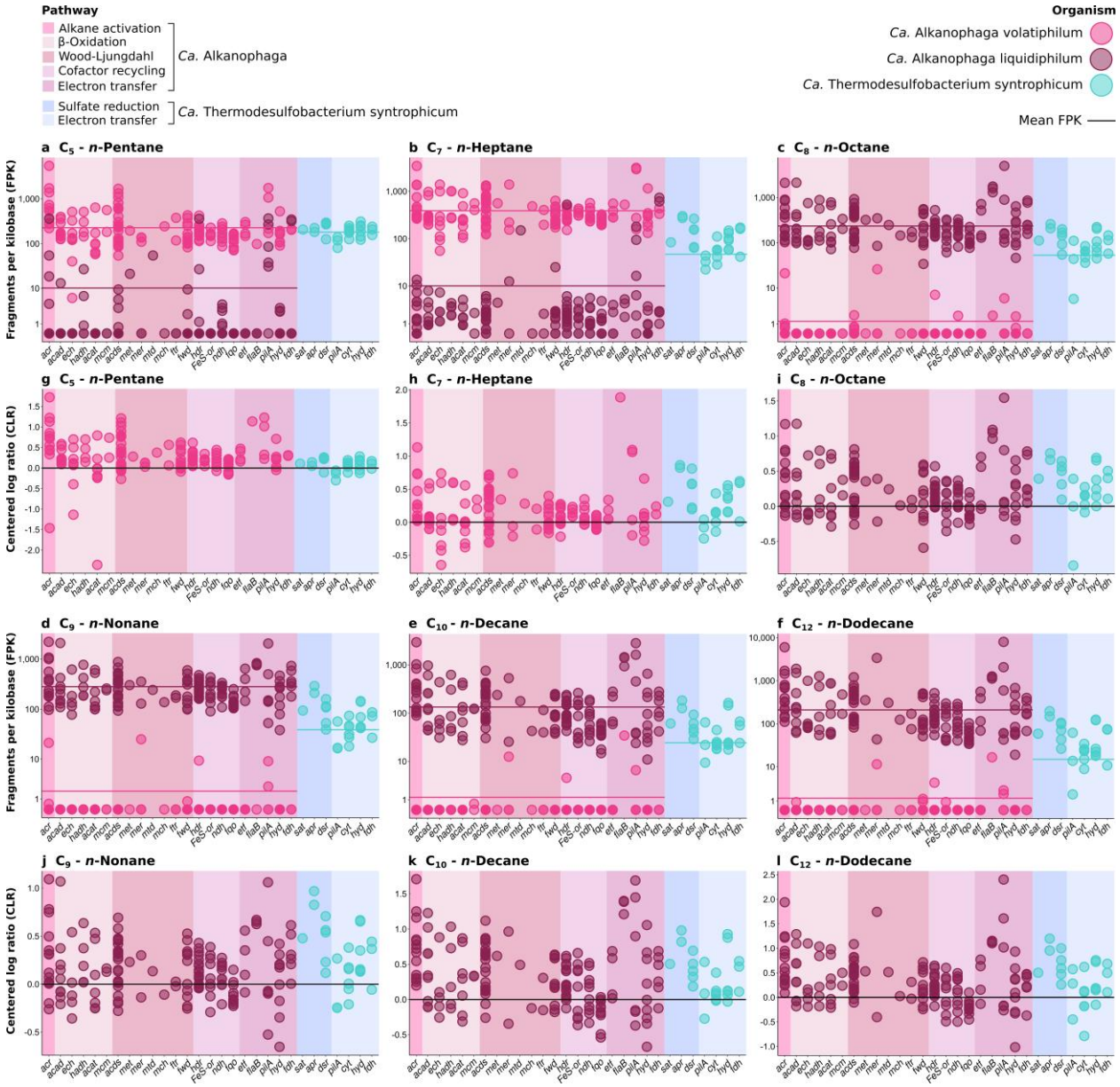


**Extended Data Figure 7 | Expression of alkane oxidation, sulfate reduction, and related genes in $C_5$-$C_{12}$ *n*-alkane-oxidizing cultures.** Transcriptome reads were mapped to the MAGs of the two *Candidatus* Alkanophaga species and to *Ca.* Thermodesulfobacterium syntrophicum. **a-f**, Fragment counts normalized to gene length (FPK) using a logarithmic y axis. The average gene expression of each organism is indicated as arithmetic mean (sum of all FPK values divided by number of genes) depicted as a horizontal line. **g-l**, Fragment counts normalized as centered log ratio (CLR). For simplicity, only values of the more active *Ca.* Alkanophaga species are shown. The x-axis shows the genes encoding: *acr*: alkyl-CoM reductase, *acad*: acyl-CoA dehydrogenase, *ech*: enoyl-CoA hydratase, *hadh*: hydroxyacyl-CoA dehydrogenase, *acat*: acetyl-CoA acetyltransferase, *mcm*: methylmalonyl-CoA mutase, *acds*: acetyl-CoA decarbonylase/synthase, *met*: 5,10-methylene tetrahydrofolate reductase, *mer*: 5,10-methylene tetrahydromethanopterin ($H_4$MPT) reductase, *mtd*: methylene-$H_4$MPT dehydrogenase, *mch*: methenyl-$H_4$MPT cyclohydrolase, *ftr*: formylmethanofuran-$H_4$MPT formyltransferase, *fwd*: tungsten-containing formylmethanofuran dehydrogenase, *hdr*: heterodisulfide reductase, *FeS-or*: [FeS]-oxidoreductase, *ndh*: NADH dehydrogenase, *fqo*: $F_{420}H_2$:quinone oxidoreductase, *etf*: electron transfer flavoprotein, *flaB*: flagellin B, *pilA*: type IV pilin, *hyd*: [NiFe]-hydrogenase, *fdh*: formate dehydrogenase, *sat*: ATP-sulfurylase, *apr*: APS-reductase, *dsr*: dissimilatory sulfite reductase, *cyt*: multi-heme *c*-type cytochrome.

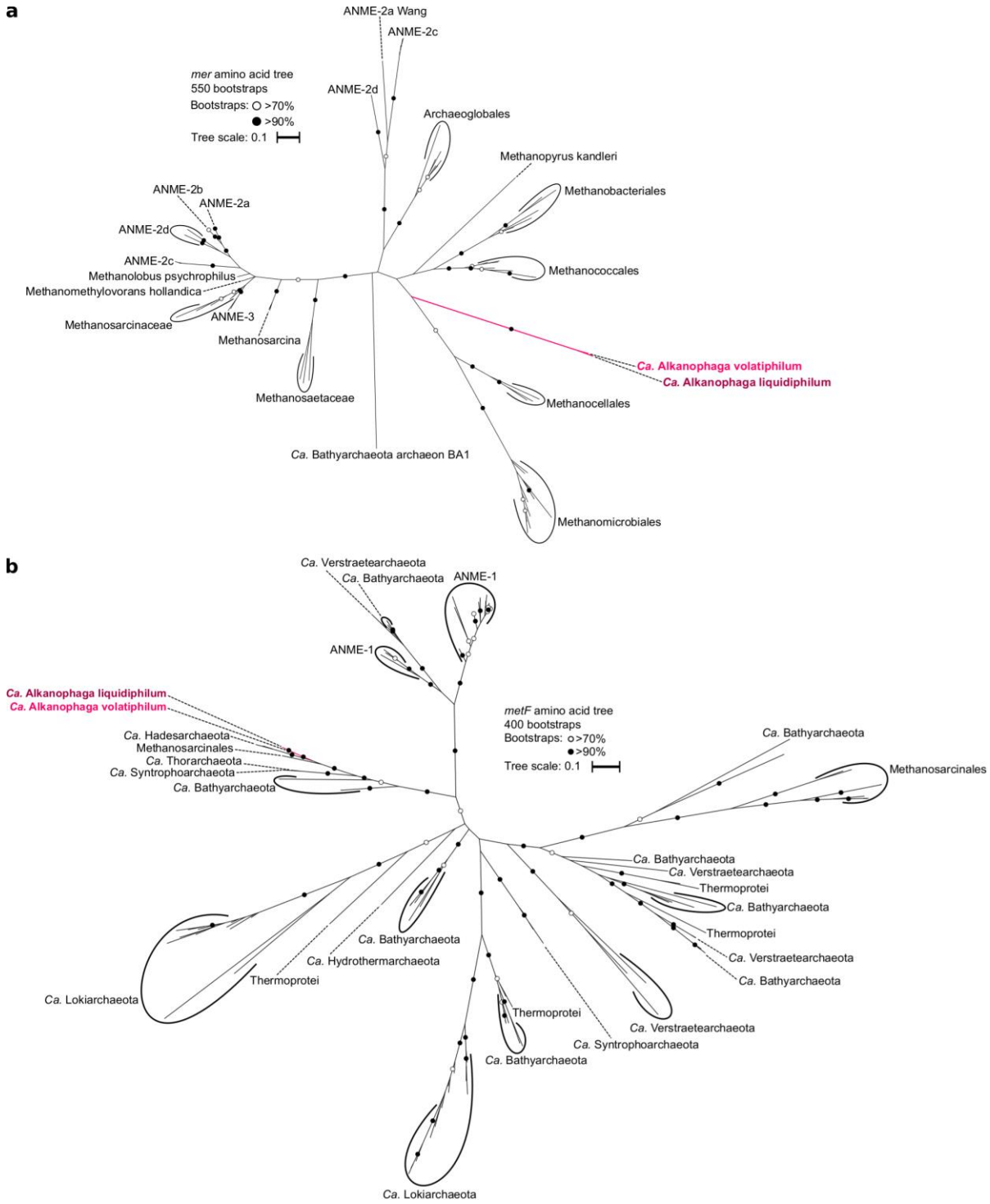


**Extended Data Figure 8 | Phylogenetic placement of (a) 5,10-methylene-$H_4$MPT reductase (*mer*) and (b) methylenetetrahydrofolate reductase (*metF*) sequences recovered from *Ca.* Alkanophaga MAGs.** Both *mer* and *metF* sequences of the two *Ca.* Alkanophaga species are highly similar to each other. The *mer* sequences, which distinguish *Ca.* Alkanophaga in the class Syntrophoarchaeia, might originate from the ancestor of Methanocellales, while *metF* sequences cluster near those of close relatives *Ca.* Syntrophoarchaeales.

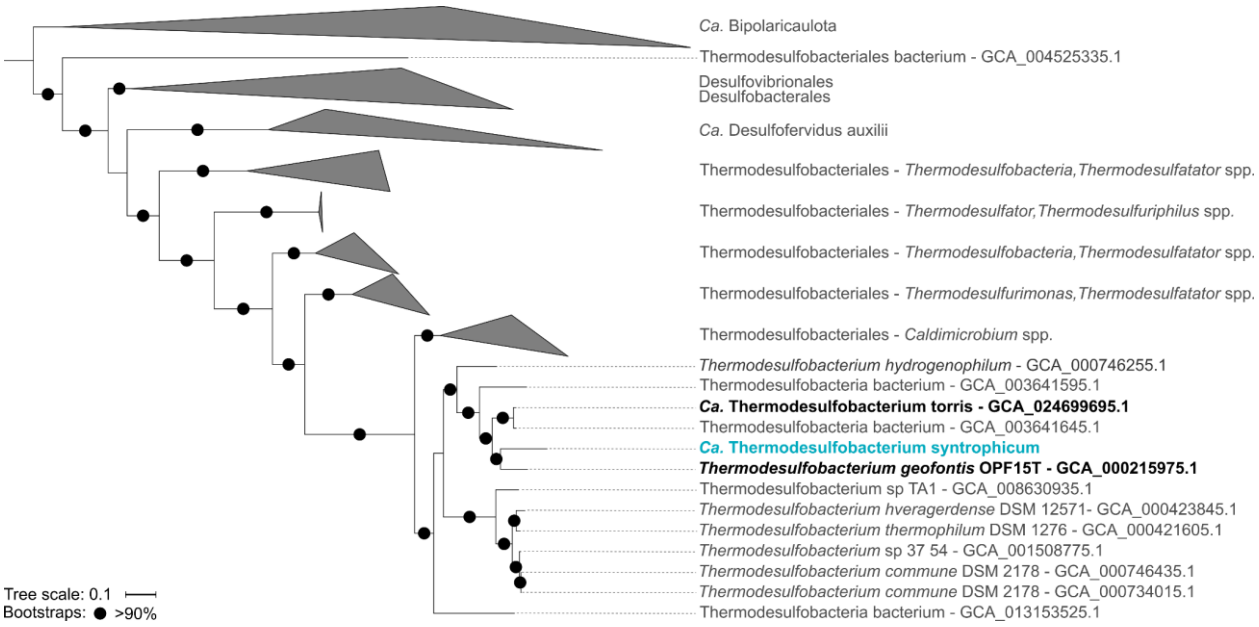


**Extended Data Figure 9 | Phylogenomic placement of *Candidatus* Thermodesulfobacterium syntrophicum based on the concatenated alignment of 71 bacterial single copy core genes.** *Ca.* T. syntrophicum is closely related to the already cultured *Thermodesulfobacterium geofontis* (OPF15T) and to *Ca.* Thermodesulfobacterium torris, which functions as partner bacterium in the thermophilic anaerobic oxidation of methane. The outgroup consists of members of the candidate phylum Bipolauricaulota. The tree scale bar indicates 10% sequence divergence.

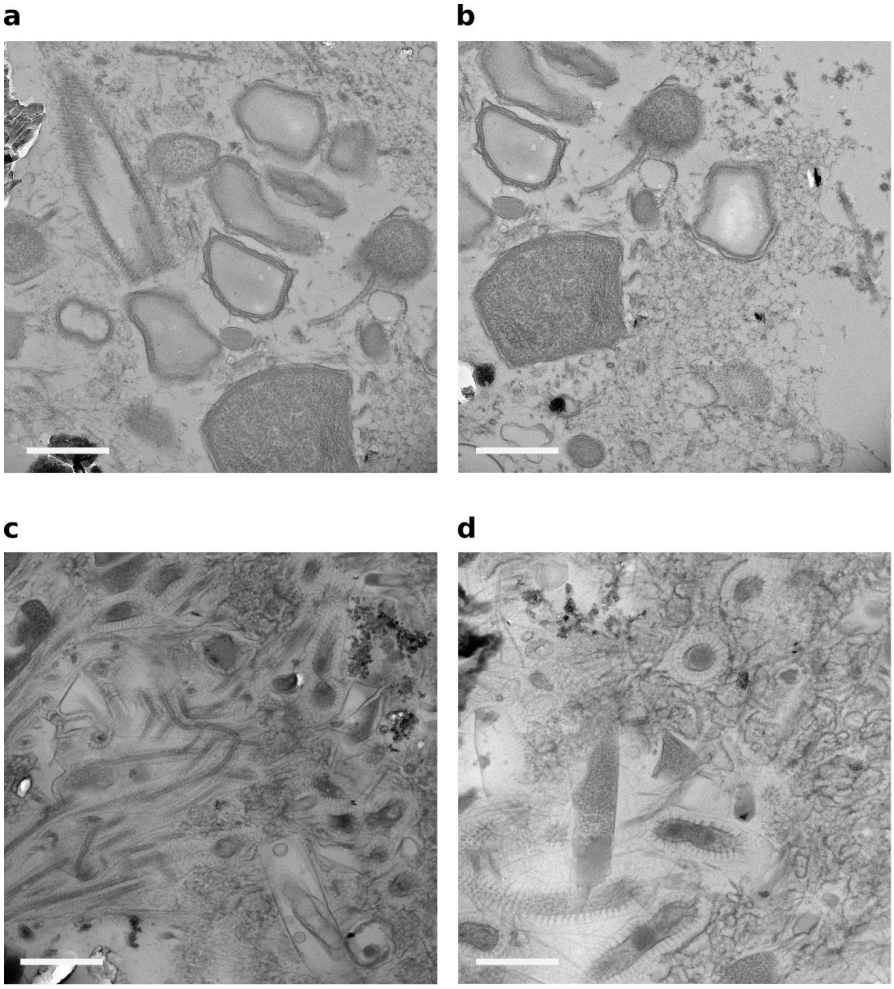


**Extended Data Figure 10 | Transmission electron micrographs of EPON 812-embedded thin-sections of (a,b) $C_6$- and (c,d) $C_{14}$-*n*-alkane-degrading culture samples.** The scale bar indicates 0.5 µm. The experiment was run once with one biological replicate per sample. Images are representative for > 5 recorded images per sample.

## Supplementary Tables

Only the Supplementary Tables 3, 5, and 6 are shown here. The extensive Supplementary Tables 1-10 are available under nature.com/articles/s41564-023-01400-3 in the section "Supplementary information".

### Overview

| | |
|---|---|
| **Supplementary Table 1** | Calculations of doubling times of $C_5$-$C_{14}$-*n*-alkane oxidizing cultures |
| **Supplementary Table 2** | Dissolved inorganic carbon (DIC) production and sulfate reduction values in $C_6$- and $C_{14}$-oxidizing cultures and estimation of carbon assimilation rates |
| **Supplementary Table 3** | Properties of metagenome-assembled genomes (MAGs) of *Candidatus* Alkanophaga and *Ca.* Thermodesulfobacterium syntrophicum |
| **Supplementary Table 4** | Relative abundances of MAGs assembled from $C_5$-$C_{14}$-alkane-oxidizing cultures |
| **Supplementary Table 5** | Coverages of *Ca.* Alkanophaga and *Ca.* T. syntrophicum MAGs in different layers of three push cores of the Guaymas Basin |
| **Supplementary Table 6** | Comparison of *acrA* sequences of *Ca.* Alkanophaga and *Ca.* Syntrophoarchaeum with BLASTp |
| **Supplementary Table 7** | Transcription of alkane oxidation (*Ca.* Alkanophaga) and sulfate reduction (*Ca.* T. syntrophicum) genes in $C_5$-$C_{14}$-alkane-oxidizing cultures |
| **Supplementary Table 8** | Amino acid identities of *Ca.* Alkanophaga, ANME-1, and *Ca.* Syntrophoarchaeum MAGs |
| **Supplementary Table 9** | Hydrogen production in $C_6$- and $C_{14}$-alkane-oxidizing cultures |
| **Supplementary Table 10** | Accession numbers of MAGs included in phylogenomic archaeal and bacterial trees and *mcrA* sequences included in phylogenetic *mcrA* tree |

**Supplementary Table 3 |** Properties of metagenome-assembled genomes (MAGs) of *Candidatus* Alkanophaga and *Ca.* Thermodesulfobacterium syntrophicum.

| | ***Candidatus* Alkanophaga volatiphilum (MAG 4)** | ***Candidatus* Alkanophaga liquidiphilum (MAG 1)** | ***Candidatus* Thermodesulfobacterium syntrophicum (MAG 24)** |
|---|---|---|---|
| Size (base pairs) | 1,850,367 | 1,914,207 | 1,624,405 |
| Contigs | 89 | 89 | 12 |
| Contig N50 (bp) | 41,546 | 37,182 | 232,863 |
| GC content (%) | 53.6 | 51.6 | 32.3 |
| Genes | 1,954 | 2,045 | 1,626 |
| 16S rRNAs | 2 | 1 | 1 |
| 23S rRNAs | 2 | 1 | 2 |
| Completeness (%) | 89.71 | 91.83 | 98.75 |
| Redundancy (%) | 1.31 | 0.65 | 1.67 |
| Strain heterogeneity (%) | 0 | 0 | 0 |

**Supplementary Table 5 |** Coverage of *Candidatus* Alkanophaga and *Ca.* Thermodesulfobacterium syntrophicum MAGs in three push cores of the Guaymas Basin. Coverages were calculated with CoverM using the raw reads as input**.** Environmental descriptions originate from McKay *et al.*, 2016.

| **Metagenome accession** | **SRR 6823441** | **SRR 6478754** | **SRR 6478753** | **SRR 6479061** | **SRR 5214304** | **SRR 6823442** | **SRR 5214303** |
|---|---|---|---|---|---|---|---|
| *Ca.* A. volatiphilum (%) | 1.00 | 0.14 | 0.25 | 0.04 | 0.25 | 0.80 | 38.57 |
| *Ca.* A. liquidiphilum (%) | 0.12 | 0.14 | 0.24 | 0.06 | 0.17 | 0.18 | 4.89 |
| *Ca.* T. syntrophicum (%) | 0.09 | 0.15 | 0.24 | 0.40 | 0.57 | 0.19 | 0.00 |
| Unmapped (%) | 99.73 | 99.57 | 99.27 | 99.50 | 99.01 | 98.84 | 56.54 |
| Core | 4569-2 | 4569-9 | 4569-9 | 4571-4 | 4571-4 | 4571-4 | 4571-4 |
| Depth (cm) | 12-15 | 0-3 | 9-12 | 0-3 | 3-6 | 12-15 | 33-36 |
| Environment | white mat | orange mat | orange mat | white mat | white mat | white mat | white mat |

**Supplementary Table 6 |** Comparison of *acrA* sequences of *Ca.* Alkanophaga and *Ca.* Syntrophoarchaeum with BLASTp.

| ***acrA* #** | **MAG 4 Locus tag** | **MAG 1 Locus tag** | **Amino acid identity (%)** | **Closest related *acrA* from *Ca.* Syntrophoarchaeaum caldarius (identity [%])** | **Closest related *acrA* from *Ca.* Syntrophoarchaeaum butanivorans (identity [%])** |
|---|---|---|---|---|---|
| 1 | OD814_000175 | OD815_001376 | 89.15 | OFV67773.1 (≥ 63) | OFV65760.1 (≥ 66) |
| 2 | OD814_000815 | OD815_001020 | 94.95 | OFV68281.1 (≥ 59) | OFV65745.1 (≥ 60) |
| 3 | OD814_000515 | OD815_001179 | 90.24 | OFV67773.1 (≥ 40) | OFV67021.1 (≥ 57) |

## References


Adam, P. S., Borrel, G., and Gribaldo, S. (2019). An archaeal origin of the Wood–Ljungdahl $H_4$MPT branch and the emergence of bacterial methylotrophy. *Nat. Microbiol.* 4, 2155–2163. doi: 10.1038/s41564-019-0534-2.

Aeckersberg, F., Bak, F., and Widdel, F. (1991). Anaerobic oxidation of saturated hydrocarbons to $CO_2$ by a new type of sulfate-reducing bacterium. *Arch. Microbiol.* 156, 5–14.

Al-Shayeb, B., Schoelmerich, M. C., West-Roberts, J., Valentin-Alvarado, L. E., Sachdeva, R., Mullen, S., et al. (2022). Borgs are giant genetic elements with potential to expand metabolic capacity. *Nature* 610, 731–736. doi: 10.1038/s41586-022-05256-1.

Alm, E. W., Oerther, D. B., Larsen, N., Stahl, D. A., and Raskin, L. (1996). The oligonucleotide probe database. *Appl. Environ. Microbiol.* 62, 3557–3559. doi: 10.1128/aem.62.10.3557-3559.1996.

Altschul, S. F., Gish, W., Miller, W., Myers, E. W., and Lipman, D. J. (1990). Basic local alignment search tool. *J. Mol. Biol.* 215, 403–410. doi: https://doi.org/10.1016/S0022-2836(05)80360-2.

Aramaki, T., Blanc-Mathieu, R., Endo, H., Ohkubo, K., Kanehisa, M., Goto, S., et al. (2020). KofamKOALA: KEGG Ortholog assignment based on profile HMM and adaptive score threshold. *Bioinformatics* 36, 2251–2252. doi: 10.1093/bioinformatics/btz859.

Bankevich, A., Nurk, S., Antipov, D., Gurevich, A. A., Dvorkin, M., Kulikov, A. S., et al. (2012). SPAdes: A New Genome Assembly Algorithm and Its Applications to Single-Cell Sequencing. *J. Comput. Biol.* 19, 455–477. doi: 10.1089/cmb.2012.0021.

Benito Merino, D., Zehnle, H., Teske, A., and Wegener, G. (2022). Deep-branching ANME-1c archaea grow at the upper temperature limit of anaerobic oxidation of methane. *Front. Microbiol.* 13, 1–16. doi: 10.3389/fmicb.2022.988871.

Bertini, I., Cavallaro, G., and Rosato, A. (2006). Cytochrome c: Occurrence and Functions. *Chem. Rev.* 106, 90–115. doi: 10.1021/cr050241v.

Beulig, F., Røy, H., McGlynn, S. E., and Jørgensen, B. B. (2019). Cryptic $CH_4$ cycling in the sulfate–methane transition of marine sediments apparently mediated by ANME-1 archaea. *ISME J.* 13, 250–262. doi: 10.1038/s41396-018-0273-z.

Boetius, A., Ravenschlag, K., Schubert, C. J., Rickert, D., Widdel, F., Gleseke, A., et al. (2000). A marine microbial consortium apparently mediating anaerobic oxidation of methane. *Nature* 407, 623–626. doi: 10.1038/35036572.

Borrel, G., Adam, P. S., McKay, L. J., Chen, L. X., Sierra-García, I. N., Sieber, C. M. K., et al. (2019). Wide diversity of methane and short-chain alkane metabolisms in uncultured archaea. *Nat. Microbiol.* 4, 603–613. doi: 10.1038/s41564-019-0363-3.

Braun, T., Vos, M. R., Kalisman, N., Sherman, N. E., Rachel, R., Wirth, R., et al. (2016). Archaeal flagellin combines a bacterial type IV pilin domain with an Ig-like domain. *Proc. Natl. Acad. Sci. U. S. A.* 113, 10352–10357. doi: 10.1073/pnas.1607756113.

Chadwick, G. L., Skennerton, C. T., Laso-Pérez, R., Leu, A. O., Speth, D. R., Yu, H., et al. (2022). Comparative genomics reveals electron transfer and syntrophic mechanisms differentiating methanotrophic and methanogenic archaea. *PLoS Biol.* 20, 1–71. doi: 10.1371/journal.pbio.3001508.

Chaumeil, P.-A. A., Mussig, A. J., Hugenholtz, P., and Parks, D. H. (2020). GTDB-Tk: a toolkit to classify genomes with the Genome Taxonomy Database. *Bioinformatics* 36, 1925–1927. doi: 10.1093/bioinformatics/btz848.

Chen, S. C., Musat, N., Lechtenfeld, O. J., Paschke, H., Schmidt, M., Said, N., et al. (2019). Anaerobic oxidation of ethane by archaea from a marine hydrocarbon seep. *Nature* 568, 108–111. doi: 10.1038/s41586-019-1063-0.

Claypool, G. E., and Kvenvolden, K. A. (1983). Methane and other hydrocarbon gases in marine sediment. *Annu. Rev. Earth Planet. Sci.* 11, 299–327. doi: 10.1146/annurev.ea.11.050183.001503.

Cord-Ruwisch, R. (1985). A quick method for the determination of dissolved and precipitated sulfides in cultures of sulfate-reducing bacteria. *J. Microbiol. Methods* 4, 33–36. doi: https://doi.org/10.1016/0167-7012(85)90005-3.

Daims, H., Brühl, A., Amann, R., Schleifer, K.-H. H., and Wagner, M. (1999). The domain-specific probe EUB338 is insufficient for the detection of all bacteria: Development and evaluation of a more comprehensive probe set. *Syst. Appl. Microbiol.* 22, 434–444. doi: 10.1016/S0723-2020(99)80053-8.

Danecek, P., Bonfield, J. K., Liddle, J., Marshall, J., Ohan, V., Pollard, M. O., et al. (2021). Twelve years of SAMtools and BCFtools. *Gigascience* 10, giab008. doi: 10.1093/gigascience/giab008.

Dolan, S. K., Wijaya, A., Geddis, S. M., Spring, D. R., Silva-Rocha, R., and Welch, M. (2018). Loving the poison: the methylcitrate cycle and bacterial pathogenesis. *Microbiology* 164, 251–259. doi: https://doi.org/10.1099/mic.0.000604.

Dombrowski, N., Teske, A. P., and Baker, B. J. (2018). Expansive microbial metabolic versatility and biodiversity in dynamic Guaymas Basin hydrothermal sediments. *Nat. Commun.* 9. doi: 10.1038/s41467-018-07418-0.

Edgar, R. C. (2004). MUSCLE: multiple sequence alignment with high accuracy and high throughput. *Nucleic Acids Res.* 32, 1792–1797. doi: 10.1093/nar/gkh340.

Eren, A. M., Esen, O. C., Quince, C., Vineis, J. H., Morrison, H. G., Sogin, M. L., et al. (2015). Anvi'o: An advanced analysis and visualization platform for 'omics data. *PeerJ* 2015, 3:e1319. doi: 10.7717/peerj.1319.

Fischer, M. A., Güllert, S., Neulinger, S. C., Streit, W. R., and Schmitz, R. A. (2016). Evaluation of 16S rRNA Gene Primer Pairs for Monitoring Microbial Community Structures Showed High Reproducibility within and Low Comparability between Datasets Generated with Multiple Archaeal and Bacterial Primer Pairs. *Front. Microbiol.* 7. doi: 10.3389/fmicb.2016.01297.

Gouy, M., Tannier, E., Comte, N., and Parsons, D. P. (2021). "Seaview Version 5: A Multiplatform Software for Multiple Sequence Alignment, Molecular Phylogenetic Analyses, and Tree Reconciliation," in *Multiple Sequence Alignment: Methods and Protocols*, ed. K. Katoh (New York, NY: Springer US), 241–260. doi: 10.1007/978-1-0716-1036-7_15.

Gruber-Vodicka, H. R., Seah, B. K. B., and Pruesse, E. (2022). phyloFlash: Rapid Small-Subunit rRNA Profiling and Targeted Assembly from Metagenomes. *mSystems* 5, e00920-20. doi: 10.1128/mSystems.00920-20.

Gunsalus, R. P., Romesser, J. A., and Wolfe, R. S. (1978). Preparation of coenzyme M analogs and their activity in the methyl coenzyme M reductase system of *Methanobacterium thermoautotrophicum*. *Biochemistry* 17, 2374–2377. doi: 10.1021/bi00605a019.

Hahn, C. J., Laso-Pérez, R., Vulcano, F., Vaziourakis, K.-M., Stokke, R., Steen, I. H., et al. (2020). *Candidatus* Ethanoperedens, a Thermophilic Genus of Archaea Mediating the Anaerobic Oxidation of Ethane. *MBio* 11, e00600-20. doi: 10.1128/mBio.00600-20.

Hahn, C. J., Lemaire, O. N., Engilberge, S., Wegener, G., and Wagner, T. (2021). Crystal structure of a key enzyme for anaerobic ethane activation. *Science* 373, 118–121.

Hallam, S. J., Girguis, P. R., Preston, C. M., Richardson, P. M., and DeLong, E. F. (2003). Identification of Methyl Coenzyme M Reductase A (*mcrA*) Genes Associated with Methane-Oxidizing Archaea. *Appl. Environ. Microbiol.* 69, 5483–5491. doi: 10.1128/AEM.69.9.5483-5491.2003.

Hamilton-Brehm, S. D., Gibson, R. A., Green, S. J., Hopmans, E. C., Schouten, S., van der Meer, M. T. J., et al. (2013). *Thermodesulfobacterium geofontis* sp. nov., a hyperthermophilic, sulfate-reducing bacterium isolated from Obsidian Pool, Yellowstone National Park. *Extremophiles* 17, 251–263. doi: 10.1007/s00792-013-0512-1.

Haug, K., Cochrane, K., Nainala, V. C., Williams, M., Chang, J., Jayaseelan, K. V., et al. (2020). MetaboLights: a resource evolving in response to the needs of its scientific community. *Nucleic Acids Res.* 48, D440–D444. doi: 10.1093/nar/gkz1019.

He, X., Chadwick, G. L., Kempes, C. P., Orphan, V. J., and Meile, C. (2021). Controls on interspecies electron transport and size limitation of anaerobically methane-oxidizing microbial consortia. *MBio* 12. doi: 10.1128/mBio.03620-20.

Hinrichs, K.-U., Hayes, J. M., Sylva, S. P., Brewer, P. G., and DeLong, E. F. (1999). Methane-consuming archaebacteria in marine sediments. *Nature* 398, 802–805. doi: 10.1038/19751.

Holler, T., Widdel, F., Knittel, K., Amann, R., Kellermann, M. Y., Hinrichs, K. U., et al. (2011). Thermophilic anaerobic oxidation of methane by marine microbial consortia. *ISME J.* 5, 1946–1956. doi: 10.1038/ismej.2011.77.

Hua, Z.-S., Wang, Y.-L., Evans, P. N., Qu, Y.-N., Goh, K. M., Rao, Y.-Z., et al. (2019). Insights into the ecological roles and evolution of methyl-coenzyme M reductase-containing hot spring Archaea. *Nat. Commun.* 10, 1–11. doi: 10.1038/s41467-019-12574-y.

Jain, C., Rodriguez-R, L. M., Phillippy, A. M., Konstantinidis, K. T., and Aluru, S. (2018). High throughput ANI analysis of 90K prokaryotic genomes reveals clear species boundaries. *Nat. Commun.* 9, 1–8. doi:

10.1038/s41467-018-07641-9.

Johansen, N. G., Ettre, L. S., and Miller, R. L. (1983). Quantitative Analysis of Hydrocarbons by Structural Group Type in Gasolines and Distillates: I. Gas Chromatography. *J. Chromatogr. A* 256, 393–417. doi: https://doi.org/10.1016/S0021-9673(01)88258-3.

Kanehisa, M., Furumichi, M., Tanabe, M., Sato, Y., and Morishima, K. (2017). KEGG: new perspectives on genomes, pathways, diseases and drugs. *Nucleic Acids Res.* 45, D353–D361. doi: 10.1093/nar/gkw1092.

Katoh, K., Asimenos, G., and Toh, H. (2009). "Multiple Alignment of DNA Sequences with MAFFT," in *Bioinformatics for DNA Sequence Analysis*, ed. D. Posada (Totowa, NJ: Humana Press), 39–64. doi: 10.1007/978-1-59745-251-9_3.

Kawka, O. E., and Simoneit, B. R. T. (1987). Survey of hydrothermally-generated petroleums from the Guaymas Basin spreading center. *Org. Geochem.* 11, 311–328. doi: 10.1016/0146-6380(87)90042-8.

Kim, D., Song, L., Breitwieser, F. P., and Salzberg, S. L. (2016). Centrifuge: Rapid and sensitive classification of metagenomic sequences. *Genome Res.* 26, 1721–1729. doi: 10.1101/gr.210641.116.

Kissin, Y. V. (1987). Catagenesis and composition of petroleum: Origin of *n*-alkanes and isoalkanes in petroleum crudes. *Geochim. Cosmochim. Acta* 51, 2445–2457. doi: 10.1016/0016-7037(87)90296-1.

Kniemeyer, O., Musat, F., Sievert, S. M., Knittel, K., Wilkes, H., Blumenberg, M., et al. (2007). Anaerobic oxidation of short-chain hydrocarbons by marine sulphate-reducing bacteria. *Nature* 449, 898–901. doi: 10.1038/nature06200.

Konstantinidis, K. T., Rosselló-Móra, R., and Amann, R. (2017). Uncultivated microbes in need of their own taxonomy. *ISME J.* 11, 2399–2406. doi: 10.1038/ismej.2017.113.

Krukenberg, V., Harding, K., Richter, M., Glöckner, F. O., Gruber-Vodicka, H. R., Adam, B., et al. (2016). *Candidatus* Desulfofervidus auxilii, a hydrogenotrophic sulfate-reducing bacterium involved in the thermophilic anaerobic oxidation of methane. *Environ. Microbiol.* 18, 3073–3091. doi: 10.1111/1462-2920.13283.

Langmead, B., and Salzberg, S. L. (2012). Fast gapped-read alignment with Bowtie 2. *Nat. Methods* 9, 357–359. doi: 10.1038/nmeth.1923.

Laso-Pérez, R., Krukenberg, V., Musat, F., and Wegener, G. (2018). Establishing anaerobic hydrocarbon-degrading enrichment cultures of microorganisms under strictly anoxic conditions. *Nat. Protoc.* 13, 1310–1330. doi: 10.1038/nprot.2018.030.

Laso-Pérez, R., Wegener, G., Knittel, K., Widdel, F., Harding, K. J., Krukenberg, V., et al. (2016). Thermophilic archaea activate butane via alkyl-coenzyme M formation. *Nature* 539, 396–401. doi: 10.1038/nature20152.

Laso-Pérez, R., Wu, F., Crémière, A., Speth, D. R., Magyar, J. S., Krupovic, M., et al. (2023). Evolutionary Diversification of Methanotrophic *Ca.* Methanophagales (ANME-1) and Their Expansive Virome. *Nat. Microbiol.* 8, 231–245. doi: 10.1101/2022.07.04.498658.

Lemaire, O. N., and Wagner, T. (2022). A Structural View of Alkyl-Coenzyme M Reductases, the First Step of Alkane Anaerobic Oxidation Catalyzed by Archaea. *Biochemistry* 61, 805–821. doi: 10.1021/acs.biochem.2c00135.

Letunic, I., and Bork, P. (2011). Interactive Tree Of Life v2: online annotation and display of phylogenetic trees made easy. *Nucleic Acids Res.* 39, W475–W478. doi: 10.1093/nar/gkr201.

Liao, Y., Smyth, G. K., and Shi, W. (2014). FeatureCounts: An efficient general purpose program for assigning sequence reads to genomic features. *Bioinformatics* 30, 923–930. doi: 10.1093/bioinformatics/btt656.

Ludwig, W., Strunk, O., Westram, R., Richter, L., Meier, H., Yadhukumar, A., et al. (2004). ARB: A software environment for sequence data. *Nucleic Acids Res.* 32, 1363–1371. doi: 10.1093/nar/gkh293.

Lynes, M. M., Krukenberg, V., Jay, Z. J., Kohtz, A. J., Gobrogge, C. A., Spietz, R. L., et al. (2023). Diversity and function of methyl-coenzyme M reductase-encoding archaea in Yellowstone hot springs revealed by metagenomics and mesocosm experiments. *ISME Commun.* 3, 22. doi: 10.1038/s43705-023-00225-9.

Ma, K., and Thauer, R. K. (1990). Purification and properties of $N^5$, $N^{10}$-methylenetetrahydromethanopterin reductase from *Methanobacterium thermoautotrophicum* (strain Marburg). *Eur. J. Biochem.* 191, 187–193. doi: https://doi.org/10.1111/j.1432-1033.1990.tb19109.x.

Maden, H., and Edward, B. (1996). Why methanopterin? Comparative bioenergetics of the reactions catalyzed by methylene tetrahydrofolate reductase and methylene tetrahydromethanopterin reductase. *Biochem. Soc.*

*Trans.* 24, 466S-466S. doi: 10.1042/bst024466s.

Marietou, A. (2021). "Sulfate reducing microorganisms in high temperature oil reservoirs," in *Advances in Applied Microbiology*, eds. G. M. Gadd and S. Sariaslani (Elsevier Inc.), 99–131. doi: 10.1016/bs.aambs.2021.03.004.

Mbadinga, S. M., Wang, L. Y., Zhou, L., Liu, J. F., Gu, J. D., and Mu, B. Z. (2011). Microbial communities involved in anaerobic degradation of alkanes. *Int. Biodeterior. Biodegrad.* 65, 1–13. doi: 10.1016/j.ibiod.2010.11.009.

McKay, L., Klokman, V. W., Mendlovitz, H. P., Larowe, D. E., Hoer, D. R., Albert, D., et al. (2016). Thermal and geochemical influences on microbial biogeography in the hydrothermal sediments of Guaymas Basin, Gulf of California. *Environ. Microbiol. Rep.* 8, 150–161. doi: 10.1111/1758-2229.12365.

Mistry, J., Chuguransky, S., Williams, L., Qureshi, M., Salazar, G. A., Sonnhammer, E. L. L., et al. (2021). Pfam: The protein families database in 2021. *Nucleic Acids Res.* 49, D412–D419. doi: 10.1093/nar/gkaa913.

Natarajan, V. P., Zhang, X., Morono, Y., Inagaki, F., and Wang, F. (2016). A modified SDS-based DNA extraction method for high quality environmental DNA from seafloor environments. *Front. Microbiol.* 7. doi: 10.3389/fmicb.2016.00986.

Ono, Y., Takeuchi, Y., and Hisanaga, N. (1981). A comparative study on the toxicity of *n*-hexane and its isomers on the peripheral nerve. *Int. Arch. Occup. Environ. Health* 48, 289–294. doi: 10.1007/BF00405616.

Parks, D. H., Imelfort, M., Skennerton, C. T., Hugenholtz, P., and Tyson, G. W. (2015). CheckM: Assessing the quality of microbial genomes recovered from isolates, single cells, and metagenomes. *Genome Res.* 25, 1043–1055. doi: 10.1101/gr.186072.114.

Quast, C., Pruesse, E., Yilmaz, P., Gerken, J., Schweer, T., Yarza, P., et al. (2013). The SILVA ribosomal RNA gene database project: improved data processing and web-based tools. *Nucleic Acids Res.* 41, D590–D596. doi: 10.1093/nar/gks1219.

Rabus, R., Hansen, T. A., and Widdel, F. (2013). "Dissimilatory Sulfate- and Sulfur-Reducing Prokaryotes," in *The Prokaryotes: Prokaryotic Physiology and Biochemistry*, eds. E. Rosenberg, E. F. DeLong, S. Lory, E. Stackebrandt, and F. Thompson (Berlin Heidelberg: Springer Berlin Heidelberg), 309–404. doi: 10.1007/978-3-642-30141-4_70.

Rabus, R., and Widdel, F. (1995). Anaerobic degradation of ethylbenzene and other aromatic hydrocarbons by new denitrifying bacteria. *Arch. Microbiol.* 163, 96–103. doi: 10.1007/BF00381782.

Rabus, R., Wilkes, H., Behrends, A., Armstroff, A., Fischer, T., Pierik, A. J., et al. (2001). Anaerobic Initial Reaction of *n*-Alkanes in a Denitrifying Bacterium: Evidence for (1-Methylpentyl)succinate as Initial Product and for Involvement of an Organic Radical in *n*-Hexane Metabolism. *J. Bacteriol.* 183, 1707–1715. doi: 10.1128/JB.183.5.1707-1715.2001.

Rojo, F. (2009). Degradation of alkanes by bacteria. *Environ. Microbiol.* 11, 2477–2490. doi: https://doi.org/10.1111/j.1462-2920.2009.01948.x.

Rotaru, A.-E., Shrestha, P. M., Liu, F., Markovaite, B., Chen, S., Nevin, K. P., et al. (2014). Direct interspecies electron transfer between *Geobacter metallireducens* and *Methanosarcina barkeri*. *Appl. Environ. Microbiol.* 80, 4599–4605. doi: 10.1128/AEM.00895-14.

Rotaru, A.-E., Shrestha, P. M., Liu, F., Ueki, T., Nevin, K., Summers, Z. M., et al. (2012). Interspecies electron transfer via hydrogen and formate rather than direct electrical connections in cocultures of *Pelobacter carbinolicus* and *Geobacter sulfurreducens*. *Appl. Environ. Microbiol.* 78, 7645–7651. doi: 10.1128/AEM.01946-12.

Sakai, S., Imachi, H., Hanada, S., Ohashi, A., Harada, H., and Kamagata, Y. (2008). *Methanocella paludicola* gen. nov., sp. nov., a methane-producing archaeon, the first isolate of the lineage 'Rice Cluster I', and proposal of the new archaeal order Methanocellales ord. nov. *Int. J. Syst. Evol. Microbiol.* 58, 929–936. doi: https://doi.org/10.1099/ijs.0.65571-0.

Scheller, S., Goenrich, M., Boecher, R., Thauer, R. K., and Jaun, B. (2010). The key nickel enzyme of methanogenesis catalyses the anaerobic oxidation of methane. *Nature* 465, 606–608. doi: 10.1038/nature09015.

Schulz, H. (1991). Beta oxidation of fatty acids. *Biochim. Biophys. Acta - Lipids Lipid Metab.* 1081, 109–120. doi: https://doi.org/10.1016/0005-2760(91)90015-A.

Seemann, T. (2014). Prokka: rapid prokaryotic genome annotation. *Bioinformatics* 30, 2068–2069. doi: 10.1093/bioinformatics/btu153.

Simoneit, B. R. T. (1990). Petroleum generation, an easy and widespread process in hydrothermal systems: an overview. *Appl. Geochemistry* 5, 3–15. doi: 10.1016/0883-2927(90)90031-Y.

Stamatakis, A. (2014). RAxML version 8: a tool for phylogenetic analysis and post-analysis of large phylogenies. *Bioinformatics* 30, 1312–1313. doi: 10.1093/bioinformatics/btu033.

Stokke, R., Roalkvam, I., Lanzen, A., Haflidason, H., and Steen, I. H. (2012). Integrated metagenomic and metaproteomic analyses of an ANME-1-dominated community in marine cold seep sediments. *Environ. Microbiol.* 14, 1333–1346. doi: https://doi.org/10.1111/j.1462-2920.2012.02716.x.

Studer, D., Michel, M., and Müller, M. (1989). High pressure freezing comes of age. *Scanning Microsc. Suppl.* 3, 253–68; discussion 268-9. Available at: http://europepmc.org/abstract/MED/2694271.

Summers, Z. M., Fogarty, H. E., Leang, C., Franks, A. E., Malvankar, N. S., and Lovley, D. R. (2010). Direct Exchange of Electrons Within Aggregates of an Evolved Syntrophic Coculture of Anaerobic Bacteria. *Science* 330, 1413–1416.

Tatusov, R. L., Koonin, E. V, and Lipman, D. J. (1997). A Genomic Perspective on Protein Families. *Science* 278, 631–637. doi: 10.1126/science.278.5338.631.

Teske, A., De Beer, D., McKay, L. J., Tivey, M. K., Biddle, J. F., Hoer, D., et al. (2016). The Guaymas Basin hiking guide to hydrothermal mounds, chimneys, and microbial mats: Complex seafloor expressions of subsurface hydrothermal circulation. *Front. Microbiol.* 7, 1–23. doi: 10.3389/fmicb.2016.00075.

Trac, L. N., Schmidt, S. N., and Mayer, P. (2018). Headspace passive dosing of volatile hydrophobic chemicals – Aquatic toxicity testing exactly at the saturation level. *Chemosphere* 211, 694–700. doi: https://doi.org/10.1016/j.chemosphere.2018.07.150.

Vishnoi, S. C., Bhagat, S. D., Kapoor, V. B., Chopra, S. K., and Krishna, R. (1987). Simple gas chromatographic determination of the distribution of normal alkanes in the kerosene fraction of petroleum. *Analyst* 112, 49–52. doi: 10.1039/AN9871200049.

Walker, D. J. F., Martz, E., Holmes, D. E., Zhou, Z., Nonnenmann, S. S., Lovley, D. R., et al. (2019). The Archaellum of *Methanospirillum hungatei* Is Electrically Conductive. *MBio* 10, e00579-19. doi: 10.1128/mBio.00579-19.

Wang, Y., Wegener, G., Hou, J., Wang, F., and Xiao, X. (2019). Expanding anaerobic alkane metabolism in the domain of Archaea. *Nat. Microbiol.* 4, 595–602. doi: 10.1038/s41564-019-0364-2.

Wang, Y., Wegener, G., Williams, T. A., Xie, R., Hou, J., Wang, F., et al. (2021). A methylotrophic origin of methanogenesis and early divergence of anaerobic multicarbon alkane metabolism. *Sci. Adv.* 7. doi: 10.1126/sciadv.abh1051.

Watkinson, R. J., and Morgan, P. (1990). Physiology of aliphatic hydrocarbon-degrading microorganisms. *Biodegradation* 1, 79–92. doi: 10.1007/BF00058828.

Wegener, G., Krukenberg, V., Riedel, D., Tegetmeyer, H. E., and Boetius, A. (2015). Intercellular wiring enables electron transfer between methanotrophic archaea and bacteria. *Nature* 526, 587–590. doi: 10.1038/nature15733.

Wegener, G., Laso-Pérez, R., Orphan, V. J., and Boetius, A. (2022). Anaerobic Degradation of Alkanes by Marine Archaea. *Annu. Rev. Microbiol.* 76, 553–577. doi: 10.1146/annurev-micro-111021-045911.

Wilhelms, A., Larter, S. R., Head, I., Farrimond, P., di-Primio, R., and Zwach, C. (2001). Biodegradation of oil in uplifted basins prevented by deep-burial sterilization. *Nature* 411, 1034–1037. doi: 10.1038/35082535.

Wongkittichote, P., Ah Mew, N., and Chapman, K. A. (2017). Propionyl-CoA carboxylase – A review. *Mol. Genet. Metab.* 122, 145–152. doi: https://doi.org/10.1016/j.ymgme.2017.10.002.

Yee, M. O., and Rotaru, A.-E. (2020). Extracellular electron uptake in Methanosarcinales is independent of multiheme c-type cytochromes. *Sci. Rep.* 10, 1–12. doi: 10.1038/s41598-019-57206-z.

Zhou, Z., Zhang, C., Liu, P., Fu, L., Laso-Pérez, R., Yang, L., et al. (2022). Non-syntrophic methanogenic hydrocarbon degradation by an archaeal species. *Nature* 601, 257–262. doi: 10.1038/s41586-021-04235-2.

## Manuscript 2

# Anaerobic oxidation of benzene and naphthalene by thermophilic microorganisms from the Guaymas Basin

Hanna Zehnle, Carolin Otersen, David Benito Merino, Gunter Wegener

Submitted to

*Frontiers in Microbiology*

Submitted: 18.08.2023

# Anaerobic oxidation of benzene and naphthalene by thermophilic microorganisms from the Guaymas Basin

Hanna Zehnle[1,2,3], Carolin Otersen[1], David Benito Merino[1,3], and Gunter Wegener[1,2]

1. Max Planck Institute for Marine Microbiology, 28359 Bremen, Germany
2. MARUM, Center for Marine Environmental Science, 28359 Bremen, Germany
3. Faculty of Geosciences, University of Bremen, 28359 Bremen, Germany

Correspondence: hzehnle@mpi-bremen.de; gwegener@marum.de

## Abstract

Unsubstituted aromatic hydrocarbons (UAHs) are recalcitrant molecules abundant in crude oil, which is accumulated in subsurface reservoirs and occasionally enters the marine environment through natural seepage or human-caused spillage. The challenging anaerobic degradation of UAHs by microorganisms, in particular under thermophilic conditions, is poorly understood. Here, we established benzene- and naphthalene-degrading cultures under sulfate-reducing conditions at 50 °C and 70 °C from Guaymas Basin sediments. Dependent on the combination of UAH and temperature, different microorganisms became enriched. A Thermoplasmatota archaeon was abundant in the benzene-degrading culture at 50 °C, but catabolic pathways remained elusive, because the archaeon lacked most known genes for benzene degradation. Two novel species of Desulfatiglandales bacteria were strongly enriched in the benzene-degrading culture at 70 °C and in the naphthalene-degrading culture at 50 °C. Both bacteria encode almost complete pathways for UAH activation and for downstream degradation. They likely activate benzene via methylation, and naphthalene via direct carboxylation, respectively. The two species constitute the first thermophilic UAH degraders of the Desulfatiglandales. In the naphthalene culture incubated at 70 °C, a Dehalococcoidia bacterium became enriched, which encoded a partial pathway for UAH degradation. Comparison of enriched bacteria with related genomes from environmental samples indicated that pathways for benzene degradation are widely distributed, while thermophily and capacity for naphthalene activation are rare. Our study highlights the capacities of uncultured thermophilic microbes for UAH degradation in petroleum reservoirs and in contaminated environments.

### Key words

Anaerobic hydrocarbon oxidation, unsubstituted aromatic hydrocarbons, petroleum hydrocarbons, thermophily, Thermoplasmatota, Desulfatiglandales, Dehalococcoidia, bioremediation, Guaymas Basin

## Introduction

Aromatic hydrocarbons (AHs) are a naturally abundant group of hydrocarbons. They are highly hydrophobic and extremely stable molecules because of their planar conformation consisting of one or more six-carbon ring systems stabilized by delocalized π electrons (Aihara, 1992). AHs constitute a major part (20-60%) of petroleum and fossil fuel, and are thus naturally abundant in subsurface petroleum reservoirs (Gibson, 1975; Pevneva et al., 2017). On Earth's surface, AHs originate mainly from incomplete combustion of fossil fuel (Blumer, 1976; Lima et al., 2005), from natural seepage on the ocean floor, and from accidental spillage during oil reservoir exploration or transport (Kawka and Simoneit, 1990; Wang et al., 1999).

The study of AH biodegradation is of high interest, because AHs are highly toxic and thus their release into the environment is associated with health hazards (WHO Regional Office for Europe, 2000). Moreover, it is important to understand dynamics of hydrocarbon degradation in deeply buried petroleum reservoirs. Despite the toxicity of AHs, microorganisms have developed metabolic pathways to degrade these compounds. Microbial degradation is the main mechanism of AH removal from the environment. AH degradation pathways differ fundamentally in the presence and absence of molecular oxygen. (Alexander, 1981; Parales et al., 2002; Parales and Haddock, 2004; Fuchs et al., 2011). Under oxic conditions, many bacteria and some halophilic archaea degrade AHs rapidly after activation via oxygenases (Bugg, 2003; Fahy et al., 2006; Tapilatu et al., 2010; Erdoğmuş et al., 2013). After ring cleavage, products converge as central intermediates like acetate, pyruvate, and succinate, which are shuttled into biomass production or enter central metabolic pathways (Fuchs, 1999). Anaerobic AH degradation yields less energy and sustains slower growth rates, therefore cultivation of the respective organisms is challenging. Still, successful enrichment or pure cultures have been produced, which have allowed insights into the mechanisms of anaerobic AH degradation. Unsubstituted AHs (UAHs), i.e. AHs without functional groups, are especially challenging to degrade and the rate-limiting step is the initial activation of the very stable aromatic ring system (Heider, 2007).

Under anoxic conditions, benzene, the smallest UAH, is oxidized by mesophilic bacteria under sulfate-, nitrate-, iron-, and manganese-reducing and in syntrophic consortia with methanogenic archaea (Musat and Widdel, 2008; Villatoro-Monzón et al., 2008; Zhang et al., 2012; Atashgahi et al., 2018; Toth et al., 2021). While methylation to toluene and hydroxylation to phenol have been proposed as activation mechanisms, carboxylation to benzoate has become the favored pathway (Ulrich et al., 2005; Abu Laban et al., 2009; Zhang et al., 2013; Eziuzor et al., 2022). Enzymes for direct methylation or hydroxylation of benzene are currently unknown, but an anaerobic benzene carboxylase (AbcAD) belonging to the UbiD/UbiX-type carboxylases was identified in iron-reducing enrichment cultures of *Peptococcaceae* bacteria (Abu Laban et al., 2010; Luo et al., 2014). All activation pathways converge in the central intermediate benzoyl-CoA (BCoA) (Porter and Young, 2014). Then, the aromatic ring system becomes dearomatized by ATP-dependent Class I benzoyl-CoA reductase (BCR) or ATP-independent class II BCR

(Boll et al., 1997, 2000; Song and Ward, 2005; Wischgoll et al., 2005; Porter and Young, 2014; Huwiler et al., 2019). Subsequent ring fissure occurs via *Thauera* type or *Rhodopseudomonas* type ring hydrolysis (Harwood et al., 1998; Carmona et al., 2009; Porter and Young, 2014). A modified *β*-oxidation pathway, the lower BCoA pathway, yields acetyl-CoA (Carmona et al., 2009), which is shuttled into biomass production or completely oxidized to $CO_2$ via the Wood-Ljungdahl (WL) or tricarboxylic acid (TCA) pathways (Krebs, 1954; Ragsdale, 1997).

Naphthalene, the next largest UAH, consists of two fused benzene rings. Several anaerobic bacteria oxidize naphthalene under sulfate-reducing (Galushko et al., 1999), iron-reducing (Kleemann and Meckenstock, 2011), and methanogenic (Christensen et al., 2004) conditions. The best-studied cultures are the pure culture of *Desulfatiglandaceae* bacterium NaphS2 and a highly enriched culture dominated (abundance >95 %) by *Desulfobacterium* strain N47 (Galushko et al., 1999; Meckenstock et al., 2000; DiDonato et al., 2010; Selesi et al., 2010; Bergmann et al., 2011b). Like for benzene, direct carboxylation is the likely activation mechanism of naphthalene in most cultures (Galushko et al., 1999; Musat et al., 2009; DiDonato et al., 2010; Kleemann and Meckenstock, 2011; Mouttaki et al., 2012; Kümmel et al., 2015). A gene cluster encoding a putative naphthalene carboxylase complex, including UbiD-like carboxylases similar to AbcA, has been described (Kümmel et al., 2015; Koelschbach et al., 2019; Heker et al., 2023). Subsequent degradation occurs via conversion to 2-naphthoyl-CoA (Bergmann et al., 2011a; Meckenstock et al., 2016; Heker et al., 2023) and a three-step reductive dearomatization (Eberlein et al., 2013a, 2013b; Estelmann et al., 2015; Meckenstock et al., 2016). A stepwise oxidation, which includes ring cleavage and removal of branched alkyl chains, produces acetyl-CoA, presumably by enzymes encoded in the *thn* operon which is found in NaphS2 and N47 (Meckenstock et al., 2016).

Temperature is an important factor for the rate of petroleum hydrocarbon degradation (Das and Chandran, 2011). While hydrocarbon biodegradation in petroleum reservoirs is assumed to take place up to 80-90 °C (Wilhelms et al., 2001), most cultured anaerobic UAH degraders grow at around 30 °C. The knowledge on thermophilic to hyperthermophilic UAH degraders is scarce. The combination of UAH degradation with sulfate reduction is of particular interest, because sulfate is an important electron acceptor introduced artificially into reservoirs during secondary oil recovery, thereby stimulating hydrocarbon degradation and reservoir souring (Marietou, 2021).

Here, we aimed to enrich UAH oxidizers operating under the least studied conditions: anaerobic metabolism, UAH degradation, and high temperatures. Therefore, we incubated hydrothermally heated oil-rich sediment from the Guaymas Basin (Gulf of California, Mexico), where AHs are naturally abundant (Kawka and Simoneit, 1990), with UAHs as electron donor and sulfate as electron acceptor at 50 °C and 70 °C.

## Methods

### *Anoxic cultivation*

The push cores 4991-13 and 4991-14 used for anoxic cultivations were collected at the "Cathedral Hill" hydrothermal vent site with submersible *Alvin* during *RV Atlantis* cruise AT42-05 to the Guaymas Basin (Gulf of California, Mexico) during dive 4991 (27° 00′ 41.1″ N, 111° 24′ 16.3″ W, 2,013 m water depth, November 17, 2018). On the ship, the push cores were transferred to glass bottles, which were sealed with rubber stoppers, purged with argon and stored at 4 °C. In the home laboratory, the cores were combined and mixed with anoxic sulfate-reducer medium (SRM) (Laso-Pérez et al., 2018) in a ratio of 1:10 (v:v). The sediment slurry was distributed into autoclaved serum bottles in 100 ml aliquots. The bottles were sealed with butyl rubber stoppers. Benzene, naphthalene, phenanthrene, and pyrene were provided as sole electron and carbon donors. The UAHs were dissolved in silicone oil, which is non-biodegradable and was previously shown to decrease AH toxicity and aid in transport of AHs to microbial cells (Ye et al., 2019). 5 ml of the silicone oil-UAH mixture were added to the slurries, supplying a final UAH concentration of 10 mM. A negative control contained 5 ml silicone oil without substrate. The headspaces were filled with 2 atm $N_2$:$CO_2$ (90:10). Two temperature treatments, 50 °C and 70 °C, were applied, and bottles were incubated at gentle shaking (40 rpm) in the dark. For each substrate and each temperature, three replicates were prepared.

Sulfide production was assessed in bi-weekly intervals via a copper sulfate assay (Cord-Ruwisch, 1985) using sulfate reduction as indicator for AH oxidation. Cultures were diluted 1:4 (v:v) in fresh SRM and supplied with fresh substrate when sulfide concentrations exceeded ~10 mM. To determine the doubling times of active microorganisms in the cultures, the sulfide production rates of cultures after the first dilution were used as a proxy, excluding dilutions with only two sulfide measuring points. Produced sulfide was displayed on a logarithmic (base 2) y-axis, and doubling times were calculated from the inclination $m$ of exponential regression lines $y = n * e^{mx}$ with the equation

$$doubling\ time\ (d) = \frac{ln(2)}{m}$$

### *DNA extraction*

After around 600 days of cultivation, cultures were sampled and DNA was extracted for metagenome sequencing. By this time, the active cultures had been diluted eight (benzene 50 °C-B50), seven (benzene 70 °C-B70), ten (naphthalene 50 °C-N50), and two (naphthalene 70 °C-N70) times. Of each culture, 40 ml were sampled, centrifuged (10 minutes, 3,100 × g, 4 °C) and the culture medium was discarded. DNA was extracted from the pellets using a modified SDS-protocol (Natarajan et al., 2016). DNA was also extracted in the same way from a 1 g pellet of dried sediment slurry (dry weight 202 mg $ml^{-1}$) that was produced from the combined cores 4991-13 and 4991-14. The final DNA concentrations were determined in a fluorometric assay. DNA yields were 0.2 µg (B50), 3.4 µg (N50), 4.0 µg (B70), 0.6 µg (N70), and 0.7 µg (original sediment). Libraries were sequenced as 2×150 bp paired-end reads on an Illumina HiSeq3000

platform at the Max-Planck-Genome-Centre (Cologne, Germany). Between 4,142,459 (B70) and 4,247,237 (N70) raw reads were obtained.

***Short-read DNA analysis***

Raw reads were quality-trimmed with BBDuk (included in BBMap version 38.79; https://sourceforge.net/projects/bbmap/; minimum quality value: 20, minimum read length: 50) (Bushnell, 2014). For the sediment slurry sample, the microbial community was estimated based on reconstructed small subunit (SSU) ribosomal RNA (rRNA) gene sequences mapped against the SILVA SSU reference database (version 138.1) (Quast et al., 2013) with phyloFlash (https://github.com/HRGV/phyloFlash) (Gruber-Vodicka et al., 2022). The trimmed reads of the culture samples were co-assembled with SPAdes (version 3.15.0; https://github.com/ablab/spades) (Bankevich et al., 2012). The output scaffolds were reformatted with anvi'o (version 7.1; https://github.com/merenlab/anvi'o/releases) (Eren et al., 2015), simplifying names and excluding contigs <2,500 bp. The trimmed reads were then mapped to the reformatted scaffolds fasta using Bowtie 2 with local read alignment setting (version 2.4.2; http://bowtie-bio.sourceforge.net/bowtie2/index.shtml) (Langmead and Salzberg, 2012). The output sequence alignment map (SAM) files were converted to binary alignment map (BAM) files with SAMtools (version 1.11; http://samtools.sourceforge.net) (Danecek et al., 2021), which were indexed with anvi'o. A contigs database was created from the reformatted scaffolds file and profile databases were created for all samples with anvi'o. Hidden Markov Model (HMM) searches for archaeal and bacterial single-copy core genes (SCGs) and genes pertaining to the dissimilatory sulfate reduction (DSR) pathway were run. Taxonomies were predicted for open reading frames (ORFs) predicted for the contigs database with the Centrifuge classifier (version 1.0.2-beta; https://ccb.jhu.edu/software/centrifuge) (Kim et al., 2016). The profile databases were merged, enforcing hierarchical clustering. Metagenome-assembled genomes (MAGs) were created in the anvi'o interactive interface through manual binning. For this purpose, branches of the hierarchically clustered dendrogram were followed systematically in a counterclockwise direction, generating bins via clicking and observing the real-time statistics on completion and redundancy based on single-copy core genes (SCGs) were observed. All MAGs were then refined manually with anvi'o, using GC content, mean coverage in all samples, and gene taxonomy as guides. The quality of the final MAGs was determined with CheckM (version 1.1.3; https://ecogenomics.github.io/CheckM) (Parks et al., 2015). Only MAGs with completion >50% and redundancy <10% after refinement were included in downstream analyses. Next, taxonomies were assigned to the MAGs using the GTDB toolkit, GTDB-Tk (version 2.1.1; https://github.com/Ecogenomics/GTDBTk) (Chaumeil et al., 2020) and relative abundances of the MAGs in the samples were calculated with CoverM (version 0.6.1; https://github.com/wwood/CoverM), which was run in genome mode. Prevalence of the MAGs in the original sediment was also estimated with CoverM using the trimmed read of the sediment slurry as input to map to the MAGs. The optimal growth temperature (OGT) was predicted for MAGs of interest with the OGT_prediction tool (version 1.0.3;

https://github.com/DavidBSauer/OGT_prediction/) (Sauer and Wang, 2019) using the included regression models for *Archaea* and *Bacteria*, which exclude genome size and 16S rRNA gene data. Average nucleotide identities (ANIs) between MAGs were determined with fastANI (version 1.33; https://github.com/ParBLiSS/FastANI) (Jain et al., 2018).

### *Genome annotation*

Contigs databases where created for the MAGs of interest with anvi'o, which automatically identifies open-reading frames using Prodigal (version 2.6.3; https://github.com/hyattpd/Prodigal) (Hyatt et al., 2010). The translated gene sequences were extracted from each MAG with anvi'o. Amino acid sequences of genes involved in AH degradation, sulfate reduction and related genes (electron transfer, carbon fixation, cell appendage formation) from the domains *Archaea* and *Bacteria* were acquired from the National Center for Biotechnology Information (NCBI) Protein and the UniProtKB databases. For putative anaerobic benzene carboxylase (AbcAD), protein sequences were collected from recent publications (Abu Laban et al., 2010; Holmes et al., 2011; Luo et al., 2014). The nucleotide sequences presumably coding for AbcA and AbcD from Abu Laban *et al.*, 2010 (GenBank accessions GU357992 and GU357991, respectively) were translated to amino acid sequences using the ExPASy translate tool (https://web.expasy.org/translate/). Additional amino acid sequences for subunits of class I BCRs (*bcrACD*/*bzdNQ*) amplified via PCR in the study by (Song and Ward, 2005), which have been deposited under GenBank accession numbers AY956841 to AY956907, were also acquired. Sequences for 3-hydroxypimeloyl-CoA dehydrogenase (*pimE*) and acetyl-CoA acyltransferase (*pimB*) were acquired from (Atashgahi et al., 2018) (locus tags contig-100_24_2 and Contig-100_24_7, respectively). For each protein file, short sequences were removed with Seqtk (version 1.3; https://github.com/lh3/seqtk). Local databases were created for the protein files with BLAST (version 2.10.1; https://www.ncbi.nlm.nih.gov/books/NBK279690/) (Altschul et al., 1990). Amino acid sequences of the MAGs were compared to the local databases with BLASTp. BLASTp output was filtered with BLAST-QC (version 0.1; https://github.com/torkian/blast-QC) (Torkian et al., 2020). Cutoff values for the identification of a given protein where: *e*-value <1e-10, identity ≥40%, and aligned length ≥80%.

### *Phylogenomic and genomic analysis of bacterial groups associated with enriched organisms*

Two phylogenomic trees were constructed from concatenated alignments of single-copy core genes (SCGs). For the first tree, all 135 publicly available MAGs classified as order Desulfatiglandales in the Genome Taxonomy Database (GTDB) taxonomy tree (https://gtdb.ecogenomic.org/tree) (Parks et al., 2022) were downloaded from NCBI including metadata (Supplementary Table 1). Due to the high number of genomes, the Desulfatiglandales MAGs were dereplicated at species level (ANI ≥95%) prior to tree reconstruction with anvi'o, which uses fastANI, picking the MAG with highest similarity to all other MAGs of a species

cluster as a representative. The phylogenomic tree was constructed with the 76 representative MAGs (Supplementary Table 2), the six Desulfatiglandales MAGs (5, 9, 34, 36, 46, and 47) from this study, and five MAGs of the Desulfobulbia, a sister group of Desulfatiglandales, as outgroup. The second tree included all 26 publicly available MAGs assigned as order SZUA-161 of the class Dehalococcoidia in the GTDB taxonomy tree (Supplementary Table 3) downloaded from NCBI, including metadata, plus the SZUA-161 MAG of this study (MAG 33) and 10 MAGs of a sister order of SZUA-161 within Dehalococcoidia, UBA6952, as outgroup. For tree reconstruction, the selected MAGs were reformatted and a contigs database was created for each MAG with anvi'o (version 7.1). The anvi'o-integrated HMM collection was run on all contigs databases to identify bacterial SCGs, which were then aligned in a concatenated manner via anvi'o, which uses the multiple sequence alignment tool MUSCLE (version 5.1; https://github.com/rcedgar/muscle) (Edgar, 2004). Trees were calculated with 30 SCGs using IQ-TREE (version 1.6.12; http://www.iqtree.org/) (Nguyen et al., 2015). IQ-TREE was run using standard model selection followed by tree inference with 100 bootstrap iterations. Two MAGs (GCA_020351915.1 and GCA_020349865.1) and one MAG (GCA_020351795.1) were automatically excluded from the Desulfatiglandales and the SZUA-161 trees by IQ-TREE because they didn't contain sufficient SCGs to infer meaningful phylogenies. Final trees were visualized with the Interactive Tree of Life (iTOL) online tool (version 6; https://itol.embl.de/) (Letunic and Bork, 2011). MAGs were compared via calculation of ANI with fastANI and amino acid identity (AAI) with the aai_wf workflow, which is part of the CompareM package (version 0.1.2; https://github.com/donovan-h-parks/CompareM).

The optimal growth temperature was predicted for the publicly available MAGs with the OGT_prediction tool (version 1.0.3). Key genes for anaerobic UAH/AH oxidation and downstream degradation were identified in Desulfatiglandales and SZUA-161 MAGs by running the previously built protein databases on the amino acid sequences of the MAGs in the same way and with the same selection criteria as described in the section "Genome annotation".

## Results

### *Thermophilic microorganisms from the Guaymas Basin degrade one- to two-ringed UAHs*

We incubated triplicate batches of an oil-rich sediment slurry from the Guaymas Basin (Fig. 1a) with UAHs ranging from one to four aromatic rings at 50 °C and 70 °C (benzene, naphthalene, phenanthrene, and pyrene, increasing in size). Cultures supplied with phenanthrene and pyrene did not produce more sulfide than a substrate-free control at either incubation temperature, indicating that UAH oxidation did not take place. In contrast, cultures supplied with benzene and naphthalene incubated at 50 °C and 70 °C started to produce sulfide shortly after the incubation start and first reached sulfide levels >10 mM after 40 (B50 culture) to 120 days (N70). Sequential dilutions strongly reduced the sediment content in the B50, B70, and N50 cultures (Fig. 1b). The average doubling time based on sulfide production was 20 days in the N50, 25 days in the B70, and 37 days in the B50 cultures, respectively (Fig. 1c,d,e, Supplementary Table 4). In the N70 cultures, dilutions resulted in decreasing sulfide production rates (Fig. 1f) accompanied by long doubling times (>200 days) after the second dilution (Supplementary Table 4).

### *Community compositions in the enrichment cultures*

After more than 1.5 years of cultivation, we retrieved short-read metagenomes from the original sediment used for incubations and from the four active cultures B50, B70, N50, and N70. From the co-assembled metagenomes, we reconstructed 47 MAGs with completeness >50% and redundancy <10%. Cultures that showed high sulfate-dependent substrate turnover (B50, B70, and N50) were more enriched in specific taxa, whereas the microbial community of the less active N70 culture remained more diverse (Fig. 2a,b, Supplementary Table 5). A previous study observed high archaea:bacteria ratios in heated Guaymas Basin sediments, which increase further with temperature (McKay et al., 2016; Ramírez et al., 2021). In our case, the B50 culture had a higher archaea:bacteria ratio than the B70 culture, contrasting this hypothesis. In the N50 culture, archaea were completely absent, but made up around 50% of the community in the N70 culture, coinciding with literature (Fig. 2b, Supplementary Table 5).

In the B50 culture, the most abundant MAG (MAG 53, relative abundance 31%) was classified as species VBQP01 sp008297795 of the archaeal phylum Thermoplasmatota (Fig. 2c, Table 1). This MAG belongs to the same species (average nucleotide identity-ANI = 98.9%) as a MAG reconstructed from an environmental metagenome from the Guaymas Basin, M8_bin1702 (GCA_008297795.1). A recent study discussed the potential of this organism to degrade aromatic compounds via the phenylacetic acid (PAA) pathway (Liu et al., 2020). The B70 and N50 cultures were dominated by a single bacterial MAG with relative abundance >50%: MAG 9 in the B70 culture and MAG 34 in the N50 culture. Both MAGs were classified as Desulfatiglandales (Table 1).

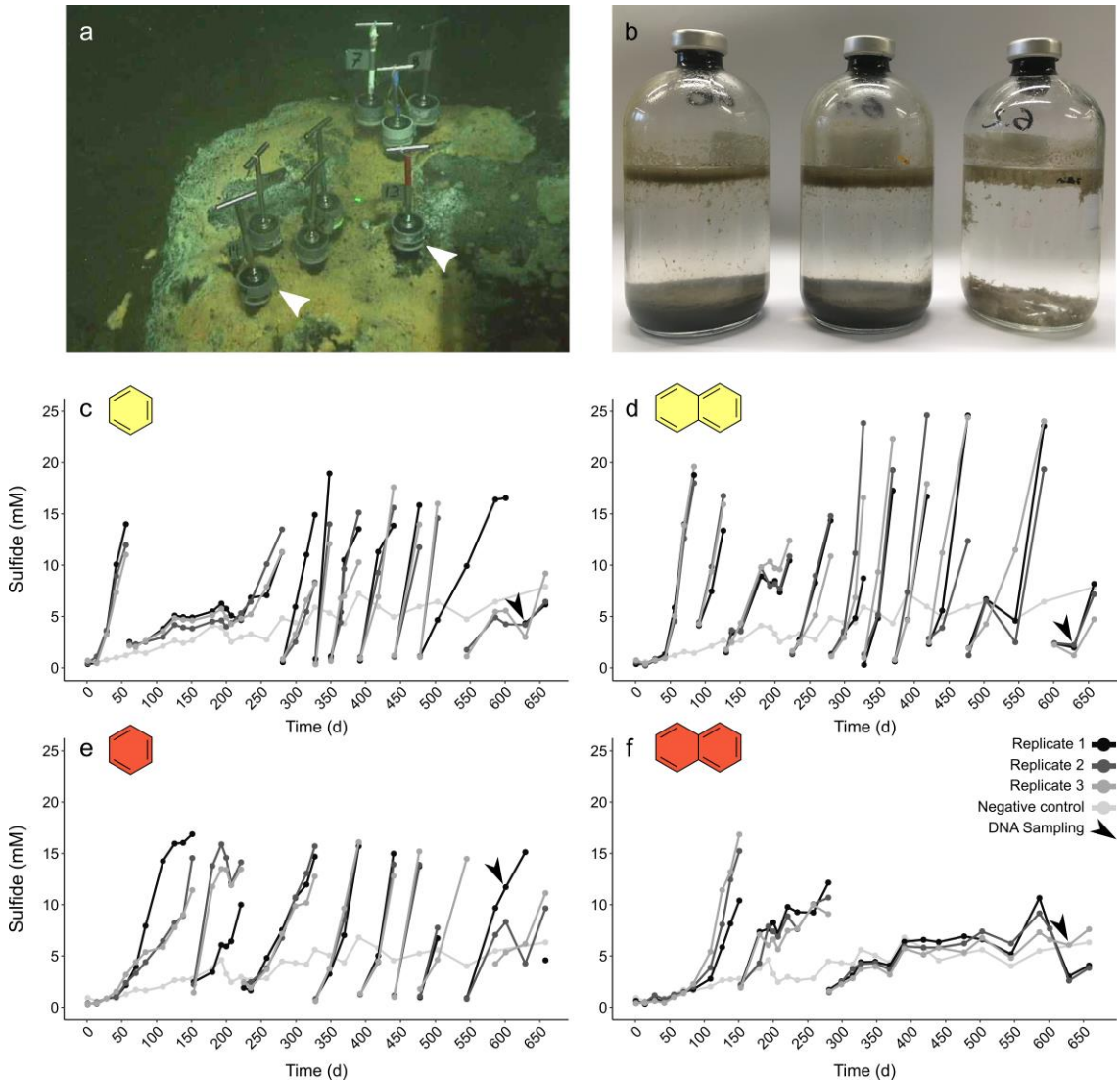


**Figure 1 | Thermophilic microorganisms from Guaymas Basin sediment oxidize aromatic hydrocarbons. a** Sampling site of petroleum hydrocarbon-rich push cores in the Guaymas Basin. Push cores used for anoxic incubations are indicated by white arrow heads. **b** Sequential dilution of sulfide-producing anoxic slurries strongly reduced sediment content (from left to right: original slurry, first dilution, second dilution). **c-f** Sulfide production in anoxic cultures supplied with benzene (**c,e**) and naphthalene (**d,f**) incubated at 50 °C (yellow filling) and 70 °C (red filling). Gaps in sulfide profiles indicate dilution events.

MAG 34 was classified up to species-level and belongs to the genus B111-G9, the representative of which was previously reconstructed from Guaymas Basin sediments (Dombrowski et al., 2018), MAG 9 was only classified at order level. In the N70 culture, MAG 33 affiliated with the bacterial family SpSt-899 of the Dehalococcoidia order SZUA-161 was the most abundant (relative abundance 12%), closely followed by archaeal MAGs of the genus *Archaeoglobus* (MAG 31, 8%), and the family WUQV01 (class Bathyarchaeia) (MAG 32, 5.3%), and a bacterial MAG (MAG 16, 5%) of the *Bipolaricaulaceae*. The communities of the cultures differed strongly from the ANME-1 dominated sediment slurry, where the enriched MAGs were only present at very low abundances (0.0-0.1%) (Supplementary Table 6).

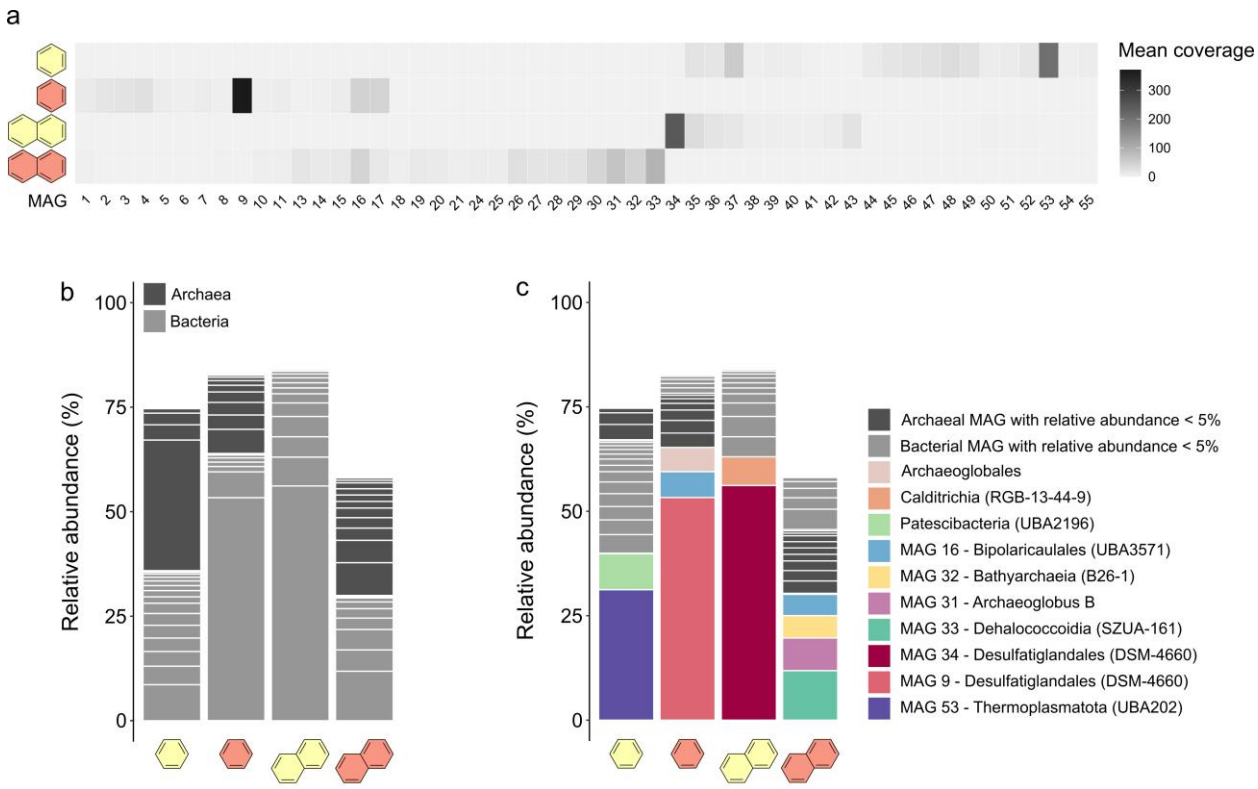


**Figure 2 | Microbial community compositions differ in anaerobic UAH-degrading cultures depending on substrate and incubation temperature. a** Mean coverages of the 47 MAGs reconstructed from the co-assembly of metagenomes of benzene- and naphthalene-supplied cultures at 50 °C and 70 °C. **b** Relative abundances of MAGs assigned to the domains archaea or bacteria in the four metagenomes. **c** Relative abundances of the MAGs on order-level.

### *UAH degradation pathways in abundant MAGs*

In the B50 culture, the most abundant MAG, MAG 53 (Thermoplasmatota), encodes only very few proteins of known pathways for the activation and oxidation of benzene, among others benzoylsuccinyl-CoA thiolase (BbsAB) of the methylation pathway, and benzoate-CoA ligase (BamY) of the carboxylation pathway (Fig. 3a). We also searched for genes encoding the PAA pathway recently discussed by Liu et al. (2020). MAG 53 encodes only three of thirteen proteins of the pathway, among others the key enzyme phenylacetate-CoA ligase (PaaK) (Jiao et al., 2022). Further, MAG 53 lacks the dissimilatory sulfate reduction (DSR) pathway. The second most abundant MAG, MAG 37 (Patescibacteria) contains even fewer genes for anaerobic benzene oxidation, and is thus a less likely candidate for benzene oxidation. We searched for the relevant pathway genes in less abundant MAGs with relative abundances of 3-5% (MAGs 48, 49, 47, 46, and 35) (Supplement Figure 1, Supplementary Table 8). MAGs 46 and 47, affiliated with Desulfatiglandales, encode a majority of the genes for benzene activation via methylation. In addition, MAG 47 encodes a partial hydroxylation pathway. While neither MAG encodes homologues of Abc, both contain *bamY* and complete or near complete pathways for reductive dearomatization (RD), ring hydrolysis (RH), and lower BCoA pathway, CO-Dehydrogenase/Acetyl-CoA Synthase complex (ACDS), and the $H_4F$ methyl branch of the Wood-Ljungdahl ($H_4F$ WL) pathway. In addition, both MAGs encode complete DSR pathways. Thus, both organisms could be capable of benzene degradation and can perform DSR. However,

because their abundance is very low, it is questionable whether they are the main benzene oxidizers in the culture. The role of the highly abundant MAG 53 remains enigmatic. More studies are required to elucidate the mechanisms in this cryptic but highly active culture.

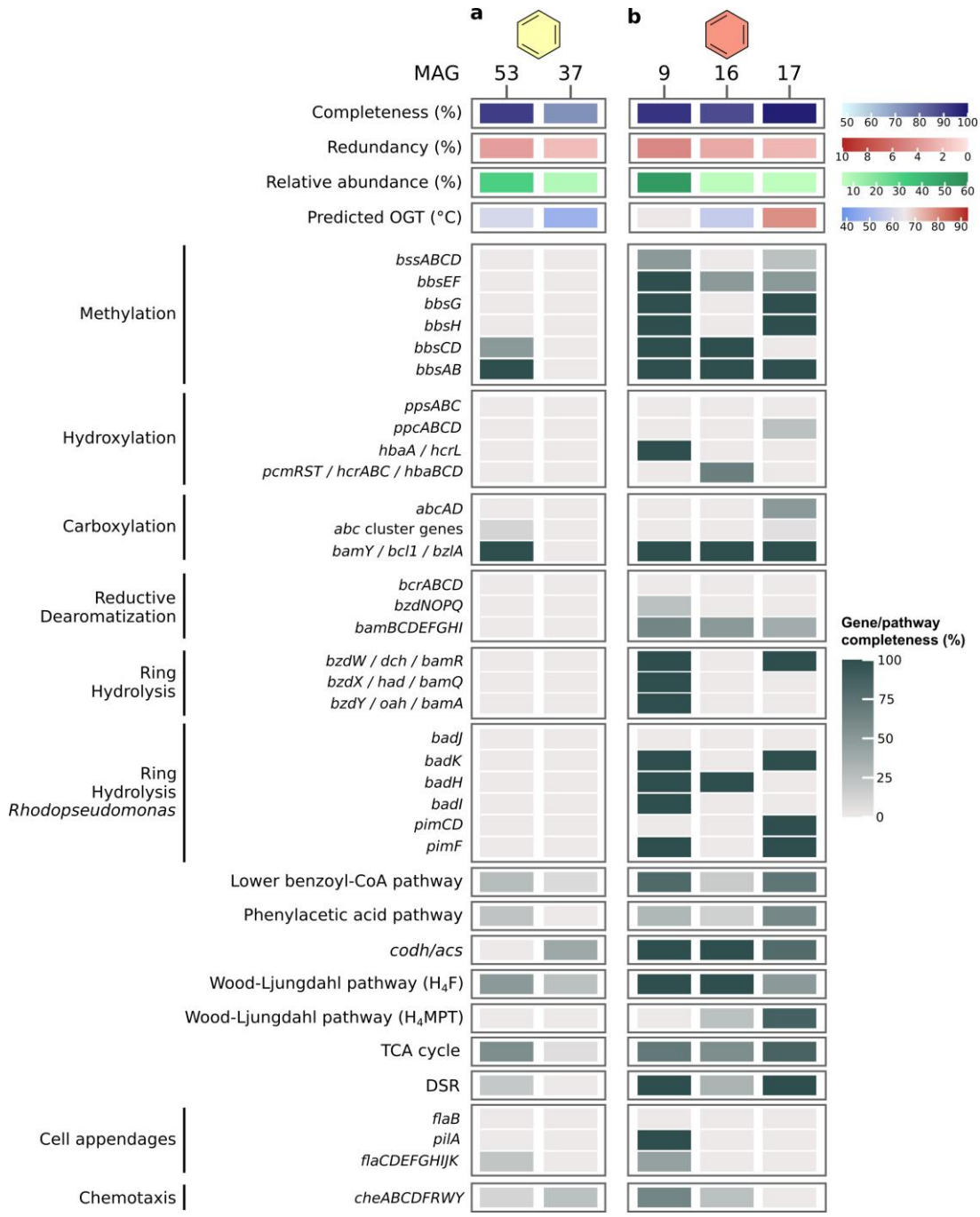


**Figure 3 | Benzene degradation pathways in MAGs recovered from benzene-oxidizing cultures at 50 °C (a) and 70 °C (b).** Genes were identified via BLASTp search against local databases of proteins of interest. For proteins and pathways encoded by several genes, completeness was calculated as percentage of present genes of total genes of the pathway/protein. For pathway genes and abbreviations see Supplementary Table 7

**Table 1 | MAGs with relative abundance ≥5% recovered from benzene- and naphthalene-oxidizing cultures at 50 °C and 70 °C.** Optimal growth temperature (OGT) was predicted with OGT_prediction and taxonomic affiliation was determined with GTDB-Tk. B50: benzene-oxidizing culture at 50 °C; B70: benzene-oxidizing culture at 70 °C, N50: naphthalene-oxidizing culture at 50 °C; N70: naphthalene-oxidizing culture at 70 °C.

| MAG | Culture | Relative abundance (%) | OGT (°C) | Domain | Phylum | Class | Order | Family | Genus | Species |
|---|---|---|---|---|---|---|---|---|---|---|
| **53** | B50 | 31.2 | 59.7 | Archaea | Thermoplasmatota | E2 | UBA202 | DSCA01 | VBQP01 | VBQP01 sp008297795 |
| **37** | B50 | 8.6 | 47.7 | Bacteria | Patescibacteria | ABY1 | UBA2196 | GWA2-42-15 | | |
| **9** | B70 | 53.3 | 65.8 | Bacteria | Desulfobacterota | DSM-4660 | Desulfatiglandales | | | |
| **16** | B70 / N70 | 6.2 / 5.1 | 56.0 | Bacteria | Bipolaricaulota | Bipolaricaulia | Bipolaricaulales | Bipolaricaulaceae | UBA3571 | |
| **17** | B70 | 5.8 | 78.6 | Archaea | Halobacteriota | Archaeoglobi | Archaeoglobales | Archaeoglobaceae | B5-G16 | |
| **34** | N50 | 56.2 | 54.5 | Bacteria | Desulfobacterota | DSM-4660 | Desulfatiglandales | Desulfatiglandaceae | B111-G9 | |
| **35** | N50 | 6.9 | 47.5 | Bacteria | Calditrichota | Calditrichia | RBG-13-44-9 | RBG-13-44-9 | | |
| **33** | N70 | 11.8 | 60.1 | Bacteria | Chloroflexota | Dehalococcoidia | SZUA-161 | SpSt-899 | | |
| **31** | N70 | 7.8 | 92.1 | Archaea | Halobacteriota | Archaeoglobi | Archaeoglobales | Archaeoglobaceae | Archaeoglobus_B | |
| **32** | N70 | 5.3 | 84.4 | Archaea | Thermoproteota | Bathyarchaeia | B26-1 | WUQV01 | | |

In the B70 culture, MAG 9 (Desulfatiglandales) encodes an almost complete pathway for benzene activation via methylation, and an almost complete class II BCR for RD (Fig. 3b). Because *abcAD* is absent from this MAG, and only a single enzyme (HbaA/HcrL) of the hydroxylation pathway is encoded, substrate activation most likely occurs via methylation. MAG 9 encodes a *Thauera* type RH pathway including BamR, BamQ, and BamA, and an almost complete *Rhodopseudomonas* type RH pathway. Additionally, a major part of the lower BCoA pathway and CODH/ACS complex, and a complete $H_4F$ WL pathway for a complete oxidation of benzene to $CO_2$ are present. A complete DSR pathway should enable this organism to combine benzene oxidation with sulfate reduction in a single cell. MAG 9 also encodes type IV pilin (PilA) and several chemotaxis genes, which could enable it to outcompete other potential benzene degraders and increase its efficiency for benzene degradation, as previously shown for the naphthalene-degrading bacterium *Pseudomonas putida* G7 (Law and Aitken, 2003). The estimated optimal growth temperature (OGT) of 65 °C for this MAG supports the thermophilic character of this organism. Low-abundance MAGs in this culture, like MAG 16 (Bipolaricaulales) and MAG 17 (Archaeoglobales), also encode proteins for anaerobic benzene degradation, such as BamY, some subunits of class II BCR, and in case of MAG 17 a complete DSR pathway. Notably, MAG 17 encodes one of two subunits of anaerobic benzene carboxylase (AbcA), which could enable it to degrade benzene via carboxylation. It is thus possible that the two organisms contribute to a small degree to benzene oxidation or sulfate reduction, but considering abundances, we expect the organism represented by MAG 9 to be the main active organism in the culture.

In the N50 culture (Fig. 4a), MAG 34 (Desulfatiglandales) exhibits vast genomic capacities for anaerobic naphthalene oxidation. First, it encodes an almost complete pathway of the known enzymes of the methylation pathway. It is also capable of activation via direct carboxylation, encoding homologues of all eight genes of the naphthalene carboxylase complex. This complex consists of three UbiD-like carboxylases, two ParA-MiND ATPase-like-proteins, and three putative linker proteins (Koelschbach et al., 2019). Moreover, MAG 34 encodes four copies of naphthoyl-CoA ligase (NCL) highly homologous to the variants of NaphS2 and N47 (amino acid identity ≥67%). NCL converts 2-naphthoate to 2-naphthoyl-CoA (Heker et al., 2023). Further, it is capable of the three-step RD of naphthalene, encoding homologues of 2-naphtoyl-CoA reductase (NCR), 5,6-dihydro-2-naphthoyl-CoA reductase (DHNCR), and both N47 and NaphS2 type of 5,6,7,8-tetrahydro-2-naphthoyl-CoA reductase (THNCR). An almost complete *thn* operon and lower BCoA pathway facilitates RH and oxidation to acetyl-CoA, followed by complete oxidation to $CO_2$ via the CODH/ACS complex and the remaining $H_4F$ WL pathway. MAG 34 encodes a complete DSR pathway, enabling the organism to shuttle electrons from naphthalene oxidation directly into sulfate reduction. The incubation temperature is very close to the estimated OGT of the organism of 55 °C. Its high relative abundance and its extensive genomic capacity for naphthalene degradation suggest that the bacterium represented by MAG 34 is the dominant, maybe even the only naphthalene oxidizer in the culture.

In the N70 culture (Fig. 4b), MAG 33 (Dehalococcoidia) encodes only one protein of the methylation pathway, and lacks naphthalene carboxylase, thus limiting its options for naphthalene activation. Yet, MAG 33 encodes NCL, two of the three reductases required for RD, and about two thirds of the *thn* operon for RH, among others the putative ring-cleaving hydrolase ThnL (Meckenstock et al., 2016). Further, it encodes an almost complete lower BCoA pathway, plus a complete CODH/ACS and $H_4F$ WL pathway, which would enable it to oxidize naphthalene to $CO_2$. MAG 33 is about 85% complete, thus it is possible that the missing 15% encode naphthalene-activating UbiD-like carboxylases and DHNCR, which would enable it to degrade naphthalene. Because none of the other MAGs with relative abundances ≥5% in this culture encode numerous genes for activation, RD, or RH, MAG 33 is the most likely candidate for naphthalene oxidation. MAG 33 encodes only one of three proteins of the DSR pathway, sulfate adenylyltransferase (Sat), and is therefore probably incapable of sulfate reduction. The next most abundant MAG, MAG 31 (Archaeoglobales), encodes an almost complete DSR pathway, which lacks only the AprA subunit of adenylylsulfate reductase. Thus, it is possible that naphthalene oxidation in this culture occurs via syntrophic interactions, potentially via direct interspecies electron transfer (DIET) of electrons released from naphthalene oxidation to MAG 31, for which MAG 31 encodes both archaeal type (FlaB) and bacterial type (PilA) cell appendages.

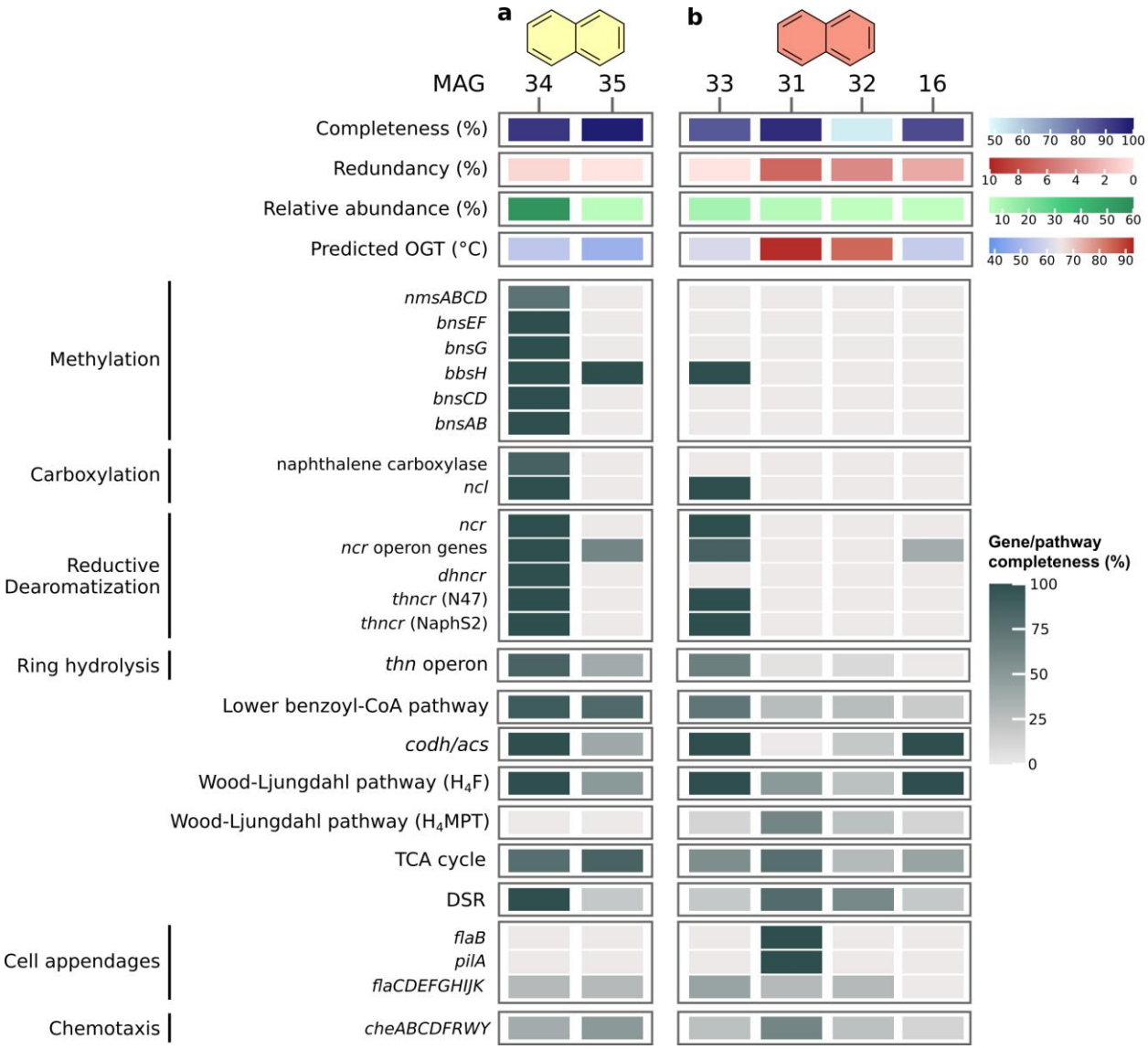


**Figure 4 | Naphthalene degradation pathways in MAGs recovered from naphthalene-oxidizing cultures at 50 °C (a) and 70 °C (b).** Genes were identified via BLASTp search against local databases of proteins of interest. For proteins and pathways encoded by several genes, completeness was calculated as percentage of present genes of total genes of the pathway/protein. For pathway genes and abbreviations see Supplementary Table 7.

We aimed to bring the results from our enrichment cultures into a wider ecological context and examined the distribution of AH degradation genes and pathways in the larger taxonomic groups of the microorganisms that we enriched in our study. We refrained from examining the phylogeny of the Thermoplasmatota MAG 53 (M8_bin1702), because the Thermoplasmatota phylogeny was well-resolved in the recent study by Liu *et al.*, 2020. Thus, we focused on two bacterial groups with which abundant MAGs from our cultures were affiliated: the order Desulfatiglandales (class DSM-4660) and the order SZUA-161 (class Dehalococcoidia).

### *Environmental distribution of Desulfatiglandales and SZUA-161*

Desulfatiglandales currently comprise 135 publicly available MAGs on GDTB, while for SZUA-161 only 26 MAGs are available at the moment. Both Desulfatiglandales and Dehalococcoidia are globally widespread members of marine sediment and subsurface communities (Inagaki et al., 2006; Parkes et al., 2014; Wasmund et al., 2014; Robador et al., 2016). Desulfatiglandales MAGs have been recovered mainly from or near the North American continent. Fewer MAGs originate from Eurasia, including the Black Sea, with only one MAG (GCA_024641835.1) stemming from the Southern Hemisphere (Fig. 5a). The few available SZUA-161 MAGs have been reconstructed from continental samples from North America, Eurasia, Asia, and Africa, plus from marine samples from the Atlantic (Fig. 5b). Both group distributions likely reflect sampling efforts rather than actual occurrence and/or abundance.

The MAGs of both orders originate from a wide array of environments, including lakes, springs, cold seeps, the seafloor and the subsurface. More than half of publicly available Desulfatiglandales MAGs (75 out of 135) originate from hydrothermal vent sediment, mainly from the Guaymas Basin (70 MAGs) and to a smaller degree (5 MAGs) from the Pescadero Basin, a recently described hydrothermal vent area (Paduan et al., 2018) located ~400 km southeast of the Guaymas Basin in the Gulf of California. Further MAGs include 17 MAGs from groundwater or aquifer samples, 9 MAGs from seawater samples from the Black Sea, the Pacific coast, and the Gulf of Mexico, and 7 MAGs from estuary sediment. For SZUA-161, hydrothermal vents are also the most common environment type, with 11 MAGs emanating from the Lost City hydrothermal field located at the Mid-Atlantic Ridge (Kelley et al., 2001). Considering the current data on both bacterial groups, it seems plausible that both are widely distributed and capable of inhabiting diverse environments, with a potential preference for hydrothermal vent areas.

Next, we examined the phylogenomic placement of Desulfatiglandales MAGs and the SZUA-161 MAG from our study in their larger taxonomic groups, and investigated the genomic potential of environmental Desulfatiglandales and SZUA-161 MAGs for anaerobic UAH degradation.

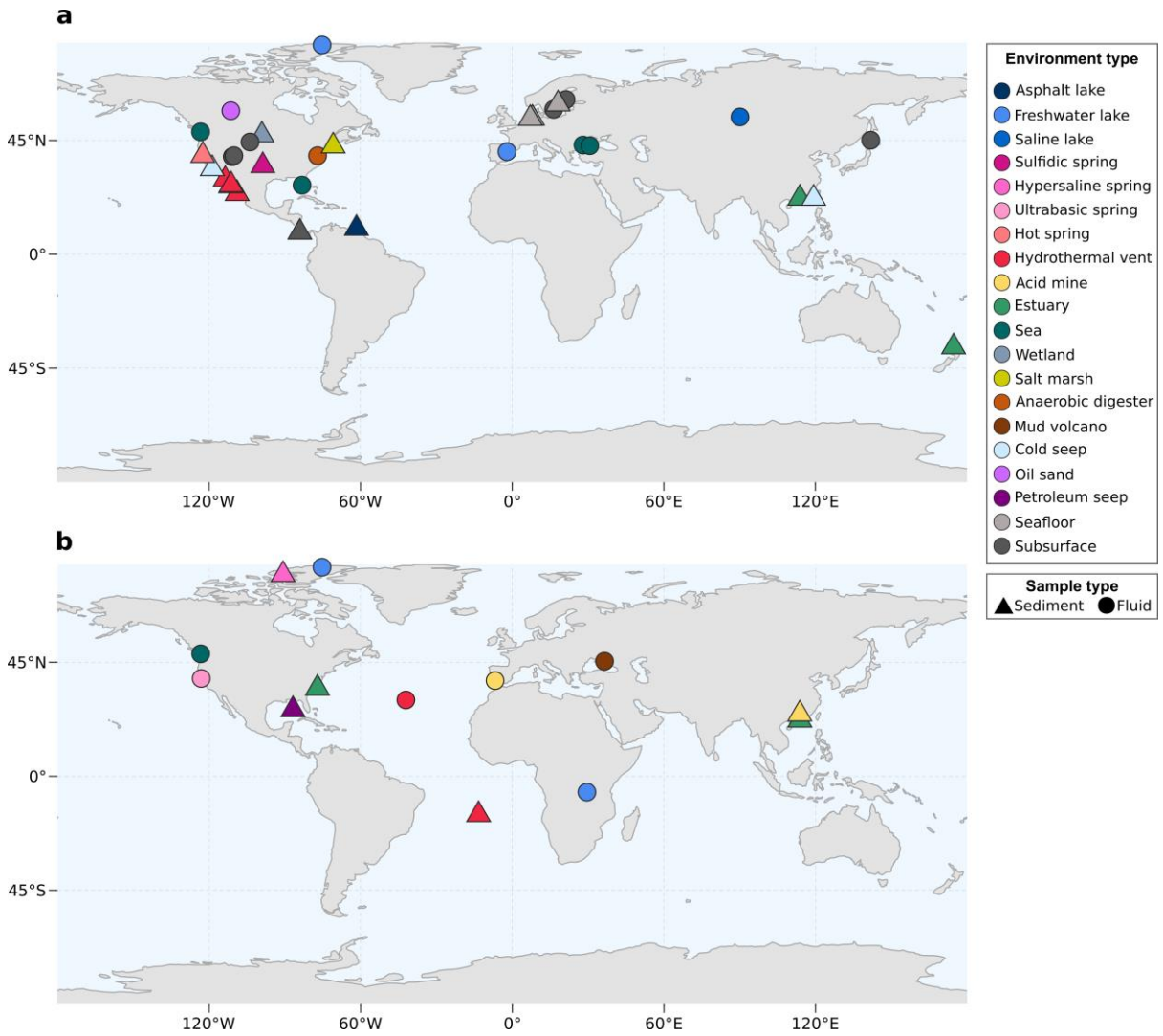


**Figure 5 | Environmental origin of bacterial MAGs of the Desulfobacterota order Desulfatiglandales (a) and of the Dehalococcoidia order SZUA-161 (b).** Coordinates were acquired from metadata accompanying the MAGs deposited at NCBI.

### *Genomic capacity for UAH degradation in Desulfatiglandales bacteria*

According to GTDB (Parks et al., 2022), Desulfatiglandales is currently the only order in the class DSM-4660, which in turn belongs to the phylum Desulfobacterota. Desulfatiglandales are defined as gram-negative, rod-shaped, strictly anaerobic, and mesophilic bacteria that utilize AH derivatives like phenol and benzoate as electron donors in combination with the reduction of sulfate and other inorganic sulfur compounds (Suzuki et al., 2014; Waite et al., 2020; Galushko and Kuever, 2021). Notable members of the order include NaphS2 (Galushko et al., 1999; DiDonato et al., 2010), *Desulfatiglans anilini*, which degrades phenol and the aromatic amine aniline (Schnell et al., 1989; Young-Beom et al., 2009; Suzuki et al., 2014), and the recently isolated phenanthrene-degrader *Desulfatiglans* TRIP_1 (Himmelberg et al., 2018; Kraiselburd et al., 2019).

Desulfatiglandales include four families: *Desulfatiglandaceae* with the type genus *Desulfatiglans* (Waite et al., 2020), B25-G16, HGW-15, and JAIPEI01. The majority (77) of publicly available MAGs fall into the family *Desulfatiglandaceae*, with 34 MAGs classified as

HGW-15, 26 MAGs as B25-G16, and only one MAG representing JAIPEI01. This phylogeny is well-resolved in our phylogenomic tree based on concatenated single-copy core genes (Fig. 6). The tree is divided into two large monophyletic groups: (1) the B25-G16 family and (2) the three other families JAIPEI01, HGW-15, and *Desulfatiglandaceae*. All six MAGs from our study fall into one monophyletic clade within the family *Desulfatiglandaceae*, which indicates that MAGs 5 and 9 are part of this family, even though they were not assigned as such by GTDB-Tk. This clade contains four additional MAGs (GCA_021163815.1, GCA_019306325.1, GCA_003646995.1, and GCA_019309225.1), all from hydrothermal vent sediment in the Guaymas Basin and the Pescadero Basin. The clade splits into two groups: (1) MAGs 5, 9, and 46 and GCA_021163815.1 (2) GCA_019306325.1, GCA_003646995.1, MAGs 47, 34, 36, and GCA_019309225.1. Based on ANI, AAI and the tree structure (Fig. 6, Supplementary Figs. 2 and 3, Supplementary Table 9), group one consists of two genera, one containing two species, represented each by MAGs 5 and 9 (ANI 78%, AAI 73%), and one containing one species represented by two MAGs, GCA_021163815.1 and MAG 46 (ANI 95%, AAI 96%) (Konstantinidis et al., 2017; Jain et al., 2018). Notably, MAGs 5 and 9 exhibit the highest estimated OGTs of all Desulfatiglandales MAGs (63 °C and 66 °C, respectively compared to an average OGT of 44 °C of all publicly available MAGs) (Supplementary Table 1). Therewith, we were able to reconstruct the MAGs of the, to this date, likely most thermophilic genus of the class, and enrich the currently most thermophilic organism and anaerobic AH degrader of the clade, represented by MAG 9, at temperatures slightly above its predicted OGT. Strikingly, the MAGs of the sister genus, MAG 46 and GCA_021163815.1, likely grow at mesophilic temperatures about 20 °C lower (OGT 44 °C). According to the same criteria, the second group consists of four species of one genus: species (1) GCA_019306325.1; species (2) GCA_003646995.1 and MAG 47; species (3) MAG 34; and species (4) MAG 36 and GCA_019309225.1. Members of group two are predicted moderate thermophiles with OGTs around 50-55 °C, which coincides with the enrichment of the MAG 34 bacterium at 50 °C.

Genes coding for central enzymes for the anaerobic AH metabolism, e.g. *bamY* and *bamA*, are widely distributed within the order Desulfatiglandales, and do not appear to be connected to specific clades. Most MAGs also encode PaaK, the key enzyme of the PAA pathway. CODH/ACS and bacterial-type $H_4F$ WL pathway are also ubiquitously present and should allow a downstream oxidation of aromatic compounds. The DSR pathway is strongly represented for coupling to sulfate reduction, even though the pathway is incomplete in about a third of the included MAGs. In some cases this may be a result of low completion, e.g. in MAGs GCA_015223015.1 and GCA_016776415.1.

About half of the MAGs encode the alpha subunit of benzylsuccinate synthase (BssA) of the methylation pathway of benzene and the alpha subunit of phenylphosphate synthase (PpsA) of the hydroxylation pathway. Interestingly, more than a third of the Desulfatiglandales MAGs encode AbcA. AbcA, in connection with BamY, could enable many yet uncultured Desulfatiglandales of degrading benzene via the carboxylation pathway. Regarding BCRs, the

*bcr* type BCR I, isolated from *Thauera aromatica* and *Rhododpseudomonas palustris* (Song and Ward, 2005), is the least distributed version, with about a third of MAGs encoding the catalytic subunit BcrA. More than three quarters of MAGs encode BzdQ, the active subunit of *bzd* type BCR I of *Azoarcus evansii* (Song and Ward, 2005). The BamB subunit of ATP-independent class II BCR is similarly as represented as BzdQ, thus both ATP-dependent and -independent BCRs seem to be used by Desulfatiglandales.

Genes for the anaerobic activation of naphthalene are less frequent in Desulfatiglandales than genes for benzene activation. We did not detect genes encoding the alpha subunit of naphthyl-2-methylsuccinate synthase (*nmsA*) for naphthalene activation via methylation (Selesi et al., 2010), in any of the MAGs. Instead, about a quarter of MAGs encode one or more copies of the UbiD-carboxylases previously identified in the naphthalene carboxylase operon (Koelschbach et al., 2019). NCL-encoding genes are present in only eight MAGs, NCR-encoding genes in 15 MAGs, DHNCR-encoding genes in 8 MAGs, and the complete operon encoding THNCR in 12 MAGs. The combined presence of all genes required for naphthalene degradation via carboxylation is rare. In fact, next to the known naphthalene-degrader NaphS2, MAG 34 from the N50 culture is the only MAG encoding the complete naphthalene degradation pathway. MAG 34 also contains key genes for the anaerobic activation of benzene, *bssA* and *abcA*. Thus this bacterium might also be capable of benzene and/or benzene derivate degradation.

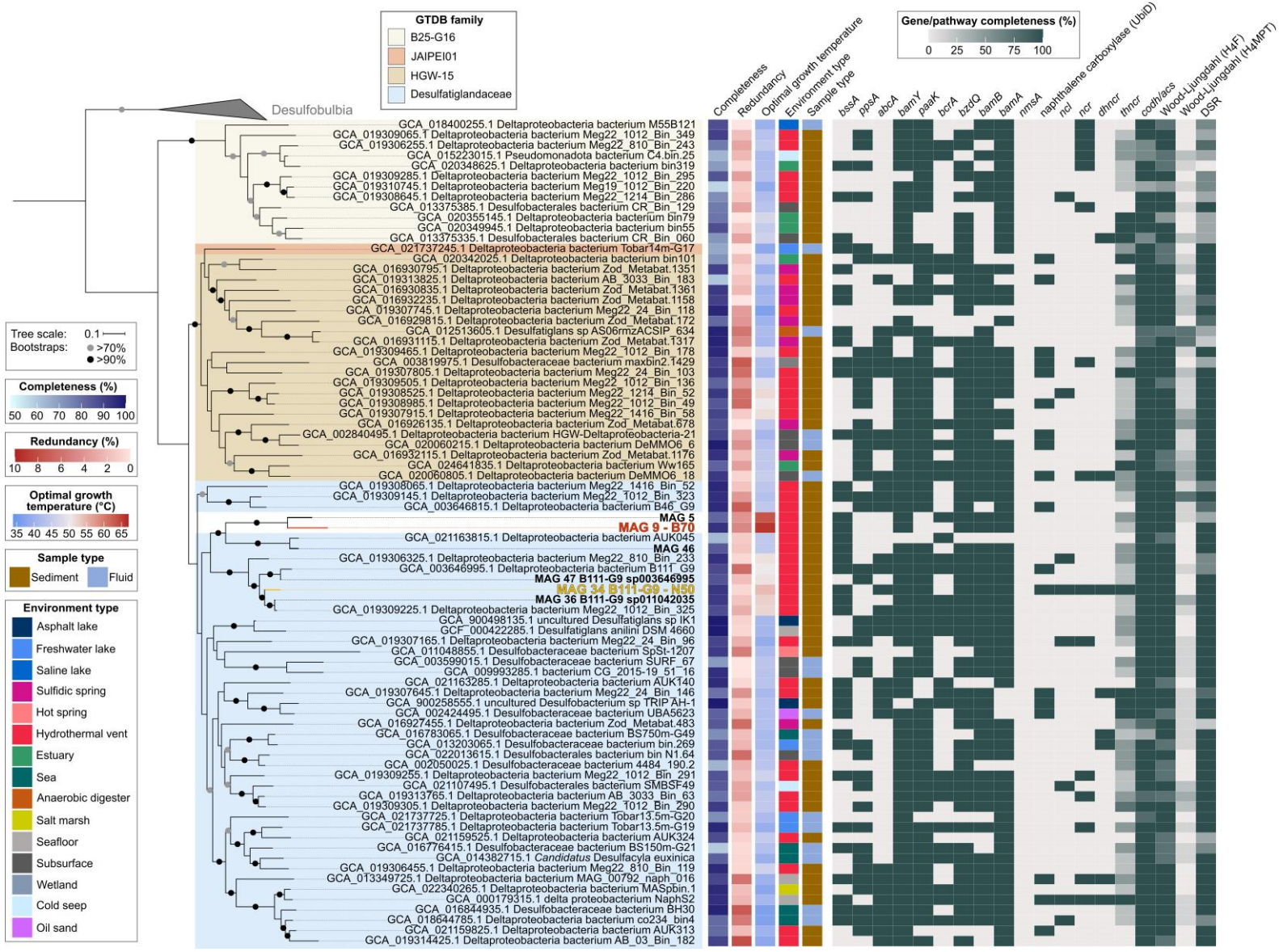


**Figure 6 | Genomic capacities for anaerobic aromatic hydrocarbon degradation in genomes of the bacterial order Desulfatiglandales.** MAGs recovered in this study are highlighted in bold, MAG 9 dominant in the benzene 70 °C (B70) culture and MAG 34 dominant in the naphthalene 50 °C (N50) culture are additionally highlighted in red and yellow, respectively. For pathway genes and abbreviations see Supplementary Table 7.

### *Genomic capacity for UAH degradation in SZUA-161 bacteria*

In GDTB, the order SZUA-161 falls into the class Dehalococcoidia and phylum Chloroflexota (Parks et al., 2022). While this specific order is not well-described yet, cultured Dehalococcoidia are known for the reductive dehalogenation of chlorinated and brominated compounds (Maymó-Gatell et al., 1997; Yan et al., 2009). Examples include *Dehalococcoides mccartyi*, which reduces chlorinated ethene and benzene (Löffler et al., 2013), and the *Dehalogenimonas* species *D. lykanthroporepellens* and *D. alkenigignens*, which reduce poylchlorinated aliphatic alkanes (Moe et al., 2009; Bowman et al., 2013). Both genera fall into the order Dehalococcoidales and use hydrogen as electron donor. Recent studies suggest a potential for both aerobic and anaerobic aromatics degradation in the Dehalococcoidia. For instance, the phenol derivatives vanillin and syringic acid stimulated growth of aerobic bacteria of the order Tepidiformales isolated from geothermal springs and thriving at 55-60 °C (Palmer et al., 2023). Further, Dehalococcoidia MAGs, one of which is part of the order SZUA-161 (GCA_004376205.1), from petroleum seeps in the Gulf of Mexico contained proteins for the anaerobic hydroxylation of the alkylbenzene *p*-cymene and class I BCRs for RD (Dong et al., 2019). Another study enriched a Dehalococcoidia bacterium closely related to *D. alkenigignens* anaerobically on lignin, which encoded an almost complete benzoate degradation pathway (Yu et al., 2023). The study further showed that most Dehalococcoidia MAGs recovered from marine sediment encoded *bcr*-type BCRs, which were absent in Dehalococcoidia MAGs from groundwater or seawater.

The order SZUA-161 currently contains 26 MAGs of two families, SZUA-161 (9 MAGs) and SpSt-899 (17 MAGs). This phylogeny is well-resolved in our tree (Fig. 7). MAG 33 from the N70 culture is situated at the root of the SpSt-899 family branch, which coincides with its taxonomic affiliation to this family. Notably, MAG 33 has a much higher estimated OGT (60°C) than all other MAGs of the order (average OGT 43°C). We therefore propose that SpSt-899 was originally more thermophilic, and later distributed into less heated environments. The closest relative to MAG 33 is the Dehalococcoidia bacterium LH_S1 (GCA_023660035.1), which belongs to a different genus (AAI 59%) (Supplementary Fig. 4a,b, Supplementary Table 10).

The SZUA-161 family encodes several key pathway genes for benzene degradation. For instance, seven out of eight MAGs encode BssA, all MAGs encode BamY, and six MAGs encode BamA. Interestingly, SZUA-161 seem to rely on ATP-dependent BCRs, since all MAGs encode BzdQ, five MAGs encode BcrA, but only two MAGs encode BamB. Naphthalene activation genes, both for the methylation and carboxylation pathway, are not encoded by members of the SZUA-161 family. Yet, two MAGs encode NCR, three MAGs encode DHNCR, and all MAGs encode one or more subunits of the four-subunit THNCR. Thus, while SZUA-161 likely cannot activate naphthalene directly, they might be able to dearomatize naphthyl-derivatives. All SZUA-161 family MAGs encode complete CODH/ACS complexes and partial or complete $H_4F$ WL pathways, which they could use for oxidation of dearomatized naphthyl-residues to $CO_2$. Surprisingly, two MAGs of the SZUA-161 family encode complete DSR

pathways, and the other six MAGs encode partial DSR pathways, insinuating that these organisms are capable of sulfate reduction, a metabolic trait that was previously not associated with members of the Dehalococcoidia.

In the SpSt-899 family, four members that are closer to the root of the clade, MAG 33, LH_S1 (GCA_023660035.1), GCA_018657655.1, and GCA_013203045.1, contain several genes for the anaerobic degradation of benzene or derivatives, e.g. *bssA* and *bamY* in two of the MAGs, and *bamA* in three of the MAGs. Those MAGs also encode several *bcrA*, *bzdQ*, and *bamB* subunits of BCRs, indicating a capacity for RD. MAG 33 is the only MAG of the group encoding a partial pathway for naphthalene degradation (NCL, NCR, and THNCR). Interestingly, one MAG of this group, GCA_013203045.1, encodes a complete and another MAG, GCA_018657655.1, an almost complete DSR pathway, indicating capacity for DSR in this group. In the remaining members of SpSt-899, genes for both benzene and naphthalene degradation are scarce. Yet, several MAGs contain isolated genes for the degradation of benzene, i.e. *bssA*, *bamY*, *bamB*, and *bamA*. Curiously, one MAG (GCA_023271155.1) encodes *abcA* for direct carboxylation of benzene and a copy of UbiD-like naphthalene carboxylase, even though it lacks many genes of the downstream degradation pathway. Most SpSt-899 MAGs encode CODH/ACS and the $H_4F$ WL pathway, even though both components are incomplete in some MAGs. All in all, we propose that capacity for UAH/AH degradation is an ancestral trait of the SpSt-899 and was lost in more recent members. However, particularly in several closely related MAGs of the AH-958 group, to which GCA_023271155.1 also belongs, the analysis is impaired by low completeness (52-66%) of the MAGs (Supplementary Fig. 4a, Supplementary Tables 2,10). More high-quality MAGs are needed for more reliable predictions about UAH/AH degradation capacity in this family.

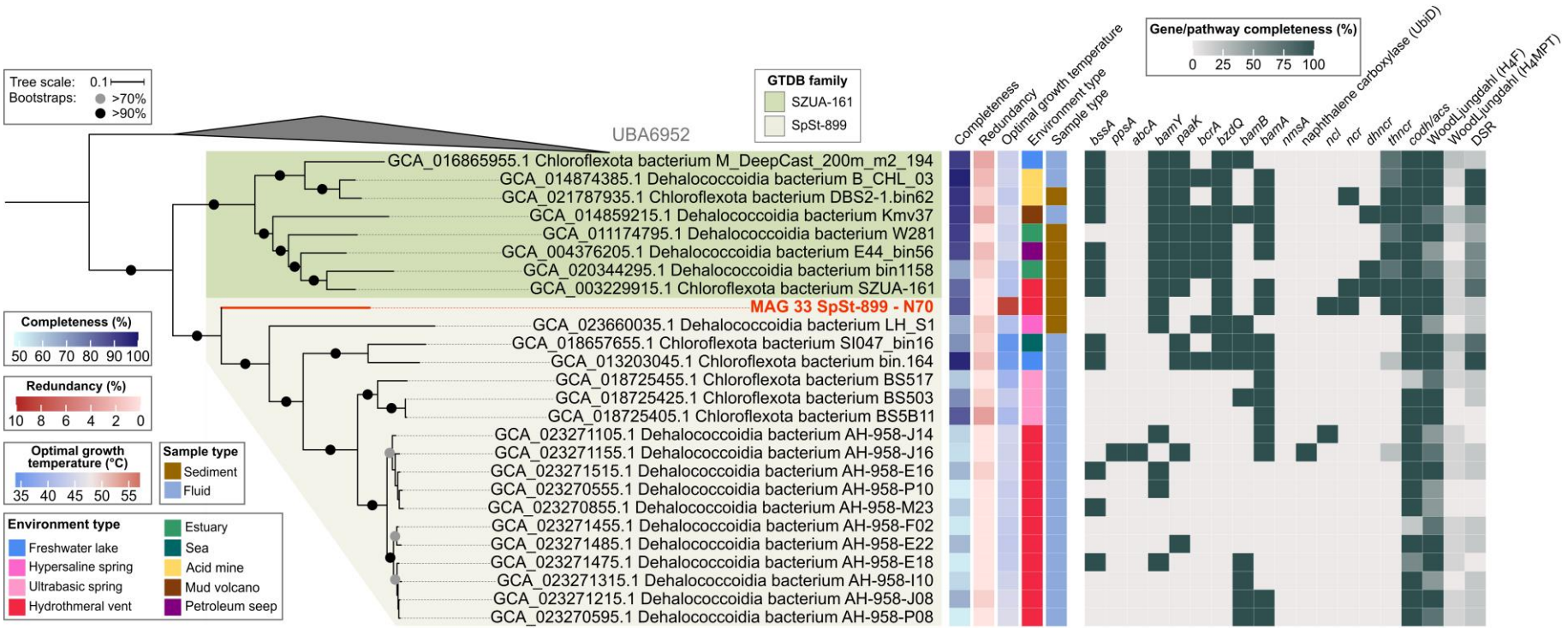


**Figure 7 | Genomic capacities for anaerobic aromatic hydrocarbon degradation in MAGs of the Dehalococcoidia order SZUA-161.** The MAG recovered in this study from the naphthalene 70 °C (N70) culture is highlighted in red. For pathway genes and abbreviations see Supplementary Table 7.

## Discussion

Most previously established UAH-degrading cultures grow at mesophilic temperatures around 30 °C (Galushko et al., 1999; Meckenstock et al., 2000; Musat et al., 2009; Zhang et al., 2012; Dong et al., 2017). A noteworthy exception is the benzene-degrading iron-reducing archaeon *Ferroglobus placidus*, which thrives at 85 °C (Holmes et al., 2011). In this study, we aimed to enrich thermophilic UAH-degrading microorganisms in connection to the reduction of sulfate, one of the most abundant terminal electron acceptors in anoxic marine sediments, from Guaymas Basin (GB) sediment (Thamdrup, 2000; Jørgensen and Kasten, 2006; Bowles et al., 2014). Previous cultivation efforts using GB sediment revealed UAH oxidation in mesophilic aerobic bacteria degrading naphthalene and phenanthrene (Bazylinski et al., 1989; Goetz and Jannasch, 1993), and anaerobic degradation of benzene by *Desulfatiglans* strains SB-21, SB-30, and BznS295 at 28-30°C (Phelps et al., 1998; Musat and Widdel, 2008). Cultures of anaerobic thermophilic UAH-degraders have, to the best of our knowledge, not previously been established from GB sediment.

In this study, we established benzene- and naphthalene-degrading cultures at 50 °C and 70 °C. We found distinct communities in each culture, suggesting that sediments contain a large variety of specified archaea and bacteria that can be enriched with different substrates and temperature combinations. Surprisingly, we found only few benzene degradation genes in the highly abundant Thermoplasmatota MAG in the B50 culture. This pathway has been previously detected mostly in bacteria. It is possible that archaeal homologues differ so much from the bacterial enzymes that they could not be detected due to the high stringency of the BLASTp search. The only known archaeal UAH degrader, *F. placidus*, uses a bacterial-type pathway for benzene degradation (Holmes et al., 2011). Alternatively, this Thermoplasmatota archaeon might employ a different, yet unknown mechanism. Recently, it was proposed that Thermoplasmatota archaea from the GB are able to degrade aromatics via the PAA pathway (Liu et al., 2020). Our MAG did include the key gene, *paaK*, but lacked most other genes of this pathway. Plus, this pathway also converges in BCoA, and BCR and the enzymes of the lower BCoA pathway are required for further oxidation, most of which are absent in MAG 53. Yet, the high relative abundance of this MAG suggests an important role in the culture. Whether and by which mechanism this archaeon degrades benzene requires further investigation.

Desulfatiglandales MAGs 9 and 34 were highly abundant in the B70 and N50 cultures, respectively, and encode plenty of genes for anaerobic UAH oxidation and a complete DSR pathway. Thus, they are most likely the UAH oxidizers in their respective cultures and combine UAH oxidation with sulfate reduction in a single cell. MAG 9 lacks AbcAD, the enzyme for direct carboxylation of benzene, which is currently the only confirmed activation mechanism (Abu Laban et al., 2010; Luo et al., 2014; Eziuzor et al., 2022). Instead, it encodes genes for degrading benzene after methylation by a yet unknown enzyme. Further studies are needed to identify the enzyme responsible for the challenging direct methylation of benzene. Yet, our study indicates that carboxylation is not the only pathway used for benzene activation in anoxic

sediments. MAG 34 encodes an almost complete operon for the anaerobic oxidation of naphthalene via carboxylation (Koelschbach et al., 2019), and further enzymes for complete naphthalene oxidation. According to our analysis of naphthalene degradation genes in the order Desulfatiglandales, MAG 34 is only the second bacterium in the clade, together with NaphS2, capable of oxidizing naphthalene via direct carboxylation. Grown at 50 °C, it is also the most thermophilic anaerobic naphthalene-degrader to date, to the best of our knowledge. With the enrichment of thermophilic species, especially MAG 9 thriving at 70 °C, the general definition of Desulfatiglandales as mesophilic may be questioned (Galushko and Kuever, 2021). We did not detect genes for processing of naphthalene (*nmsA*) after activation via direct methylation in the Desulfatiglandales. Thus, methylation does not seem to be a frequent mechanism for naphthalene activation, which is in accordance with previous studies (Zhang and Young, 1997; Musat et al., 2009; DiDonato et al., 2010).

In the N70 culture, we identified MAG 33 of the Dehalococcoidia order SZUA-161 as the most likely naphthalene oxidizer. The genomic potential for anaerobic aromatics degradation was previously reported for the traditionally hydrogenotrophic organohalide-respiring Dehalococcoidia (Calvo-Martin et al., 2022; Palmer et al., 2023). We found such potential also in the order SZUA-161, particularly in the family SZUA-161, as evidenced by the presence of key genes. While a true confirmation of AH/UAH degradation activity of Dehalococcoidia requires further experimental evidence, e.g. transcriptomics and proteomics, it seems that this clade holds more versatile metabolisms than previously believed. Whether Dehalococcidia may be able to combine AH/UAH degradation to dehalogenation is an intriguing question for the future.

Because the GB exhibits similar characteristics to deeply-buried petroleum reservoirs, i.e. high temperatures, absence of oxygen and presence of UAHs in surface-near sediment layers, the microorganisms enriched in this study might thrive in such yet under-sampled reservoirs (Sierra-Garcia and Oliveira, 2013), where they could contribute to reservoir souring (Tanji et al., 2014). Particularly the Desulfatiglandales bacterium in the B70 culture operates close to the temperature limit of reservoir sterilization of 80-90 °C (Wilhelms et al., 2001). Future studies using advanced sampling and sequencing techniques could reveal the presence and activity of these bacteria in such reservoirs.

*Acknowledgments*

We thank the DFG under Germany's Excellence Initiative/Strategy through the Cluster of Excellence EXC 2077 "The Ocean Floor—Earth's Uncharted Interface" (project no. 390741603) and the Max Planck Society for funding this project. Further, we thank captain, crew and chief scientist Prof. Andreas Teske of *RV Atlantis* cruise AT42-05 and the Alfred Wegener Institute in Bremerhaven (Germany) for providing computational resources.

*Author contributions*

H.Z. designed the study and did laboratory work. G.W. conducted sampling on board. C.O., D.B.M., and H.Z. ran bioinformatical analyses. H.Z. wrote the manuscript with contributions from all coauthors.

## Supplementary Figures

### Overview

| | |
|---|---|
| **Supplementary Figure 1** | Pathways for activation and oxidation of benzene in low-abundance MAGs present in the benzene 50 °C culture |
| **Supplementary Figure 2** | Average nucleotide identities (ANIs) between DSM-4660 MAGs |
| **Supplementary Figure 3** | Average amino acid identities (AAIs) between DSM-4660 MAGs |
| **Supplementary Figure 4** | ANIs and AAIs between SZUA-161 MAGs |

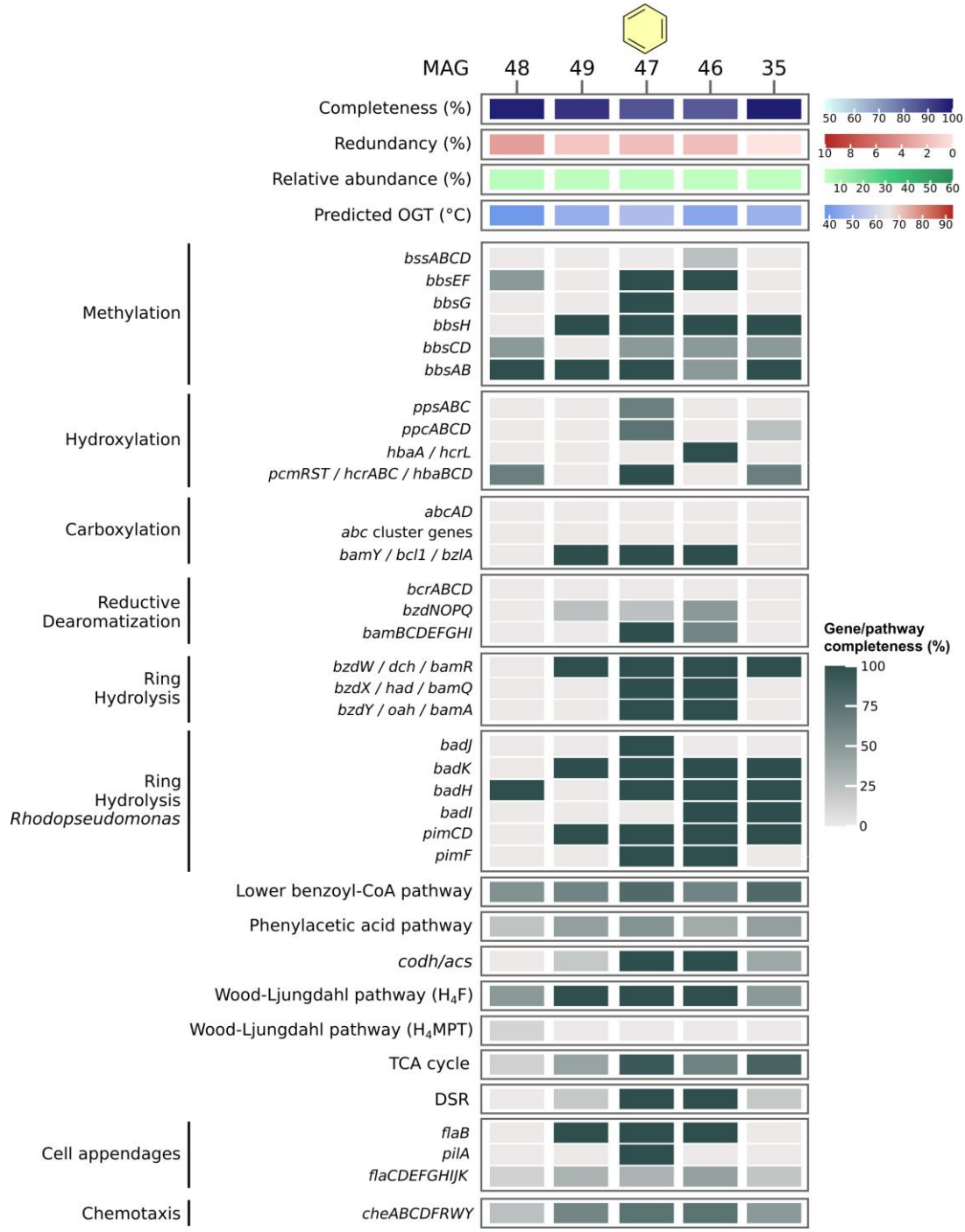


**Supplementary Figure 1 |** Pathways for activation and oxidation of benzene in MAGs present with relative abundances between 3-5% in the benzene 50 °C culture. For proteins and pathways encoded by several genes, completeness was calculated as percentage of present genes of total genes of the pathway/protein. For pathway genes and abbreviations see Supplementary Table 7.

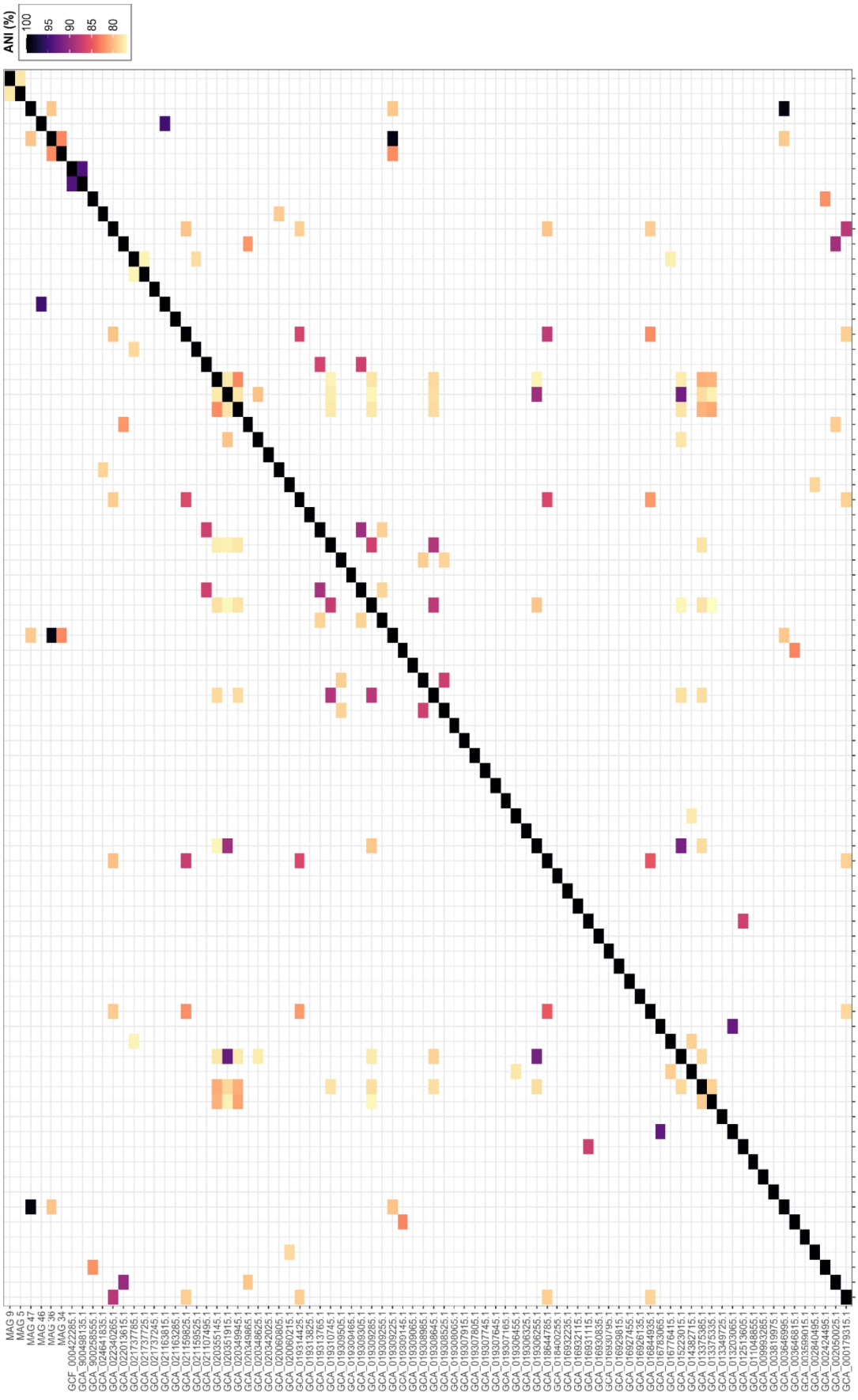


**Supplementary Figure 2** | Average nucleotide identity (ANI) between publicly availablY DSM-4660 MAGs and DSM-4660 MAGs from this study.

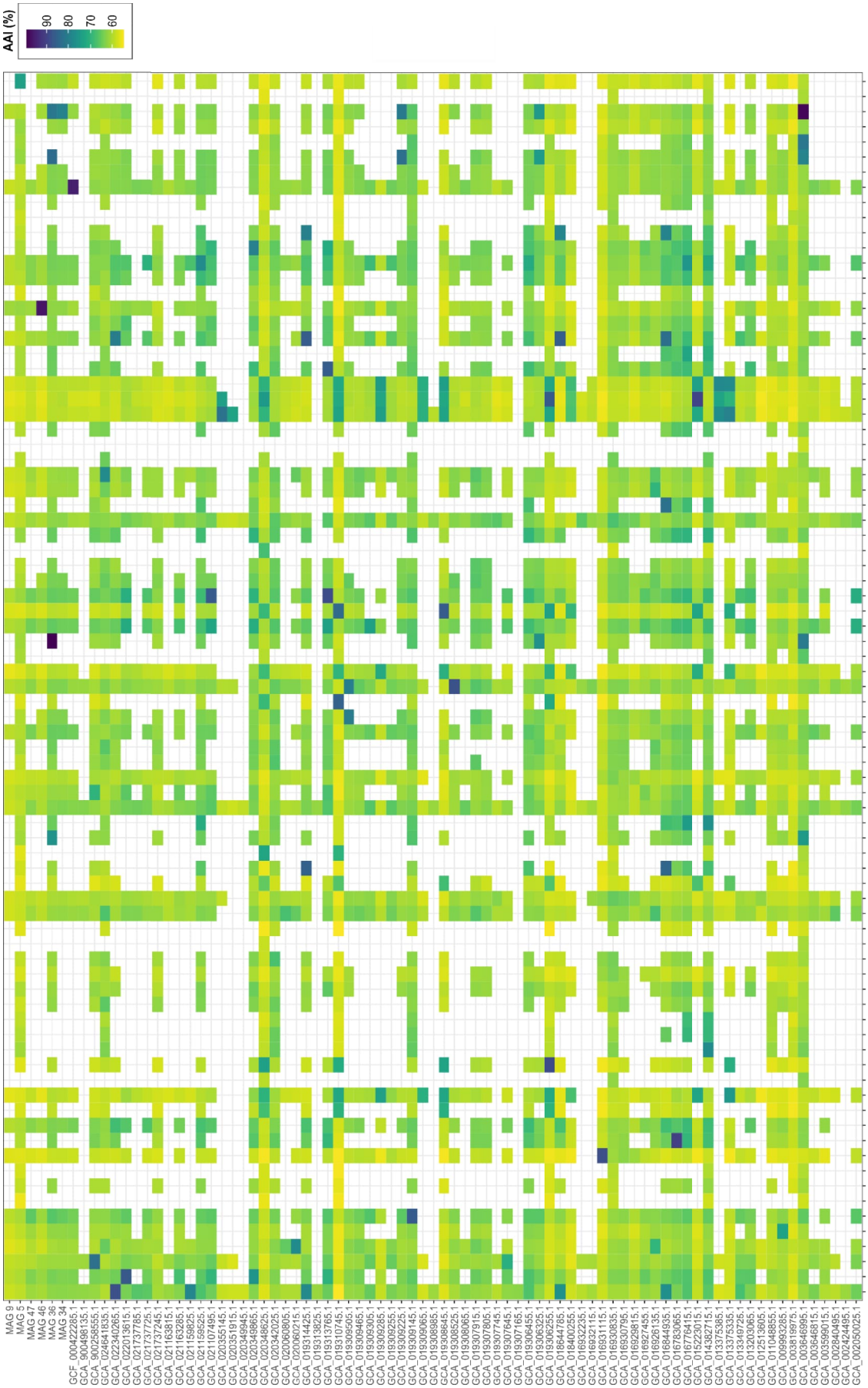


**Supplementary Figure 3** | Average amino acid identity (AAI) between publicly availably DSM-4660 MAGs and DSM-4660 MAGs from this study.

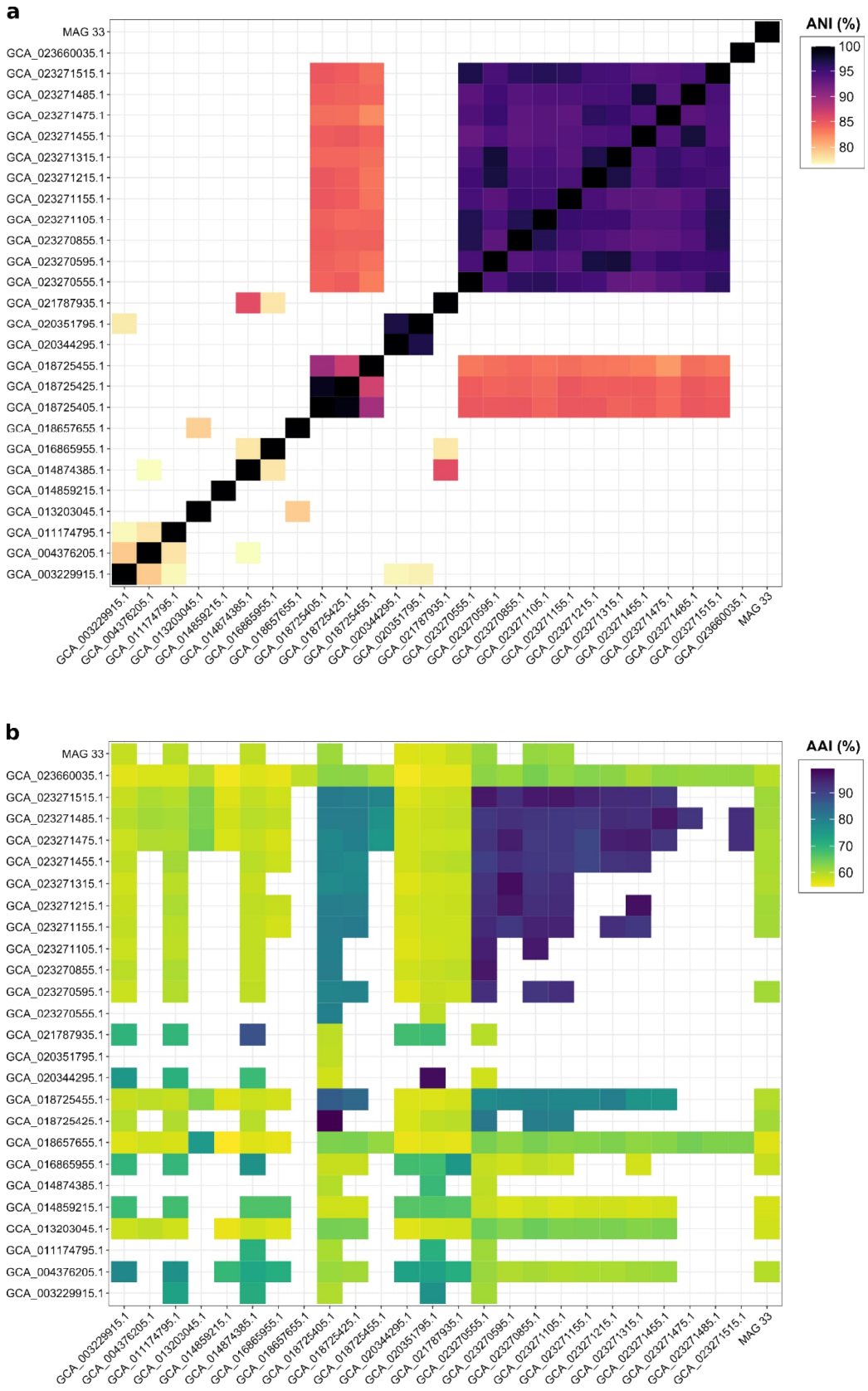


**Supplementary Figure 4 |** Average nucleotide identity (ANI) (**a**) and average amino acid identity (AAI) (**b**) between publicly available MAGs of the bacterial order SZUA-161 and of the SZUA-161 MAG, MAG 33, reconstructed in this study.

## Supplementary Tables

The Supplementary Tables 4, 5, 6, 9, and 10 are available under:
https://figshare.com/s/1d6a4e231b9041cdda2a

### Overview

| | |
|---|---|
| **Supplementary Table 1** | Metadata on DSM-4660 MAGs |
| **Supplementary Table 2** | Genome clusters of DSM-4660 MAGs |
| **Supplementary Table 3** | Metadata on SZUA-161 MAGs |
| **Supplementary Table 4** | Calculation of doubling times of UAH-degrading cultures |
| **Supplementary Table 5** | Relative abundance of MAGs in UAH-degrading cultures |
| **Supplementary Table 6** | Read counts per nearest taxonomic unit (NTU) of reconstructed 16S rRNA gene sequences in original sediment and relative abundances of MAGs from UAH-degrading cultures in original sediment |
| **Supplementary Table 7** | Details on pathways and genes involved in the anaerobic degradation of benzene and naphthalene |
| **Supplementary Table 8** | Details on low-abundance MAGs in the benzene-oxidizing culture at 50 °C |
| **Supplementary Table 9** | ANI and AAI values of DSM-4660 MAGs |
| **Supplementary Table 10** | ANI and AAI values of SZUA-161 MAGs |

**Supplementary Table 1 |** Metadata on publicly available DSM-4660 MAGs included in this study. BioSample accession plus organism and isolate names were acquired from NCBI. Completeness and redundancy was acquired from GTDB-Tk. The optimal growth temperature (OGT) was inferred with OGT_prediction (see "Method" section).

| Accession | BioSample | Organism name | Isolate | Completeness (%) | Redundancy (%) | OGT (°C) |
|---|---|---|---|---|---|---|
| GCA_000179315.1 | SAMN02436561 | delta proteobacterium NaphS2 | | 94.5 | 2.4 | 41.2 |
| GCA_001874005.1 | SAMN04328281 | Desulfobacteraceae bacterium CG2_30_51_40 | CG2_30_51_40 | 95.8 | 0.0 | 43.6 |
| GCA_002050025.1 | SAMN06288223 | Desulfobacteraceae bacterium 4484_190.2 | 4484_190.2 | 64.4 | 2.6 | 43.4 |
| GCA_002424495.1 | SAMN06456449 | Desulfobacteraceae bacterium UBA5623 | UBA5623 | 83.3 | 2.5 | 42.6 |
| GCA_002772275.1 | SAMN06659666 | Deltaproteobacteria bacterium CG23_combo_of_CG06-09_8_20_14_all_51_20 | CG23_combo_of_CG06-09_8_20_14_all_51_20 | 92.2 | 0.0 | 43.3 |
| GCA_002783705.1 | SAMN06659920 | Deltaproteobacteria bacterium CG_4_8_14_3_um_filter_51_11 | CG_4_8_14_3_um_filter_51_11 | 91.9 | 0.0 | 43.2 |
| GCA_002784205.1 | SAMN06659861 | Deltaproteobacteria bacterium CG_4_10_14_3_um_filter_51_14 | CG_4_10_14_3_um_filter_51_14 | 91.4 | 0.0 | 43.3 |
| GCA_002789975.1 | SAMN06660056 | Deltaproteobacteria bacterium CG_4_9_14_3_um_filter_51_14 | CG_4_9_14_3_um_filter_51_14 | 91.3 | 0.7 | 43.2 |
| GCA_002840495.1 | SAMN06767650 | Deltaproteobacteria bacterium HGW-Deltaproteobacteria-21 | HGW-Deltaproteobacteria-21 | 89.2 | 3.0 | 41.0 |
| GCA_002840535.1 | SAMN06767643 | Deltaproteobacteria bacterium HGW-Deltaproteobacteria-15 | HGW-Deltaproteobacteria-15 | 98.7 | 2.7 | 41.0 |
| GCA_003599015.1 | SAMN08499061 | Desulfobacteraceae bacterium | SURF_67 | 70.5 | 0.0 | 43.6 |
| GCA_003646795.1 | SAMN09215079 | Deltaproteobacteria bacterium | B5_G2 | 73.8 | 3.1 | 51.6 |
| GCA_003646815.1 | SAMN09215278 | Deltaproteobacteria bacterium | B46_G9 | 95.7 | 7.2 | 44.3 |
| GCA_003646865.1 | SAMN09214972 | Deltaproteobacteria bacterium | B37_G16 | 81.3 | 0.7 | 52.0 |
| GCA_003646875.1 | SAMN09214971 | Deltaproteobacteria bacterium | B33_G16 | 84.8 | 0.7 | 42.1 |
| GCA_003646935.1 | SAMN09214970 | Deltaproteobacteria bacterium | B25_G16 | 79.8 | 1.4 | 43.7 |
| GCA_003646975.1 | SAMN09214968 | Deltaproteobacteria bacterium | B17_G16 | 81.7 | 0.7 | 44.6 |

| | | | | | | |
|---|---|---|---|---|---|---|
| GCA_003646995.1 | SAMN09215277 | Deltaproteobacteria bacterium | B111_G9 | 88.4 | 6.3 | 50.3 |
| GCA_003819975.1 | SAMN10417363 | Desulfobacteraceae bacterium | maxbin2.1429 | 90.1 | 7.3 | 42.3 |
| GCA_009993285.1 | SAMN13287382 | bacterium | CG_2015-19_51_16 | 94.6 | 0.0 | 43.3 |
| GCA_009993525.1 | SAMN13287371 | bacterium | CG_2015-17_51_13 | 94.0 | 1.0 | 43.8 |
| GCA_011040805.1 | SAMN09638283 | Desulfobacteraceae bacterium | HyVt-119 | 79.7 | 2.8 | 43.1 |
| GCA_011042035.1 | SAMN09638339 | Desulfobacteraceae bacterium | HyVt-17 | 68.9 | 2.1 | 52.9 |
| GCA_011048855.1 | SAMN09639126 | Desulfobacteraceae bacterium | SpSt-1207 | 91.6 | 5.4 | 41.6 |
| GCA_011051075.1 | SAMN09638484 | Deltaproteobacteria bacterium | HyVt-30 | 87.7 | 1.8 | 47.0 |
| GCA_012513605.1 | SAMN13894512 | Desulfatiglans sp. | AS06rmzACSIP_634 | 97.4 | 5.8 | 41.9 |
| GCA_013203065.1 | SAMN14944601 | Desulfobacteraceae bacterium | bin.269 | 85.3 | 2.4 | 41.5 |
| GCA_013349725.1 | SAMN14911656 | Deltaproteobacteria bacterium | MAG_00792_naph_016 | 89.3 | 5.9 | 39.9 |
| GCA_013375335.1 | SAMN14414639 | Desulfobacterales bacterium | CR_Bin_060 | 71.3 | 3.2 | 45.9 |
| GCA_013375385.1 | SAMN14414638 | Desulfobacterales bacterium | CR_Bin_129 | 77.6 | 3.4 | 43.4 |
| GCA_014382715.1 | SAMN15784269 | Candidatus Desulfacyla euxinica | | 83.5 | 0.7 | 39.7 |
| GCA_014382905.1 | SAMN15784260 | Desulfobacterales bacterium | NIOZ-UU19 | 94.7 | 8.7 | 42.0 |
| GCA_015223015.1 | SAMN16387413 | Pseudomonadota bacterium | C4.bin.25 | 64.4 | 2.3 | 41.6 |
| GCA_016776415.1 | SAMN16436252 | Desulfobacteraceae bacterium | BS150m-G21 | 59.9 | 0.5 | 42.7 |
| GCA_016782905.1 | SAMN16436358 | Desulfobacteraceae bacterium | BS750m-G56 | 79.9 | 5.2 | 42.5 |
| GCA_016783025.1 | SAMN16436352 | Desulfobacteraceae bacterium | BS750m-G50 | 54.8 | 0.2 | 41.3 |
| GCA_016783065.1 | SAMN16436351 | Desulfobacteraceae bacterium | BS750m-G49 | 73.6 | 1.9 | 41.6 |
| GCA_016785045.1 | SAMN16436251 | Desulfobacteraceae bacterium | BS150m-G20 | 54.6 | 0.0 | 40.8 |
| GCA_016844935.1 | SAMN17213154 | Desulfobacteraceae bacterium | BH30 | 97.1 | 7.3 | 36.6 |
| GCA_016926135.1 | SAMN17242139 | Deltaproteobacteria bacterium | Zod_Metabat.678 | 86.7 | 0.0 | 44.2 |
| GCA_016927455.1 | SAMN17242070 | Deltaproteobacteria bacterium | Zod_Metabat.483 | 85.0 | 6.3 | 42.8 |
| GCA_016929815.1 | SAMN17241952 | Deltaproteobacteria bacterium | Zod_Metabat.172 | 81.6 | 4.0 | 40.1 |
| GCA_016930795.1 | SAMN17241896 | Deltaproteobacteria bacterium | Zod_Metabat.1351 | 90.7 | 0.9 | 39.6 |
| GCA_016930835.1 | SAMN17241898 | Deltaproteobacteria bacterium | Zod_Metabat.1361 | 92.3 | 2.3 | 39.9 |
| GCA_016931115.1 | SAMN17241884 | Deltaproteobacteria bacterium | Zod_Metabat.1317 | 97.4 | 4.5 | 41.3 |
| GCA_016932115.1 | SAMN17241832 | Deltaproteobacteria bacterium | Zod_Metabat.1176 | 94.1 | 2.0 | 44.3 |

Supplementary Table 1 (continued)

| | | | | | | |
|---|---|---|---|---|---|---|
| GCA_016932235.1 | SAMN17241825 | Deltaproteobacteria bacterium | Zod_Metabat.1158 | 90.7 | 0.0 | 41.0 |
| GCA_018400255.1 | SAMN19006008 | Deltaproteobacteria bacterium | M55B121 | 87.3 | 0.0 | 39.9 |
| GCA_018644785.1 | SAMN14913697 | Deltaproteobacteria bacterium | co234_bin4 | 81.2 | 5.6 | 36.7 |
| GCA_018814905.1 | SAMN19297944 | Pseudomonadota bacterium | Modern_marine.mb.154 | 95.0 | 0.7 | 42.4 |
| GCA_018824685.1 | SAMN19298129 | Pseudomonadota bacterium | Modern_marine_glass_biofilm.mb.54 | 91.3 | 0.7 | 42.4 |
| GCA_019306145.1 | SAMN17179507 | Deltaproteobacteria bacterium | Meg22_810_Bin_82 | 75.0 | 1.2 | 42.6 |
| GCA_019306165.1 | SAMN17179506 | Deltaproteobacteria bacterium | Meg22_810_Bin_43 | 89.4 | 3.6 | 43.1 |
| GCA_019306225.1 | SAMN17179505 | Deltaproteobacteria bacterium | Meg22_810_Bin_34 | 90.6 | 3.2 | 43.7 |
| GCA_019306255.1 | SAMN17179502 | Deltaproteobacteria bacterium | Meg22_810_Bin_243 | 77.4 | 3.2 | 44.5 |
| GCA_019306265.1 | SAMN17179504 | Deltaproteobacteria bacterium | Meg22_810_Bin_24 | 87.9 | 0.1 | 44.0 |
| GCA_019306325.1 | SAMN17179500 | Deltaproteobacteria bacterium | Meg22_810_Bin_233 | 94.2 | 0.7 | 51.3 |
| GCA_019306415.1 | SAMN17179495 | Deltaproteobacteria bacterium | Meg22_810_Bin_172 | 96.5 | 4.1 | 47.8 |
| GCA_019306445.1 | SAMN17179494 | Deltaproteobacteria bacterium | Meg22_810_Bin_16 | 89.7 | 0.7 | 50.5 |
| GCA_019306455.1 | SAMN17179493 | Deltaproteobacteria bacterium | Meg22_810_Bin_119 | 95.8 | 0.7 | 46.0 |
| GCA_019306645.1 | SAMN17179484 | Deltaproteobacteria bacterium | Meg22_46_Bin_59 | 81.8 | 0.0 | 45.7 |
| GCA_019306805.1 | SAMN17179476 | Deltaproteobacteria bacterium | Meg22_46_Bin_232 | 87.1 | 6.6 | 41.5 |
| GCA_019306825.1 | SAMN17179475 | Deltaproteobacteria bacterium | Meg22_46_Bin_228 | 93.2 | 5.5 | 39.0 |
| GCA_019307165.1 | SAMN17179458 | Deltaproteobacteria bacterium | Meg22_24_Bin_96 | 89.5 | 2.6 | 39.0 |
| GCA_019307645.1 | SAMN17179434 | Deltaproteobacteria bacterium | Meg22_24_Bin_146 | 79.6 | 4.2 | 41.2 |
| GCA_019307745.1 | SAMN17179429 | Deltaproteobacteria bacterium | Meg22_24_Bin_118 | 96.7 | 3.7 | 36.7 |
| GCA_019307765.1 | SAMN17179428 | Deltaproteobacteria bacterium | Meg22_24_Bin_117 | 93.2 | 1.9 | 46.0 |
| GCA_019307805.1 | SAMN17179426 | Deltaproteobacteria bacterium | Meg22_24_Bin_103 | 92.6 | 6.3 | 41.5 |
| GCA_019307815.1 | SAMN17179424 | Deltaproteobacteria bacterium | Meg22_1618_Bin_54 | 96.8 | 0.7 | 51.9 |
| GCA_019307885.1 | SAMN17179422 | Deltaproteobacteria bacterium | Meg22_1618_Bin_164 | 94.2 | 0.9 | 51.3 |
| GCA_019307915.1 | SAMN17179418 | Deltaproteobacteria bacterium | Meg22_1416_Bin_58 | 89.7 | 1.3 | 51.4 |
| GCA_019307945.1 | SAMN17179421 | Deltaproteobacteria bacterium | Meg22_1618_Bin_163 | 97.4 | 1.3 | 44.9 |
| GCA_019308065.1 | SAMN17179416 | Deltaproteobacteria bacterium | Meg22_1416_Bin_52 | 96.3 | 1.6 | 44.0 |
| GCA_019308255.1 | SAMN17179401 | Deltaproteobacteria bacterium | Meg22_1214_Bin_373 | 94.8 | 0.7 | 51.3 |
| GCA_019308525.1 | SAMN17179405 | Deltaproteobacteria bacterium | Meg22_1214_Bin_52 | 92.5 | 6.0 | 51.9 |

Supplementary Table 1 (continued)

| | | | | | | |
|---|---|---|---|---|---|---|
| GCA_019308605.1 | SAMN17179396 | Deltaproteobacteria bacterium | Meg22_1214_Bin_29 | 92.9 | 0.7 | 45.0 |
| GCA_019308645.1 | SAMN17179394 | Deltaproteobacteria bacterium | Meg22_1214_Bin_286 | 73.5 | 1.4 | 42.0 |
| GCA_019308725.1 | SAMN17179392 | Deltaproteobacteria bacterium | Meg22_1214_Bin_275 | 84.2 | 1.9 | 52.6 |
| GCA_019308745.1 | SAMN17179391 | Deltaproteobacteria bacterium | Meg22_1214_Bin_272 | 93.6 | 1.3 | 48.7 |
| GCA_019308765.1 | SAMN17179390 | Deltaproteobacteria bacterium | Meg22_1214_Bin_261 | 94.8 | 0.7 | 47.5 |
| GCA_019308785.1 | SAMN17179388 | Deltaproteobacteria bacterium | Meg22_1214_Bin_234 | 90 | 0.3 | 45.7 |
| GCA_019308815.1 | SAMN17179389 | Deltaproteobacteria bacterium | Meg22_1214_Bin_242 | 95.5 | 0 | 51.2 |
| GCA_019308945.1 | SAMN17179381 | Deltaproteobacteria bacterium | Meg22_1214_Bin_142 | 93.2 | 0.7 | 45.3 |
| GCA_019308985.1 | SAMN17179378 | Deltaproteobacteria bacterium | Meg22_1012_Bin_49 | 85.5 | 6.5 | 50.4 |
| GCA_019309025.1 | SAMN17179377 | Deltaproteobacteria bacterium | Meg22_1012_Bin_48 | 91.6 | 0.9 | 50.3 |
| GCA_019309065.1 | SAMN17179375 | Deltaproteobacteria bacterium | Meg22_1012_Bin_349 | 90.6 | 1.9 | 43.2 |
| GCA_019309145.1 | SAMN17179368 | Deltaproteobacteria bacterium | Meg22_1012_Bin_323 | 94.8 | 3.9 | 42.7 |
| GCA_019309225.1 | SAMN17179369 | Deltaproteobacteria bacterium | Meg22_1012_Bin_325 | 87.7 | 2.7 | 52.2 |
| GCA_019309255.1 | SAMN17179364 | Deltaproteobacteria bacterium | Meg22_1012_Bin_291 | 86.1 | 1.9 | 46.2 |
| GCA_019309285.1 | SAMN17179365 | Deltaproteobacteria bacterium | Meg22_1012_Bin_295 | 86.1 | 3.6 | 42.6 |
| GCA_019309305.1 | SAMN17179363 | Deltaproteobacteria bacterium | Meg22_1012_Bin_290 | 91.6 | 1.3 | 44.2 |
| GCA_019309325.1 | SAMN17179362 | Deltaproteobacteria bacterium | Meg22_1012_Bin_256 | 86 | 1.7 | 44.9 |
| GCA_019309385.1 | SAMN17179358 | Deltaproteobacteria bacterium | Meg22_1012_Bin_237 | 96.5 | 0.7 | 45.3 |
| GCA_019309425.1 | SAMN17179357 | Deltaproteobacteria bacterium | Meg22_1012_Bin_192 | 94.8 | 1.9 | 51.1 |
| GCA_019309465.1 | SAMN17179356 | Deltaproteobacteria bacterium | Meg22_1012_Bin_178 | 96.1 | 1.3 | 47.7 |
| GCA_019309505.1 | SAMN17179352 | Deltaproteobacteria bacterium | Meg22_1012_Bin_136 | 83 | 3.9 | 48.7 |
| GCA_019309905.1 | SAMN17179333 | Deltaproteobacteria bacterium | Meg22_02_Bin_134 | 89.8 | 7.2 | 41.1 |
| GCA_019310485.1 | SAMN17179304 | Deltaproteobacteria bacterium | Meg19_1012_Bin_503 | 94.2 | 0.7 | 51.1 |
| GCA_019310505.1 | SAMN17179301 | Deltaproteobacteria bacterium | Meg19_1012_Bin_436 | 83.5 | 2.1 | 43.3 |
| GCA_019310525.1 | SAMN17179303 | Deltaproteobacteria bacterium | Meg19_1012_Bin_445 | 96.8 | 1.3 | 47.4 |
| GCA_019310645.1 | SAMN17179296 | Deltaproteobacteria bacterium | Meg19_1012_Bin_291 | 62.1 | 0 | 43.4 |
| GCA_019310725.1 | SAMN17179292 | Deltaproteobacteria bacterium | Meg19_1012_Bin_230 | 91.9 | 2.6 | 42.1 |
| GCA_019310745.1 | SAMN17179291 | Deltaproteobacteria bacterium | Meg19_1012_Bin_220 | 57.1 | 1.1 | 38.5 |
| GCA_019310765.1 | SAMN17179289 | Deltaproteobacteria bacterium | Meg19_1012_Bin_167 | 95.7 | 1.6 | 45.4 |

Supplementary Table 1 (continued)

| | | | | | | |
|---|---|---|---|---|---|---|
| GCA_019310785.1 | SAMN17179290 | Deltaproteobacteria bacterium | Meg19_1012_Bin_18 | 88.7 | 1.3 | 43.1 |
| GCA_019310805.1 | SAMN17179288 | Deltaproteobacteria bacterium | Meg19_1012_Bin_154 | 95.5 | 1.3 | 44.8 |
| GCA_019310925.1 | SAMN17179283 | Deltaproteobacteria bacterium | Meg19_1012_Bin_10 | 66.4 | 0 | 46.6 |
| GCA_019313765.1 | SAMN17179210 | Deltaproteobacteria bacterium | AB_3033_Bin_63 | 79.4 | 3.5 | 44.3 |
| GCA_019313825.1 | SAMN17179207 | Deltaproteobacteria bacterium | AB_3033_Bin_183 | 60.7 | 1.7 | 43.2 |
| GCA_019314425.1 | SAMN17179176 | Deltaproteobacteria bacterium | AB_03_Bin_182 | 90 | 7.9 | 38.0 |
| GCA_020060215.1 | SAMN18076614 | Deltaproteobacteria bacterium | DeMMO6_6 | 98.7 | 4.2 | 43.1 |
| GCA_020060805.1 | SAMN18076585 | Deltaproteobacteria bacterium | DeMMO6_18 | 92.6 | 0.8 | 45.2 |
| GCA_020342025.1 | SAMN17669525 | Deltaproteobacteria bacterium | bin101 | 72 | 1.9 | 44.8 |
| GCA_020348625.1 | SAMN17669613 | Deltaproteobacteria bacterium | bin319 | 70.4 | 0.7 | 42.0 |
| GCA_020349865.1 | SAMN17669666 | Desulfobacteraceae bacterium | bin575 | 69.1 | 1.6 | 42.8 |
| GCA_020349945.1 | SAMN17669662 | Deltaproteobacteria bacterium | bin55 | 87.7 | 1.3 | 44.9 |
| GCA_020351915.1 | SAMN17669693 | Deltaproteobacteria bacterium | bin73 | 89.1 | 3.2 | 41.3 |
| GCA_020355085.1 | SAMN17669709 | Deltaproteobacteria bacterium | bin80 | 73.1 | 1.3 | 42.3 |
| GCA_020355145.1 | SAMN17669706 | Deltaproteobacteria bacterium | bin79 | 78.7 | 0 | 47.0 |
| GCA_021107495.1 | SAMN21083277 | Desulfobacterales bacterium | SMBSF49 | 84.8 | 3.3 | 42.6 |
| GCA_021159525.1 | SAMN18353820 | Deltaproteobacteria bacterium | AUK324 | 88 | 1 | 44.7 |
| GCA_021159825.1 | SAMN18353809 | Deltaproteobacteria bacterium | AUK313 | 81 | 2.1 | 40.1 |
| GCA_021163285.1 | SAMN18353636 | Deltaproteobacteria bacterium | AUK140 | 95.5 | 0.7 | 43.4 |
| GCA_021163655.1 | SAMN18353549 | Deltaproteobacteria bacterium | AUK053 | 91.3 | 0.9 | 42.8 |
| GCA_021163815.1 | SAMN18353541 | Deltaproteobacteria bacterium | AUK045 | 63.4 | 1.3 | 44.2 |
| GCA_021737245.1 | SAMN21020508 | Deltaproteobacteria bacterium | Tobar14m-G17 | 67.3 | 0 | 38.2 |
| GCA_021737425.1 | SAMN21020505 | Deltaproteobacteria bacterium | Tobar14m-G14 | 93.9 | 2.6 | 41.7 |
| GCA_021737725.1 | SAMN21020428 | Deltaproteobacteria bacterium | Tobar13.5m-G20 | 73.2 | 1.3 | 41.6 |
| GCA_021737785.1 | SAMN21020427 | Deltaproteobacteria bacterium | Tobar13.5m-G19 | 96.5 | 2.2 | 39.5 |
| GCA_022013615.1 | SAMN19414155 | Desulfobacterales bacterium | bin N1.64 | 85.9 | 6.3 | 43.3 |
| GCA_022340265.1 | SAMN20958559 | Deltaproteobacteria bacterium | MASpbin.1 | 95.8 | 1.9 | 37.9 |
| GCA_024641835.1 | SAMN19289861 | Deltaproteobacteria bacterium | Ww165 | 82.9 | 3.6 | 44.3 |

Supplementary Table 1 (continued)

| | | | | | | |
|---|---|---|---|---|---|---|
| GCA_900258555.1 | SAMEA104556992 | uncultured Desulfobacterium sp. | TRIP AH-1 | 99.4 | 1.3 | 42.8 |
| GCA_900498135.1 | SAMEA4803637 | uncultured Desulfatiglans sp. | IK1 | 99.4 | 1 | 41.2 |
| GCF_000422285.1 | SAMN02441472 | Desulfatiglans anilini DSM 4660 | | 99.4 | 0.7 | 40.8 |

Supplementary Table 1 (continued)

**Supplementary Table 2 |** Genome clusters of 135 DSM-4660 MAGs after dereplication at species-level (average nucleotide identity ≥95%), including representative genome selected by anvi'o.

| Cluster | Cluster size | Representative genome | Genomes |
|---|---|---|---|
| **1** | 3 | GCA_019307805.1 | GCA_019306805.1, GCA_019307805.1, GCA_019309905.1 |
| **2** | 6 | GCA_019309285.1 | GCA_019309285.1, GCA_021163655.1, GCA_003646875.1, GCA_019306145.1, GCA_019310645.1, GCA_011040805.1 |
| **3** | 6 | GCA_019306325.1 | GCA_003646795.1, GCA_003646865.1, GCA_019309425.1, GCA_019306325.1, GCA_019308815.1, GCA_019307815.1 |
| **4** | 1 | GCA_011048855.1 | GCA_011048855.1 |
| **5** | 4 | GCA_019309465.1 | GCA_019310525.1, GCA_019309465.1, GCA_003646875.18, GCA_019306415.1 |
| **6** | 1 | GCA_019313825.1 | GCA_019313825.1 |
| **7** | 2 | GCA_019306255.1 | GCA_019310725.1, GCA_019306255.1 |
| **8** | 1 | GCA_020355145.1 | GCA_020355145.1 |
| **9** | 5 | GCA_019309255.1 | GCA_019306645.1, GCA_019307765.1, GCA_019309255.1, GCA_003646875.19, GCA_019310925.1 |
| **10** | 1 | GCA_016932235.1 | GCA_016932235.1 |
| **11** | 1 | GCA_003646995.1 | GCA_003646995.1 |
| **12** | 3 | GCA_019309305.1 | GCA_019306165.1, GCA_019310785.1, GCA_019309305.1 |
| **13** | 3 | GCA_014382715.1 | GCA_014382715.1, GCA_016783025.1, GCA_016785045.1 |
| **14** | 6 | GCA_019307915.1 | GCA_019309025.1, GCA_019306445.1, GCA_003646875.12, GCA_019307885.1, GCA_019310485.1, GCA_019307915.1 |
| **15** | 1 | GCA_018644785.1 | GCA_018644785.1 |
| **16** | 2 | GCA_002840495.1 | GCA_002840535.1, GCA_002840495.1 |
| **17** | 1 | GCA_019308525.1 | GCA_019308525.1 |
| **18** | 4 | GCA_019309065.1 | GCA_003646935.1, GCA_019310505.1, GCA_019309065.1, GCA_019306225.1 |
| **19** | 1 | GCA_016929815.1 | GCA_016929815.1 |
| **20** | 2 | GCA_019309505.1 | GCA_019309505.1, GCA_003646875.17 |
| **21** | 1 | GCA_019308985.1 | GCA_019308985.1 |
| **22** | 1 | GCA_024641835.1 | GCA_024641835.1 |
| **23** | 1 | GCA_019313765.1 | GCA_019313765.1 |
| **24** | 1 | GCA_019314425.1 | GCA_019314425.1 |
| **25** | 1 | GCA_016931115.1 | GCA_016931115.1 |
| **26** | 1 | GCA_015223015.1 | GCA_015223015.1 |
| **27** | 5 | GCA_019306455.1 | GCA_019306455.1, GCA_019309385.1, GCA_011051075.1, GCA_019310765.1, GCA_019308945.1 |
| **28** | 3 | GCA_019309225.1 | GCA_011042035.1, GCA_019309225.1, GCA_019308725.1 |
| **29** | 1 | GCA_021737785.1 | GCA_021737785.1 |
| **30** | 7 | GCA_009993285.1 | GCA_002789975.1, GCA_009993525.1, GCA_001874005.1, GCA_002772275.1, GCA_009993285.1, GCA_002783705.1, GCA_002784205.1 |
| **31** | 1 | GCA_003819975.1 | GCA_003819975.1 |
| **32** | 1 | GCA_019310745.1 | GCA_019310745.1 |
| **33** | 1 | GCA_016930835.1 | GCA_016930835.1 |
| **34** | 2 | GCA_020348625.1 | GCA_020348625.1, GCA_020355085.1 |
| **35** | 2 | GCA_019307165.1 | GCA_019307165.1, GCA_019306825.1 |
| **36** | 1 | GCA_002424495.1 | GCA_002424495.1 |
| **37** | 1 | GCA_019307745.1 | GCA_019307745.1 |
| **38** | 1 | GCA_022340265.1 | GCA_022340265.1 |
| **39** | 1 | GCA_021737245.1 | GCA_021737245.1 |
| **40** | 5 | GCA_016776415.1 | GCA_018814905.1, GCA_014382905.1, GCA_018824685.1, GCA_016776415.1, GCA_016782905.1 |
| **41** | 2 | GCA_021737725.1 | GCA_021737425.1, GCA_021737725.1 |
| **42** | 1 | GCA_016844935.1 | GCA_016844935.1 |
| **43** | 1 | GCA_016926135.1 | GCA_016926135.1 |
| **44** | 1 | GCA_021159525.1 | GCA_021159525.1 |
| **45** | 7 | GCA_019308065.1 | GCA_019308605.1, GCA_019307945.1, GCA_019306265.1, GCA_019308065.1, GCA_003646975.1, GCA_019310805.1, GCA_019309325.1 |

| | | | |
|---|---|---|---|
| **46** | 1 | GCA_022013615.1 | GCA_022013615.1 |
| **47** | 1 | GCA_020351915.1 | GCA_020351915.1 |
| **48** | 1 | GCA_003599015.1 | GCA_003599015.1 |
| **49** | 1 | GCA_021163815.1 | GCA_021163815.1 |
| **50** | 1 | GCA_013349725.1 | GCA_013349725.1 |
| **51** | 1 | GCA_020060215.1 | GCA_020060215.1 |
| **52** | 1 | GCA_020342025.1 | GCA_020342025.1 |
| **53** | 1 | GCA_012513605.1 | GCA_012513605.1 |
| **54** | 1 | GCA_018400255.1 | GCA_018400255.1 |
| **55** | 1 | GCA_000179315.1 | GCA_000179315.1 |
| **56** | 1 | GCA_019309145.1 | GCA_019309145.1 |
| **57** | 1 | GCA_016783065.1 | GCA_016783065.1 |
| **58** | 1 | GCA_016930795.1 | GCA_016930795.1 |
| **59** | 1 | GCF_000422285.1 | GCF_000422285.1 |
| **60** | 1 | GCA_900498135.1 | GCA_900498135.1 |
| **61** | 1 | GCA_900258555.1 | GCA_900258555.1 |
| **62** | 1 | GCA_019308645.1 | GCA_019308645.1 |
| **63** | 1 | GCA_020349865.1 | GCA_020349865.1 |
| **64** | 1 | GCA_021163285.1 | GCA_021163285.1 |
| **65** | 1 | GCA_019307645.1 | GCA_019307645.1 |
| **66** | 1 | GCA_013375335.1 | GCA_013375335.1 |
| **67** | 1 | GCA_020060805.1 | GCA_020060805.1 |
| **68** | 1 | GCA_021107495.1 | GCA_021107495.1 |
| **69** | 1 | GCA_020349945.1 | GCA_020349945.1 |
| **70** | 1 | GCA_002050025.1 | GCA_002050025.1 |
| **71** | 1 | GCA_003646815.1 | GCA_003646815.1 |
| **72** | 1 | GCA_016927455.1 | GCA_016927455.1 |
| **73** | 1 | GCA_013375385.1 | GCA_013375385.1 |
| **74** | 1 | GCA_016932115.1 | GCA_016932115.1 |
| **75** | 1 | GCA_021159825.1 | GCA_021159825.1 |
| **76** | 1 | GCA_013203065.1 | GCA_013203065.1 |

Supplementary Table 2 (continued)

**Supplementary Table 3 |** Metadata on publicly available SZUA-161 MAGs included in this study. BioSample accession, and organism and isolate names were acquired from NCBI. Completeness and redundancy was acquired from GTDB-Tk. The optimal growth temperature (OGT) was inferred with OGT_prediction (see "Method" section).

| Accession | BioSample | Organism | Isolate | Completeness (%) | Redundancy (%) | OGT (°C) |
|---|---|---|---|---|---|---|
| GCA_003229915.1 | SAMN09240145 | Chloroflexota bacterium | SZUA-161 | 81.9 | 0.0 | 41.3 |
| GCA_004376205.1 | SAMN11124421 | Dehalococcoidia bacterium | E44_bin56 | 88.8 | 2.0 | 44.8 |
| GCA_011174795.1 | SAMN14094343 | Dehalococcoidia bacterium | W281 | 91.3 | 0.0 | 44.1 |
| GCA_013203045.1 | SAMN14944593 | Chloroflexota bacterium | bin.164 | 96.7 | 2.0 | 35.2 |
| GCA_014859215.1 | SAMN15871848 | Dehalococcoidia bacterium | Kmv37 | 92.7 | 3.0 | 44.7 |
| GCA_014874385.1 | SAMN15828998 | Dehalococcoidia bacterium | B_CHL_03 | 97.7 | 2.2 | 44.3 |
| GCA_016865955.1 | SAMN10966618 | Chloroflexota bacterium | M_DeepCast_200m_m2_194 | 91.8 | 3.1 | 43.9 |
| GCA_018657655.1 | SAMN14914550 | Chloroflexota bacterium | SI047_bin16 | 73.2 | 1.0 | 34.1 |
| GCA_018725405.1 | SAMN08978946 | Chloroflexota bacterium | BS5B11 | 85.1 | 3.5 | 40.5 |
| GCA_018725425.1 | SAMN08978947 | Chloroflexota bacterium | BS503 | 74.2 | 1.0 | 43.1 |
| GCA_018725455.1 | SAMN08978945 | Chloroflexota bacterium | BS517 | 59.7 | 0.0 | 39.4 |
| GCA_020344295.1 | SAMN17669546 | Dehalococcoidia bacterium | bin1158 | 67.3 | 1.0 | 41.8 |
| GCA_020351795.1 | SAMN17669699 | Dehalococcoidia bacterium | bin748 | 70.1 | 2.0 | 41.3 |
| GCA_021787935.1 | SAMN20842954 | Chloroflexota bacterium | DBS2-1.bin62 | 93.7 | 1.1 | 42.9 |
| GCA_023270555.1 | SAMN27740660 | Dehalococcoidia bacterium | AH-958-P10 | 51.5 | 0.0 | 43.4 |
| GCA_023270595.1 | SAMN27740658 | Dehalococcoidia bacterium | AH-958-P08 | 51.6 | 0.0 | 45.8 |
| GCA_023270855.1 | SAMN27740650 | Dehalococcoidia bacterium | AH-958-M23 | 59.1 | 0.0 | 43.9 |
| GCA_023271105.1 | SAMN27740640 | Dehalococcoidia bacterium | AH-958-J14 | 57.3 | 0.0 | 44.7 |
| GCA_023271155.1 | SAMN27740641 | Dehalococcoidia bacterium | AH-958-J16 | 55.1 | 0.0 | 44.4 |
| GCA_023271215.1 | SAMN27740638 | Dehalococcoidia bacterium | AH-958-J08 | 65.5 | 1.0 | 45.4 |
| GCA_023271315.1 | SAMN27740632 | Dehalococcoidia bacterium | AH-958-I10 | 56.4 | 0.0 | 44.2 |
| GCA_023271455.1 | SAMN27740626 | Dehalococcoidia bacterium | AH-958-F02 | 53.0 | 0.0 | 43.2 |
| GCA_023271475.1 | SAMN27740623 | Dehalococcoidia bacterium | AH-958-E18 | 52.4 | 0.0 | 43.1 |
| GCA_023271485.1 | SAMN27740625 | Dehalococcoidia bacterium | AH-958-E22 | 63.4 | 0.0 | 42.9 |
| GCA_023271515.1 | SAMN27740622 | Dehalococcoidia bacterium | AH-958-E16 | 64.0 | 1.0 | 44.4 |
| GCA_023660035.1 | SAMN18613319 | Dehalococcoidia bacterium LH_S1 | LH_S1 | 66.2 | 1.5 | 41.3 |

**Supplementary Table 7 |** Pathways and genes involved in the anaerobic degradation of benzene and naphthalene

| Pathway part | Gene(s) | Protein encoded |
|---|---|---|
| Benzene methylation | *bssABCD* | Benzylsuccinate synthase |
| Benzene methylation | *bbsEF* | Succinyl-CoA:benzylsuccinate CoA-transferase |
| Benzene methylation | *bbsG* | Benzylsuccinyl-CoA dehydrogenase |
| Benzene methylation | *bbsH* | Phenylitaconyl-CoA hydratase |
| Benzene methylation | *bbsCD* | 2-[Hydroxy(phenyl)methyl]-succinyl-CoA dehydrogenase |
| Benzene methylation | *bbsAB* | Benzoylsuccinyl-CoA thiolase |
| Benzene hydroxylation | *ppsABC* | Phenylphosphate synthase |
| Benzene hydroxylation | *ppcABCD* | Phenylphosphate carboxylase |
| Benzene hydroxylation | *hbaA / hcrL* | 4-Hydroxybenzoate-CoA ligase |
| Benzene hydroxylation | *pcmRST / hcrABC / hbaBCD* | 4-Hydroxybenzoyl-CoA reductase |
| Benzene carboxylation | *abcAD* | Benzene carboxylase |
| Benzene carboxylation | *bamY / bcl1 / bzlA* | Benzoate-CoA ligase |
| Reductive dearomatization (benzene) | *bcrABCD* | Type I benzoyl-CoA reductase (ATP-dependent) (BCR I) *Thauera*-type |
| Reductive dearomatization (benzene) | *bzdNOPQ* | Type I benzoyl-CoA reductase (ATP-dependent) (BCR I) *Azoarcus*-type |
| Reductive dearomatization (benzene) | *bamBCDEFGHI* | Type II benzoyl-CoA reductase (ATP-independent) (BCR II) |
| Ring hydrolysis | *bzdW / dch / bamR* | Cyclohexa-1,5-dienecarbonyl-CoA hydratase |
| Ring hydrolysis | *bzdX / had / bamQ* | 6-Hydroxycyclohex-1-ene-1-carboxyl-CoA dehydrogenase |
| Ring hydrolysis | *bzdY / oah / bamA* | 6-Oxocyclohex-1- ene-1-carbonyl-CoA hydrolase |
| Ring hydrolysis (*Rhodopseudomonas*) | *badJ* | Cyclohexanecarboxyl-CoA dehydrogenase |
| Ring hydrolysis (*Rhodopseudomonas*) | *badK* | Cyclohex-1-ene-1-carboxyl-CoA hydratase |
| Ring hydrolysis (*Rhodopseudomonas*) | *badH* | 2-Hydroxycyclohexanecarboxyl-CoA dehydrogenase |
| Ring hydrolysis (*Rhodopseudomonas*) | *badI* | 2-Ketocyclohexanecarboxyl-CoA hydrolase |
| Ring hydrolysis (*Rhodopseudomonas*) | *pimCD* | Pimeloyl-CoA dehydrogenase (large-C & small-D subunit) |
| Ring hydrolysis (*Rhodopseudomonas*) | *pimF* | Enoyl-CoA hydratase |
| Lower benzoyl-CoA pathway | *pimE* | 3-Hydroxypimeloyl-CoA dehydrogenase |
| Lower benzoyl-CoA pathway | *pimB* | Acetyl-CoA acyltransferase |
| Lower benzoyl-CoA pathway | *gcdH* | Glutaryl-CoA dehydrogenase (decarboxylating) (facultative anaerobes) |
| Lower benzoyl-CoA pathway | *gdh* | Glutaryl-CoA dehydrogenase (non-decarboxylating) (obligate anaerobes) |
| Lower benzoyl-CoA pathway | *gcdABCD* | Glutaconyl-CoA decarboxylase (obligate anaerobes) (energy-conserving) |
| Lower benzoyl-CoA pathway | | 3-Hydroxybutyryl-CoA dehydratase |
| Lower benzoyl-CoA pathway | | 3-Hydroxybutyryl-CoA dehydrogenase |
| Lower benzoyl-CoA pathway | *acat* | Acetoacetyl-CoA thiolase |
| Phenylacetic acid pathway | *paaK* | Phenylacetate-CoA ligase |
| Phenylacetic acid pathway | *paaI* | Acyl-CoA thioesterase |
| Phenylacetic acid pathway | *paaABCDE* | 1,2-Phenylacetyl-CoA epoxidase complex |
| Phenylacetic acid pathway | *paaG* | 1,2-Epoxyphenylacetyl-CoA isomerase |
| Phenylacetic acid pathway | *paaZ* | Bifunctional protein (aldehyde dehydrogenase/enoyl-CoA hydratase) |
| Phenylacetic acid pathway | *paaY* | Thioesterase |
| Phenylacetic acid pathway | *paaJ* | 3-Oxoadipyl-CoA thiolase |
| Phenylacetic acid pathway | *paaF* | 2,3-Dehydroadipyl-CoA hydratase |
| Phenylacetic acid pathway | *paaH* | 3-Hydroxyadipyl-CoA dehydrogenase |
| Phenylacetic acid pathway | *paaX / paaR* | Transcriptional regulator/repressor |
| Naphthalene methylation | *nmsABCD* | Naphthyl-2-methylsuccinyl synthase |

| | | |
|---|---|---|
| Naphthalene methylation | *bnsEF* | Naphthyl-2-methylsuccinyl-CoA transferase |
| Naphthalene methylation | *bnsG* | Naphthyl-2-methyl-succinyl-CoA dehydrogenase |
| Naphthalene methylation | *bnsH* | Naphthyl-2-methylene succinyl-CoA hydratase |
| Naphthalene methylation | *bnsCD* | Naphthyl-2-hydroxymethyl-succinyl-CoA dehydrogenase |
| Naphthalene methylation | *bnsAB* | Napthyl-2-oxomethyl-succinyl-CoA thiolase |
| Naphthalene carboxylation | | Naphthalene carboxylase (UbiD-like carboxylase cluster) |
| Naphthalene carboxylation | *ncl* | Naphthoyl-CoA ligase |
| Reductive dearomatization (naphthalene) | *ncr* | 2-Napthtoyl-CoA reductase |
| Reductive dearomatization (naphthalene) | *dhncr* | 5,6-Dihydro-2-naphthyl-CoA reductase |
| Reductive dearomatization (naphthalene) | *thnBCDE* | 5,6,7,8-Tetrahydro-2-naphthoyl-CoA reductase (THNCR) |
| *thn* Operon | *thnR* | TetR family transcriptional regulator |
| *thn* Operon | *thnA* | Enoyl-CoA hydratase/hydrolase/isomerase |
| *thn* Operon | *thnF* | Ferredoxin |
| *thn* Operon | *thnG* | Oxidoreductase |
| *thn* Operon | *thnH* | Acyl dehydratase MaoC like |
| *thn* Operon | *thnI* | Acyl dehydratase MaoC like |
| *thn* Operon | *thnJ* | Acetyl-CoA acetyltransferase/thiolase |
| *thn* Operon | *thnK* | 3-Hydroxyacyl-CoA dehydrogenase |
| *thn* Operon | *thnL* | Enoyl-CoA hydratase/hydrolase/isomerase |
| *thn* Operon | *thnM* | Enoyl-CoA hydratase/hydrolase/isomerase |
| *thn* Operon | *thnN* | Metal-dependent amidohydrolase |
| *thn* Operon | *thnO* | Acyl-CoA dehydrogenase |
| *thn* Operon | *thnW* | 3-Oxoacyl-ACP reductase |
| *thn* Operon | *thnP* | Acetyl-CoA transferase/hydrolase |
| *thn* Operon | *thnQ* | Acyl-CoA:acetate-lyase AtuA like |
| *thn* Operon | *thnS* | Acyl-CoA:acetate-lyase AtuA like |
| *thn* Operon | *thnX* | 3-Oxoacyl-ACP reductase |
| *thn* Operon | *thnY* | 3-Hydroxyacyl-CoA dehydrogenase |
| *thn* Operon | *thnT* | Acyl-CoA dehydrogenase |
| *thn* Operon | *thnU* | Enoyl-CoA hydratase/hydrolase/isomerase |
| *thn* Operon | *thnV* | Acetyl-CoA acetyltransferase/thiolase |
| CO-dehydrogenase/acetyl-CoA synthase (CODH/ACS) | *cdhA / acsB* | CODH/ACS alpha subunit |
| CO-dehydrogenase/acetyl-CoA synthase (CODH/ACS) | *cdhC / acsA* | CODH/ACS beta subunit |
| CO-dehydrogenase/acetyl-CoA synthase (CODH/ACS) | *cdhE / acsC* | CODH/ACS gamma subunit |
| CO-dehydrogenase/acetyl-CoA synthase (CODH/ACS) | *cdhD / acsD* | CODH/ACS delta subunit |
| CO-dehydrogenase/acetyl-CoA synthase (CODH/ACS) | *cdhB / acsE* | CODH/ACS epsilon subunit |
| Wood-Ljungdahl ($H_4$F methyl branch) | *metF* | 5,10-Methylene-H4F reductase |
| Wood-Ljungdahl ($H_4$F methyl branch) | *folD* | 5,10-Methenyl-$H_4$F cyclohydrolase / 5,10-methylene-$H_4$F dehydrogenase |
| Wood-Ljungdahl ($H_4$F methyl branch) | *fhs* | 10-Formyl-$H_4$F synthetase |
| Wood-Ljungdahl ($H_4$F methyl branch) | *fdhF* | Formate dehydrogenase |
| Wood-Ljungdahl ($H_4$MPT methyl branch) | *mer* | Methylene-$H_4$MPT reductase |
| Wood-Ljungdahl ($H_4$MPT methyl branch) | *mtd / hmd* | Methylene-$H_4$MPT dehydrogenase |
| Wood-Ljungdahl ($H_4$MPT methyl branch) | *mch* | Methenyl-$H_4$MPT cyclohydrolase |
| Wood-Ljungdahl ($H_4$MPT methyl branch) | *ftr* | Formylmethanofuran:$H_4$MPT formyltransferase |

Supplementary Table 7 (continued)

| | | |
|---|---|---|
| Wood-Ljungdahl ($H_4$MPT methyl branch) | *fwdABCD / fmdABCD* | Formylmethanofuran dehydrogenase |
| Tricarboxylic acid cycle | *cit* | Citrate synthase |
| Tricarboxylic acid cycle | *acn* | Aconitate hydratase |
| Tricarboxylic acid cycle | *idh* | Isocitrate dehydrogenase |
| Tricarboxylic acid cycle | | Alpha-ketoglutarate dehydrogenase |
| Tricarboxylic acid cycle | *scsAB* | Succinyl-CoA synthetase / succinate-CoA ligase |
| Tricarboxylic acid cycle | *sdhABCD* | Succinate dehydrogenase |
| Tricarboxylic acid cycle | *fumABC* | Fumarase |
| Tricarboxylic acid cycle | *mdh* | Malate dehydrogenase |
| Dissimilatory sulfate reduction | *sat* | ATP sulfurylase / sulfate adenylyltransferase |
| Dissimilatory sulfate reduction | *aprAB* | Adenylylsulfate reductase |
| Dissimilatory sulfate reduction | *dsrAB* | Dissimilatory sulfite reductase |
| Cell appendages | *flaB/flgA* | Structural pilin |
| Cell appendages | *flaCDE* | Membrane protein with a motor or switch function |
| Cell appendages | *flaF* | Flagellin |
| Cell appendages | *flaG* | Flagellin |
| Cell appendages | *flaH* | Membrane protein with a motor or switch function |
| Cell appendages | *flaI* | ATPase |
| Cell appendages | *flaJ* | Membrane protein with a motor or switch function |
| Cell appendages | *flaK/flgE* | Pre-archaellin-processing peptidase |
| Cell appendages | *pilA* | Type IV major pilin |
| Chemotaxis | *cheA* | Chemotaxis protein |
| Chemotaxis | *cheB* | Chemotaxis response regulator |
| Chemotaxis | *cheC* | CheY-P phosphatase |
| Chemotaxis | *cheD* | Methyl-accepting chemotaxis protein |
| Chemotaxis | *cheF* | Chemotaxis protein |
| Chemotaxis | *cheR* | Chemotaxis protein methyltransferase |
| Chemotaxis | *cheW* | Chemotaxis protein |
| Chemotaxis | *cheY* | Chemotaxis response regulator |

Supplementary Table 7 (continued)

**Supplementary Table 8** | MAGs occurring with relative abundances of 3-5% in the benzene-oxidizing culture at 50 °C. Optimal growth temperature (OGT) was predicted with OGT_prediction, taxonomic affiliation was determined with GTDB-Tk.

| MAG | Relative abundance (%) | OGT (°C) | Domain | Phylum | Class | Order | Family | Genus | Species |
|---|---|---|---|---|---|---|---|---|---|
| **48** | 4.4 | 39.9 | Bacteria | Patescibacteria | ABY1 | UBA2196 | GWA2-42-15 | | |
| **49** | 3.7 | 46.4 | Bacteria | Caldisericota | Caldisericia | B22-G15 | B22-G15 | B22-G15 | B22-G15 sp003648245 |
| **47** | 3.5 | 51.1 | Archaea | Thermoplasmatota | E2 | DHVEG-1 | DHVEG-1 | B44-G15 | |
| **46** | 3.2 | 44.2 | Bacteria | Desulfobacterota | DSM-4660 | Desulfatiglandales | Desulfatiglandaceae | B111-G9 | B111-G9 sp003646995 |
| **35** | 3.1 | 47.5 | Bacteria | Desulfobacterota | DSM-4660 | Desulfatiglandales | Desulfatiglandaceae | | |

## References

Abu Laban, N., Selesi, D., Jobelius, C., and Meckenstock, R. U. (2009). Anaerobic benzene degradation by Gram-positive sulfate-reducing bacteria. *FEMS Microbiol. Ecol.* 68, 300–311. doi: 10.1111/j.1574-6941.2009.00672.x.

Abu Laban, N., Selesi, D., Rattei, T., Tischler, P., and Meckenstock, R. U. (2010). Identification of enzymes involved in anaerobic benzene degradation by a strictly anaerobic iron-reducing enrichment culture. *Environ. Microbiol.* 12, 2783–2796. doi: 10.1111/j.1462-2920.2010.02248.x.

Aihara, J. (1992). Why Aromatic Compounds Are Stable. *Sci. Am.* 266, 62–69.

Alexander, M. (1981). Biodegradation of Chemicals of Environmental Concern. *Science* 211, 132–138. doi: 10.1126/science.7444456.

Altschul, S. F., Gish, W., Miller, W., Myers, E. W., and Lipman, D. J. (1990). Basic local alignment search tool. *J. Mol. Biol.* 215, 403–410. doi: https://doi.org/10.1016/S0022-2836(05)80360-2.

Atashgahi, S., Hornung, B., Van Der Waals, M. J., Da Rocha, U. N., Hugenholtz, F., Nijsse, B., et al. (2018). A benzene-degrading nitrate-reducing microbial consortium displays aerobic and anaerobic benzene degradation pathways. *Sci. Rep.* 8, 1–12. doi: 10.1038/s41598-018-22617-x.

Bankevich, A., Nurk, S., Antipov, D., Gurevich, A. A., Dvorkin, M., Kulikov, A. S., et al. (2012). SPAdes: A New Genome Assembly Algorithm and Its Applications to Single-Cell Sequencing. *J. Comput. Biol.* 19, 455–477. doi: 10.1089/cmb.2012.0021.

Bazylinski, D. A., Wirsen, C. O., Jannasch, H. W., A., B. D., O., W. C., and W., J. H. (1989). Microbial Utilization of Naturally Occurring Hydrocarbons at the Guaymas Basin Hydrothermal Vent Site. *Appl. Environ. Microbiol.* 55, 2832–2836. doi: 10.1128/aem.55.11.2832-2836.1989.

Bergmann, F. D., Selesi, D., and Meckenstock, R. U. (2011a). Identification of new enzymes potentially involved in anaerobic naphthalene degradation by the sulfate-reducing enrichment culture N47. *Arch. Microbiol.* 193, 241–250. doi: 10.1007/s00203-010-0667-4.

Bergmann, F., Selesi, D., Weinmaier, T., Tischler, P., Rattei, T., and Meckenstock, R. U. (2011b). Genomic insights into the metabolic potential of the polycyclic aromatic hydrocarbon degrading sulfate-reducing *Deltaproteobacterium* N47. *Environ. Microbiol.* 13, 1125–1137. doi: 10.1111/j.1462-2920.2010.02391.x.

Blumer, M. (1976). Polycyclic Aromatic Compounds in Nature. *Sci. Am.* 234, 34–45. Available at: http://www.jstor.org/stable/24950303.

Boll, M., Albracht, S. S. P., and Fuchs, G. (1997). Benzoyl-CoA reductase (dearomatizing), a key enzyme of anaerobic aromatic metabolism - A study of adenosinetriphosphatase activity, ATP stoichiometry of the reaction and EPR properties of the enzyme. *Eur. J. Biochem.* 244, 840–851. doi: 10.1111/j.1432-1033.1997.00840.x.

Boll, M., Laempe, D., Eisenreich, W., Bacher, A., Mittelberger, T., Heinze, J., et al. (2000). Nonaromatic Products from Anoxic Conversion of Benzoyl-CoA with Benzoyl-CoA Reductase and Cyclohexa-1,5-diene-1-carbonyl-CoA Hydratase. *J. Biol. Chem.* 275, 21889–21895. doi: https://doi.org/10.1074/jbc.M001833200.

Bowles, M. W., Mogolĺon, J. M., Kasten, S., Zabel, M., and Hinrichs, K. U. (2014). Global rates of marine sulfate reduction and implications for sub-sea-floor metabolic activities. *Science* 344, 889–891. doi: 10.1126/science.1249213.

Bowman, K. S., Nobre, M. F., da Costa, M. S., Rainey, F. A., and Moe, W. M. (2013). *Dehalogenimonas alkenigignens* sp. nov., a chlorinated-alkane-dehalogenating bacterium isolated from groundwater. *Int. J. Syst. Evol. Microbiol.* 63, 1492–1498. doi: https://doi.org/10.1099/ijs.0.045054-0.

Bugg, T. (2003). Dioxygenase Enzymes: Catalytic Mechanisms and Chemical Models. *Tetrahedron* 59, 7075–7101. doi: 10.1016/S0040-4020(03)00944-X.

Bushnell, B. (2014). BBMap: A Fast, Accurate, Splice-Aware Aligner. in *Conference: 9th Annual Genomics of Energy & Environment Meeting, Walnut Creek, CA* Available at: https://www.osti.gov/biblio/1241166.

Calvo-Martin, E., Teira, E., Álvarez-Salgado, X. A., Rocha, C., Jiang, S., Justel-Díez, M., et al. (2022). On the hidden diversity and niche specialization of the microbial realm of subterranean estuaries. *Environ. Microbiol.* 24, 5859–5881. doi: 10.1111/1462-2920.16160.

Carmona, M., Zamarro, M. T., Blázquez, B., Durante-Rodríguez, G., Juárez, J. F., Valderrama, J. A., et al. (2009). Anaerobic Catabolism of Aromatic Compounds: a Genetic and Genomic View. *Microbiol. Mol. Biol. Rev.* 73, 71–133. doi: 10.1128/mmbr.00021-08.

Chaumeil, P.-A. A., Mussig, A. J., Hugenholtz, P., and Parks, D. H. (2020). GTDB-Tk: a toolkit to classify genomes with the Genome Taxonomy Database. *Bioinformatics* 36, 1925–1927. doi: 10.1093/bioinformatics/btz848.

Christensen, N., Batstone, D., He, Z., Angelidaki, I., and Schmidt, J. (2004). Removal of polycyclic aromatic hydrocarbons (PAH) from sewage sludge by anaerobic degradation. *Water Sci. Technol.* 50, 237–244. doi: 10.2166/wst.2004.0580.

Cord-Ruwisch, R. (1985). A quick method for the determination of dissolved and precipitated sulfides in cultures of sulfate-reducing bacteria. *J. Microbiol. Methods* 4, 33–36. doi: https://doi.org/10.1016/0167-7012(85)90005-3.

Danecek, P., Bonfield, J. K., Liddle, J., Marshall, J., Ohan, V., Pollard, M. O., et al. (2021). Twelve years of SAMtools and BCFtools. *Gigascience* 10, giab008. doi: 10.1093/gigascience/giab008.

Das, N., and Chandran, P. (2011). Microbial Degradation of Petroleum Hydrocarbon Contaminants: An Overview. *Biotechnol. Res. Int.* 2011, 1–13. doi: 10.4061/2011/941810.

DiDonato, R. J., Young, N. D., Butler, J. E., Chin, K. J., Hixson, K. K., Mouser, P., et al. (2010). Genome sequence of the deltaproteobacterial strain NaphS2 and analysis of differential gene expression during anaerobic growth on naphthalene. *PLoS One* 5. doi: 10.1371/journal.pone.0014072.

Dombrowski, N., Teske, A. P., and Baker, B. J. (2018). Expansive microbial metabolic versatility and biodiversity in dynamic Guaymas Basin hydrothermal sediments. *Nat. Commun.* 9. doi: 10.1038/s41467-018-07418-0.

Dong, X., Dröge, J., Von Toerne, C., Marozava, S., McHardy, A. C., and Meckenstock, R. U. (2017). Reconstructing metabolic pathways of a member of the genus *Pelotomaculum* suggesting its potential to oxidize benzene to carbon dioxide with direct reduction of sulfate. *FEMS Microbiol. Ecol.* 93, 1–9. doi: 10.1093/femsec/fiw254.

Dong, X., Greening, C., Rattray, J. E., Chakraborty, A., Chuvochina, M., Mayumi, D., et al. (2019). Metabolic potential of uncultured bacteria and archaea associated with petroleum seepage in deep-sea sediments. *Nat. Commun.* 10, 1–12. doi: 10.1038/s41467-019-09747-0.

Eberlein, C., Estelmann, S., Seifert, J., Von Bergen, M., Müller, M., Meckenstock, R. U., et al. (2013a). Identification and characterization of 2-naphthoyl-coenzyme A reductase, the prototype of a novel class of dearomatizing reductases. *Mol. Microbiol.* 88, 1032–1039. doi: 10.1111/mmi.12238.

Eberlein, C., Johannes, J., Mouttaki, H., Sadeghi, M., Golding, B. T., Boll, M., et al. (2013b). ATP-dependent/-independent enzymatic ring reductions involved in the anaerobic catabolism of naphthalene. *Environ. Microbiol.* 15, 1832–1841. doi: 10.1111/1462-2920.12076.

Edgar, R. C. (2004). MUSCLE: multiple sequence alignment with high accuracy and high throughput. *Nucleic Acids Res.* 32, 1792–1797. doi: 10.1093/nar/gkh340.

Erdoğmuş, S. F., Mutlu, B., Korcan, S. E., Güven, K., and Konuk, M. (2013). Aromatic hydrocarbon degradation by halophilic archaea isolated from Çamaltı Saltern, Turkey. *Water. Air. Soil Pollut.* 224, 1449. doi: 10.1007/s11270-013-1449-9.

Eren, A. M., Esen, O. C., Quince, C., Vineis, J. H., Morrison, H. G., Sogin, M. L., et al. (2015). Anvi'o: An advanced analysis and visualization platform for 'omics data. *PeerJ* 2015, 3:e1319. doi: 10.7717/peerj.1319.

Estelmann, S., Blank, I., Feldmann, A., and Boll, M. (2015). Two distinct old yellow enzymes are involved in naphthyl ring reduction during anaerobic naphthalene degradation. *Mol. Microbiol.* 95, 162–172. doi: 10.1111/mmi.12875.

Eziuzor, S. C., Corrêa, F. B., Peng, S., Schultz, J., Kleinsteuber, S., da Rocha, U. N., et al. (2022). Structure and functional capacity of a benzene-mineralizing, nitrate-reducing microbial community. *J. Appl. Microbiol.* 132, 2795–2811. doi: 10.1111/jam.15443.

Fahy, A., McGenity, T. J., Timmis, K. N., and Ball, A. S. (2006). Heterogeneous aerobic benzene-degrading communities in oxygen-depleted groundwaters. *FEMS Microbiol. Ecol.* 58, 260–270. doi: 10.1111/j.1574-6941.2006.00162.x.

Fuchs, G. (1999). "Oxidation of organic compounds," in *Biology of the Prokaryotes*, eds. J. Lengeler, G. Drews, and H. Schlegel (Stuttgart: Thieme), 187–233.

Fuchs, G., Boll, M., and Heider, J. (2011). Microbial degradation of aromatic compounds- From one strategy to four. *Nat. Rev. Microbiol.* 9, 803–816. doi: 10.1038/nrmicro2652.

Galushko, A., and Kuever, J. (2021). "*Desulfatiglandaceae*," in *Bergey's Manual of Systematics of Archaea and Bacteria*, 1–3. doi: https://doi.org/10.1002/9781118960608.fbm00325.

Galushko, A., Minz, D., Schink, B., and Widdel, F. (1999). Anaerobic degradation of naphthalene by a pure culture of a novel type of marine sulphate-reducing bacterium. *Environ. Microbiol.* 1, 415–420. doi: 10.1046/j.1462-2920.1999.00051.x.

Gibson, D. T. (1975). "XI. Microbial Degradation of Aromatic Hydrocarbons," in *The Role of Microorganisms in the Recovery of Oil: Proceedings, 1976 Engineering Foundation Conferences* (Tidewater Inn, Easton, Maryland), 51–55.

Goetz, F. E., and Jannasch, H. W. (1993). Aromatic hydrocarbon-degrading bacteria in the petroleum-rich sediments of the guaymas basin hydrothermal vent site: Preference for aromatic carboxylic acids. *Geomicrobiol. J.* 11, 1–18. doi: 10.1080/01490459309377928.

Gruber-Vodicka, H. R., Seah, B. K. B., and Pruesse, E. (2022). phyloFlash: Rapid Small-Subunit rRNA Profiling and Targeted Assembly from Metagenomes. *mSystems* 5, e00920-20. doi: 10.1128/mSystems.00920-20.

Harwood, C. S., Burchhardt, G., Herrmann, H., and Fuchs, G. (1998). Anaerobic metabolism of aromatic compounds via the benzoyl-CoA pathway. *FEMS Microbiol. Rev.* 22, 439–458. doi: 10.1111/j.1574-6976.1998.tb00380.x.

Heider, J. (2007). Adding handles to unhandy substrates: anaerobic hydrocarbon activation mechanisms. *Curr. Opin. Chem. Biol.* 11, 188–194. doi: 10.1016/j.cbpa.2007.02.027.

Heker, I., Haberhauer, G., and Meckenstock, R. U. (2023). Naphthalene Carboxylation in the Sulfate-Reducing Enrichment Culture N47 Is Proposed to Proceed via 1,3-Dipolar Cycloaddition to the Cofactor Prenylated Flavin Mononucleotide. *Appl. Environ. Microbiol.* 89, e01927-22. doi: 10.1128/aem.01927-22.

Himmelberg, A. M., Brüls, T., Farmani, Z., Weyrauch, P., Barthel, G., Schrader, W., et al. (2018). Anaerobic degradation of phenanthrene by a sulfate-reducing enrichment culture. *Environ. Microbiol.* 20, 3589–3600. doi: 10.1111/1462-2920.14335.

Holmes, D. E., Risso, C., Smith, J. A., and Lovley, D. R. (2011). Anaerobic oxidation of benzene by the hyperthermophilic archaeon *Ferroglobus placidus*. *Appl. Environ. Microbiol.* 77, 5926–5933. doi: 10.1128/AEM.05452-11.

Huwiler, S. G., Löffler, C., Anselmann, S. E. L., Stärk, H. J., Von Bergen, M., Flechsler, J., et al. (2019). One-megadalton metalloenzyme complex in *Geobacter metallireducens* involved in benzene ring reduction beyond the biological redox window. *Proc. Natl. Acad. Sci. U. S. A.* 116, 2259–2264. doi: 10.1073/pnas.1819636116.

Hyatt, D., Chen, G.-L., LoCascio, P. F., Land, M. L., Larimer, F. W., and Hauser, L. J. (2010). Prodigal: prokaryotic gene recognition and translation initiation site identification. *BMC Bioinformatics* 11, 119. doi: 10.1186/1471-2105-11-119.

Inagaki, F., Nunoura, T., Nakagawa, S., Teske, A., Lever, M., Lauer, A., et al. (2006). Biogeographical distribution and diversity of microbes in methane hydrate-bearing deep marine sediments on the Pacific Ocean Margin. *Proc. Natl. Acad. Sci.* 103, 2815–2820. doi: 10.1073/pnas.0511033103.

Jain, C., Rodriguez-R, L. M., Phillippy, A. M., Konstantinidis, K. T., and Aluru, S. (2018). High throughput ANI analysis of 90K prokaryotic genomes reveals clear species boundaries. *Nat. Commun.* 9, 1–8. doi: 10.1038/s41467-018-07641-9.

Jiao, M., He, W., Ouyang, Z., Shi, Q., and Wen, Y. (2022). Progress in structural and functional study of the bacterial phenylacetic acid catabolic pathway, its role in pathogenicity and antibiotic resistance. *Front. Microbiol.* 13, 1–18. doi: 10.3389/fmicb.2022.964019.

Jørgensen, B. B., and Kasten, S. (2006). "Sulfur Cycling and Methane Oxidation," in *Marine Geochemistry*, 271–309. doi: 10.1007/3-540-32144-6_8.

Kawka, O. E., and Simoneit, B. R. T. (1990). Polycyclic aromatic hydrocarbons in hydrothermal petroleums from the Guaymas Basin spreading center. *Appl. Geochemistry* 5, 17–27. doi: 10.1016/0883-2927(90)90032-Z.

Kelley, D. S., Karson, J. A., Blackman, D. K., Früh-Green, G. L., Butterfield, D. A., Lilley, M. D., et al. (2001). An

off-axis hydrothermal vent field near the Mid-Atlantic Ridge at 30° N. *Nature* 412, 145–149. doi: 10.1038/35084000.

Kim, D., Song, L., Breitwieser, F. P., and Salzberg, S. L. (2016). Centrifuge: Rapid and sensitive classification of metagenomic sequences. *Genome Res.* 26, 1721–1729. doi: 10.1101/gr.210641.116.

Kleemann, R., and Meckenstock, R. U. (2011). Anaerobic naphthalene degradation by Gram-positive, iron-reducing bacteria. *FEMS Microbiol. Ecol.* 78, 488–496. doi: 10.1111/j.1574-6941.2011.01193.x.

Koelschbach, J. S., Mouttaki, H., Merl-Pham, J., Arnold, M. E., and Meckenstock, R. U. (2019). Identification of naphthalene carboxylase subunits of the sulfate-reducing culture N47. *Biodegradation* 30, 147–160. doi: 10.1007/s10532-019-09872-z.

Konstantinidis, K. T., Rosselló-Móra, R., and Amann, R. (2017). Uncultivated microbes in need of their own taxonomy. *ISME J.* 11, 2399–2406. doi: 10.1038/ismej.2017.113.

Kraiselburd, I., Brüls, T., Heilmann, G., Kaschani, F., Kaiser, M., and Meckenstock, R. U. (2019). Metabolic reconstruction of the genome of candidate *Desulfatiglans* TRIP_1 and identification of key candidate enzymes for anaerobic phenanthrene degradation. *Environ. Microbiol.* 21, 1267–1286. doi: 10.1111/1462-2920.14527.

Krebs, H. A. (1954). "The Tricarboxylic Acid Cycle," in *Chemical Pathways of Metabolism*, ed. D. M. B. T. Greenberg (Academic Press), 109–171. doi: https://doi.org/10.1016/B978-1-4832-3147-1.50009-3.

Kümmel, S., Herbst, F. A., Bahr, A., Duarte, M., Pieper, D. H., Jehmlich, N., et al. (2015). Anaerobic naphthalene degradation by sulfate-reducing *Desulfobacteraceae* from various anoxic aquifers. *FEMS Microbiol. Ecol.* 91, 1–13. doi: 10.1093/femsec/fiv006.

Langmead, B., and Salzberg, S. L. (2012). Fast gapped-read alignment with Bowtie 2. *Nat. Methods* 9, 357–359. doi: 10.1038/nmeth.1923.

Laso-Pérez, R., Krukenberg, V., Musat, F., and Wegener, G. (2018). Establishing anaerobic hydrocarbon-degrading enrichment cultures of microorganisms under strictly anoxic conditions. *Nat. Protoc.* 13, 1310–1330. doi: 10.1038/nprot.2018.030.

Law, A. M. J., and Aitken, M. D. (2003). Bacterial Chemotaxis to Naphthalene Desorbing from a Nonaqueous Liquid. *Appl. Environ. Microbiol.* 69, 5968–5973. doi: 10.1128/AEM.69.10.5968-5973.2003.

Letunic, I., and Bork, P. (2011). Interactive Tree Of Life v2: online annotation and display of phylogenetic trees made easy. *Nucleic Acids Res.* 39, W475–W478. doi: 10.1093/nar/gkr201.

Lima, A. L. C., Farrington, J. W., and Reddy, C. M. (2005). Combustion-Derived Polycyclic Aromatic Hydrocarbons in the Environment–A Review. *Environ. Forensics* 6, 109–131. doi: 10.1080/15275920590952739.

Liu, W. W., Pan, J., Feng, X., Li, M., Xu, Y., Wang, F., et al. (2020). Evidences of aromatic degradation dominantly via the phenylacetic acid pathway in marine benthic Thermoprofundales. *Environ. Microbiol.* 22, 329–342. doi: 10.1111/1462-2920.14850.

Löffler, F. E., Yan, J., Ritalahti, K. M., Adrian, L., Edwards, E. A., Konstantinidis, K. T., et al. (2013). *Dehalococcoides mccarty*i gen. nov., sp. nov., obligately organohalide-respiring anaerobic bacteria relevant to halogen cycling and bioremediation, belong to a novel bacterial class, Dehalococcoidia classis nov., order Dehalococcoidales ord. nov. and famil. *Int. J. Syst. Evol. Microbiol.* 63, 625–635. doi: 10.1099/ijs.0.034926-0.

Luo, F., Gitiafroz, R., Devine, C. E., Gong, Y., Hug, L. A., Raskin, L., et al. (2014). Metatranscriptome of an anaerobic benzene-degrading, nitrate-reducing enrichment culture reveals involvement of carboxylation in benzene ring activation. *Appl. Environ. Microbiol.* 80, 4095–4107. doi: 10.1128/AEM.00717-14.

Marietou, A. (2021). "Sulfate reducing microorganisms in high temperature oil reservoirs," in *Advances in Applied Microbiology*, eds. G. M. Gadd and S. Sariaslani (Elsevier Inc.), 99–131. doi: 10.1016/bs.aambs.2021.03.004.

Maymó-Gatell, X., Chien, Y., Gossett, J. M., and Zinder, S. H. (1997). Isolation of a Bacterium That Reductively Dechlorinates Tetrachloroethene to Ethene. *Science* 276, 1568–1571. doi: 10.1126/science.276.5318.1568.

McKay, L., Klokman, V. W., Mendlovitz, H. P., Larowe, D. E., Hoer, D. R., Albert, D., et al. (2016). Thermal and geochemical influences on microbial biogeography in the hydrothermal sediments of Guaymas Basin, Gulf of California. *Environ. Microbiol. Rep.* 8, 150–161. doi: 10.1111/1758-2229.12365.

Meckenstock, R. U., Annweiler, E., Michaelis, W., Richnow, H. H., and Schink, B. (2000). Anaerobic Naphthalene

Degradation by a Sulfate-Reducing Enrichment Culture. *Appl. Environ. Microbiol.* 66, 2743–2747. doi: 10.1128/AEM.66.7.2743-2747.2000.

Meckenstock, R. U., Boll, M., Mouttaki, H., Koelschbach, J. S., Cunha Tarouco, P., Weyrauch, P., et al. (2016). Anaerobic degradation of benzene and polycyclic aromatic hydrocarbons. *J. Mol. Microbiol. Biotechnol.* 26, 92–118. doi: 10.1159/000441358.

Moe, W. M., Yan, J., Nobre, M. F., da Costa, M. S., and Rainey, F. A. (2009). *Dehalogenimonas lykanthroporepellens* gen. nov., sp. nov., a reductively dehalogenating bacterium isolated from chlorinated solvent-contaminated groundwater. *Int. J. Syst. Evol. Microbiol.* 59, 2692–2697. doi: https://doi.org/10.1099/ijs.0.011502-0.

Mouttaki, H., Johannes, J., and Meckenstock, R. U. (2012). Identification of naphthalene carboxylase as a prototype for the anaerobic activation of non-substituted aromatic hydrocarbons. *Environ. Microbiol.* 14, 2770–2774. doi: 10.1111/j.1462-2920.2012.02768.x.

Musat, F., Galushko, A., Jacob, J., Widdel, F., Kube, M., Reinhardt, R., et al. (2009). Anaerobic degradation of naphthalene and 2-methylnaphthalene by strains of marine sulfate-reducing bacteria. *Environ. Microbiol.* 11, 209–219. doi: 10.1111/j.1462-2920.2008.01756.x.

Musat, F., and Widdel, F. (2008). Anaerobic degradation of benzene by a marine sulfate-reducing enrichment culture, and cell hybridization of the dominant phylotype. *Environ. Microbiol.* 10, 10–19. doi: 10.1111/j.1462-2920.2007.01425.x.

Natarajan, V. P., Zhang, X., Morono, Y., Inagaki, F., and Wang, F. (2016). A modified SDS-based DNA extraction method for high quality environmental DNA from seafloor environments. *Front. Microbiol.* 7. doi: 10.3389/fmicb.2016.00986.

Nguyen, L.-T., Schmidt, H. A., von Haeseler, A., and Minh, B. Q. (2015). IQ-TREE: A Fast and Effective Stochastic Algorithm for Estimating Maximum-Likelihood Phylogenies. *Mol. Biol. Evol.* 32, 268–274. doi: 10.1093/molbev/msu300.

Paduan, J. B., Zierenberg, R. A., Clague, D. A., Spelz, R. M., Caress, D. W., Troni, G., et al. (2018). Discovery of Hydrothermal Vent Fields on Alarcón Rise and in Southern Pescadero Basin, Gulf of California. *Geochemistry, Geophys. Geosystems* 19, 4788–4819. doi: https://doi.org/10.1029/2018GC007771.

Palmer, M., Covington, J., Thomas, S., Seymour, C., Johnston, J., and Bowen, B. (2023). Thermophilic Dehalococcoidia with unusual traits shed light on an unexpected past. *ISME J.* 17, 952–966. doi: 10.1038/s41396-023-01405-0.

Parales, R. E., Bruce, N. C., Schmid, A., and P, W. L. (2002). Biodegradation, Biotransformation, and Biocatalysis (B3). *Appl. Environ. Microbiol.* 68, 4699–4709. doi: 10.1128/AEM.68.10.4699-4709.2002.

Parales, R. E., and Haddock, J. D. (2004). Biocatalytic degradation of pollutants. *Curr. Opin. Biotechnol.* 15, 374–379. doi: https://doi.org/10.1016/j.copbio.2004.06.003.

Parkes, R. J., Cragg, B., Roussel, E., Webster, G., Weightman, A., and Sass, H. (2014). A review of prokaryotic populations and processes in sub-seafloor sediments, including biosphere:geosphere interactions. *Mar. Geol.* 352, 409–425. doi: https://doi.org/10.1016/j.margeo.2014.02.009.

Parks, D. H., Chuvochina, M., Rinke, C., Mussig, A. J., Chaumeil, P. A., and Hugenholtz, P. (2022). GTDB: An ongoing census of bacterial and archaeal diversity through a phylogenetically consistent, rank normalized and complete genome-based taxonomy. *Nucleic Acids Res.* 50, D785–D794. doi: 10.1093/nar/gkab776.

Parks, D. H., Imelfort, M., Skennerton, C. T., Hugenholtz, P., and Tyson, G. W. (2015). CheckM: Assessing the quality of microbial genomes recovered from isolates, single cells, and metagenomes. *Genome Res.* 25, 1043–1055. doi: 10.1101/gr.186072.114.

Pevneva, G. S., Fursenko, E. A., Voronetskaya, N. G., Mozhayskaya, M. V., Golovko, A. K., Nesterov, I. I., et al. (2017). Hydrocarbon composition and structural parameters of resins and asphaltenes of naphthenic oils of northern West Siberia. *Russ. Geol. Geophys.* 58, 425–433. doi: 10.1016/j.rgg.2016.09.018.

Phelps, C. D., Kerkhof, L. J., and Young, L. Y. (1998). Molecular characterization of a sulfate-reducing consortium which mineralizes benzene. *FEMS Microbiol. Ecol.* 27, 269–279. doi: 10.1016/S0168-6496(98)00073-7.

Porter, A. W., and Young, L. Y. (2014). "Benzoyl-CoA, a Universal Biomarker for Anaerobic Degradation of Aromatic Compounds," in *Advances in Applied Microbiology* (Elsevier Inc.), 167–203. doi: 10.1016/B978-0-12-800260-5.00005-X.

Quast, C., Pruesse, E., Yilmaz, P., Gerken, J., Schweer, T., Yarza, P., et al. (2013). The SILVA ribosomal RNA gene database project: improved data processing and web-based tools. *Nucleic Acids Res.* 41, D590–D596. doi: 10.1093/nar/gks1219.

Ragsdale, S. W. (1997). The Eastern and Western branches of the Wood/Ljungdahl pathway: how the East and West were won. *BioFactors* 6, 3–11. doi: https://doi.org/10.1002/biof.5520060102.

Ramírez, G. A., Mara, P., Sehein, T., Wegener, G., Chambers, C. R., Joye, S. B., et al. (2021). Environmental factors shaping bacterial, archaeal and fungal community structure in hydrothermal sediments of Guaymas Basin, Gulf of California. *PLoS One* 16, 1–31. doi: 10.1371/journal.pone.0256321.

Robador, A., Müller, A. L., Sawicka, J. E., Berry, D., Hubert, C. R. J., Loy, A., et al. (2016). Activity and community structures of sulfate-reducing microorganisms in polar, temperate and tropical marine sediments. *ISME J.* 10, 796–809. doi: 10.1038/ismej.2015.157.

Sauer, D. B., and Wang, D. N. (2019). Predicting the optimal growth temperatures of prokaryotes using only genome derived features. *Bioinformatics* 35, 3224–3231. doi: 10.1093/bioinformatics/btz059.

Schnell, S., Bak, F., and Pfennig, N. (1989). Anaerobic degradation of aniline and dihydroxybenzenes by newly isolated sulfate-reducing bacteria and description of *Desulfobacterium anilini*. *Arch. Microbiol.* 152, 556–563.

Selesi, D., Jehmlich, N., Von Bergen, M., Schmidt, F., Rattei, T., Tischler, P., et al. (2010). Combined genomic and proteomic approaches identify gene clusters involved in anaerobic 2-methylnaphthalene degradation in the sulfate-reducing enrichment culture N47. *J. Bacteriol.* 192, 295–306. doi: 10.1128/JB.00874-09.

Sierra-Garcia, I. N., and Oliveira, V. M. (2013). "Microbial Hydrocarbon Degradation: Efforts to Understand Biodegradation in Petroleum Reservoirs," in *Biodegradation - Engineering and Technology*, 47–72. Available at: http://www.intechopen.com/books/biodegradation-engineering-and-technology/microbial-hydrocarbon-degradation-efforts-to-understand-biodegradation-in-petroleum-reservoirs.

Song, B., and Ward, B. B. (2005). Genetic diversity of benzoyl coenzyme a reductase genes detected in denitrifying isolates and estuarine sediment communities. *Appl. Environ. Microbiol.* 71, 2036–2045. doi: 10.1128/AEM.71.4.2036-2045.2005.

Suzuki, D., Li, Z., Cui, X., Zhang, C., and Katayama, A. (2014). Reclassification of *Desulfobacterium anilini* as *Desulfatiglans anilini* comb. nov. within *Desulfatiglans* gen. nov., and description of a 4-chlorophenol-degrading sulfate-reducing bacterium, *Desulfatiglans parachlorophenolica* sp. nov. *Int. J. Syst. Evol. Microbiol.* 64, 3081–3086. doi: 10.1099/ijs.0.064360-0.

Tanji, Y., Toyama, K., Hasegawa, R., and Miyanaga, K. (2014). Biological souring of crude oil under anaerobic conditions. *Biochem. Eng. J.* 90, 114–120. doi: 10.1016/j.bej.2014.05.023.

Tapilatu, Y. H., Grossi, V., Acquaviva, M., Militon, C., Bertrand, J.-C., and Cuny, P. (2010). Isolation of hydrocarbon-degrading extremely halophilic archaea from an uncontaminated hypersaline pond (Camargue, France). *Extremophiles* 14, 225–231. doi: 10.1007/s00792-010-0301-z.

Thamdrup, B. (2000). "Bacterial Manganese and Iron Reduction in Aquatic Sediments," in *Advances in Microbial Ecology*, ed. B. Schink (Boston, MA: Springer US), 41–84. doi: 10.1007/978-1-4615-4187-5_2.

Torkian, B., Hann, S., Preisner, E., and Norman, R. S. (2020). BLAST-QC: automated analysis of BLAST results. *Environ. Microbiome* 15, 15. doi: 10.1186/s40793-020-00361-y.

Toth, C. R. A., Luo, F., Bawa, N., Webb, J., Guo, S., Dworatzek, S., et al. (2021). Anaerobic benzene biodegradation linked to the growth of highly specific bacterial clades. *Environ. Sci. Technol.* 55, 7970–7980. doi: 10.1021/acs.est.1c00508.

Ulrich, A. C., Beller, H. R., and Edwards, E. A. (2005). Metabolites Detected during Biodegradation of $^{13}C_6$-Benzene in Nitrate-Reducing and Methanogenic Enrichment Cultures. *Environ. Sci. Technol.* 39, 6681–6691. doi: 10.1021/es050294u.

Villatoro-Monzón, W. R., Morales-Ibarria, M. G., Velázquez, E. K., Ramírez-Saad, H., and Razo-Flores, E. (2008). Benzene Biodegradation under Anaerobic Conditions Coupled with Metal Oxides Reduction. *Water. Air. Soil Pollut.* 192, 165–172. doi: 10.1007/s11270-008-9643-x.

Waite, D. W., Chuvochina, M., Pelikan, C., Parks, D. H., Yilmaz, P., Wagner, M., et al. (2020). Proposal to reclassify the proteobacterial classes Deltaproteobacteria and Oligoflexia, and the phylum Thermodesulfobacteria into four phyla reflecting major functional capabilities. *Int. J. Syst. Evol. Microbiol.*

70, 5972–6016. doi: 10.1099/ijsem.0.004213.

Wang, Z., Fingas, M., and Page, D. S. (1999). Oil spill identification. *J. Chromatogr. A* 843, 369–411. doi: https://doi.org/10.1016/S0021-9673(99)00120-X.

Wasmund, K., Schreiber, L., Lloyd, K. G., Petersen, D. G., Schramm, A., Stepanauskas, R., et al. (2014). Genome sequencing of a single cell of the widely distributed marine subsurface Dehalococcoidia, phylum Chloroflexi. *ISME J.* 8, 383–397. doi: 10.1038/ismej.2013.143.

WHO Regional Office for Europe (2000). Chapter 5.2 Benzene. *Air Qual. Guidel. - Second Ed.* 3, 1–18. Available at: http://scholar.google.com/scholar?hl=en&btnG=Search&q=intitle:Chapter+5.2#8.

Wilhelms, A., Larter, S. R., Head, I., Farrimond, P., di-Primio, R., and Zwach, C. (2001). Biodegradation of oil in uplifted basins prevented by deep-burial sterilization. *Nature* 411, 1034–1037. doi: 10.1038/35082535.

Wischgoll, S., Heintz, D., Peters, F., Erxleben, A., Sarnighausen, E., Reski, R., et al. (2005). Gene clusters involved in anaerobic benzoate degradation of *Geobacter metallireducens*. *Mol. Microbiol.* 58, 1238–1252. doi: https://doi.org/10.1111/j.1365-2958.2005.04909.x.

Yan, J., Rash, B. A., Rainey, F. A., and Moe, W. M. (2009). Isolation of novel bacteria within the Chloroflexi capable of reductive dechlorination of 1,2,3-trichloropropane. *Environ. Microbiol.* 11, 833–843. doi: https://doi.org/10.1111/j.1462-2920.2008.01804.x.

Ye, J. X., Lin, T. H., Hu, J. T., Poudel, R., Cheng, Z. W., Zhang, S. H., et al. (2019). Enhancing chlorobenzene biodegradation by *Delftia tsuruhatensis* using a water-silicone oil biphasic system. *Int. J. Environ. Res. Public Health* 16. doi: 10.3390/ijerph16091629.

Young-Beom, A., Jong-Chan, C., J., Z. G., and M., H. M. (2009). Degradation of Phenol via Phenylphosphate and Carboxylation to 4-Hydroxybenzoate by a Newly Isolated Strain of the Sulfate-Reducing Bacterium *Desulfobacterium anilini*. *Appl. Environ. Microbiol.* 75, 4248–4253. doi: 10.1128/AEM.00203-09.

Yu, T., Wu, W., Liang, W., Wang, Y., Hou, J., Chen, Y., et al. (2023). Anaerobic degradation of organic carbon supports uncultured microbial populations in estuarine sediments. *Microbiome* 11, 1–14. doi: 10.1186/s40168-023-01531-z.

Zhang, T., Bain, T. S., Nevin, K. P., Barlett, M. A., and Lovley, D. R. (2012). Anaerobic benzene oxidation by *Geobacter* species. *Appl. Environ. Microbiol.* 78, 8304–8310. doi: 10.1128/AEM.02469-12.

Zhang, T., Tremblay, P. L., Chaurasia, A. K., Smith, J. A., Bain, T. S., and Lovley, D. R. (2013). Anaerobic benzene oxidation via phenol in *Geobacter metallireducens*. *Appl. Environ. Microbiol.* 79, 7800–7806. doi: 10.1128/AEM.03134-13.

Zhang, X., and Young, L. Y. (1997). Carboxylation as an initial reaction in the anaerobic metabolism of naphthalene and phenanthrene by sulfidogenic consortia. *Appl. Environ. Microbiol.* 63, 4759–4764. doi: 10.1128/aem.63.12.4759-4764.1997.

## Manuscript 3

# The core lipidome of anaerobic alkane-oxidizing archaea and their sulfate-reducing partner bacteria

Hanna Zehnle, Christopher Klaembt, Qing-Zeng Zhu, Gunter Wegener, and Florence Schubotz

Manuscript in preparation

# The core lipidome of anaerobic alkane-oxidizing archaea and their sulfate-reducing partner bacteria

Hanna Zehnle[1,2,3], Christopher Klaembt[2], Qing-Zeng Zhu[2], Gunter Wegener[1,2], and Florence Schubotz[2]

1. Max Planck Institute for Marine Microbiology, 28359 Bremen, Germany
2. MARUM, Center for Marine Environmental Science, 28359 Bremen, Germany
3. Faculty of Geosciences, University of Bremen, 28359 Bremen, Germany

Correspondence: gwegener@marum.de; fschubotz@marum.de

## Abstract

Consortia of anaerobic methanotrophic/anaerobic multicarbon alkane-degrading archaea (ANME/ANKA) and their partner sulfate-reducing bacteria (SRB) mediate alkane cycling in gas- and oil-rich environments. These consortia are active over a wide temperature range, which requires adaptations of the cell membrane to maintain adequate membrane permeability and stability. Here, we characterized the membrane core lipid (CL) inventory of long-term enrichment cultures of ANME/ANKA and partner SRB, thriving at 20-70 °C, via state-of-the art mass spectrometry. CL compositions differed strongly between cultures depending on incubation temperature, substrate, and prevalent ANME/ANKA and SRB. Archaeol and macrocyclic archaeol dominated in a low-temperature methane-oxidizing culture, while dialkyl tetraether lipids (GDGTs) were more abundant at higher temperatures. Cross-linkage between biphytanyl groups (GMGTs), additional methylation of tetraethers, and the GMGT derivatives GMD and H-shaped tetrol increased with incubation temperature, while hydroxylated GDGTs were associated with lower temperatures. Tetraethers of bacterial origin, branched GDGTs (brGDGTs), and of yet unresolved biological origin, hybrid isoprenoidal/branched GDGTs (IB-GDGTs), overly branched GDGTs (OB-GDGTs), and sparsely branched GDGTs (SB-GDGTs) accounted for up to 10% of total CLs, hinting at a possible biological origin in the cultures.

***Key words***

Alkane-oxidizing archaea, sulfate-reducing bacteria, core membrane lipids, thermophily, mass spectrometry

## Introduction

*n*-Alkanes (hereafter referred to as alkanes) are linear molecules, consisting only of carbon and hydrogen. Forming the major part of natural gas and petroleum, they occur naturally in gas- and oil-rich habitats like cold seeps, hydrothermal vent areas, and subsurface petroleum reservoirs (Simoneit, 1990; Wilhelms et al., 2001; Boetius and Suess, 2004; Sephton and Hazen, 2013; Åström et al., 2018). Alkanes constitute an energy-rich substrate for anaerobic microorganisms. Anaerobic methanotrophic archaea (ANME) mediate the anaerobic oxidation of methane (AOM) in anoxic environments and remove about 90% of all marine methane via oxidation to $CO_2$, (Reeburgh, 1996; Boetius and Suess, 2004; Lösekann et al., 2007). ANME fall into three clades, ANME-1, ANME-2, and ANME-3 (Hinrichs et al., 1999; Boetius et al., 2000; Orphan et al., 2001; Niemann et al., 2006; Knittel and Boetius, 2009), which oxidize methane over a wide temperature range of -1.5-70°C, with thermophilic AOM currently exclusively attributed to ANME-1 (Boetius et al., 2009; Holler et al., 2011; Benito Merino et al., 2022). Most ANME form syntrophic consortia with sulfate-reducing bacteria (SRB). Mesophilic ANME-1 associate with bacteria of Seep-SRB2 bacteria (within the Genome Taxonomy Database -GTDB- order Dissulfuribacterales) (Ruff et al., 2016; Krukenberg et al., 2018), while thermophilic ANME-1 partner with *Candidatus* Desulfofervidus auxilii of the HotSeep1 clade at 50 °C (Holler et al., 2011; Krukenberg et al., 2016). Recently, a new partner bacterium was discovered for the upper limit of AOM at 70 °C, where ANME-1c partner with *Ca.* Thermodesulfobacterium torris (Benito Merino et al., 2022). ANME-2 partner with the Desulfobacterales clade Seep-SRB1, Seep-SRB2 or seepDBB (*Desulfobulbaceae*-DBB) (Orphan et al., 2001; Pernthaler et al., 2008; Schreiber et al., 2010; Kleindienst et al., 2012; Green-Saxena et al., 2014; Ruff et al., 2016), and ANME-3 with Seep-SRB1a and DBB (Niemann et al., 2006; Lösekann et al., 2007; Schreiber et al., 2010).

Recently, other related archaea were cultured, which oxidize multi-carbon gaseous and liquid alkanes similarly to ANME. These archaea are referred to as anaerobic multicarbon alkane-degrading archaea (ANKA) (Wegener et al., 2022). *Ca.* Argoarchauem ethanivorans and *Ca.* Ethanoperedens thermophilum oxidize ethane ($C_2$) (Chen et al., 2019; Hahn et al., 2020), *Ca.* Syntrophoarchaeum caldarius and *Ca.* S. butanivorans oxidize propane ($C_3$) and butane ($C_4$) (Laso-Pérez et al., 2016), and *Ca.* Alkanophaga volatiphilum and *Ca.* A. liquidiphilum grow on liquid alkanes between pentane ($C_5$) and tetradecane ($C_{14}$) (Zehnle et al., 2023). These ANKA require a syntrophic sulfate-reducing partner, like most ANME. ANKA thrive at a wide temperature range, and growth temperature seems to select the SRB they partner with. *Ca.* A. ethanivorans, which grows at 12 °C, likely partners with two SRB of the Seep-SRB1 group, Eth_SRB1 and Eth_SRB2 (Chen et al., 2019), while *Ca.* E. thermophilum, growing at 37 and 50 °C, and *Ca.* Syntrophoarchaeum spp., growing at 50 °C, partner with *Ca.* D. auxilii, like thermophilic ANME-1 (Holler et al., 2011; Laso-Pérez et al., 2016; Hahn et al., 2020). *Ca.* Alkanophaga spp., grown at 70 °C, partner with a *Thermodesulfobacterium* species, like ANME-1c grown at the same temperature (Benito Merino et al., 2022; Zehnle et al., 2023).

Such different growth temperatures require specific adaptations, including modifications of the cell membrane, which encapsulates the cells of all living organisms (Lamparter and Galic, 2020). The cell membrane needs to balance optimal ion permeability and rigidity, which can be achieved by customizing the membrane lipids (MLs) which make up the membrane (Valentine, 2007; Lamparter and Galic, 2020). Previous studies of enrichment cultures of ANKA and their partner SRB lacked structural analyses of the MLs of both syntrophic partners. Lipid-based studies provide important complementary information to nucleic acid-based analyses, which are often the starting point for studying and identifying microbial communities. Intact MLs consist of hydrophobic tails linked to a glycerol backbone, which in turn is connected to a polar head group, together forming the amphiphilic cell membrane of living organisms (Sturt et al., 2004). Fundamental structural differences exist between archaeal and bacterial MLs. Bacterial MLs resemble those of eukaryotic cells, and consist of fatty acid tails ester-linked to *sn*-glycerol-3-phosphate (G3P). On the other hand, archaeal MLs are made up of highly methylated isoprenoid tails ether-linked to *sn*-glycerol-1-phosphate (G1P) (Koga et al., 1998). Archaea often connect these diether lipids to form membrane-spanning, extremely stable glycerol dibiphytanyl glycerol tetraethers (GDGTs) (Lombard et al., 2012; Schouten et al., 2013; Jain et al., 2014). This challenging tail-to-tail reaction of inert carbon atoms was only recently revealed to be catalyzed by radical S-adenosylmethionine (SAM) proteins (Lloyd et al., 2022; Zeng et al., 2022). The boundaries in this apparent "lipid divide" between the domains of life have become blurry in recent years, with ether-linked and non-isoprenoid membrane-spanning lipids reported in bacteria (Schouten et al., 2007; Lorenzen et al., 2014; Sahonero-Canavesi et al., 2022).

Non-polar core lipids (CLs), i.e. the glycerol backbone with the hydrophobic tails, can remain intact in marine sediments for a long time, under the right circumstances on million year timescales (Kuypers et al., 2001; Brocks et al., 2005; Summons et al., 2022). Microorganisms modify their CLs in a multitude of ways to maintain optimal membrane rigidity and permeability under various environmental conditions (Valentine, 2007). Such modifications are often connected to specific taxonomic groups (De Rosa et al., 1980; Rossel et al., 2008; Sinninghe Damsté et al., 2011). Therefore, CLs are useful biosignatures for past microbial life in the geological record (Eigenbrode, 2008; Summons et al., 2022). In archaea, ML modifications include methylation, hydroxylation, and even cross-linking of the phytanyl or biphytanyl chains in both diether and tetraether lipids as well as inclusion of cyclopentane and cyclohexane moieties (Michaelis and Albrecht, 1979; De Rosa et al., 1980; Comita et al., 1984; Hinrichs et al., 2000; Rossel et al., 2008; Liu et al., 2012b; Knappy et al., 2015; Tourte et al., 2022). While most enzymes performing such challenging modifications remain elusive, recently it was shown that like in case of tetraether formation, radical SAM proteins are responsible for cyclopentane ring formation in GDGTs in the thermophilic model archaeon *Sulfolobus acidocaldarius* (Zeng et al., 2019; Yang et al., 2023). Temperature is an important environmental factor shaping CL modifications (Valentine, 2007; Cario et al., 2015; Sollich et al., 2017). Correlations of certain CL modifications with temperature serve to reconstruct paleological seawater surface

temperatures. For instance, the TetraEther lipid indeX $TEX_{86}$ bases on ratios of GDGTs with a different degree of cyclization found in marine sediments (Schouten et al., 2002). $TEX_{86}$ includes crenarchaeol, a distinct GDGT containing four cyclopentane moieties and one cyclohexane ring presumably produced exclusively by marine planktonic archaea of the class Nitrosphaeria (previously phylum Thaumarchaeota) (Schouten et al., 2002; Sinninghe Damsté et al., 2002; Pester et al., 2011).

Bacteria also modify their tetraether CLs, termed branched GDGTs (brGDGTs), with cyclopentane moieties and additional methyl groups depending on pH and temperature (Weijers et al., 2007). Such brGDGTs were originally associated with anoxic terrestrial environments like peat and soil, and are thus used as a proxy for terrigenous organic matter input into marine environments (Sinninghe Damsté et al., 2000; Hopmans et al., 2004; Weijers et al., 2007; Ceccopieri et al., 2019). A confirmed biological source of brGDGTs are strains of Acidobacteriota, a diverse bacterial phylum abundant in soil (Lee et al., 2008; Sinninghe Damsté et al., 2018; Chaudhary et al., 2019; Chen et al., 2022). Recently, brGDGTs have been increasingly detected in marine oxygen minimum zones and anoxic sediments, including hydrothermal vent sites (Hu et al., 2012; Rotaru et al., 2012; Abdelgadir et al., 2014; Lü et al., 2019). Interestingly, brGDGT concentrations in offshore hypoxic and anoxic marine environments exceed concentrations which can be explained by terrestrial input, indicating *in situ* production by yet unknown bacterial groups (Xie et al., 2013). In addition to brGDGTs, three other groups of GDGTs have been described, which include hybrid isoprenoidal/branched GDGTs (IB-GDGTs), overly branched GDGTs (OB-GDGTs), and sparsely branched GDGTs (SB-GDGTs) (Liu et al., 2012c). These GDGTs are widespread in the anoxic marine environment, and assumed to be produced *in situ* by anaerobic microbial populations (Xie et al., 2014). However, their exact biological origin remains unclear, which is why they have been referred to as “orphan lipids” (Xie et al., 2014).

In this study, we complement recent descriptions of enrichment cultures of ANKA and partner SRB with a mass-spectrometry-based analysis of CLs from culture extracts. We aimed to identify specific CL modifications which might serve as biosignatures, and potentially contribute to the resolution of the biological source of the orphan lipids.

## Methods

### *Anaerobic cultivation*

Anaerobic alkane-oxidizing consortia (Table 1) were cultured in sulfate-reducer medium as described previously (Laso-Pérez et al., 2018) at their favored growth temperature with their respective substrates under gentle shaking (40 rpm) in the dark. The ethane-oxidizing culture growing at 20 °C (E20) was set up as described previously (Laso-Pérez et al., 2018; Hahn et al., 2020) from push core 4870-32 collected with submersible *Alvin* at the moderately warm, yellow "Aceto Balsamico" mat (27°00'28.2"N 111°24'26.2"W, temperature at 20 cm depth ~20 °C (Teske et al., 2016) in the Guaymas Basin (Gulf of California, Mexico) during *RV Atlantis* cruise AT37-06 in December 2016.

### *DNA extraction & sequencing for E20 culture*

After the second dilution of the culture, a 2 ml sample was collected from the E20 culture and centrifuged (10 min, 4,000 rpm, 4 °C). DNA was extracted from the pellet with the Qiagen DNeasy PowerSoil Kit according to the manufacturer's instructions. DNA yield determined via fluorometric measurement was 2.5 µg. DNA was sequenced at the Max-Planck-Genome-Centre (Cologne, Germany) as 2 × 250 paired-end reads on an Illumina HiSeq2500 platform. 6,198,838 reads were obtained.

### *Short-read DNA analysis for E20 culture*

Raw reads were trimmed with the BBDuk script included in BBMap (version 38.79; https://sourceforge.net/projects/bbmap/) (minimum length: 50, minimum quality value: 20). Trimmed reads were assembled with SPAdes (version 3.15.5; https://github.com/ablab/spades) (Bankevich et al., 2012). SPAdes was run with BayesHammer error correction and default *k*-mer increments (21, 33, 55, 77, 99, and 121). The assembly file was reformatted with anvi'o (version 7.1; https://anvio.org/) (Eren et al., 2015), simplifying names and excluding contigs shorter than 1,000 nucleotides. Trimmed reads were mapped to the reformatted assembly with Bowtie2 (version 2.5.1; https://bowtie-bio.sourceforge.net/bowtie2/) (Langmead and Salzberg, 2012). The output sequence alignment map (SAM) file was converted to a binary alignment map (BAM) file with SAMtools (version 1.16.1; http://samtools.sourceforge.net) (Danecek et al., 2021) and indexed with anvi'o. A contigs database for the reformatted assembly and a profile database for the indexed BAM file were created with anvi'o. Anvi'o-included Hidden Markov Models (HMMs) for archaeal and bacterial single-copy core genes (SCGs) plus own HMMs for methyl-coenzyme M reductases (Mcrs) and proteins of the dissimilatory sulfate reduction (DSR) pathway were run on the contigs database with anvi'o. Contigs were binned automatically using MetaBAT 2 (version 2.15; https://bitbucket.org/berkeleylab/metabat) (Kang et al., 2019). Metagenome-assembled genomes (MAGs) were refined manually using anvi'o. MAGs were quality-checked with CheckM (version 1.2.2; https://ecogenomics.github.io/CheckM) (Parks et al., 2015) and only MAGs with completeness ≥50% and redundancy ≤10% were kept. Taxonomies were assigned to MAGs with GTDB-Tk (version 2.1.1;

https://github.com/Ecogenomics/GTDBTk) (Chaumeil et al., 2020) and relative abundances of MAGs were assessed with CoverM (version 0.6.1; https://github.com/wwood/CoverM) run in genome mode. MAGs were compared via fastANI (version 1.33; https://github.com/ParBLiSS/FastANI) (Jain et al., 2018), which determines average nucleotide identities (ANIs).

### *Search for proteins involved in membrane lipid modifications encoded by ANME/ANKA and their partner SRB*

Protein sequences were extracted from previously published MAGs of ANME/ANKA and partner SRBs (accessions see Table 1) plus the likely ANKA/SRB MAGs from the E20 culture with anvi'o, which uses open reading frame prediction by Prodigal (version 2.6.3; https://github.com/hyattpd/Prodigal) (Hyatt et al., 2010). Recently published protein sequences involved in specific ML modifications were downloaded from the National Center for Biotechnology Information (NCBI) database. Local databases were created for the proteins with BLAST (version 2.10.1; https://www.ncbi.nlm.nih.gov/books/NBK279690/) (Altschul et al., 1990). Amino acid sequences of the MAGs were compared to the local databases with BLASTp. The BLASTp output was filtered with BLAST-QC (version 0.1; https://github.com/torkian/blast-QC) (Torkian et al., 2020). Cutoff values for the identification of a given protein were: *e*-value <1e-50, identity ≥30%, and query coverage ≥70%.

**Table 1** | Overview over anaerobic alkane-oxidizing enrichment cultures included in the study and accession numbers of MAGs used for genomic analyses. NA: not available.

| Culture abbreviation | *n*-Alkane substrate | Incubation temperature (°C) | Dominant ANME/ANKA | Partner SRB | Culture origin | Reference |
|---|---|---|---|---|---|---|
| M20 | Methane ($CH_4$) | 20 | ANME-2c<br>NA | Seep-SRB2<br>NA | Gulf of Mexico | Wegener et al., 2016 |
| M37 | Methane ($CH_4$) | 37 | ANME-1a<br>GCA_003194425.1 | Seep-SRB2<br>GCA_003194485.1 | Guaymas Basin | Wegener et al., 2016<br>Krukenberg et al., 2018 |
| M50 | Methane ($CH_4$) | 50 | ANME-1a<br>GCA_003194435.1 | *Ca.* Desulfofervidus auxilii<br>GCA_001577525.1 | Guaymas Basin | Holler et al., 2011<br>Krukenberg et al., 2016 |
| M70 | Methane ($CH_4$) | 70 | ANME-1c<br>GCA_024699715.1 | *Ca.* Thermodesulfobacterium torris<br>GCA_024699695.1 | Guaymas Basin | Benito Merino et al., 2022 |
| E20 | Ethane ($C_2H_6$) | 20 | *Ca.* Ethanoperedens ex4572_44 | Eth_SRB2, Seep-SRB2, Eth_SRB1 | Guaymas Basin | This study |
| E37 | Ethane ($C_2H_6$) | 37 | *Ca.* Ethanoperedens thermophilum<br>GCA_012910725.1 | *Ca.* Desulfofervidus auxilii<br>GCA_001577525.1 | Guaymas Basin | Hahn et al., 2020 |
| E50 | Ethane ($C_2H_6$) | 50 | *Ca.* Ethanoperedens thermophilum<br>GCA_012910725.1 | *Ca.* Desulfofervidus auxilii<br>GCA_001577525.1 | Guaymas Basin | Hahn et al., 2020 |
| P50 | Propane ($C_3H_8$) | 50 | *Ca.* Syntrophoarchaeum caldarius<br>GCA_001766815.1 | *Ca.* Desulfofervidus auxilii<br>GCA_001577525.1 | Guaymas Basin | Laso-Pérez et al., 2016 |
| B50 | Butane ($C_4H_{10}$) | 50 | *Ca.* Syntrophoarchaeum butanivorans<br>GCA_001766825.1 | *Ca.* Desulfofervidus auxilii<br>GCA_001577525.1 | Guaymas Basin | Laso-Pérez et al., 2016 |
| H70 | Hexane ($C_6H_{14}$) | 70 | *Ca.* Alkanophaga volatiphilum<br>GCA_029259545.1 | *Ca.* Thermodesulfobacterium syntrophicum<br>GCA_029259515.1 | Guaymas Basin | Zehnle et al., 2023 |
| T70 | Tetradecane ($C_{14}H_{30}$) | 70 | *Ca.* Alkanophaga liquidiphilum<br>GCA_029259535.1 | *Ca.* Thermodesulfobacterium syntrophicum<br>GCA_029259515.1 | Guaymas Basin | Zehnle et al., 2023 |
| HD70 | Hexadecane ($C_{16}H_{34}$) | 70 | *Ca.* Cerberiarchaeum oleivorans | *Ca.* Thermodesulfobacterium torris | Guaymas Basin | Benito Merino (2023)<br>AT37-06 enrichment |

### *Total lipid extraction*

Two replicate samples were collected from each culture and pelleted via centrifugation (10 min, 4,000 rpm). Total lipids were extracted from the pellets following an adapted Bligh and Dyer extraction method (Bligh and Dyer, 1959; Sturt et al., 2004). All used glassware was pre-combusted at 450 °C for 10 h or rinsed with methanol (MeOH), dichloromethane/methanol (DCM/MeOH) (2:1, v:v) and pure DCM to remove any lipids and other organic contaminants. Chemicals were acquired from Sigma Aldrich (Hamburg, Germany).

For total lipid extraction, the culture pellet was resuspended in 0.8 ml 50 mM phosphate buffer (8,7 g $K_2HPO_4$ $l^{-1}$; pH adjusted to 7.4 with HCl), 1 ml dichloromethane (DCM), and 2 ml methanol (MeOH) per gram pellet. The mixture was sonicated for 10 min in an ultrasonic bath and then centrifuged (2,000 rpm, 10 min). The supernatant was transferred to a separatory funnel, and the extraction from the pellet was repeated once more in the same way. Then, the extraction was repeated twice more with the following new proportions, targeting specifically archaeal tetraether lipids (GDGTs) (Nishihara and Koga, 1987; Sturt et al., 2004): 0.8 ml trichloroacetic acid (TCA) buffer (pH adjusted to 2 with KOH), 1 ml DCM, 2ml MeOH per gram pellet. Next, equal volumes of DCM and Milli-Q-grade $H_2O$ were added to the separatory funnel to separate the solution into an aqueous and an organic phase. The separatory funnel was agitated to mix phases and the organic phase was subsequently collected in a glass container. The aqueous phase was extracted three more times with DCM, collecting all organic phases together. Finally, the combined organic fraction was washed three times with Milli-Q-$H_2O$. The organic fraction was then transferred to a TurboVap flask, and the majority of solvent was evaporated in the TurboVap evaporator under $N_2$ flux for 30-45 min at 34 °C. The remaining solvent, which included total lipids, was transferred to a Zinsser vial. The total lipid extract (TLE) was dried in the Zinsser vial under $N_2$ flux. TLEs were frozen at -20 °C until measurements.

### *Mass spectrometry and raw data analysis*

CLs were analyzed on a Dionex Ultimate 3000RS ultra high-pressure liquid chromatography (UHPLC) system connected to a Bruker maXis ultra-high resolution quadrupole time-of-flight mass spectrometer, equipped with an atmospheric pressure chemical ionization (APCI) II source a following the method described by Becker et al. (2013). Separation of compounds occurred on two acquity BEH HILIC amide columns (1.7 µm, 2.1 × 300 mm) in tandem maintained at 50 °C, and *n*-hexane as eluent A and *n*-hexane:isopropanol, 90:10, v:v as eluent B. A constant flow rate of 0.5 ml $min^{-1}$ and the following gradient was employed: linear gradient from 3% B to 5% B in 2 min, followed by a linear gradient to 10% B in 8 min, 20% B in 10 min, 50% B in 15 min and finally 100% B in 10 min, which was held for 6 min. The columns were equilibrated with 3% B for 9 min before the next injection. Raw data was analyzed with Bruker Compass 1.9 and Bruker Data Analysis Version 4.4 (Bruker Daltonics, Bremen, Germany).

### *CL compositional and statistical analyses*

Total abundances of CL lipid groups were converted to relative abundances to allow comparison between samples. Statistical analyses were carried out using R software (version 4.1.2; https://www.R-project.org/) (R Core Team, 2022) in the RStudio environment (version 2023.03.1; https://www.rstudio.com/) (RStudio Team, 2019). Two-dimensional non-metric multidimensional scaling (NMDS) to examine (dis)similarities of the CL composition between samples was run with the *metaMDS* function of the *vegan* package (version 2.5-7; https://CRAN.R-project.org/package=vegan) using relative abundances of all detected CLs as input and Bray-Curtis dissimilarity as distance measure (Bray and Curtis, 1957; Oksanen et al., 2020). Statistical significance of individual and combined effects of categorical variables on CL composition was examined via permutational multivariate analysis of variance (PERMANOVA) using the *adonis2* function of the *vegan* package. Spearman's rank correlation to test correlations between groups was carried out with the *cor* and *cor.test* functions of the R-integrated *stats* package (version 4.1.2).

The ring index (RI) was calculated to determine the cyclization degree of unmodified GDGTs using average relative abundances of GDGT with up to four cyclopentane rings of the duplicates as follows after Pearson et al. (2004):

$$\mathrm{RI} = \frac{0 \times [\mathrm{GDGT{-}0}] + 1 \times [\mathrm{GDGT{-}1}] + 2 \times [\mathrm{GDGT{-}2}] + 3 \times [\mathrm{GDGT{-}3}] + 4 \times [\mathrm{GDGT{-}4}]}{[\mathrm{GDGT{-}0}] + [\mathrm{GDGT{-}1}] + [\mathrm{GDGT{-}2}] + [\mathrm{GDGT{-}3}] + [\mathrm{GDGT{-}4}]}$$

The methylation index (MI) was calculated to define the degree of methylation of branched tetraethers as follows after Liu et al. (2014):

$$\mathrm{MI_{OB/br/SB}} = ([\text{SB-GDGT-III}] + 2 \times [\text{SB-GDGT-II}] + 3 \times [\text{SB-GDGT-I}] + 4 \times [\text{brGDGT-Ia}] + 5 \times [\text{brGDGT-IIa}] + 6 \times [\text{brGDGT-IIIa}] + 7 \times [\text{OB-GDGT-VI}] + 8 \times [\text{OB-GDGT-V}] + 9 \times [\text{OB-GDGT-IV}] + 10 \times [\text{OB-GDGT-III}] + 11 \times [\text{OB-GDGT-II}] + 12 \times [\text{OB-GDGT-I}]) / ([\Sigma \text{ SB-GDGTs}] + [\Sigma \text{ brGDGTs}] + [\Sigma \text{ OB-GDGTs}])$$

## Results

In this study, we analyzed CLs from methane-oxidizing cultures growing at four different temperatures: consortia of ANME-2c/Seep-SRB2 (20 °C-M20) (Wegener et al., 2016), ANME-1a/Seep-SRB2 (37 °C-M37) (Wegener et al., 2016; Krukenberg et al., 2018), ANME-1a/*Ca.* Desulfofervidus auxilii (50 °C-M50) (Holler et al., 2011; Krukenberg et al., 2016), and ANME-1c/*Ca.* Thermodesulfobacterium torris (70 °C-M70) (Benito Merino et al., 2022). Further, we studied ethane-oxidizing cultures at three temperatures: *Ca.* Ethanoperedens thermophilum/*Ca.* D. auxilii (37 °C-E37 and 50 °C-E50) (Hahn et al., 2020) and a previously undescribed culture growing at ambient temperature (E20). A propane-oxidizing culture (P50) (*Ca.* Syntrophoarchaeum caldarius/*Ca.* D. auxilii) and a butane-oxidizing culture (B50) (*Ca.* S. butanivorans/*Ca.* D. auxilii) (Laso-Pérez et al., 2016) were grown at 50 °C. Hexane-oxidizing cultures of *Ca.* Alkanophaga volatiphilum/*Ca.* T. syntrophicum (H70), tetradecane-oxidizing cultures of *Ca.* A. liquidiphilum/*Ca.* T. syntrophicum (T70) (Zehnle et al., 2023) and hexadecane-oxidizing cultures of *Ca.* Cerberiarchaeum oleivorans/*Ca.* T. torris (HD70) (Benito Merino, 2023) growing at 70 °C were also included (for overview over cultures see Table 1). As a first step, we aimed to identify the ethane-oxidizer and sulfate-reducer in the E20 culture.

### *A* Ca. *Ethanoperedens archaeon is abundant in the E20 culture*

From the short-read metagenome of the E20 culture, we recovered a highly abundant (relative abundance 37.5%) (Table 2), high-quality (completeness 91.2%, redundancy 1.0%) MAG, MAG 12. MAG 12 encodes a complete Mcr/Acr operon (*mcrABG*/*acrABG*), the alkane-activating enzyme of ANME and ANKA (Shima et al., 2012; Laso-Pérez et al., 2016; Lemaire and Wagner, 2022). This MAG is highly similar (ANI >99%) to a previously published MAG reconstructed from Guaymas Basin sediment (Methanosarcinales archaeon ex4572_44, GCA_002254825.2) (Dombrowski et al., 2017), and thus belongs to the same species (Jain et al., 2018). This MAG was previously studied by Hahn et al. (2020), where it was shown to belong to the same genus as *Ca.* E. thermophilum in the GoM-Arc1 cluster. Further, its *acrA* sequence was highly similar to the one of *Ca.* E. thermophilum, and it encoded the Wood-Ljungdahl pathway, but no genes for the *β*-oxidation pathway, which would be required for the oxidation of alkanes larger than ethane (Hahn et al., 2020). Thus, the archaeon represented by this MAG was presumed to be an anaerobic ethane oxidizer as well (Hahn et al., 2020). No other reconstructed MAG encoded Mcr/Acr subunits. Thus, we presume that MAG 12 is the sole ethane oxidizer in our culture.

The next most abundant MAG, MAG 16 (relative abundance 4.1%, completeness 97.7%, redundancy 4.5%) classified as Desulfobacterales genus S5133MH16, encodes a complete dissimilatory sulfate reduction (DSR) pathway. This MAG is of the same genus as one potential partner SRB for *Ca.* Argoarchaeum ethanivorans in ethane-oxidizing enrichments at 12 °C, Eth-SRB2 (GCA_004193595.1) (ANI 88%) (Chen et al., 2019). Two other potential sulfate reducers with a full DSR pathway in the metagenome are MAGs 3 (completeness 95.2%, redundancy

0.6%, assigned to family UBA3076 of order Dissulfuribacterales) and 9 (completeness 97.4%, redundancy 8.2%, assigned to genus Desulfatia of family ETH-SRB1) with relative abundances of 3.0% and 2.2%, respectively. MAG 3 is of the same genus as two previously reconstructed Seep-SRB2 MAGs (GCA_030262715.1 and GCA_030262755.1, ANI 79% and 78%, respectively) from the recently described hydrothermal vent area Pescadero Basin located South of the Guaymas Basin in the Gulf of California (Paduan et al., 2018; Murali et al., 2022). MAG 9 is of the same genus as the second potential partner SRB for *Ca.* A. ethanivorans, Eth_SRB1 (GCA_004193555.1) (ANI 80%), which forms a genus closely related to the genus Seep-SRB1a (Chen et al., 2019; Murali et al., 2022). Based on relative abundances, presence of the DSR pathway, and taxonomic affiliation, it is conceivable that all three bacteria are active sulfate reducers in our culture.

### *CL compositions and major CL groups*

As a first part of the CL analysis, we compared the CL compositions between samples via NMDS ordination (Fig. 1a) and PERMANOVA (Table 3). Samples with the same substrate and temperature combination in general clustered closely together (Fig. 1a), an exception being the M70 culture, in which the composition of the duplicates seems to be very different. Samples of cultures incubated at 70 °C clustered closely together, indicating a similar CL composition. Interestingly, both duplicates of the B50 culture, in which *Ca.* Syntrophoarchaeum butanivorans is the active ANKA, are part of this 70 °C cluster, and fall far away from the P50 culture, in which the closely related *Ca.* S. caldarius oxidizes propane. Of the remaining samples, the M37 and M50 samples fall closely together, as do the E37, E50, and P50 samples. Both 20 °C samples apparently are composed very differently from the remaining samples, and from each other. Substrate, temperature, archaeal genus, bacterial genus, as well as the combination of substrate and temperature all had statistically significant effects on CL composition (Table 3). The vast majority (average 97±3.7%) of detected CLs were of archaeal origin, with 3±3.7% of bacterial (brGDGTs) and unknown (IB-GDGTs, OB-GDGTs, and SB-GDGTs) origin (Fig. 1b). The M37 and M70 culture exhibited the highest percentages of bacterial/unknown CLs (10% and 11% of all CLs, respectively).

**Table 2 |** Relative abundances obtained with CoverM and taxonomic classification with closest relative obtained with GTDB-Tk of all MAGs recovered from the ethane-oxidizing culture at 20 °C. Remaining reads were unmapped. ANI: average nucleotide identity; NA: not available; *: MAG encodes Mcr/Acr; ▲: MAG encodes complete dissimilatory sulfate reduction pathway.

| MAG | Relative abundance (%) | Domain | Phylum | Class | Order | Family | Genus | Species | Closest relative (ANI ≥95%) |
|---|---|---|---|---|---|---|---|---|---|
| **12*** | 37.5 | Archaea | Halobacteriota | Methanosarcinia | Methanosarcinales | EX4572-44 | EX4572-44 | EX4572-44 sp002254825 | GCA_002254825.2 |
| **16▲** | 4.1 | Bacteria | Desulfobacterota | Desulfobacteria | Desulfobacterales | UBA11574 | S5133MH16 | | GCA_001751005.1 |
| **14** | 3.9 | Bacteria | Chloroflexota | Dehalococcoidia | Dehalococcoidales | UBA5627 | W693 | | GCA_011170385.1 |
| **3▲** | 2.9 | Bacteria | Desulfobacterota | Dissulfuribacteria | Dissulfuribacterales | UBA3076 | | | NA |
| **5** | 2.9 | Bacteria | Atribacterota | JS1 | SB-45 | 34-128 | 34-128 | | NA |
| **11** | 2.5 | Archaea | Nanoarchaeota | Nanoarchaeia | Woesearchaeales | DSVV01 | | | GCA_016935125.1 |
| **9▲** | 2.2 | Bacteria | Desulfobacterota | Desulfobacteria | Desulfobacterales | ETH-SRB1 | Desulfaltia | | NA |
| **4** | 1.4 | Archaea | Nanoarchaeota | Nanoarchaeia | Woesearchaeales | | | | GCA_018653365.1 |
| **6** | 1.3 | Archaea | Halobacteriota | Methanosarcinia | Methanosarcinales | EX4572-44 | Ethanoperedens | | GCA_012910725.1 |
| **2** | 1.0 | Bacteria | Patescibacteria | ABY1 | BM507 | UBA12075 | B7-G4 | B7-G4 sp003647675 | GCA_003647675.1 |
| **8** | 0.9 | Bacteria | Desulfobacterota | DSM-4660 | Desulfatiglandales | Desulfatiglandaceae | | | GCA_002050025.1 |

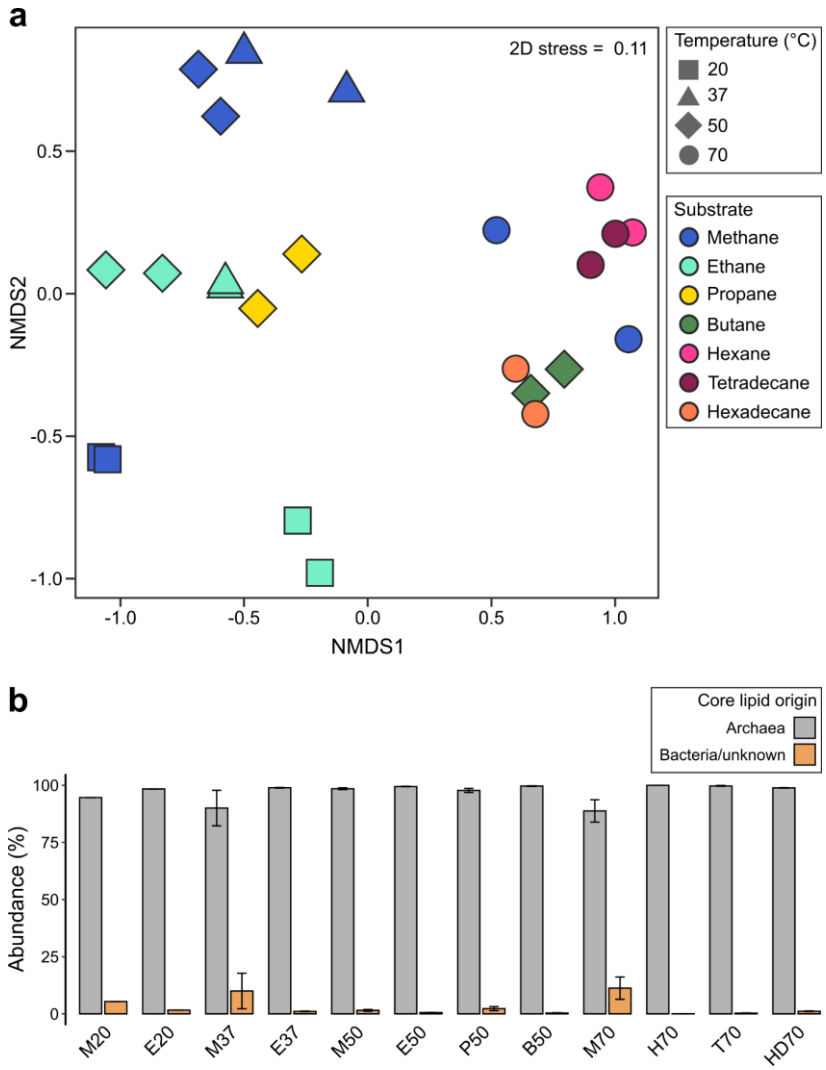


**Figure 1 | Compositional analysis of core lipids in alkane-oxidizing cultures via NMDS ordination (a) and ratios of core lipids of archaeal vs. bacterial/unknown origin (b).**

**Table 3 | Individual and combined effects of variables on core lipid composition determined via PERMANOVA.** Significance levels: 0: '***', 0.001: '**', 0.01: '*', 0.05: '.' Only statistically significant effects are shown.

| Variable | p-Value | Significance |
|---|---|---|
| Substrate | 0.001 | *** |
| Temperature | 0.001 | *** |
| Substrate:temperature | 0.004 | ** |
| Archaeal genus | 0.001 | *** |
| Bacterial genus | 0.001 | *** |

Next, we looked into major CL groups in the samples, using average relative abundances of the duplicates. Among the archaeal CLs (Fig. 2a), archaeol, the simplest diether lipid, was the major CL in the M20 culture (relative abundance within archaeal CLs 77%), followed by macrocyclic archaeol (MAR) with 20%. In all other cultures, diether lipids (archaeol and derivatives) were far less abundant and tetraether lipids constituted the majority of CLs. While all MAGs of the ANME/ANKA encoded at least one homologue of the recently described tetraether synthase (Lloyd et al., 2022; Zeng et al., 2022) for the synthesis of such lipids, peculiarly, *Ca.* S. butanivorans does not encode such a homologue (Supplementary Table 1). Whether this archaeon encodes a tetraether synthase in the ~10% that are missing from this MAG (completeness 89%), or if it uses a variant that is too divergent from the identified proteins to be identified via BLASTp, can currently only be speculated upon. In all cultures except M20, the majority of CLs were unmodified GDGTs with varying number of cyclopentane moieties (see Fig. 3a,b). Structural isomers of GDGT and the diether derivative of GDGT, glycerol dialkyl diether (GDD), plus its isomers were also detected in several cultures, e.g. the HD70 culture, where GDGT isomers were particularly abundant (7% of archaeal CLs). In all ethane cultures (E20, E37, and E50), hydroxylated GDGTs were detected with relative abundances up to 13%, most of which contained one hydroxyl group and no cyclopentane units (1OH-GDGT-0). 2OH- and 3OH-GDGTs were detected at minor relative abundances (≤1%) in the E37, E50, E20, P50, and B50 cultures.

A drastic switch in CL composition occurs from cultures incubated at 50 °C and 70 °C. The B50 culture is an exception to this, and its CL composition is more similar to the CL compositions of cultures incubated at higher temperatures, as was indicated already by the compositional analysis above. B50 and the 70 °C cultures contained lower abundances of archaeol (<20%) and varying relative abundances of unmodified GDGTs (18% in HD70 compared to 59% in T70). Tetraethers with cross-linkage between the biphytanyl chains, glycerol monoalkyl glycerol tetraethers (GMGTs), and modified GMGTs with one and two additional methyl groups (1Me-GMGTs and 2Me-GMGTs) were found in all cultures of this group. In addition, the GMGT derivatives glycerol monoalkyl diether (GMD) and H-shaped tetrol were highly abundant in this group. GMGTs and derivatives made up between 31% (T70) and 59% (HD70) of archaeal CLs in the cultures incubated at 70 °C, plus 42% in B50. GMGTs and derivatives were also present in the E37 and P50 cultures, but with lower abundances (12% and 6%, respectively). The 70 °C cultures also contained low relative abundances of mono- and dimethylated GDGTs (1Me-GDGTs and 2Me-GDGTs) and their derivative diethers (1Me-GDDs and 2Me-GDDs). 1Me-GDGT was most abundant in the T70 culture (3%) and 2Me-GDGT in the HD70 culture (0.8%). These methylated GDGTs were virtually absent in cultures incubated at lower temperatures.

Within the CLs of bacterial/unknown origin, brGDGTs made up the majority in the M20, E20, H70, and HD70 cultures with relative abundances between 47 and 69% in the bacterial/unknown CL fraction (Fig. 2b). In the E37 culture and all cultures incubated at 50 °C,

overly branched non-isoprenoidal tetraether (OB-GDGT) was the prevalent bacterial/unknown CL (51-77%). Notably, relatively high relative abundances of the structurally intriguing hybrid isoprenoidal/branched tetraether, IB-GDGT, were detected in M37, M70, T70, and HD70 cultures. In the M37 and M70 cultures, IB-GDGT made up 48 and 88% of bacterial/unknown CLs, and 8% of total CLs, respectively. Cultures incubated at up to 50 °C also contained low abundances (maximally 6% of bacterial/unknown CLs in M20), of sparsely branched non-isoprenoid tetraether lipids (SB-GDGTs). Those lipids were absent in cultures incubated at 70 °C.

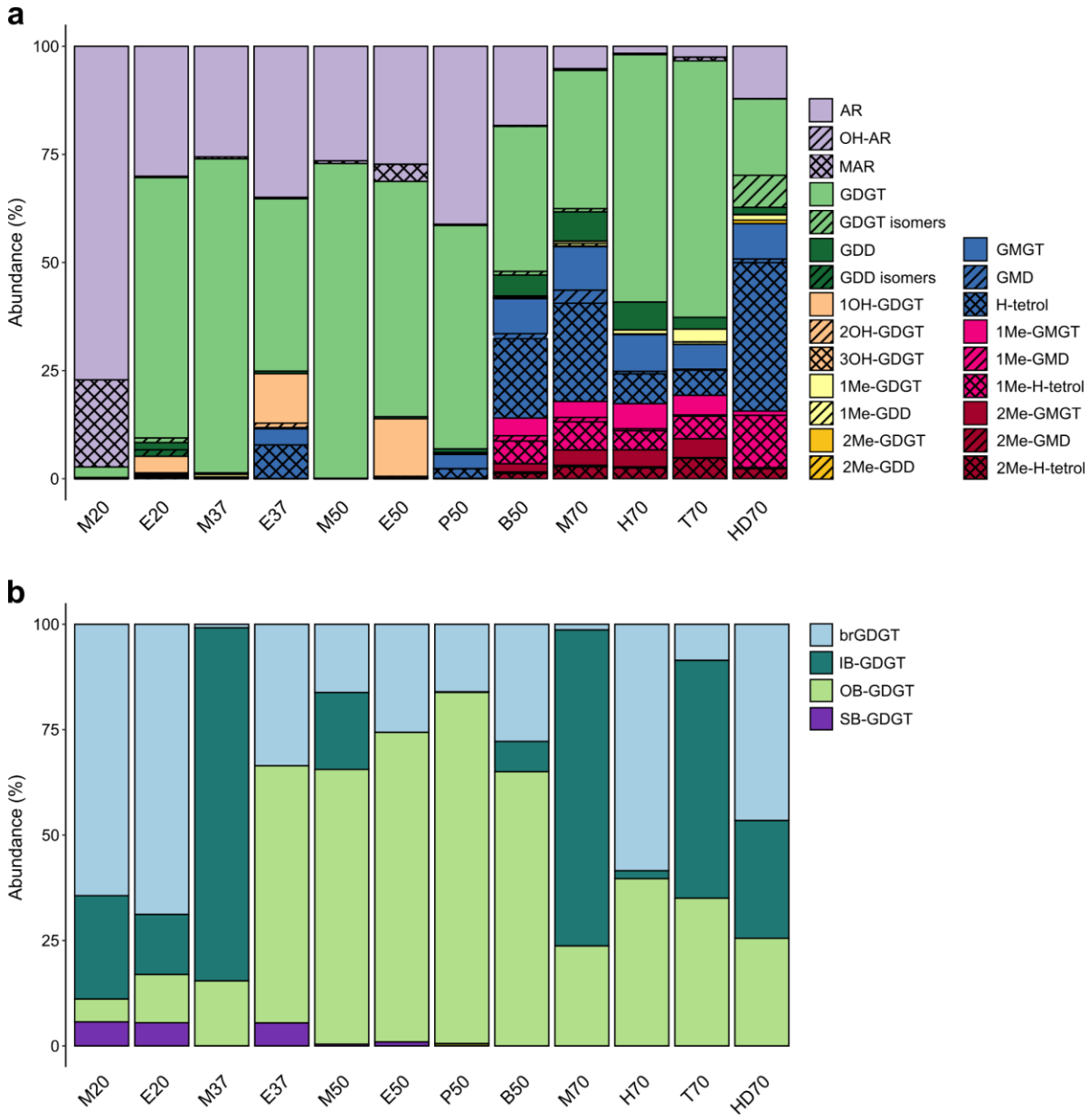


**Figure 2 | Relative abundances of (a) archaeal diether and tetraether core lipids, and (b) tetraether core lipids of bacterial and unknown origin in the alkane-oxidizing cultures.** For each culture, the average relative abundance of the respective lipid in the two duplicate samples is displayed. For culture abbreviations see Table 1. For lipid structures see Supplementary Figures 1-3.

### *Degrees of cyclization in GDGTs and GMGTs*

Next, we looked at the degree of integration of cyclopentane moieties, i.e. cyclization, in unmodified and methylated archaeal dialkyl tetraethers (GDGTs) (Fig. 3) and monoalkyl tetraethers (GMGTs) (Fig. 4). It needs to be noted that relative abundances of variants are respective to the sum of all variants of the tetraether lipid in question, and that relative abundances of the whole lipid group vary strongly between samples as seen in Fig. 2. For unmodified GDGTs and GDDs, lipids with up to six cyclopentane units were detected (Fig. 3a and 3b, respectively). While *Ca*. Syntrophoarchaeum butanivorans, both *Ca.* Alkanophaga and *Ca.* Cerberiarchaeum MAGs encoded one or more homologues of the recently described tetraether ring synthases GrsA and GrsB, the ANME-1c, both *Ca.* Ethanoperedens, and the *Ca*. Syntrophoarchaeum caldarius MAGs lacked homologues of these proteins (Zeng et al., 2019) (Supplementary Table 1). It is likely that GrsA produces GDGT-1-4 from acyclic GDGT and that GrsB adds further cyclopentane rings to GDGT-4, producing GDGT-5-8 (Zeng et al., 2019). Coinciding with this absence of GDGT ring synthase, the E37, E50, and P50 cultures synthesized predominantly acyclic variants of GDGT and GDD (Fig. 3a,b). However, in the E20 culture, GDGT-1/GDD-1 and GDGT-2/GDD-2 were detected, and interestingly, crenarchaeol and GDD-cren were highly abundant (43%/63%). It cannot be excluded that crenarchaeol originated from sediment which the culture still contained. However, the crenarchaeol/GDD-cren abundances seem too high to be background signal, and no Nitrosphaeria MAGs were recovered from the culture which could produce these compounds (Table 2). Whether this *Ca.* Ethanoperedens archaeon is indeed the source of crenarchaeol, and if so, by which means it synthesizes this complex lipid without the known ring synthases, remains to be investigated.

In the M20, E37, E50, P50, B50, and HD70 cultures, acyclic GDGT-0/GDD-0 was dominant. These cultures contained only minor abundances of lipids with multiple cyclopentane moieties. The M37 culture exhibited similar abundances of all GDGT/GDD variants with 0-4 cyclopentane moieties (GDGT-0-4/GDD-0-4). In the M50, M70, H70, and T70 cultures, GDGT-4/GDD-4 was the prevalent variant (32-42% of total GDGT/46-64% of total GDD), with GDGT-0-3/GDD-0-3 also being present at considerable abundances. Because ANME-1c does not encode the previously described ring synthases (Supplementary Table 1), it is surprising that the M70 culture exhibits such a high degree of cyclization. Possibly this archaeon uses less homologous proteins for the same purpose. The ring index (RI), which indicates degree of cyclization, did not increase monotonically with increasing temperature, as would be expected (Supplementary Figure 4a) (Zhang et al., 2016). For instance, HD70 incubated at 70 °C had one of the lowest RIs of all cultures, while M37 and M50 all had relatively high RIs for their incubation temperature. Spearman's rank index indicated a moderate positive correlation between temperature and RI, however, this correlation was not statistically significant (Supplementary Table 2).

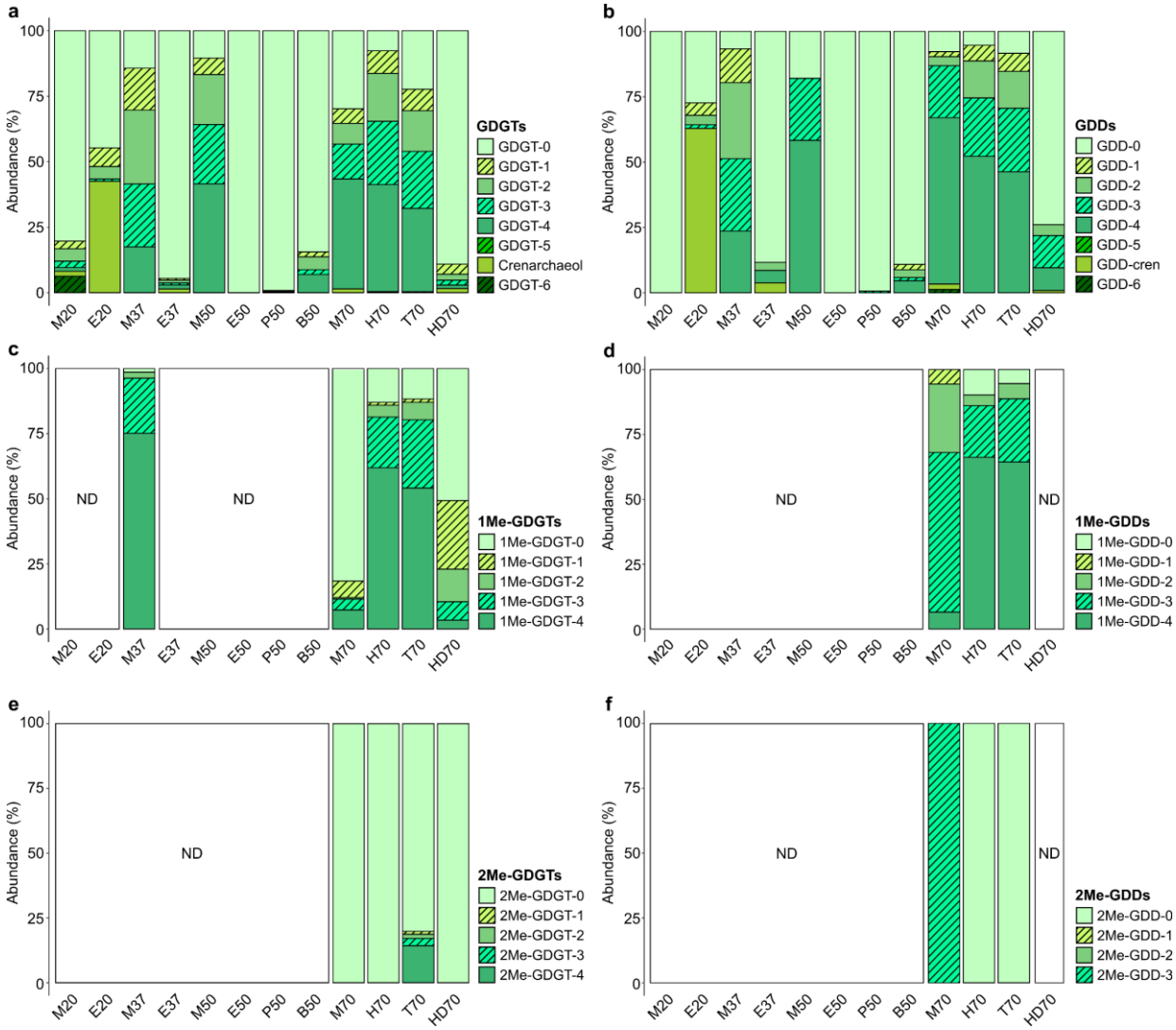


**Figure 3 | Relative abundances of unmodified (a,b), mono-(b,c), and dimethylated (e,f) GDGTs and their diether (GDD) derivatives with varying number of integrated cyclopentane units in alkane-oxidizing cultures.** Isomers and non-isomers were combined and relative abundance of a given variant is percentage of the variant of the sum of all variants. ND: not detected. For lipid structures see Supplementary Figure 1.

Among the 1Me-GDGT detected in the M37 cultures and all 70 °C cultures, 1Me-GDGT-4 was the most abundant variant in the M37, H70, and T70 cultures (62-75%), followed by 1Me-GDGT-3 (19-26%), whereas 1Me-GDGT-0 followed by 1Me-GDGT-1 were prevalent in M70 and HD70 (Fig. 3c). 1Me-GDGT-2 and 1Me-GDGT-3 were also detected at lower abundances. 1Me-GDDs were only found in M70, H70, and T70 cultures (Fig. 3d). Here, the cyclization patterns of H70 and T70 resembled those of 1Me-GDGT variants (Fig. 3c), whereas 1Me-GDD-3 was the prevalent variant detected in M70. For 2Me-GDGT and the corresponding GDD, which were detected only in minor abundances in the total CL pool of the 70 °C cultures, the variant without cyclopentane units was prevalent in all samples except for M70, where 2Me-GDD-3 was the only variant encountered. T70 was the only culture which contained 2Me-GDGT with one to four included cyclopentane rings (2Me-GDGT-1-4).

GMGTs were predominantly detected in the B50 and all 70 °C cultures, to a lower degree in the E37 and P50 cultures, and to a minor degree in the remaining cultures (Fig. 2a). Among

the unmodified GMGTs, variants with up to five cyclopentane rings (GMGT-5) were found (Fig. 4a). Acyclic GMGT-0 was the prevalent variant in most cultures, except for M37, in which GMGT-2 was slightly more abundant, and H70, in which GMGT-4 was the most abundant (60% of GMGTs and 5% of total CL pool). GMDs with up to six cyclopentane moieties were detected in the P50, B50, and all 70 °C cultures, and were absent in all other cultures (Fig. 4b). GMD-0 was the most abundant variant, except for M70 and H70, in which GMD-4 was prevalent. The cyclization patterns of H-tetrol, of which variants with up to four cyclopentane rings were detected (Fig. 4c), mirrors the one of GMGT, in that the acyclic variant is the most abundant in most cultures except for M70, H70, and T70 which have high abundances of H-tetrol-4 and also H-tetrol-3. Among monomethylated GMGT and its degradation/intermediate products, M70, H70, and T70 exhibited again high abundances of the four-cyclic and three-cyclic variants, whereas the acyclic variant was dominant in B50 and HD70 (Fig. 4d,e,f). 2Me-GMGT constituted a minor fraction of the total CL pool of the E20, B50, and 70 °C cultures, with maximum relative abundance of 2% (GMGT-4 in T70). The H70 and T70 cultures had very similar cyclization patterns, with 2Me-GMGT-3 and 2Me-GMGT-4 each making up around 40-50% of 2Me-GMGTs, whereas acyclic 2Me-GMGT-0 made up around 50% in B50, M70, and HD70, with the other half composed of 2Me-GMGT-1-4 (Fig. 4g). This pattern is reflected in 2Me-GMDs and 2Me-H-tetrol compositions, where the four-cyclic variant was highly abundant in H70 and T70, and also M70, and the acyclic variant prevailing in B50 and HD70 (Fig. 4h,i).

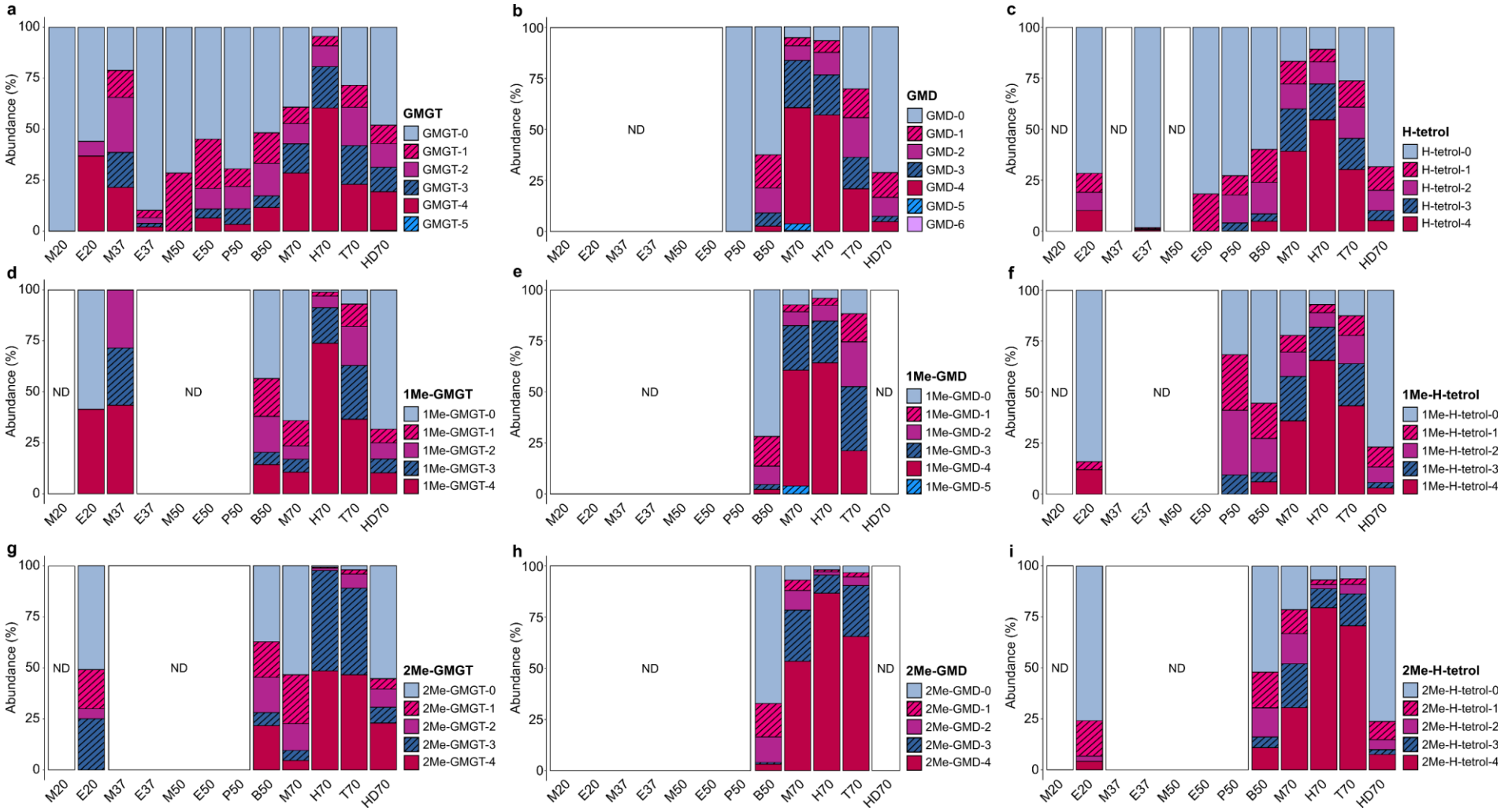


**Figure 4 | Relative abundances of unmodified (a,b,c), mono-(d,e,f), and dimethylated (g,h,i) GMGTs and their diether (GMDs) and H-tetrol derivatives with varying number of integrated cyclopentane units in alkane-oxidizing cultures.** Relative abundance of a given variant is percentage of the variant of the sum of all variants. ND: not detected. For lipid structures see Supplementary Figure 2.

### *Degree of methylation in CLs of bacterial/unknown origin*

The tetraether lipids of bacterial and unknown origin, brGDGTs, SB-GDGTs, OB-GDGTs, and IB-GDGTs are further differentiated by their degree of methylation, and brGDGT variants can include up to two cycplopentane rings (Liu et al., 2012c, 2014) (Supplementary Figure 3). Within the brGDGT fraction, the acyclic brGDGT-Ia, brGDGT-IIa, and brGDGT-IIIa were the most common variants in almost all cultures, except for HD70, where variants with one cyclopentane ring were more abundant (Fig. 5a). Among the IB-GDGT, relative abundances of the variants varied strongly between cultures (Fig. 5b). In the M70 culture, which exhibited the highest total relative abundances of IB-GDGTs, less methylated IB-GDGT-V was the most abundant variant (2% of total CL pool), followed by IB-GDGT-IV (1.8%) and IB-GDGT-III (1.7%). For OB-GDGTs, the methylation degree seemed to decrease with temperature, with 70 °C cultures containing more maximally methylated OB-GDGT-I (Fig. 5c). SB-GDGTs were only detected in cultures up to 50 °C, and were almost exclusively SB-GDGT-I and SB-GDGT-II (Fig. 5d). The methylation index ($MI_{OB/br/SB}$) had a moderate positive correlation with temperature, however, this correlation was not statistically significant (Supplementary Figure 4b, Supplementary Table 2).

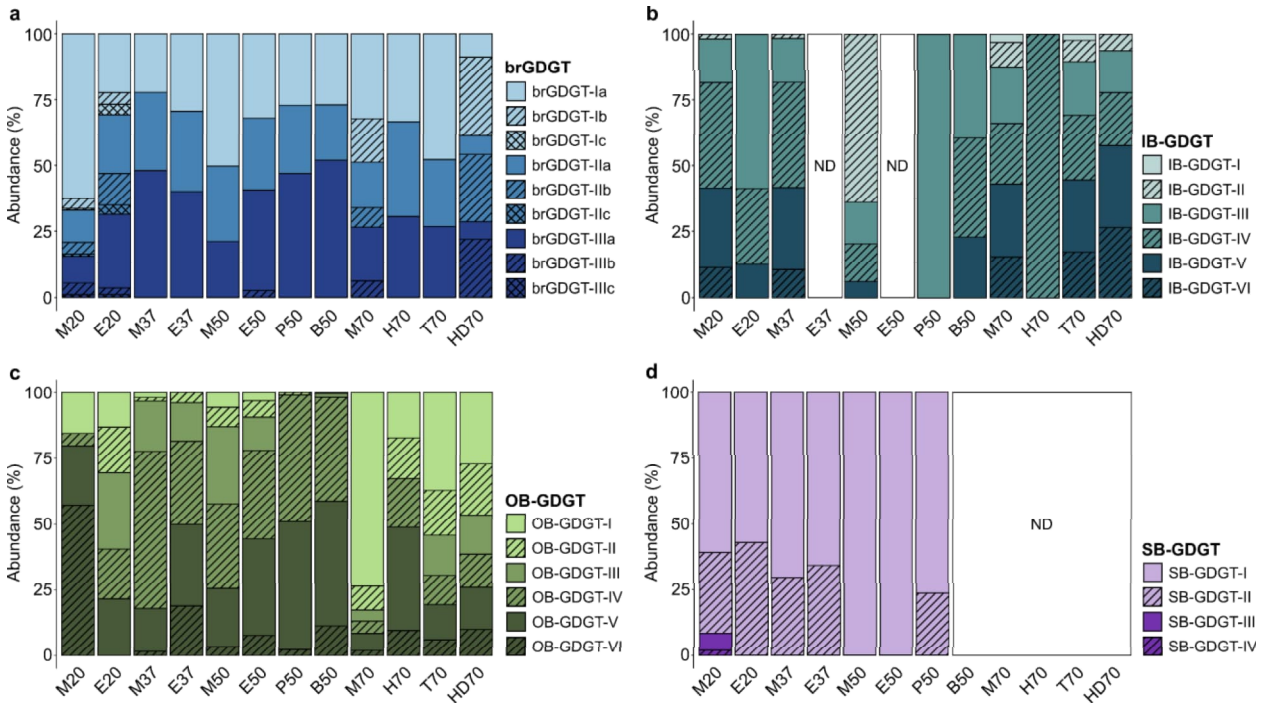


**Figure 5 | Relative abundances of variants of (a) brGDGTs (b) IB-GDGTs (c) OB-GDGTs and (d) SB-GDGTs in alkane-oxidizing cultures.** Relative abundance of a given variant is percentage of the variant of the sum of all variants of the respective lipid group. For lipid structures see Supplementary Figure 3.

### *Effect of temperature on major CL group abundances*

We investigated correlations between relative abundances of CL groups and between CL groups and temperature with Spearman's rank correlation (Fig. 6). Coinciding with the previous observations of CL compositions, correlations formed two groups, one of which entailed CLs correlating positively with an increase in temperature, while in the other group CLs correlated negatively with higher temperatures. The former comprises mono- and dimethylated GDGT (Me-GDGT) and their derivative diethers (Me-GDD), as well as unmodified and methylated GMGT (GMGT and Me-GMGT) and their derivatives (GMD and H-tetrol). Archaeol, all hydroxylated GDGTs, brGDGT, SB-GDGT, and OB-GDGT correlated negatively with an increase in temperature. This negative correlation is strongest for archaeol, 1OH-GDGT, and SB-GDGT. Correlations of individual CL groups in general coincided with that, in that lipids that correlated positively with temperature correlated positively with each other, and negatively with lipids that correlated negatively with higher temperature, and vice versa. Exceptions were 2OH-GDGT and 3OH-GDGT, which correlate negatively with IB-GDGT, even though all three correlated negatively with temperature. GDGT isomers, which were particularly abundant in the HD70 culture, exhibited a slightly positive correlation with several CL groups that correlated positively with temperature, e.g. 2Me-GDGTs, GMGTs, and Me-GMGTs, even though they themselves did not correlate significantly with temperature.

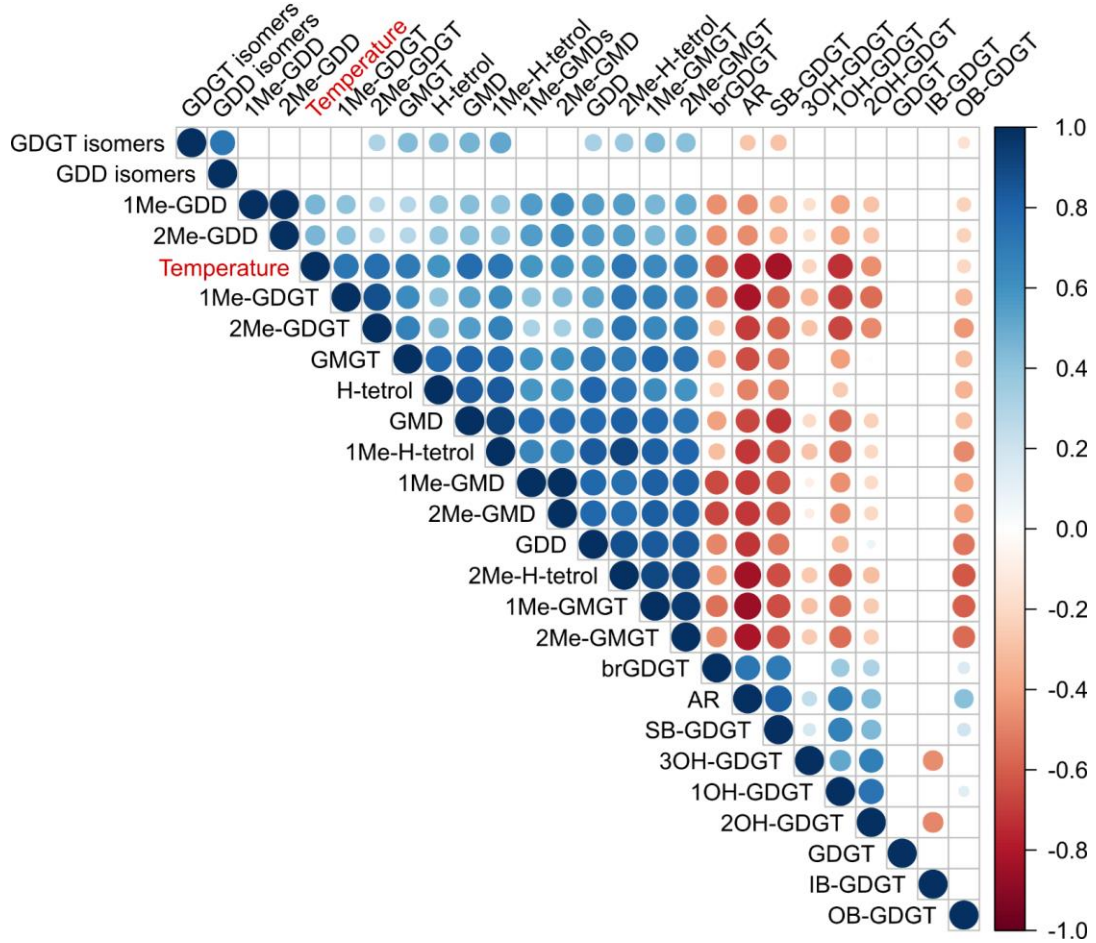


**Figure 6 | Spearman's rank correlation between core lipid groups and between core lipid groups and temperature.** Only statistically significant correlations (p-value <0.01) are shown.

## Discussion

In this study, we described a novel ethane-oxidizing culture growing at 20 °C (E20) and analyzed the core lipids (CLs) of a series of cultures oxidizing alkanes from methane ($C_1$) to hexadecane ($C_{16}$) and growing at a wide range of temperatures between 20 °C and 70 °C. From the E20 culture, we reconstructed a MAG of a highly abundant archaeon of the GoM-Arc1 clade closely related to the known ethane-oxidizer *Ca.* Ethanoperedens thermophilum (Hahn et al., 2020). This extends the growing list of ANKA established in recent years, and bridges a gap between the psychrophilic ethane oxidizer *Ca.* Argoarchaeum ethanivorans, growing at 12 °C, and the mildly thermophilic *Ca.* E. thermophilum, growing at 37 °C and 50 °C (Chen et al., 2019; Hahn et al., 2020).

### *Archaeal CLs*

The CL compositions of the cultures depended strongly on substrate, incubation temperature, and ANME/ANKA and SRB prevalent in the culture. The diether archaeol was predominant only in the M20/ANME-2c culture and decreased strongly with temperature. This coincides partly with previous literature, where archaeol was a main CL of ANME-2 archaea (Rossel et al., 2008). However, this previous study also found high abundances of OH-archaeol, which we did not find in the M20 culture. Instead, macrocyclic archaeol (MAR) was abundant, which is unexpected because previously this lipid was believed to constitute an adaptation to high environmental temperatures. For instance, MAR has been reported predominantly associated with (hyper)thermophilic methanogens, e.g. *Methanocaldococcus jannaschii*, which grows at 85 °C and produces more MAR at higher temperatures (Comita et al., 1984; Sprott et al., 1991; Arakawa et al., 2001). In our ANME-1 cultures, and at higher temperatures, archaeol was less abundant and predominantly GDGT was detected. This coincides with previous observations of high abundances of GDGT and low abundances of archaeol in ANME-1 (Rossel et al., 2008) and in thermophilic archaea in general (Matsuno et al., 2009). Monohydroxylated GDGT (1OH-GDGT) with up to two cyclopentane rings was observed in all three ethane-oxidizing cultures, thus this CL has potential as a biomarker for ethane-oxidizing archaea in marine sediments. However, this CL was also found in marine Nitrosphaeria (Elling et al., 2017) and its distribution in other sedimentary archaea remains to be explored. Hydroxylated GDGTs were absent in cultures incubated at 70 °C. This negative correlation with increasing temperature was statistically significant. Previously, increasing OH-GDGT concentrations were observed at lower temperatures, coinciding with this observation (Huguet et al., 2013).

In cultures incubated at 70 °C, we observed a strong switch in CL composition compared to lower temperatures, and lipids were characterized by a higher degree of methylation and cross-linked tetraethers (GMGTs), plus high abundances of the GMGTs derivatives GMD and H-shaped tetrol. The effect of GDGT methylation and its connection to temperature has not been completely resolved yet, and mono- to trimethylated GDGTs have been detected in both mesophilic and (hyper)thermophilic, mostly methanogenic, Halobacteriota (Meador et al., 2014;

Bauersachs et al., 2015; Knappy et al., 2015; Yoshinaga et al., 2015). Our study supports the notion that methylation is an adaptation to high temperatures, and indicative of thermophilic archaea, which matches environmental observations (Sollich et al., 2017). We obtained similar results for GMGTs, which correlated positively with temperature, as observed previously in other (hyper)thermophilic archaea. For instance, *Pyrococcus furiosus* and *Ca.* Aciduliprofundum boonei synthesized GMGTs at temperatures ≥70 °C (Schouten et al., 2008; Tourte et al., 2022). Interestingly, we detected GMGTs, both unmethylated and methylated, at substantial abundances already at 50 °C in the B50/*Ca.* S. butanivorans culture. This extends the synthesis of these CLs to lower temperatures. The GMGT derivatives GMDs and H-tetrols might be degradation products of the corresponding intact tetraether, or intermediates during tetraether synthesis, or both (Liu et al., 2016). Yet, the GDGT derivatives GDDs have been detected in both mesophilic (*Nitrosopumilus maritimus*) and hyperthermophilic archaea (e.g. *Methanothermococcus thermolitotrophicus*), where they might carry a yet unknown biological function (Liu et al., 2012a; Meador et al., 2014). In terms of the cyclization degree of GDGTs, previously a higher degree of cyclization was observed at higher temperatures (De Rosa et al., 1980). This notion was recently supported by increased gene expression and activities of the enzymes responsible for integration of cyclopentane units, GDGT ring synthases, in the hyperthermophilic archaeon *Sulfolobus caldarius* (Yang et al., 2023). However, also a lower degree of cyclization at higher temperatures has been reported (Bale et al., 2019), and in another study it was suggested that pH and ion strength have a higher impact on cyclization than temperature (Macalady et al., 2004). In our study, the cyclization degree seemed to be more connected to the phylogeny of the culture organisms than to temperature. For instance, all ethane-oxidizing cultures of *Ca.* Ethanoperedens spp. had very low cyclization degrees, all methane-oxidizing cultures of ANME-1 had a similarly high cyclization degree of cyclization, irrespective of the incubation temperature, and the HD70 culture incubated at 70 °C had one of the lowest RIs of all cultures (Fig. 3a,b, Supplementary Figure 4a). Thus, a strict connection between cyclization degree and temperature in all archaea may be questioned.

### *Tetraether CLs of bacterial and unknown origin*

While tetraether lipids other than the known archaeal CLs were present at low abundances in our cultures, those were still considerable in some cases, especially in the M37 and M70 cultures. We detected all four major branched tetraether CL groups, with IB-GDGTs being the most abundant group in the M37 and M70 culture (~8% of total CLs). This is intriguing, because biological sources of this hybrid lipid, which entails both archaea-like isoprenoid and bacteria-like branched chains, were previously unknown. While further studies of intact polar lipids are required to confirm this notion, it seems that those methane-oxidizing cultures indeed produce such IB-GDGTs. Whether these lipids are produced by archaea or bacteria, or by both groups, remains a compelling question for the future. In the marine environment, IB-GDGTs have been detected in oxygen minimum zones, deep anoxic water, and sediment, together with the minimally methylated SB-GDGTs and the maximally methylated

OB-GDGTs (Liu et al., 2012c; Xie et al., 2014). While the orphan lipids are presumably synthesized in anoxic marine environments, brGDGTs are apparently synthesized in both terrestrial and marine environments (Liu et al., 2014). It was previously suggested that brGDGTs which include cyclopentane units have a terrestrial origin, while acyclic brGDGTs have a marine origin (Liu et al., 2014). Corroborating this, most brGDGTs found in our cultures were of the acyclic kind, the most abundant being brGDGT-Ia, which made up 2% of total CLs in the M20 culture. Additionally, an increase in methylation was observed for OB-, SB-, and brGDGTs in deep anoxic water which was hypothesized to be an adaptation to harsh redox conditions (Liu et al., 2014). In our cultures, the methylation index of branched GDGTs was in general higher for cultures incubated at higher temperatures, thus methylation of branched GDGTs could constitute an adaptation to higher temperature in a similar manner as is the case for isoprenoid GDGTs. In terms of genomic capacity for the biosynthesis of such lipids, we found homologues for bacterial ether lipid formation proteins in all partner SRB MAGs (Supplementary Table 3) (Lorenzen et al., 2014; Sahonero-Canavesi et al., 2022). The partner SRB at 70 °C, *Thermodesulfobacterium* spp., in addition encode membrane-spanning lipid synthase (Mss) for tetraether synthesis (Supplementary Table 3) (Sahonero-Canavesi et al., 2022). Thus, these bacteria seem capable of synthesizing diether and tetraether lipids. Our study implies at least low-level production of brGDGTs and orphan lipids from microorganisms in the cultures. Further studies based on metatranscriptome analyses in combination with stable isotope probing could corroborate the production of these CLs from SRB.

In conclusion, alkane-oxidizing cultures displayed a diverse core lipidome which was greatly influenced by temperature, but also by the taxonomic groups present in the culture. Observations of specific tetraether lipids, e.g. dimethylated GMGTs with up to four cyclopentane rings and IB-GDGTs, which were previously scarcely detected in cultures, suggest that these archaea and bacteria are biological sources of those lipids, which could in the future help to predict taxonomic groups and functions from environmental samples, particularly from gas- and oil-rich environments. Further studies of intact polar lipids are required to validate these results.

*Acknowledgments*

We thank the DFG under Germany's Excellence Initiative/Strategy through the Clusters of Excellence EXC 2077 "The Ocean Floor—Earth's Uncharted Interface" (project no. 390741603) and the Max Planck Society for funding this project. We thank Susanne Menger, Anja Seebeck, Rafael Laso Pérez, Cedric Hahn, and David Benito Merino for maintaining the alkane-oxidizing cultures and for providing culture samples, Charlotte Decker for the introduction to total lipid extractions, Xavier Prieto for performing initial mass spectrometry experiments, and the whole Organic Geochemistry group at MARUM for support of the study.

*Author contributions*

G.W., F.S., and H.Z. designed the study. H.Z. did bioinformatical analyses. C.K., Q.-Z.Z., and H.Z. extracted total lipids. F.S. performed mass spectrometry. F.S. analyzed the raw mass spectrometry data, F.S. and H.Z. performed further analyses. H.Z. wrote the manuscript with contributions from all coauthors.

## Supplementary Figures

### Overview

| | |
|---|---|
| **Supplementary Figure 1** | Structures of archaeal dialkyl core lipids |
| **Supplementary Figure 2** | Structures of archaeal monoalkyl core lipids |
| **Supplementary Figure 3** | Structures of tetraether core lipids of bacterial and unknown origin |
| **Supplementary Figure 4** | Ring index (RI) of isoprenoid GDGTs (a) and methylation index of branched GDGTs ($MI_{OB/br/SB}$) |

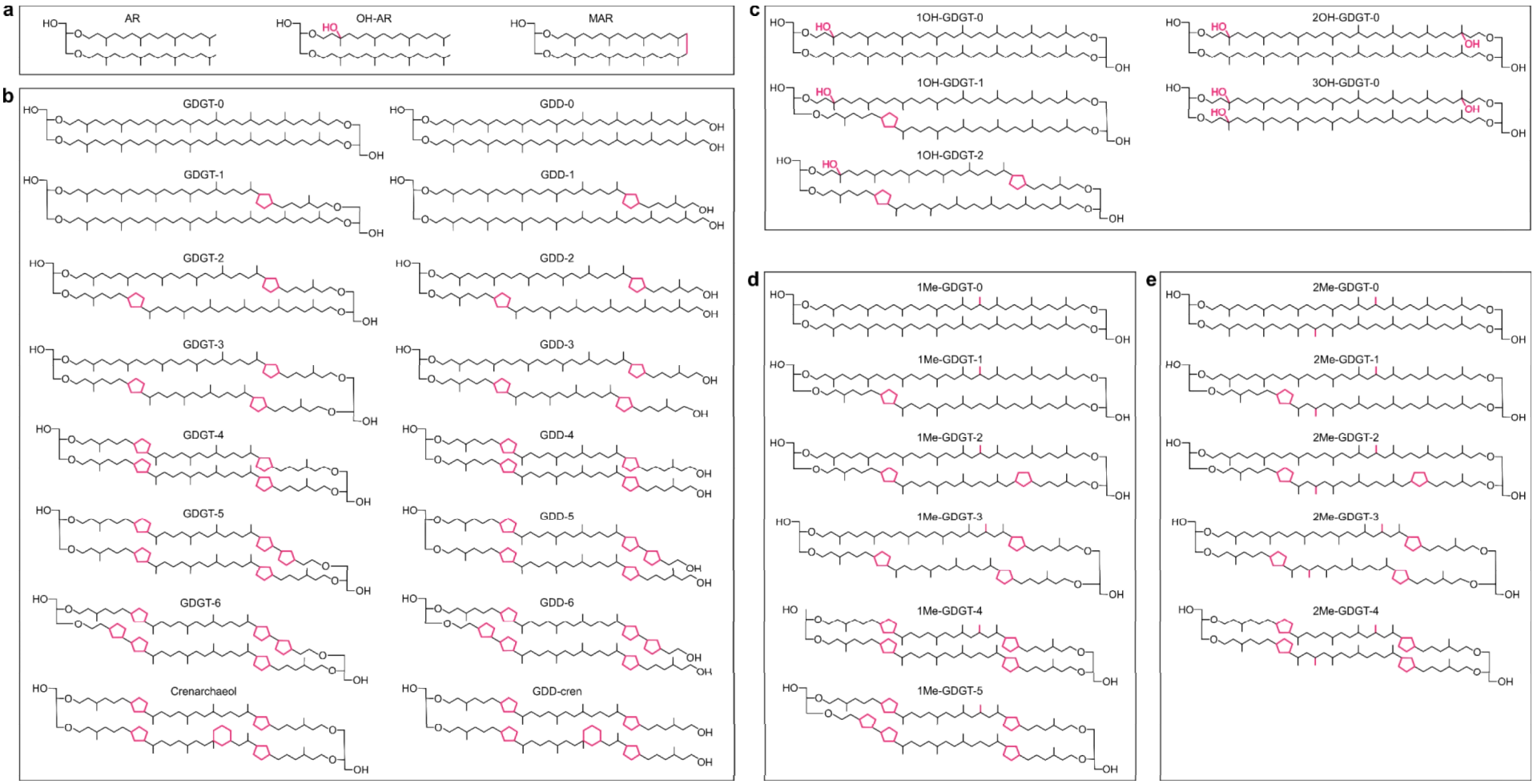


**Supplementary Figure 1 |** Structures of archaeal dialkyl core lipids detected in alkane-oxidizing cultures. (**a**) archaeol and derivatives (**b**) Series of isoprenoid glycerol dialkyl glycerol tetraether (GDGT) and glycerol dibiphytanol diether (GDD) lipids (**c**) mono-, di-, and trihydroxyl GDGTs (**d**) monomethylated GDGTs (**e**) dimethylated GDGTs. Formation of diether lipids from tetraether lipids shown in (**d**,**e**) (1Me-GDD and 2Me-GDD) is analogous to GDDs shown in (**b**), with one glycerol unit missing and one terminal hydroxyl group located on each biphytanyl moiety

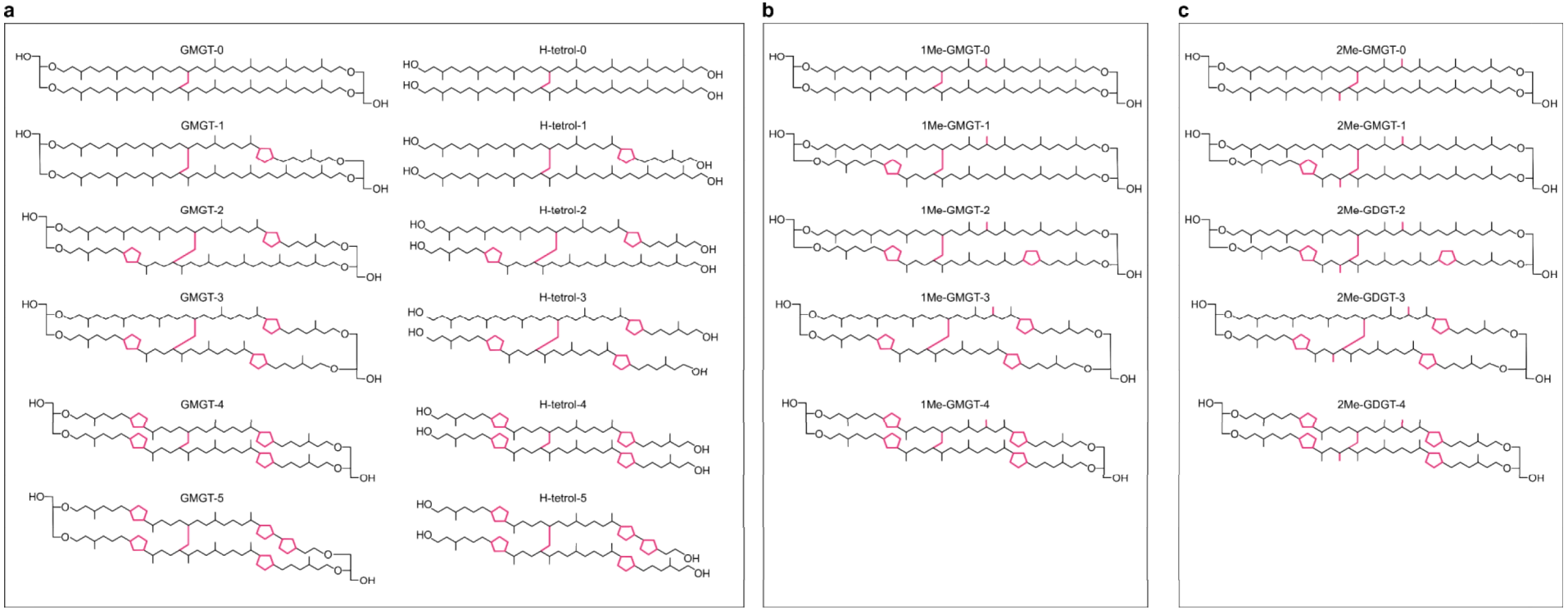


**Supplementary Figure 2 |** Structures of archaeal monoalkyl core lipids detected in alkane-oxidizing cultures (**a**) Series of glycerol monoalkyl glycerol tetraether (GMGT) lipids and H-shaped tetrol derivatives. (b) Monomethylated GMGTs, (c) dimethylated GMGTs. H-tetrol formation from tetraether lipids shown in (**b,c**) corresponds to H-tetrols shown in (**a**), with both glycerol units missing and two terminal hydroxyl groups located on each biphytanyl moiety. Formation of diether lipids (GMDs) of tetraether lipids in (**a,b,c**) is analogous to GDDs shown in Supplementary Figure **1b**, with one glycerol unit missing and one terminal hydroxyl groups located on each biphytanyl moiety.

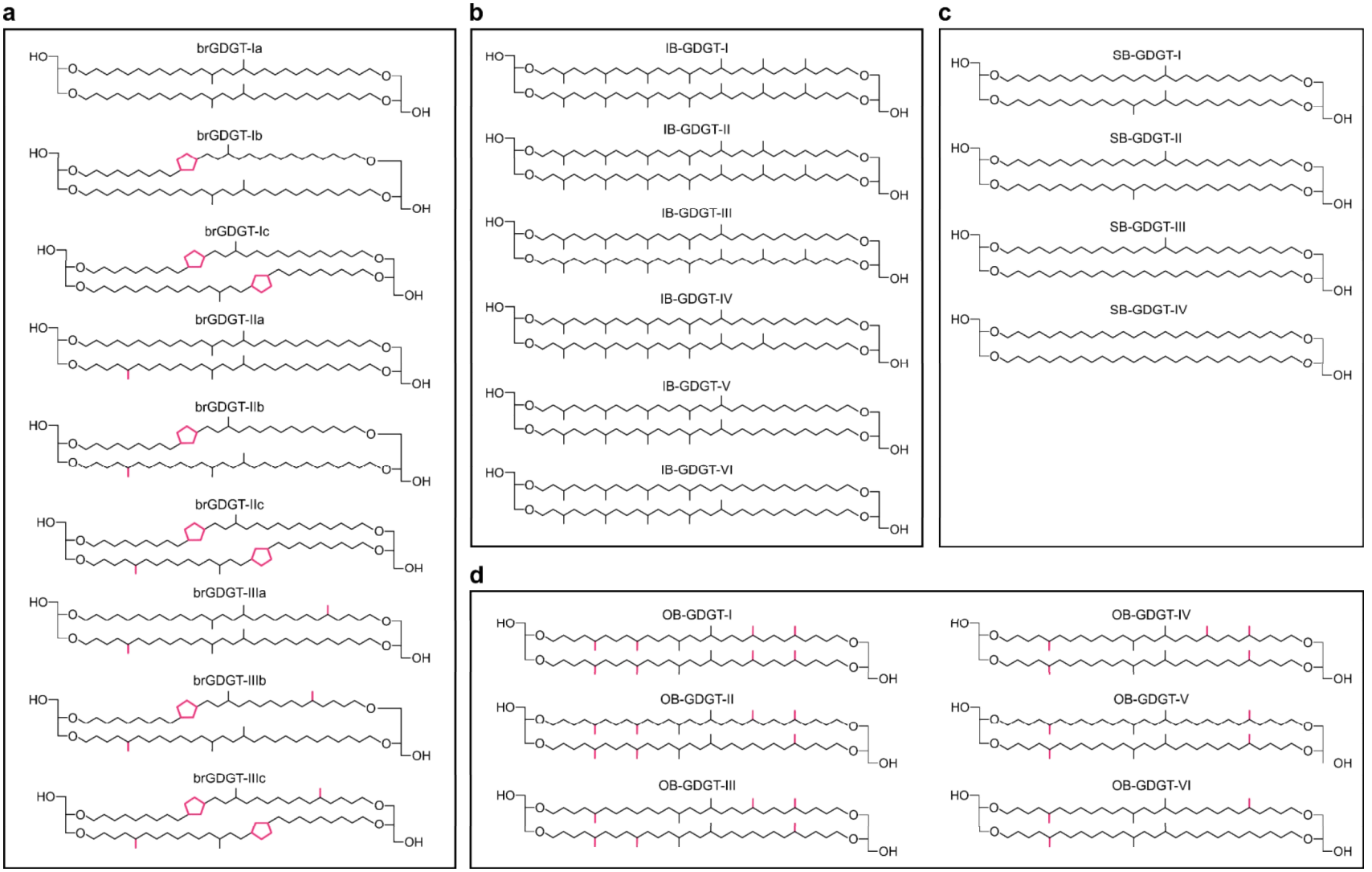


**Supplementary Figure 3** | Structures of tetraether core lipids of bacterial and unknown origin detected in alkane-oxidizing cultures. Series of (**a**) branched glycerol dialkyl glycerol tetraether (brGDGT) (**b**) hybrid isoprenoidal/branched GDGT (IB-GDGT) (c) sparsely branched GDGT (SB-GDGT) (d) overly branched GDGT (OB-GDGT).

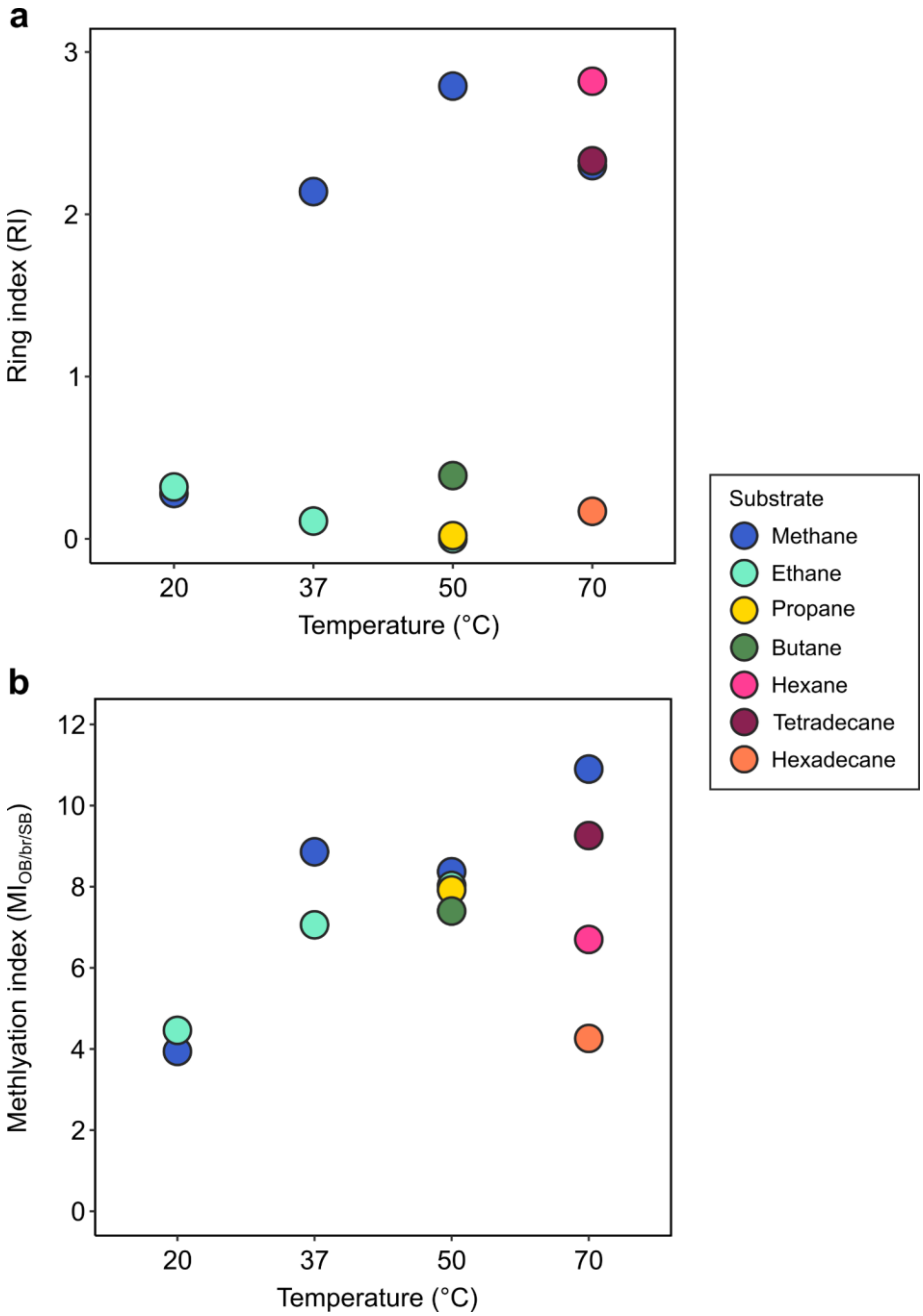


**Supplementary Figure 4 |** Ring index (RI) of isoprenoid GDGTs (a) and methylation index of branched GDGTs ($MI_{OB/br/SB}$) in anaerobic alkane-oxidizing cultures.

## Supplementary Tables

**Supplementary Table 1 |** Homologues of proteins involved in tetraether formation and integration of cyclopentane rings into tetraether lipids in archaea detected in MAGs of ANME and ANKA. Percentages indicate identity of homologues to the reference sequences obtained with BLASTp (e-value $\leq 1 \times 10^{-50}$ and query coverage ≥30%). In cases where multiple homologues where found, their identities are indicated in the same field separated by a vertical line. Tes: tetraether synthase (Zeng et al., 2022), GDGT-MAS: GDGT–macrocyclic archaeol synthase (Lloyd et al., 2022), GrsA: GDGT ring synthase A (Zeng et al., 2019), GrsB: GDGT ring synthase B (Zeng et al., 2019), ND: not detected. For genome accessions and details on cultures see Table 1.

| ANME/ANKA | Tes | GDGT-MAS | GrsA | GrsB |
|---|---|---|---|---|
| ANME-1a (M37) | 39.3 | 51.5 | 33.5 | 31.6 |
| ANME-1a (M50) | 42.4 \| 35.2 | 55.1 \| 45.4 | 33.6 | 31.3 |
| ANME-1c | 32.9 \| 42.1 | 40.7 \| 56.3 | ND | ND |
| *Ca.* Ethanoperedens ex4572_44 | 41.0 | 53.6 | ND | ND |
| *Ca.* Ethanoperedens thermophilum | 42.0 | 56.0 | ND | ND |
| *Ca.* Syntrophoarchaeum caldarius | 39.0 | 51.8 | ND | ND |
| *Ca.* Syntrophoarchaeum butanivorans | ND | ND | 35.5 | 51.5 \| 53.7 |
| *Ca.* Alkanophaga volatiphilum | 40.7 \| 37.0 | 58.0 \| 43.6 | 37.2 \| 32.7 \| 36.0 | 33.7 \| 39.1 \| 33.5 |
| *Ca.* Alkanophaga liquidiphilum | 35.3 \| 40.3 | 41.3 \| 56.5 | 36.0 | 33.5 |
| *Ca.* Cerberiarchaeum oleivorans | 51.1 \| 50.5 | 47.6 \| 46.1 | 32.3 \| 33.0 | 32.7 \| 31.1 |

**Supplementary Table 2 |** Spearman's rank correlation between isoprenoidal GDGT ring indices (RI) and branched GDGT methylation indices ($MI_{OB/br/SB}$) with incubation temperature. For details on cultures see Table 1. *p*-Values <0.1 would be statistically significant.

| Measure | rho | *p*-Value |
|---|---|---|
| RI | 0.34 | 0.62 |
| MI | 0.40 | 0.79 |

**Supplementary Table 3 |** Homologues of proteins involved in ether bond and tetraether formation in bacteria detected in MAGs of SRB from alkane-oxidizing cultures. Percentages indicate identity of homologues to the reference sequences obtained with BLASTp (e-value $\leq 1 \times 10^{-50}$ and query coverage ≥30%). In cases where multiple homologues where found, their identities are indicated in the same field separated by a vertical line. ElbD: ether lipid biodsynthesis protein D (Lorenzen et al., 2014), Ger: glycerol ester reductase (Sahonero-Canavesi et al., 2022), Mss: membrane-spanning lipid synthase (Sahonero-Canavesi et al., 2022), ND: not detected. For genome accessions and details on cultures see Table 1.

| SRB | ElbD | Ger | Mss |
|---|---|---|---|
| Seep-SRB2 (E20) | ND | ND | ND |
| Eth_SRB2 | 31.3 | 40.8 \| 41.5 | ND |
| Eth_SRB1 | ND | 35.0 \| 47.4 | ND |
| Seep-SRB2 (M37) | 30.1 \| 31.4 | 31.1 | ND |
| *Ca.* Desulfofervidus auxilii | 31.8 | 33.1 | ND |
| *Ca.* Thermodesulfobacterium torris | ND | 32.5 | 32.9 |
| *Ca.* Thermodesulfobacterium syntrophicum | ND | 32.2 | 32.8 |

## References


Abdelgadir, A., Chen, X., Liu, J., Xie, X., Zhang, J., Zhang, K., et al. (2014). Characteristics, Process Parameters, and Inner Components of Anaerobic Bioreactors. *Biomed Res. Int.* 2014, 841573. doi: 10.1155/2014/841573.

Altschul, S. F., Gish, W., Miller, W., Myers, E. W., and Lipman, D. J. (1990). Basic local alignment search tool. *J. Mol. Biol.* 215, 403–410. doi: https://doi.org/10.1016/S0022-2836(05)80360-2.

Arakawa, K., Eguchi, T., and Kakinuma, K. (2001). 36-Membered Macrocyclic Diether Lipid is Advantageous for Archaea to Thrive under the Extreme Thermal Environments. *Bull. Chem. Soc. Jpn.* 74, 347–356. doi: 10.1246/bcsj.74.347.

Åström, E. K. L., Carroll, M. L., Ambrose Jr., W. G., Sen, A., Silyakova, A., and Carroll, J. (2018). Methane cold seeps as biological oases in the high-Arctic deep sea. *Limnol. Oceanogr.* 63, S209–S231. doi: https://doi.org/10.1002/lno.10732.

Bale, N. J., Palatinszky, M., Rijpstra, W. I. C., Herbold, C. W., Wagner, M., and Sinninghe Damsté, J. S. (2019). Membrane Lipid Composition of the Moderately Thermophilic Ammonia-Oxidizing Archaeon "*Candidatus* Nitrosotenuis uzonensis" at Different Growth Temperatures. *Appl. Environ. Microbiol.* 85, e01332-19. doi: 10.1128/AEM.01332-19.

Bankevich, A., Nurk, S., Antipov, D., Gurevich, A. A., Dvorkin, M., Kulikov, A. S., et al. (2012). SPAdes: A New Genome Assembly Algorithm and Its Applications to Single-Cell Sequencing. *J. Comput. Biol.* 19, 455–477. doi: 10.1089/cmb.2012.0021.

Bauersachs, T., Weidenbach, K., Schmitz, R. A., and Schwark, L. (2015). Distribution of glycerol ether lipids in halophilic, methanogenic and hyperthermophilic archaea. *Org. Geochem.* 83–84, 101–108. doi: https://doi.org/10.1016/j.orggeochem.2015.03.009.

Becker, K. W., Lipp, J. S., Zhu, C., Liu, X. L., and Hinrichs, K. U. (2013). An improved method for the analysis of archaeal and bacterial ether core lipids. *Org. Geochem.* 61, 34–44. doi: 10.1016/j.orggeochem.2013.05.007.

Benito Merino, D. (2023). Archaea and bacteria mediating anaerobic alkane degradation at its upper temperature limit. https://doi.org/10.26092/elib/2276

Benito Merino, D., Zehnle, H., Teske, A., and Wegener, G. (2022). Deep-branching ANME-1c archaea grow at the upper temperature limit of anaerobic oxidation of methane. *Front. Microbiol.* 13, 1–16. doi: 10.3389/fmicb.2022.988871.

Bligh, E. G., and Dyer, W. J. (1959). A rapid method of total lipid extraction and purification. *Can. J. Biochem. Physiol.* 37, 911–917.

Boetius, A., Holler, T., Knittel, K., Felden, J., and Wenzhöfer, F. (2009). "The Seabed as Natural Laboratory: Lessons From Uncultivated Methanotrophs," in *Uncultivated Microorganisms*, ed. S. S. Epstein (Berlin, Heidelberg: Springer Berlin Heidelberg), 293–316. doi: 10.1007/978-3-540-85465-4_15.

Boetius, A., Ravenschlag, K., Schubert, C. J., Rickert, D., Widdel, F., Gleseke, A., et al. (2000). A marine microbial consortium apparently mediating anaerobic oxidation of methane. *Nature* 407, 623–626. doi: 10.1038/35036572.

Boetius, A., and Suess, E. (2004). Hydrate Ridge: a natural laboratory for the study of microbial life fueled by methane from near-surface gas hydrates. *Chem. Geol.* 205, 291–310. doi: https://doi.org/10.1016/j.chemgeo.2003.12.034.

Bray, J. R., and Curtis, J. T. (1957). An Ordination of the Upland Forest Communities of Southern Wisconsin. *Ecol. Monogr.* 27, 325–349. doi: https://doi.org/10.2307/1942268.

Brocks, J. J., Love, G. D., Summons, R. E., Knoll, A. H., Logan, G. A., and Bowden, S. A. (2005). Biomarker evidence for green and purple sulphur bacteria in a stratified Palaeoproterozoic sea. *Nature* 437, 866–870. doi: 10.1038/nature04068.

Cario, A., Grossi, V., Schaeffer, P., and Oger, P. M. (2015). Membrane homeoviscous adaptation in the piezo-hyperthermophilic archaeon *Thermococcus barophilus*. *Front. Microbiol.* 6. doi: 10.3389/fmicb.2015.01152.

Ceccopieri, M., Carreira, R. S., Wagener, A. L. R., Hefter, J., and Mollenhauer, G. (2019). Branched GDGTs as Proxies in Surface Sediments From the South-Eastern Brazilian Continental Margin. *Front. Earth Sci.* 7, 1–14. doi: 10.3389/feart.2019.00291.

Chaudhary, D. K., Khulan, A., and Kim, J. (2019). Development of a novel cultivation technique for uncultured soil bacteria. *Sci. Rep.* 9, 6666. doi: 10.1038/s41598-019-43182-x.

Chaumeil, P.-A. A., Mussig, A. J., Hugenholtz, P., and Parks, D. H. (2020). GTDB-Tk: a toolkit to classify genomes with the Genome Taxonomy Database. *Bioinformatics* 36, 1925–1927. doi: 10.1093/bioinformatics/btz848.

Chen, S. C., Musat, N., Lechtenfeld, O. J., Paschke, H., Schmidt, M., Said, N., et al. (2019). Anaerobic oxidation of ethane by archaea from a marine hydrocarbon seep. *Nature* 568, 108–111. doi: 10.1038/s41586-019-1063-0.

Chen, Y., Zheng, F., Yang, H., Yang, W., Wu, R., Liu, X., et al. (2022). The production of diverse brGDGTs by an *Acidobacterium* providing a physiological basis for paleoclimate proxies. *Geochim. Cosmochim. Acta* 337, 155–165. doi: https://doi.org/10.1016/j.gca.2022.08.033.

Comita, P. B., Gagosian, R. B., Pang, H., and Costello, C. E. (1984). Structural elucidation of a unique macrocyclic membrane lipid from a new, extremely thermophilic, deep-sea hydrothermal vent Archaebacterium, *Methanococcus jannaschii*. *J. Biol. Chem.* 259, 15234–15241. doi: 10.1016/s0021-9258(17)42540-3.

Danecek, P., Bonfield, J. K., Liddle, J., Marshall, J., Ohan, V., Pollard, M. O., et al. (2021). Twelve years of SAMtools and BCFtools. *Gigascience* 10, giab008. doi: 10.1093/gigascience/giab008.

De Rosa, M., Gambacorta, A., Nicolaus, B., and Bu'lock, J. D. (1980). Complex lipids of Caldariella acidophila, a thermoacidophile archaebacterium. *Phytochemistry* 19, 821–825.

Dombrowski, N., Seitz, K. W., Teske, A. P., and Baker, B. J. (2017). Genomic insights into potential interdependencies in microbial hydrocarbon and nutrient cycling in hydrothermal sediments. *Microbiome* 5, 106. doi: 10.1186/s40168-017-0322-2.

Eigenbrode, J. L. (2008). "Fossil Lipids for Life-Detection: A Case Study from the Early Earth Record," in *Strategies of Life Detection*, eds. O. Botta, J. L. Bada, J. Gomez-Elvira, E. Javaux, F. Selsis, and R. Summons (Boston, MA: Springer US), 161–185. doi: 10.1007/978-0-387-77516-6_12.

Elling, F. J., Könneke, M., Nicol, G. W., Stieglmeier, M., Bayer, B., Spieck, E., et al. (2017). Chemotaxonomic characterisation of the thaumarchaeal lipidome. *Environ. Microbiol.* 19, 2681–2700. doi: https://doi.org/10.1111/1462-2920.13759.

Eren, A. M., Esen, O. C., Quince, C., Vineis, J. H., Morrison, H. G., Sogin, M. L., et al. (2015). Anvi'o: An advanced analysis and visualization platform for 'omics data. *PeerJ* 2015, 3:e1319. doi: 10.7717/peerj.1319.

Green-Saxena, A., Dekas, A. E., Dalleska, N. F., and Orphan, V. J. (2014). Nitrate-based niche differentiation by distinct sulfate-reducing bacteria involved in the anaerobic oxidation of methane. *ISME J.* 8, 150–163. doi: 10.1038/ismej.2013.147.

Hahn, C. J., Laso-Pérez, R., Vulcano, F., Vaziourakis, K.-M., Stokke, R., Steen, I. H., et al. (2020). *Candidatus* Ethanoperedens, a Thermophilic Genus of Archaea Mediating the Anaerobic Oxidation of Ethane. *MBio* 11, e00600-20. doi: 10.1128/mBio.00600-20.

Hinrichs, K.-U., Hayes, J. M., Sylva, S. P., Brewer, P. G., and DeLong, E. F. (1999). Methane-consuming archaebacteria in marine sediments. *Nature* 398, 802–805. doi: 10.1038/19751.

Hinrichs, K.-U., Pancost, R. D., Summons, R. E., Sprott, G. D., Sylva, S. P., Sinninghe Damsté, J. S., et al. (2000). Mass spectra of *sn*-2-hydroxyarchaeol, a polar lipid biomarker for anaerobic methanotrophy. *Geochemistry, Geophys. Geosystems* 1, 11–13. doi: 10.1029/2000gc000042.

Holler, T., Widdel, F., Knittel, K., Amann, R., Kellermann, M. Y., Hinrichs, K. U., et al. (2011). Thermophilic anaerobic oxidation of methane by marine microbial consortia. *ISME J.* 5, 1946–1956. doi: 10.1038/ismej.2011.77.

Hopmans, E. C., Weijers, J. W. H., Schefuß, E., Herfort, L., Sinninghe Damsté, J. S., and Schouten, S. (2004). A novel proxy for terrestrial organic matter in sediments based on branched and isoprenoid tetraether lipids. *Earth Planet. Sci. Lett.* 224, 107–116. doi: https://doi.org/10.1016/j.epsl.2004.05.012.

Hu, J., Meyers, P. A., Chen, G., Peng, P., and Yang, Q. (2012). Archaeal and bacterial glycerol dialkyl glycerol tetraethers in sediments from the Eastern Lau Spreading Center, South Pacific Ocean. *Org. Geochem.* 43, 162–167. doi: https://doi.org/10.1016/j.orggeochem.2011.10.012.

Huguet, C., Fietz, S., and Rosell-Melé, A. (2013). Global distribution patterns of hydroxy glycerol dialkyl glycerol tetraethers. *Org. Geochem.* 57, 107–118. doi: 10.1016/j.orggeochem.2013.01.010.

Hyatt, D., Chen, G.-L., LoCascio, P. F., Land, M. L., Larimer, F. W., and Hauser, L. J. (2010). Prodigal: prokaryotic gene recognition and translation initiation site identification. *BMC Bioinformatics* 11, 119. doi: 10.1186/1471-2105-11-119.

Jain, C., Rodriguez-R, L. M., Phillippy, A. M., Konstantinidis, K. T., and Aluru, S. (2018). High throughput ANI analysis of 90K prokaryotic genomes reveals clear species boundaries. *Nat. Commun.* 9, 1–8. doi: 10.1038/s41467-018-07641-9.

Jain, S., Caforio, A., and Driessen, A. J. M. (2014). Biosynthesis of archaeal membrane ether lipids. *Front. Microbiol.* 5, 1–16. doi: 10.3389/fmicb.2014.00641.

Kang, D. D., Li, F., Kirton, E., Thomas, A., Egan, R., An, H., et al. (2019). MetaBAT 2: An adaptive binning algorithm for robust and efficient genome reconstruction from metagenome assemblies. *PeerJ* 2019, 1–13. doi: 10.7717/peerj.7359.

Kleindienst, S., Ramette, A., Amann, R., and Knittel, K. (2012). Distribution and *in situ* abundance of sulfate-reducing bacteria in diverse marine hydrocarbon seep sediments. *Environ. Microbiol.* 14, 2689–2710. doi: 10.1111/j.1462-2920.2012.02832.x.

Knappy, C., Barillà, D., Chong, J., Hodgson, D., Morgan, H., Suleman, M., et al. (2015). Mono-, di- and trimethylated homologues of isoprenoid tetraether lipid cores in archaea and environmental samples: Mass spectrometric identification and significance. *J. Mass Spectrom.* 50, 1420–1432. doi: 10.1002/jms.3709.

Knittel, K., and Boetius, A. (2009). Anaerobic Oxidation of Methane: Progress with an Unknown Process. *Annu. Rev. Microbiol.* 63, 311–334. doi: 10.1146/annurev.micro.61.080706.093130.

Koga, Y., Kyuragi, T., Nishihara, M., and Sone, N. (1998). Did archaeal and bacterial cells arise independently from noncellular precursors? A hypothesis stating that the advent of membrane phospholipid with enantiomeric glycerophosphate backbones caused the separation of the two lines of descent. *J. Mol. Evol.* 46, 54–63. doi: 10.1007/PL00006283.

Krukenberg, V., Harding, K., Richter, M., Glöckner, F. O., Gruber-Vodicka, H. R., Adam, B., et al. (2016). *Candidatus* Desulfofervidus auxilii, a hydrogenotrophic sulfate-reducing bacterium involved in the thermophilic anaerobic oxidation of methane. *Environ. Microbiol.* 18, 3073–3091. doi: 10.1111/1462-2920.13283.

Krukenberg, V., Riedel, D., Gruber-Vodicka, H. R., Buttigieg, P. L., Tegetmeyer, H. E., Boetius, A., et al. (2018). Gene expression and ultrastructure of meso- and thermophilic methanotrophic consortia. *Environ. Microbiol.* 20, 1651–1666. doi: 10.1111/1462-2920.14077.

Kuypers, M. M. M., Blokker, P., Erbacher, J., Kinkel, H., Pancost, R. D., Schouten, S., et al. (2001). Massive expansion of marine archaea during a mid-Cretaceous oceanic anoxic event. *Science* 293, 92–94. doi: 10.1126/science.1058424.

Lamparter, L., and Galic, M. (2020). Cellular Membranes, a Versatile Adaptive Composite Material. *Front. Cell Dev. Biol.* 8. doi: 10.3389/fcell.2020.00684.

Langmead, B., and Salzberg, S. L. (2012). Fast gapped-read alignment with Bowtie 2. *Nat. Methods* 9, 357–359. doi: 10.1038/nmeth.1923.

Laso-Pérez, R., Krukenberg, V., Musat, F., and Wegener, G. (2018). Establishing anaerobic hydrocarbon-degrading enrichment cultures of microorganisms under strictly anoxic conditions. *Nat. Protoc.* 13, 1310–1330. doi: 10.1038/nprot.2018.030.

Laso-Pérez, R., Wegener, G., Knittel, K., Widdel, F., Harding, K. J., Krukenberg, V., et al. (2016). Thermophilic archaea activate butane via alkyl-coenzyme M formation. *Nature* 539, 396–401. doi: 10.1038/nature20152.

Lee, S.-H., Ka, J.-O., and Cho, J.-C. (2008). Members of the phylum Acidobacteria are dominant and metabolically active in rhizosphere soil. *FEMS Microbiol. Lett.* 285, 263–269. doi: 10.1111/j.1574-6968.2008.01232.x.

Lemaire, O. N., and Wagner, T. (2022). A Structural View of Alkyl-Coenzyme M Reductases, the First Step of Alkane Anaerobic Oxidation Catalyzed by Archaea. *Biochemistry* 61, 805–821. doi: 10.1021/acs.biochem.2c00135.

Liu, X. L., Birgel, D., Elling, F. J., Sutton, P. A., Lipp, J. S., Zhu, R., et al. (2016). From ether to acid: A plausible degradation pathway of glycerol dialkyl glycerol tetraethers. *Geochim. Cosmochim. Acta* 183, 138–152. doi: 10.1016/j.gca.2016.04.016.

Liu, X. L., Lipp, J. S., Schröder, J. M., Summons, R. E., and Hinrichs, K. U. (2012a). Isoprenoid glycerol dialkanol diethers: A series of novel archaeal lipids in marine sediments. *Org. Geochem.* 43, 50–55. doi: 10.1016/j.orggeochem.2011.11.002.

Liu, X. L., Lipp, J. S., Simpson, J. H., Lin, Y. S., Summons, R. E., and Hinrichs, K. U. (2012b). Mono- and dihydroxyl glycerol dibiphytanyl glycerol tetraethers in marine sediments: Identification of both core and

intact polar lipid forms. *Geochim. Cosmochim. Acta* 89, 102–115. doi: 10.1016/j.gca.2012.04.053.

Liu, X. L., Summons, R. E., and Hinrichs, K. U. (2012c). Extending the known range of glycerol ether lipids in the environment: Structural assignments based on tandem mass spectral fragmentation patterns. *Rapid Commun. Mass Spectrom.* 26, 2295–2302. doi: 10.1002/rcm.6355.

Liu, X. L., Zhu, C., Wakeham, S. G., and Hinrichs, K.-U. (2014). In situ production of branched glycerol dialkyl glycerol tetraethers in anoxic marine water columns. *Mar. Chem.* 166, 1–8. doi: 10.1016/j.marchem.2014.08.008.

Lloyd, C. T., Iwig, D. F., Wang, B., Cossu, M., Metcalf, W. W., Boal, A. K., et al. (2022). Discovery, structure and mechanism of a tetraether lipid synthase. *Nature* 609, 197–203. doi: 10.1038/s41586-022-05120-2.

Lombard, J., López-García, P., and Moreira, D. (2012). The early evolution of lipid membranes and the three domains of life. *Nat. Rev. Microbiol.* 10, 507–515. doi: 10.1038/nrmicro2815.

Lorenzen, W., Ahrendt, T., Bozhüyük, K. A. J., and Bode, H. B. (2014). A multifunctional enzyme is involved in bacterial ether lipid biosynthesis. *Nat. Chem. Biol.* 10, 425–427. doi: 10.1038/nchembio.1526.

Lösekann, T., Knittel, K., Nadalig, T., Fuchs, B., Niemann, H., Boetius, A., et al. (2007). Diversity and Abundance of Aerobic and Anaerobic Methane Oxidizers at the Haakon Mosby Mud Volcano, Barents Sea. *Appl. Environ. Microbiol.* 73, 3348–3362. doi: 10.1128/AEM.00016-07.

Lü, X., Liu, X., Xu, C., Song, J., Li, X., Yuan, H., et al. (2019). The origins and implications of glycerol ether lipids in China coastal wetland sediments. *Sci. Rep.* 9, 1–11. doi: 10.1038/s41598-019-55104-y.

Macalady, J. L., Vestling, M. M., Baumler, D., Boekelheide, N., Kaspar, C. W., and Banfield, J. F. (2004). Tetraether-linked membrane monolayers in *Ferroplasma* spp: a key to survival in acid. *Extremophiles* 8, 411–419. doi: 10.1007/s00792-004-0404-5.

Matsuno, Y., Sugai, A., Higashibata, H., Fukuda, W., Ueda, K., Uda, I., et al. (2009). Effect of growth temperature and growth phase on the lipid composition of the archaeal membrane from *Thermococcus kodakaraensis*. *Biosci. Biotechnol. Biochem.* 73, 104–108. doi: 10.1271/bbb.80520.

Meador, T., Gagen, E., Loscar, M., Goldhammer, T., Yoshinaga, M., Wendt, J., et al. (2014). *Thermococcus kodakarensis* modulates its polar membrane lipids and elemental composition according to growth stage and phosphate availability. *Front. Microbiol.* 5. doi: 10.3389/fmicb.2014.00010.

Michaelis, W., and Albrecht, P. (1979). Molecular fossils of archaebacteria in kerogen. *Naturwissenschaften* 66, 420–422. doi: 10.1007/BF00368078.

Murali, R., Yu, H., Speth, D. R., Wu, F., Metcalfe, K. S., Malmstrom, R. R., et al. (2022). Physiological adaptation of sulfate reducing bacteria in syntrophic partnership with methanotrophic archaea. doi: https://doi.org/10.1101/2022.11.23.517749.

Niemann, H., Losekann, T., de Beer, D., Elvert, M., Nadalig, T., Knittel, K., et al. (2006). Novel microbial communities of the Haakon Mosby mud volcano and their role as a methane sink. *Nature* 443, 854–858.

Nishihara, M., and Koga, Y. (1987). Extraction and Composition of Polar Lipids from the Archaebacterium, *Methanobacterium thermoautotrophicum* : Effective Extraction of Tetraether Lipids by an Acidified Solvent 1. *J. Biochem.* 101, 997–1005. doi: 10.1093/oxfordjournals.jbchem.a121969.

Oksanen, J., Blanchet, F. G., Friendly, M., Kindt, R., Legendre, P., McGlinn, D., et al. (2020). vegan: Community Ecology Package. *R Packag. version 2.5-7*. Available at: https://cran.r-project.org/package=vegan.

Orphan, V. J., Hinrichs, K.-U., Ussler, W., Paull, C. K., Taylor, L. T., Sylva, S. P., et al. (2001). Comparative Analysis of Methane-Oxidizing Archaea and Sulfate-Reducing Bacteria in Anoxic Marine Sediments. *Appl. Environ. Microbiol.* 67, 1922–1934. doi: 10.1128/AEM.67.4.1922-1934.2001.

Paduan, J. B., Zierenberg, R. A., Clague, D. A., Spelz, R. M., Caress, D. W., Troni, G., et al. (2018). Discovery of Hydrothermal Vent Fields on Alarcón Rise and in Southern Pescadero Basin, Gulf of California. *Geochemistry, Geophys. Geosystems* 19, 4788–4819. doi: https://doi.org/10.1029/2018GC007771.

Parks, D. H., Imelfort, M., Skennerton, C. T., Hugenholtz, P., and Tyson, G. W. (2015). CheckM: Assessing the quality of microbial genomes recovered from isolates, single cells, and metagenomes. *Genome Res.* 25, 1043–1055. doi: 10.1101/gr.186072.114.

Pearson, A., Huang, Z., Ingalls, A. E., Romanek, C. S., Wiegel, J., Freeman, K. H., et al. (2004). Nonmarine Crenarchaeol in Nevada Hot Springs. *Appl. Environ. Microbiol.* 70, 5229–5237. doi: 10.1128/AEM.70.9.5229-5237.2004.

Pernthaler, A., Dekas, A. E., Brown, C. T., Goffredi, S. K., Embaye, T., and Orphan, V. J. (2008). Diverse syntrophic partnerships from deep-sea methane vents revealed by direct cell capture and metagenomics. *Proc. Natl. Acad. Sci. U. S. A.* 105, 7052–7057. doi: 10.1073/pnas.0711303105.

Pester, M., Schleper, C., and Wagner, M. (2011). The Thaumarchaeota: an emerging view of their phylogeny and ecophysiology. *Curr. Opin. Microbiol.* 14, 300–306. doi: https://doi.org/10.1016/j.mib.2011.04.007.

R Core Team (2022). R: A Language and Environment for Statistical Computing. Available at: https://www.r-project.org/.

Reeburgh, W. S. (1996). ""Soft Spots" in the Global Methane Budget," in *Microbial Growth on C1 Compounds: Proceedings of the 8th International Symposium on Microbial Growth on C1 Compounds, held in San Diego, U.S.A., 27 August -- 1 September 1995*, eds. M. E. Lidstrom and F. R. Tabita (Dordrecht: Springer Netherlands), 334–342. doi: 10.1007/978-94-009-0213-8_44.

Rossel, P. E., Lipp, J. S., Fredricks, H. F., Arnds, J., Boetius, A., Elvert, M., et al. (2008). Intact polar lipids of anaerobic methanotrophic archaea and associated bacteria. *Org. Geochem.* 39, 992–999. doi: 10.1016/j.orggeochem.2008.02.021.

Rotaru, A.-E., Shrestha, P. M., Liu, F., Ueki, T., Nevin, K., Summers, Z. M., et al. (2012). Interspecies electron transfer via hydrogen and formate rather than direct electrical connections in cocultures of *Pelobacter carbinolicus* and *Geobacter sulfurreducens*. *Appl. Environ. Microbiol.* 78, 7645–7651. doi: 10.1128/AEM.01946-12.

RStudio Team (2019). RStudio: Integrated Development Environment for R. Available at: http://www.rstudio.com/.

Ruff, S. E., Kuhfuss, H., Wegener, G., Lott, C., Ramette, A., Wiedling, J., et al. (2016). Methane seep in shallow-water permeable sediment harbors high diversity of anaerobic methanotrophic communities, Elba, Italy. *Front. Microbiol.* 7, 1–20. doi: 10.3389/fmicb.2016.00374.

Sahonero-Canavesi, D. X., Siliakus, M. F., Asbun, A. A., Koenen, M., Von Meijenfeldt, F. A. B., Boeren, S., et al. (2022). Disentangling the lipid divide: Identification of key enzymes for the biosynthesis of membrane-spanning and ether lipids in Bacteria. *Sci. Adv.* 8, 1–16. doi: 10.1126/sciadv.abq8652.

Schouten, S., Baas, M., Hopmans, E. C., Reysenbach, A. L., and Damsté, J. S. S. (2008). Tetraether membrane lipids of *Candidatus* "Aciduliprofundum boonei", a cultivated obligate thermoacidophilic euryarchaeote from deep-sea hydrothermal vents. *Extremophiles* 12, 119–124. doi: 10.1007/s00792-007-0111-0.

Schouten, S., Hopmans, E. C., Schefuß, E., and Sinninghe Damsté, J. S. (2002). Distributional variations in marine crenarchaeotal membrane lipids: a new tool for reconstructing ancient sea water temperatures? *Earth Planet. Sci. Lett.* 204, 265–274. doi: https://doi.org/10.1016/S0012-821X(02)00979-2.

Schouten, S., Hopmans, E. C., and Sinninghe Damsté, J. S. (2013). The organic geochemistry of glycerol dialkyl glycerol tetraether lipids: A review. *Org. Geochem.* 54, 19–61. doi: 10.1016/j.orggeochem.2012.09.006.

Schouten, S., van der Meer, M. T. J., Hopmans, E. C., Rijpstra, W. I. C., Reysenbach, A.-L., Ward, D. M., et al. (2007). Archaeal and Bacterial Glycerol Dialkyl Glycerol Tetraether Lipids in Hot Springs of Yellowstone National Park. *Appl. Environ. Microbiol.* 73, 6181–6191. doi: 10.1128/AEM.00630-07.

Schreiber, L., Holler, T., Knittel, K., Meyerdierks, A., and Amann, R. (2010). Identification of the dominant sulfate-reducing bacterial partner of anaerobic methanotrophs of the ANME-2 clade. *Environ. Microbiol.* 12, 2327–2340. doi: https://doi.org/10.1111/j.1462-2920.2010.02275.x.

Sephton, M. A., and Hazen, R. M. (2013). On the Origins of Deep Hydrocarbons. *Rev. Mineral. Geochemistry* 75, 449–465. doi: 10.2138/rmg.2013.75.14.

Shima, S., Krueger, M., Weinert, T., Demmer, U., Kahnt, J., Thauer, R. K., et al. (2012). Structure of a methyl-coenzyme M reductase from Black Sea mats that oxidize methane anaerobically. *Nature* 481, 98–101. doi: 10.1038/nature10663.

Simoneit, B. R. T. (1990). Petroleum generation, an easy and widespread process in hydrothermal systems: an overview. *Appl. Geochemistry* 5, 3–15. doi: 10.1016/0883-2927(90)90031-Y.

Sinninghe Damsté, J. S., Hopmans, E. C., Pancost, R. D., Schouten, S., and Geenevasen, J. A. J. (2000). Newly discovered non-isoprenoid glycerol dialkyl glycerol tetraether lipids in sediments. *Chem. Commun.*, 1683–1684. doi: 10.1039/B004517I.

Sinninghe Damsté, J. S., Rijpstra, W. I. C., Foesel, B. U., Huber, K. J., Overmann, J., Nakagawa, S., et al. (2018). An overview of the occurrence of ether- and ester-linked iso-diabolic acid membrane lipids in microbial cultures of the Acidobacteria: Implications for brGDGT paleoproxies for temperature and pH. *Org. Geochem.*

124, 63–76. doi: 10.1016/j.orggeochem.2018.07.006.

Sinninghe Damsté, J. S., Rijpstra, W. I. C., Hopmans, E. C., Weijers, J. W. H., Foesel, B. U., Overmann, J., et al. (2011). 13,16-Dimethyl Octacosanedioic Acid (iso-Diabolic Acid), a Common Membrane-Spanning Lipid of Acidobacteria Subdivisions 1 and 3. *Appl. Environ. Microbiol.* 77, 4147–4154. doi: 10.1128/AEM.00466-11.

Sinninghe Damsté, J. S., Schouten, S., Hopmans, E. C., van Duin, A. C. T., and Geenevasen, J. A. J. (2002). Crenarchaeol. *J. Lipid Res.* 43, 1641–1651. doi: 10.1194/jlr.M200148-JLR200.

Sollich, M., Yoshinaga, M. Y., Häusler, S., Price, R. E., Hinrichs, K. U., and Bühring, S. I. (2017). Heat stress dictates microbial lipid composition along a thermal gradient in marine sediments. *Front. Microbiol.* 8, 1–19. doi: 10.3389/fmicb.2017.01550.

Sprott, G. D., Meloche, M., and Richards, J. C. (1991). Proportions of diether, macrocyclic diether, and tetraether lipids in Methanococcus jannaschii grown at different temperatures. *J. Bacteriol.* 173, 3907–3910. doi: 10.1128/jb.173.12.3907-3910.1991.

Sturt, H. F., Summons, R. E., Smith, K., Elvert, M., and Hinrichs, K. U. (2004). Intact polar membrane lipids in prokaryotes and sediments deciphered by high-performance liquid chromatography/electrospray ionization multistage mass spectrometry - New biomarkers for biogeochemistry and microbial ecology. *Rapid Commun. Mass Spectrom.* 18, 617–628. doi: 10.1002/rcm.1378.

Summons, R. E., Welander, P. V., and Gold, D. A. (2022). Lipid biomarkers: molecular tools for illuminating the history of microbial life. *Nat. Rev. Microbiol.* 20, 174–185. doi: 10.1038/s41579-021-00636-2.

Teske, A., De Beer, D., McKay, L. J., Tivey, M. K., Biddle, J. F., Hoer, D., et al. (2016). The Guaymas Basin hiking guide to hydrothermal mounds, chimneys, and microbial mats: Complex seafloor expressions of subsurface hydrothermal circulation. *Front. Microbiol.* 7, 1–23. doi: 10.3389/fmicb.2016.00075.

Torkian, B., Hann, S., Preisner, E., and Norman, R. S. (2020). BLAST-QC: automated analysis of BLAST results. *Environ. Microbiome* 15, 15. doi: 10.1186/s40793-020-00361-y.

Tourte, M., Schaeffer, P., Grossi, V., and Oger, P. M. (2022). Membrane adaptation in the hyperthermophilic archaeon *Pyrococcus furiosus* relies upon a novel strategy involving glycerol monoalkyl glycerol tetraether lipids. *Environ. Microbiol.* 24, 2029–2046. doi: 10.1111/1462-2920.15923.

Valentine, D. L. (2007). Adaptations to energy stress dictate the ecology and evolution of the Archaea. *Nat. Rev. Microbiol.* 5, 316–323. doi: 10.1038/nrmicro1619.

Wegener, G., Krukenberg, V., Ruff, S. E., Kellermann, M. Y., and Knittel, K. (2016). Metabolic capabilities of microorganisms involved in and associated with the anaerobic oxidation of methane. *Front. Microbiol.* 7, 1–16. doi: 10.3389/fmicb.2016.00046.

Wegener, G., Laso-Pérez, R., Orphan, V. J., and Boetius, A. (2022). Anaerobic Degradation of Alkanes by Marine Archaea. *Annu. Rev. Microbiol.* 76, 553–577. doi: 10.1146/annurev-micro-111021-045911.

Weijers, J. W. H., Schouten, S., van den Donker, J. C., Hopmans, E. C., and Sinninghe Damsté, J. S. (2007). Environmental controls on bacterial tetraether membrane lipid distribution in soils. *Geochim. Cosmochim. Acta* 71, 703–713. doi: https://doi.org/10.1016/j.gca.2006.10.003.

Wilhelms, A., Larter, S. R., Head, I., Farrimond, P., di-Primio, R., and Zwach, C. (2001). Biodegradation of oil in uplifted basins prevented by deep-burial sterilization. *Nature* 411, 1034–1037. doi: 10.1038/35082535.

Xie, S., Lipp, J. S., Wegener, G., Ferdelman, T. G., and Hinrichs, K.-U. (2013). Turnover of microbial lipids in the deep biosphere and growth of benthic archaeal populations. *Proc. Natl. Acad. Sci.* 110, 6010–6014. doi: 10.1073/pnas.1218569110.

Xie, S., Liu, X. L., Schubotz, F., Wakeham, S. G., and Hinrichs, K. U. (2014). Distribution of glycerol ether lipids in the oxygen minimum zone of the Eastern Tropical North Pacific Ocean. *Org. Geochem.* 71, 60–71. doi: 10.1016/j.orggeochem.2014.04.006.

Yang, W., Chen, H., Chen, Y., Chen, A., Feng, X., Zhao, B., et al. (2023). Thermophilic archaeon orchestrates temporal expression of GDGT ring synthases in response to temperature and acidity stress. *Environ. Microbiol.* 25, 575–587. doi: 10.1111/1462-2920.16301.

Yoshinaga, M. Y., Gagen, E. J., Wörmer, L., Broda, N. K., Meador, T. B., Wendt, J., et al. (2015). *Methanothermobacter thermautotrophicus* modulates its membrane lipids in response to hydrogen and nutrient availability. *Front. Microbiol.* 6, 1–9. doi: 10.3389/fmicb.2015.00005.

Zehnle, H., Laso-Pérez, R., Lipp, J., Riedel, D., Merino, D. B., Teske, A., et al. (2023). *Candidatus* Alkanophaga

archaea from Guaymas Basin hydrothermal vent sediment oxidize petroleum alkanes. *Nat. Microbiol.* 8, 1199–1212. doi: 10.1038/s41564-023-01400-3.

Zeng, Z., Chen, H., Yang, H., Chen, Y., Yang, W., Feng, X., et al. (2022). Identification of a protein responsible for the synthesis of archaeal membrane-spanning GDGT lipids. *Nat. Commun.* 13. doi: 10.1038/s41467-022-29264-x.

Zeng, Z., Liu, X. L., Farley, K. R., Wei, J. H., Metcalf, W. W., Summons, R. E., et al. (2019). GDGT cyclization proteins identify the dominant archaeal sources of tetraether lipids in the ocean. *PNAS* 116, 22505–22511. doi: 10.1073/pnas.1909306116.

Zhang, Y. G., Pagani, M., and Wang, Z. (2016). Ring Index: A new strategy to evaluate the integrity of TEX86 paleothermometry. *Paleoceanography* 31, 220–232. doi: 10.1002/2015PA002848.

# Discussion

The aim of my PhD thesis was to culture and describe novel HC-degrading microorganisms that operate under anoxic conditions and at high temperatures. In addition, I studied the membrane lipids of established anaerobic alkane-degrading consortia growing under a wide temperature range. Some key and common themes of the previous chapters that will be discussed here concern the capacity of microbes to utilize toxic and chemically inert compounds, different strategies of activating unreactive molecules, and the nature and requirements of syntrophy and thermophily.

In the two cultivation-based studies, I incubated petroleum-rich sediment from the Guaymas Basin (GB) hydrothermal vent site with different electron donors as carbon and energy source and sulfate as electron acceptor, attempting to accelerate the growth and activity of native microorganisms in the sediment with the capacity to degrade those compounds. I characterized successful enrichment cultures with a focus on the predominant microorganisms, analyzed their taxonomic relations and revealed their metabolic capacities. I obtained thermophilic cultures oxidizing mid-chain alkanes and unsubstituted aromatic hydrocarbons (UAHs), which I will discuss below. The focus will be on the established alkane-oxidation cultures, because they were the main project of this thesis.

## 5.1 Functional elucidation of a novel ANKA clade

In the first cultivation trial (**chapter 2**), I supplied mid-sized alkanes in the gasoline- and diesel-range as substrates and incubated the sediment slurries at 70 °C. This set-up based on enrichments of ANME/ANKA oxidizing gaseous alkanes ($C_1$-$C_4$) using Mcrs/Acrs that were known at the start of my PhD (Boetius et al., 2000; Knittel and Boetius, 2009; Laso-Pérez et al., 2016; Chen et al., 2019; Hahn et al., 2020). Acr-based archaeal alkane degradation for alkanes >$C_4$ was unknown. Combined with the plethora of environmental *acrA* sequences with unknown function, I suspected that yet uncultured archaea could oxidize these mid-chain alkanes. Aside from these archaea oxidizing alkanes via Mcrs/Acrs, archaeal alkane degraders were scarce, while bacteria were known to oxidize most alkanes >$C_2$ (Widdel et al., 2010). An exception was the $C_{10}$-$C_{21}$-oxidizing thermophilic archaeon *Archaeoglobus fulgidus* growing at 70 °C, which likely utilizes fumarate addition for alkane activation (Khelifi et al., 2014). This mechanism is associated with bacteria, and *A. fulgidus* likely acquired the necessary pathway genes, including a *masD*/*assA* homologue, via horizontal gene transfer (HGT) from a bacterium (Khelifi et al., 2014). Thus, alkanes from $C_5$-$C_9$ were not confirmed substrates of archaea in general, and alkanes >$C_4$ were not confirmed substrates of Acr-using archaea. During the course of my PhD, Zhou et al. (2022) revealed the Acr-based degradation of long-chain alkanes by *Ca.* Methanoliparum.

### 5.1.1 Challenges of mid-chain alkane oxidation

At standard conditions, $C_5$-$C_{14}$ alkanes comprise the phase transition from gaseous to liquid, and pentane ($C_5$), while quite volatile, is the first liquid alkane in the homologous series of alkanes ($C_nH_{2n+2}$). Volatility of these alkanes decreases with increasing chain length. The shorter, more volatile compounds ($C_5$-$C_9$) constitute the most toxic alkanes, and are often the least favored alkane substrates of microorganisms. Instead, long-chain alkanes ($C_{10}$-$C_{18}$) are preferred (Foster, 1962; Klug and Markovetz, 1971; de Carvalho et al., 2009). For instance, the aerobic alkane-degrading bacterium *Alcanivorax borkumensis* shows its fastest growth on $C_{12}$-$C_{19}$ alkanes, and grows slower on shorter ($C_6$-$C_9$) and longer alkanes ($C_{20}$-$C_{30}$) (Naether et al., 2013). The growth of yeasts, such as *Candida* 107 and *Saccharomyces carlsbergensis* was inhibited by short alkanes <$C_{10}$ (Gill and Ratledge, 1972b). While the exact mechanism(s) of the toxic effect of alkanes on microorganisms is not entirely clear, studies have shown several points of attack. For instance, decane ($C_{10}$) reduced the glucose assimilation rate in *Candida* strains to about 1% compared to controls without $C_{10}$ (Gill and Ratledge, 1972a). The cytoplasmic membrane seems to be a major point of attack of short alkanes (Sikkema et al., 1995). X-ray diffraction showed that short alkanes like $C_6$ and $C_8$ enter the hydrophobic space of the membrane and impair the organization of membrane lipids by interfering with interactions between hydrophobic tails (McIntosh et al., 1980; Sikkema et al., 1995). Witholt et al. (1990) observed damages to the cell membrane in the aerobic $C_6$-$C_{16}$-degrading bacterium *Pseudomonas oleovorans* after the exponential growth phase had ceased. They suspected that the alkane substrates assemble into apolar droplets which abstract lipid components from the outer membrane. Microorganisms have evolved protective mechanisms against the toxicity of shorter alkanes. For instance, *A. borkumensis* produces biosurfactants like glucolipids (Abraham et al., 1998). These surfactants lower the surface tension of the hydrophobic substrates by emulsifying them (Abraham et al., 1998). This facilitates higher bioaccessibility and easier degradation (Rouse et al., 1994).

### 5.1.2 *Candidatus* Alkanophaga - a novel thermophilic ANKA genus

The cultivation trials with mid-chain alkanes were successful, and I obtained eight enrichment cultures, in which alkanes between $C_5$ and $C_{14}$ were consumed. Substrate-dependent sulfate-reduction activities indicated doubling times of ~2-6 weeks, with strong variations between the cultures. The fastest growing culture was the $C_{12}$-culture with a doubling time of 13 days. This is similar to the growth rate of the $C_3$-$C_4$-oxidizing *Ca.* Syntrophoarchaeum spp., and double of the, considering anoxic conditions, rapidly growing $C_2$-oxidizing *Ca.* Ethanoperedens thermophilum (Laso-Pérez et al., 2016; Hahn et al., 2020). The $C_5$ culture grew very slowly (doubling times >100 days), even though the microbial community resembled that of the more active $C_6$-$C_7$ cultures. Because the incubation conditions were the same in all cultures, these slow doubling times could be the result of toxic effects of $C_5$ on cell structures, including the

membrane, or the catabolic enzymes of the HC-degrading microorganisms were not well adapted to this substrate.

I identified the alkane-degrading microorganisms as two species of a previously uncharacterized archaeal genus, which were abundant in all cultures. A phylogenomic analysis placed them at the root of the methane-oxidizers ANME-1, and taxonomic classification combined with genome comparisons placed them within the family ANME-1. This clade forms a third group in the class Syntrophoarchaeia, next to ANME-1 and the $C_3$-and $C_4$-oxidizers of *Ca.* Syntrophoarchaeum. Because one of the species was prevalent in cultures oxidizing shorter, more volatile alkanes ($C_5$-$C_7$) and the other one was prevalent in $C_8$-$C_{14}$-oxidizing cultures, I designated them *Ca.* Alkanophaga volatiphilum and *Ca.* Alkanophaga liquidiphilum, respectively.

### 5.1.3 The enigmatic substrate versatility of Acrs

For the activation of alkanes, both *Ca.* Alkanophaga species do not encode MasD/AssA, but each encodes three Acrs. This is the second highest number of Acrs reported in an organism, second only to the four Acrs in *Ca.* Syntrophoarchaeum. The purpose of the high number of Acrs in *Ca.* Alkanophaga and *Ca.* Syntrophoarchaeum is difficult to ascertain. Sequences in the *acrA* branch of the *mcrA*/*acrA* phylogenetic tree fall into three clusters. Two of the *acrA*s of *Ca.* Alkanophaga fall into the second cluster, while the third *acrA* is placed in the third cluster (Figure 1). *Ca.* Syntrophoarchaeum has three *acrA*s in the second cluster, and both species contain an *acrA* sequence that is only distantly related to the one of the other species. This individual sequence is placed in cluster one for *Ca.* S. caldarius and in cluster three for *Ca.* S. butanivorans. Cluster one contains sequences of $C_2$-oxidizing archaea of the GoM-Arc1 clade, while cluster three contains sequences of the confirmed or suspected long-chain alkane oxidizers *Ca.* Methanoliparum, Hadarchaeota, and Bathyarchaeia (Evans et al., 2015; Chen et al., 2019; Laso-Pérez et al., 2019; Hahn et al., 2020; Zhou et al., 2022). Cluster two is mostly made up of the *Ca.* Alkanophaga and *Ca.* Syntrophoarchaeum sequences, plus one sequence of the Archaeoglobales archaeon *Ca.* Polytropus marinifundus (Boyd et al., 2019). Thus, one could hypothesize that sequences of the first cluster activate $C_2$, sequences of the second cluster activate short- to mid-chain alkanes (~$C_3$-$C_{14}$), and sequences of the third cluster activate long-chain alkanes (~≥$C_{16}$).

However, as often in biology, things are not so simple. For instance, *Ca.* Alkanophaga clearly express the *acrA* of the third cluster the highest for all alkanes between $C_5$-$C_{14}$, while the other two *acrA*s have a low to moderate expression. Similarly, the highest expressed *acrA* in the $C_4$-oxidizing *Ca*. S. butanivorans is the one of the third cluster of supposed long-chain alkane oxidizers (Laso-Pérez et al., 2016). Further, substrate tests with short-chain alkanes ($C_1$-$C_6$) showed that *Ca.* S. caldarius cannot degrade $C_2$, despite disposing of an *acrA* similar to the one of confirmed $C_2$ oxidizers (Laso-Pérez, 2018). Lastly, in these tests *Ca.* Syntrophoarchaeum only grew on $C_3$ and $C_4$, despite their high number of *acrA*s (Laso-Pérez, 2018).

Thus, the placement of *acrA* sequence(s) in the *mcrA*/*acrA* phylogenetic tree alone does not allow a solid prediction of the growth substrate of specific uncultured ANKA. Other factors like temperature, pH, nutrient availability, and protection mechanisms against alkane toxicity might modulate the substrate range. But if additional information is considered, for instance the environment the MAG was obtained from, and the presence or absence of other catabolic genes including the *β*-oxidation pathway, a reasonable estimation could be made. There does seem to be a quite clear structural distinction between the $C_2$-activating Acr and Acrs activating alkanes $\geq C_3$. The crystal structure of the $C_2$-activating Acr entails a hydrophobic tunnel leading to the active site which likely prevents larger alkanes from being metabolized (Hahn et al., 2021). Thus, an uncultured ANKA encoding an *acrA* highly similar to those of confirmed $C_2$ oxidizers might be restricted to that substrate as well. In contrast, structural models of the $\geq C_3$-activating Acrs of *Ca.* S. butanivorans and *Ca.* Methanoliparum feature a wider cleft (Lemaire and Wagner, 2022). This Acr is likely less selective regarding the length of the alkane substrate, and other factors could be more decisive on substrate range. For instance, the presence and selectivity of specific membrane transporters for alkane import into the cell could influence the substrate range of an ANKA. Some proteins involved in alkane uptake into the cell in bacteria were shown to be substrate specific. For example, *Pseudomonas putida* GPo1 uses alkane monooxygenase (AlkB), an integral membrane protein, to import $C_7$-$C_{16}$ alkanes (Grant et al., 2014). Kim et al. (2002) reported a selective uptake of $C_{16}$ in *Rhodococcus erythropolis* S+14He when supplied with a mixture of alkanes. *Alcanivorax dieselolei* B5, which can degrade the full range of alkanes between $C_5$-$C_{36}$, apparently uses three different membrane proteins for the uptake of $C_8$-$C_{12}$, $C_{16}$-$C_{24}$, and $C_{28}$-$C_{36}$ alkanes, respectively (Liu and Shao, 2005; Wang and Shao, 2014). Efficient and fast uptake of alkanes at the membrane may also mitigate potential damaging effects of these compounds to the membrane. The lack of a specific membrane transporter could explain why an archaeon might not be capable of degrading a specific alkane despite encoding an Acr that in theory is capable of activating that alkane. The study of presence and functioning of such membrane transporters in ANKA is still pending.

This highlights the need for more cultivation-based approaches, which can be carried out with *Ca.* Alkanophaga. Cell extracts could be used for *in vitro* assays to confirm the function and substrate range of the Acrs, as shown decades ago for methanogens (Gunsalus and Wolfe, 1980; Ellermann et al., 1988). If sufficient biomass can be produced from the relatively slow-growing cultures, it would be very valuable to attempt crystallization of the highly expressed Acr. While it is challenging to separate highly similar proteins like the three Acrs encoded by *Ca.* Alkanophaga, Shima et al. (2012) generated a homogenous Mcr crystal from mixed ANME-1 and ANME-2-related Mcr populations in an environmental sample. The authors attributed their success to a naturally slow crystallization process when different protein variants combine. Thus, conveniently homogenous protein species preferably assemble into a crystal (Shima et al., 2012). A crystal structure of a mid- to long-chain activating Acr would complement the only existing Acr structure of the $C_2$-activating Acr of *Ca.* E. thermophilum (Hahn et al., 2021). Such a novel

structure might reveal characteristics, potentially including posttranslational modifications (PTMs), which mediate substrate specificity. Previously, unusual PTMs were found in the active site of the Mcr of both methanogens and methanotrophs (Ermler et al., 1997; Shima et al., 2012; Wagner et al., 2017). The exact function of these PTMs remains unknown. Further, potential modifications of the $F_{430}$ cofactor and its coordination to the Acr, which might also modulate substrate binding, could be studied in the process. It would also be valuable to test the expression of *Ca.* Alkanophaga Acrs under different physiological conditions, e.g. varying pH, temperature, and substrate concentration. Interestingly, the hydrogenotrophic methanogen *Methanobacterium thermoautotrophicum*, which contains two Mcrs, expressed one Mcr in the early growth phase and the second Mcr at the late growth phase and under $H_2$ limitation (Rospert et al., 1990). The second Mcr showed lower specific activity, thus the switch in Mcrs may serve to conserve energy under low-energy conditions (Rospert et al., 1990). Further studies may reveal if the three Acrs of *Ca.* Alkanophaga serve a similar purpose.

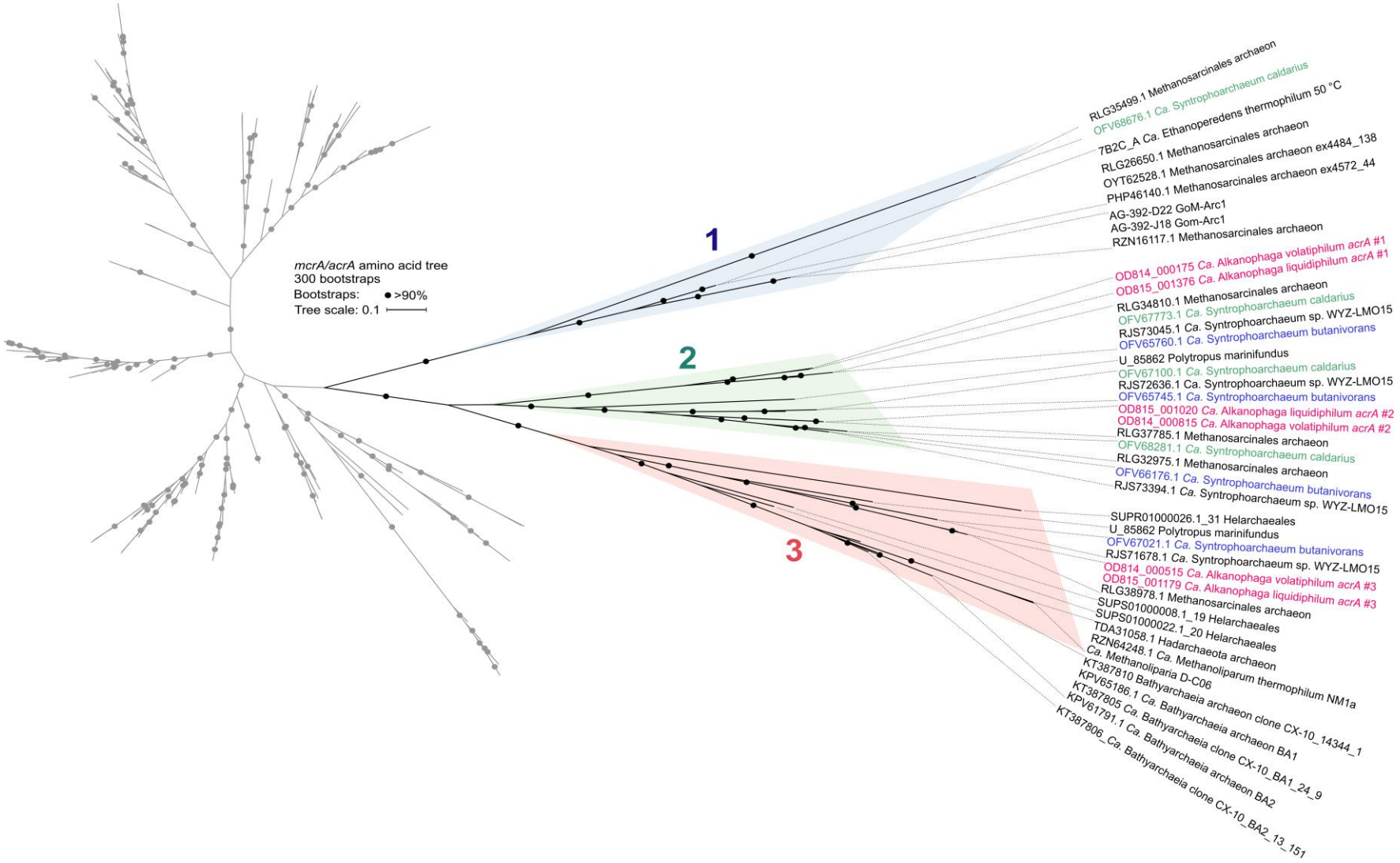


**Figure 1 |** Clusters of sequences in the divergent *acrA* branch of the *mcrA*/*acrA* phylogenetic tree. These sequences are presumably used for multi-carbon alkane metabolism. Sequences of *Ca.* Alkanophaga spp., *Ca.* Syntrophoarchaeum caldarius, and *Ca.* S. butanivorans are highlighted in pink, green, and blue, respectively. The grayed out sequences belong to methanogenic and methanotrophic archaea.

### 5.1.4 Evolutionary considerations

The origin and evolution of both Mcr and Acr within the archaea have been a focal point of recent studies (Wang et al., 2021; Garcia et al., 2022). Those studies included the previously published MAG of *Ca.* Alkanophaga liquidiphilum, ANME-1 B39_G2, which was recovered directly from GB sediment (Dombrowski et al., 2018), in their analysis. Based on the presence of Acrs and the *β*-oxidation and WL pathways, it was estimated that this archaeon is an ANKA (Dombrowski et al., 2018; Wang et al., 2021). Wang et al. (2021) and Garcia et al. (2022) proposed based on phylogenies that the class Syntrophoarchaeia emerged as multi-carbon alkane-oxidizers, and not as methanotrophs. Both studies revealed an additional branch of the Syntrophorachaeia, represented by *Ca.* Santabarbaracales. *Ca.* Santabarbaracales MAGs originate from an oil seep in the Pacific Ocean offshore Santa Barbara (California, USA) (Hawley et al., 2014b, 2014a; Nayfach et al., 2021). Like *Ca.* Alkanophaga, *Ca.* Santabarbaracales encode three *acrA*s (Wang et al., 2021). Phylogenetic analysis by Garcia et al. (2022) placed *Ca.* Santabarbaracales between *Ca.* Syntrophoarchaeales, the order including *Ca.* Syntrophoarchaeum, and *Ca.* Alkanophaga (Figure 2). Thus, *Ca.* Santabarbaracales are very likely also ANKA.

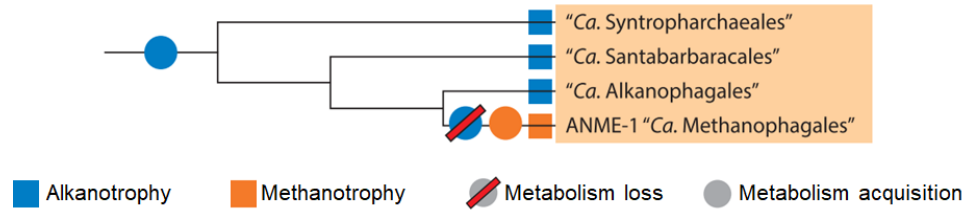


**Figure 2** | Alkane metabolism in the class Syntrophoarchaeia. Modified from Garcia et al. (2022)

With the enrichment of *Ca.* Alkanophaga on mid-chain alkanes, the previous estimations of the metabolism of this clade were confirmed. It is also the closest clade to the branching point where multi-carbon metabolism was lost in the Syntrophoarchaeia. Based on the recent studies, ANME-1 must have lost the multiple Acrs of their ANKA ancestors at this branching point, and acquired a canonical Mcr (Borrel et al., 2019; Wang et al., 2021). The order of those two events is unclear. It is conceivable that the ANME-1 ancestor first acquired the Mcr for methane metabolism before losing the Acrs. This Mcr likely originated from methyl-reducing methanogens within the recently described superclass Acherontia, a deeply branching clade situated closely at the divergence of Halobacteriota and Thermoproteota (previously TACK superphylum) (Rinke et al., 2021; Wang et al., 2021). After the acquisition of the Mcr, an environmental change might have occurred and methane become much more available than longer alkanes. This could have happened through dispersion of cells into other habitats. In these new conditions, the Mcr brought an evolutionary advantage. Because the Acrs were no longer needed, they were eliminated from the genome(s) through genome streamlining. Thereby, ANME-1 specialized on methantrophy and diverged from the ANKA of the Syntrophoarchaeia. Similar to that scenario, Garcia et al. (2022) proposed that a HGT event of an Acr to the GoM-Arc1 clade shifted the metabolism from methanotrophy to ethanotrophy in the

Methanosarcinales. In conclusion, these recent discoveries suggest that Syntrophoarchaeia are rather "a clade of ANKA that also contain ANME", than "a clade of ANME that also contain ANKA".

The exact origin of the Acr, i.e. the point of divergence from the canonical Mcr, is still under discussion. (Wang et al., 2021) proposed based on phylogenies that the first Acr was the $C_2$-activating Acr, which emerged from a gene duplication event of the *mcrABG* operon before the radiation of Euryarchaeota (now reclassified as several new phyla by GTDB) (Rinke et al., 2021). This Acr would then have evolved to utilize larger alkanes and was vertically and horizontally distributed within the archaea (Wang et al., 2021). Garcia et al. (2022) also suspected a duplication event as the origin of the Acr, and hypothesized based on observations by Borrel et al. (2019) that this event may have taken place at the root of the Syntrophoarchaeia followed by distribution to other archaeal clades via HGT. Thus, the ANKA of Syntrophoarchaeia might have been the original multi-carbon alkane oxidizers within the archaea.

### 5.1.5 Syntrophy between ANME/ANKA and sulfate reducers

With *Ca.* Thermodesulfobacterium syntrophicum, I enriched and identified a new partner SRB for ANKA. A bacterium of this genus also acts as partner SRB for thermophilic ANME-1c growing at 70 °C (Benito Merino et al., 2022). This is in contrast to the ANME/ANKA growing at 50 °C, which all partner with *Ca.* Desulfofervidus auxilii (Holler et al., 2011b; Laso-Pérez et al., 2016; Hahn et al., 2020). The higher incubation temperature of 70 °C likely selected for a more thermophilic clade.

A key observation in this study was the absence of multi-heme *c*-type cytochromes (MHCs) from *Ca.* Alkanophaga MAGs, which contrasts previously described syntrophic ANME and ANKA. This opened up the question how electrons are transferred from *Ca.* Alkanophaga to *Ca*. T. syntrophicum. Previously, different studies gave different results on the role and necessity of MHCs for direct interspecies electron transfer (DIET). In some studies MHCs were the main components of intercellular nanowires (Baquero et al., 2023; Gu et al., 2023), while in other studies microorganisms without MHCs were capable of DIET via conductive cell appendages (Reguera et al., 2005; Yee and Rotaru, 2020; Liu et al., 2022). A simple explanation would be that two types of conductive nanowires exist, one type is formed by stacked MHCs and the other bases on cell appendages like pili and flagella. Cell appendages were very highly expressed during alkane oxidation, in particular by *Ca.* Alkanophaga, indicating an essential function. The possibility of at least partial electron transfer through soluble electron carriers like formate and $H_2$ remains, as both syntrophic partners encode membrane-bound hydrogenases and formate dehydrogenases. However, initial physiological experiments did not point towards a high relevance of those molecules as electron carriers. I also attempted to isolate *Ca.* T. syntrophicum via a dilution series with $H_2$ as substrate, but these attempts were unsuccessful. *Ca.* D. auxilii was previously isolated on $H_2$ when incubated at 60 °C, 10 °C higher than when it

forms syntrophic consortia with ANME/ANKA (Holler et al., 2011b; Krukenberg et al., 2016; Laso-Pérez et al., 2016; Hahn et al., 2020). Previously isolated Thermodesulfobacteria, including *Thermodesulfobacterium geofontis* and *T. hydrogeniphilum*, can utilize $H_2$ as growth substrate and grow optimally at 75-80 °C (Jeanthon et al., 2002; Hamilton-Brehm et al., 2013). Thus, it could be valuable to attempt the isolation of *Ca.* T. syntrophicum again at a higher temperature of ~80 °C, which might exclude the partner ANKA, as *Ca.* Alkanophaga only showed activity until 75 °C. Interestingly, the novel $C_{16}$-oxidizing ANKA of the Hadarchaeota, *Ca.* Cerberiarchaeum oleivorans, which likely forms syntrophic interaction with *Ca.* Thermodesulfobacterium torris, also lacks MHCs but encodes cell appendage proteins (Benito Merino, 2023). Further experiments are necessary to determine the exact mechanism involved in electron transfer. These could include additional microscopy-based analyses, including staining of filaments to determine their identity.

The question of which unknown combinations of syntrophic ANME/ANKA and sulfate-reducing microorganisms could mediate the anaerobic oxidation of alkanes, and which factors determine these associations, is intriguing. A similar optimal growth temperature seems to be a main requirement. Currently, all described sulfate-reducing partners of ANME/ANKA are bacteria. Yet, ANME/ANKA could hypothetically also partner with sulfate-reducing archaea, such as Archaeoglobales. Syntrophic interactions exclusively between archaea have been described previously for heterotrophic hyperthermophiles, including *Thermococcus celer* and *Pyrococcus furiosus*, in cocultures with methanogenic archaea (Bonch-Osmolovskaya and Stetter, 1991). Some important insights have been gained on how syntrophy is established between two partners. For instance, it was observed that syntrophic partners assemble to form aggregates upon supply of the growth substrate. The thermophilic bacterium *Pelotomaculum thermopropionicum* strain SI and the methanogen *Methanothermobacter thermautotrophicus* strain ΔH were found dispersed in their respective medium when grown individually, but formed dense aggregates when grown in coculture (Ishii et al., 2005). Flagella originating from the bacterium, which wrapped around the *M. thermautotrophicus* cells, were involved in the coaggregation process. Ishii et al. (2005) suspected that these filaments established the first contact between the syntrophic partners. In a follow-up study, it was discovered that the flagellar cap protein FliD of the flagella produced by *P. thermopropionicum* strongly stimulated the expression of over 50 genes in the methanogenic archaeon, including genes involved in methanogenesis (Shimoyama et al., 2009). Thus, in addition to their potential role in electron transfer, flagella likely play an important role in establishing the necessary cell-to-cell connections and synchronizing the metabolisms of the syntrophic partners. In larger aggregates, extracellular polymeric substances (EPS) were spotted in the intercellular space (Ishii et al., 2005). Previous studies showed that EPS can play an important role in cell-to-cell connections and adhesion to surfaces (Tsuneda et al., 2003; Liu et al., 2004; Xiao and Zheng, 2016). Krumholz et al. (2015) tested the effect of specific gene mutations in the SRB *Desulfovibrio alaskensis* G20 on syntrophy with the butyrate-oxidizing bacterium *Syntrophomonas wolfei*. *D.*

*alaskensis* mutant strains lacking essential genes of flagellum, pili, and EPS biosynthesis were incapable of syntrophy, highlighting the importance of those factors. In addition, outer membrane components were essential for syntrophy (Krumholz et al., 2015). In accordance with that, Sieber et al. (2012) previously suggested that syntrophic partners might recognize each other through cell surface components similar to the Toll-like receptors of the immune system, which detect the flagella of pathogens (Takeda and Akira, 2004).

The exact mechanisms of how syntrophy is induced and stabilized and the degree of specificity of this interaction are still not well resolved. From what is known today, it seems likely that ANME/ANKA and potential partner sulfate reducers need to be able to produce the previously recognized as essential components for syntrophy to be successful. Filaments seem to play an important role in the interaction. Other previously established alkane-oxidizing consortia also highly expressed cell appendages during alkane oxidation, and dense cell-to-cell connections are visible in the intercellular space of the consortia (Wegener et al., 2015; Laso-Pérez et al., 2016; Krukenberg et al., 2018; Hahn et al., 2020; Benito Merino et al., 2022). It would be interesting to study whether the ANME/ANKA actively select for specific partners via communication with cells of potential partners, i.e. via quorum sensing or chemotaxis-inducing factors. While quorum sensing was mainly studied in bacteria, presence and activity of a bacterial-like quorum sensing circuit was reported in the methanogenic archaeon *Methanosaeta harundinacea* 6Ac (Zhang et al., 2012). Charlesworth et al. (2020) reported quorum sensing activity in various archaeal isolates, and hypothesized that this mechanism might be important for communication between archaea and bacteria.

### 5.1.6 Future perspectives for Mcr/Acr-based research

With the enrichment of *Ca.* Alkanophaga, it is confirmed that ANME and ANKA oxidize alkanes between $C_1$ and $\geq C_{20}$ via Mcrs/Acrs. It remains to be explored whether all Acr-based mechanisms have now been described. The enrichment of more psychrophilic ANKA clades oxidizing mid- to long-chain alkanes would be a valuable indication that ANKA could contribute to bioremediation of petroleum-contaminated sites, which are often not heated. An intriguing question is whether the equilibrium of the alkane oxidation pathway could be reversed to produce substantial amounts of alkanes. Hahn et al. (2020) observed small fractions of $C_2$ formation by *Ca.* E. thermophilum when incubating cultures with $^{13}C$-labelled inorganic carbon, removing sulfate and adding hydrogen as electron donor. The $C_2$ formation rate was however only a small fraction of the $C_2$ oxidation rate, and is likely attributed to natural back flux. A back flux of 5-13% was reported previously in consortia mediating AOM through radiotracer experiments (Holler et al., 2011a). An option would be to test the expression, function and reversibility of Acrs in other anaerobic and faster-growing archaea, e.g. methanogens like *Methanosarcina* spp. (Kohler and Metcalf, 2012), because the slow growth rate of ANME and ANKA makes such experiments challenging. Another potential application, the harvesting of energy from ANME/ANKE-based alkane oxidation in microbial fuel cells by decoupling the syntrophic

partners, was also discussed previously (Scheller et al., 2016; Scheller, 2018; Kondaveeti et al., 2019). Such a system could be used to combine bioremediation of wastewater with energy production (Malik et al., 2023). Scheller (2018) also discussed the possibility to reverse this process, and shuttle excess energy (e.g. from solar cells) into the production of alkanes.

## 5.2 Anaerobic microorganisms degrade UAHs at high temperatures

In the second cultivation trial (**chapter 3**), I incubated GB sediment with various UAHs, and obtained cultures growing with benzene and naphthalene at 50 °C and 70 °C. The larger UAHs phenanthrene and pyrene were not degraded in this study. With increasing size, hydrophobicity and therewith chemical recalcitrance of UAHs increases (Ghosal et al., 2016). Further, larger UAHs are considered more mutagenic than small ones, because of their capacity to intercalate between the bases of the DNA (Wolfe et al., 1987; Ghosal et al., 2016). Thus, the degradation of larger UAHs potentially requires protection mechanisms that are very energy-costly under anoxic conditions. Such mechanisms include the active efflux of UAHs out of the cell when hazardous concentrations are reached, which was reported in the aerobic UAH-degrading bacterium *Pseudomonas fluorescens* LP6a (Bugg et al., 2000). *P. fluorescens* LP6a degrades both naphthalene and phenanthrene, but actively exports only phenanthrene (Bugg et al., 2000). Because UAHs were observed to enter the cell of degrading microorganisms via free diffusion (Bateman et al., 1986; Bugg et al., 2000), it is also possible that the low-permeability membranes that are required at high temperatures restrict the entry of these molecules into the cell.

The cultures that showed sulfate-reducing activity on UAHs all had very different microbial communities. The naphthalene culture incubated at 70 °C stayed relatively complex, and different strategies could be employed to reach a more enriched status. Potentially, lower substrate concentrations should be tested to see if the microorganisms' growth can be accelerated. I studied the potential mechanisms of UAH degradation in these cultures. In the benzene culture at 50 °C, the absence of many of the known genes involved in anaerobic UAH oxidation in the highly abundant Thermoplasmatota MAG opened up questions on which alternative mechanism could be used. Metatranscriptome and proteome analyses as well as tests with different substrates and intermediates could help elucidate the catabolic pathways in this culture. In the benzene-oxidizing culture incubated at 70 °C, and the naphthalene-oxidizing culture at 50 °C (N50), two bacteria of the Desulfatiglandales were highly abundant, and encoded most proteins involved in anaerobic UAH degradation.

A key question in UAH degradation is the initial activation of the very stable compounds. While the bacterium in the N50 culture very likely activates naphthalene via direct carboxylation, genomic analysis of the B70 culture pointed towards degradation after methylation of benzene. But because no protein involved in direct methylation of benzene has been identified so far, the critical initial step of benzene oxidation could not be resolved in the scope of this study.

Methylation was a popular theory for UAH activation in initial studies (Ulrich et al., 2005; Safinowski and Meckenstock, 2006). It was proposed that such a methylation could occur through an aromatic substitution Friedel-Crafts-type reaction, which is exergonic when using the biological methyl group donors S-adenosylmethionine (SAM) or tetrahydrofolate (Coates et al., 2002; Vogt et al., 2011). SAM-dependent methylation of benzene by an unknown enzyme has been reported in human bone marrow (Flesher and Myers, 1991). Thus, it could be hypothesized that a protein of the radical SAM superfamily might catalyze such a reaction. Radical SAM proteins are known for catalyzing unusual and challenging reactions between C-C bonds, including methylations, through a radical mechanism (Sofia et al., 2001). For instance, the recently described archaeal tetraether synthase, which catalyzes the tail-to-tail condensation of lipid tails to form membrane-spanning lipids, is a radical SAM protein (Lloyd et al., 2022; Zeng et al., 2022). Radical SAM proteins catalyzing the methylation of aromatic compounds have been reported from *Streptomyces* spp., which use these methyltransferases during the biosynthesis of antibiotics (Tengg et al., 2012; Pavkov-Keller et al., 2017). The initial theory of UAH methylation was abandoned later because of lack of support from cultures (Musat and Widdel, 2008). Recent studies have focused mostly on investigating and describing mechanisms and reactions involved in the carboxylation pathway of UAH degradation, particularly UbiD-carboxylase-based activation, see e.g. (Abu Laban et al., 2010; Bergmann et al., 2011; Luo et al., 2014; Koelschbach et al., 2019; Heker et al., 2023). Potentially, with the enrichment of the B70 culture, which likely activates benzene via methylation, more efforts could be undertaken to identify proteins involved in other forms of UAH activation. Further enrichment and analyses of these cultures via e.g. metatranscriptomics, proteomics, and metabolite detection are necessary to further investigate and validate which mechanisms are used.

Anaerobic thermophilic bacterial UAH degraders have not been studied intensely so far. For alkane-degrading SRB, the upper growth temperature seems to be around 60-65 °C (Mbadinga et al., 2011). My study shows the potential of SRB to degrade recalcitrant HCs at temperatures up to 70 °C. Prior to that, most anaerobic bacteria that oxidize UAHs were isolated at around 30 °C. Potentially, with further enrichment trials using HC-rich sediment from heated sited like the GB, more thermophilic UAH degraders could be isolated. The only UAH degrader growing at high temperatures was the iron-reducer *Ferroglobus placidus* oxidizing benzene at 85 °C (Holmes et al., 2011). Similar to *A. fulgidus*, which oxidizes alkanes at 70 °C using the bacterial mechanism of fumarate addition, *F. placidus* oxidizes benzene via a bacterial mechanism, including anaerobic benzene carboxylase for benzene activation (Holmes et al., 2011; Khelifi et al., 2014). So far, no independent UAH activation and degradation mechanism for UAHs, like the Mcr/Acr-based oxidation of alkanes, has been reported in archaea. Thus, there could be some kind of trade-off between thermophily and (un)reactivity of a compound that a heterotrophic organism can use as carbon and energy source. This comes back to what was stated by Valentine (2007), that archaea seem to have focused on energy conservation based on rather simple metabolisms, which gave them an advantage at living in extreme habitats, including very

high temperatures ≥70 °C. Bacteria on the other hand focused instead on the diversification of their metabolism to utilize a broader range of substrates, which was more energy-costly and made them more suitable for less heated environments. Potentially, the capacity to oxidize the very stable UAHs at high temperatures requires special energy-conserving mechanisms to make this lifestyle feasible that only few microorganisms could achieve. For bacteria that do grow at high temperatures, like the Desulfatiglandales species in the B70 culture, such modifications often include adopting a more "archaeal-like" cell membrane, which reduce futile ion cycling and thereby conserve energy (Valentine, 2007).

## 5.3 Core membrane lipids of ANME/ANKA-enrichment cultures

In **chapter 4**, I studied the hydrophobic core membrane lipids of twelve established enrichment cultures of ANME/ANKA and partner SRB growing at temperatures between 20-70 °C. In addition, I analyzed the metagenome of a novel $C_2$-oxidizing culture, which was included in the study. In this culture, a novel GoM-Arc1 clade *Ca.* Ethanoperedens archaeon was highly abundant. This culture will be interesting for further investigation, at it is active at ambient temperature and thereby bridges a gap between psychrophilic and thermophilic $C_2$ oxidation (Chen et al., 2019; Hahn et al., 2020). The core lipid (CL) analysis showed that temperature, substrate, and the archaeon and bacterium prevalent in the culture all had a significant effect on the membrane lipid (ML) composition. Notable results included the absence of OH-AR in an ANME-2-dominated culture growing at 20 °C, which was previously considered characteristic for this clade (Niemann and Elvert, 2008). Instead, MAR was present at relatively high abundances in this culture. This CL was previously associated with hyperthermophiles (Comita et al., 1984; Arakawa et al., 2001). The novel $C_2$-oxidizing culture at 20 °C contained high abundances of crenarchaeol, which was previously not found outside of the pelagic Thaumarchaeota (now Nitrosphaeria) (Sinninghe Damsté et al., 2002; Pester et al., 2011). This warrants further investigation. A switch seems to occur at 70 °C, because cultures incubated at that temperature had a very different CL composition than cultures growing at lower temperatures. Variants of GMGT with varying degree of cyclization were highly abundant at that growth temperature, in line with previous observations (Bauersachs and Schwark, 2016). Of particular interest are GMGT variants with additional methylations (1Me-GMGT and 2Me-GMGT), which were previously detected in deep layers of heated sites in the GB, including Ultra Mound and Cathedral Hill (Song, 2020), and in other marine sediment heated to above 80 °C (Sollich et al., 2017), but their biological origin was unclear. These CLs and derivates were found in all cultures incubated at 70 °C. Thus, thermophilic ANKA are potential producers of these CLs in heated environments. Interestingly, the CL composition of the $C_4$-oxidizing culture of *Ca.* Syntrophoarchaeum and *Ca.* D. auxilii growing at 50 °C was highly similar to those of cultures growing at 70 °C. This culture contained high abundances of GMGTs and derivates. Previously, these lipid were associated with hyperthermorphilic archaea (Sollich et al., 2017; Tourte et al., 2022). Another interesting CL group was IB-GDGT, which exhibits a hybrid structure with

components of both archaeal and bacterial lipid architecture (Liu et al., 2012). Further studies, including analysis of the intact polar lipids and stable isotope probing, are necessary to trace back the intriguing CL structures to their biological origin with confidence.

Considering the CL composition switch at 70 °C, and the apparent upper temperature limit of most SRB of ~60-65 °C, it is tempting to speculate that growth at ≥70 °C requires the ability to synthesize special low-permeability MLs which are considered characteristic of archaea, and that most SRB cannot synthesize such lipids. In accordance with this, (Siliakus et al., 2017) stated that thermophilic bacteria growing at >70 °C produce MLs reminiscent of archaeal MLs, including ether-bonds and membrane-spanning lipids (MSLs). In contrast, MLs of meso- to thermophilic bacteria growing at <70 °C include other less drastic modifications, like increased saturation and branching of fatty acid tails (Siliakus et al., 2017). At high temperatures and/or anoxic conditions, archaea and bacteria share a high number of genes, which was found to be mainly because of HGT from archaea to bacteria (Fuchsman et al., 2017). Such a high number of common genes was not detected for high salt conditions (Fuchsman et al., 2017). Coleman et al. (2018) reported extensive horizontal gene transfer of ML biosynthesis genes between archaea and bacteria, which often lead to the formation of archaeal-like MLs in bacteria. Thus, it seems that bacteria need to become more "archaea-like" to be able to thrive in heated anoxic environments. Curiously, bacteria which synthesize ester-based MSLs do not encode a homologue of the recently described archaeal tetraether synthase, but use a different radical SAM protein for tail-to-tail condensation of fatty acid terminal C atoms (Lloyd et al., 2022; Sahonero-Canavesi et al., 2022; Zeng et al., 2022). This leaves the option open that bacteria evolved, at least in part, their own mechanisms of high-temperature membrane adaptations. However, the precursor of bacterial ether-based MSLs, and the biosynthesis of these lipids, are still unknown. The examination of the sources of unknown tetraether lipids, i.e. SB-GDGTs, OB-GDGTs, and the hybrid IB-GDGTs, in the alkane-oxidizing cultures could help elucidate the bacterial production of such lipids.

Some of the MLs that were identified in this study have the potential to serve as biosignatures for clades of ANKA. Further study of the MLs of these cultures will help to resolve the production and exact origin of these lipids. Such biosignatures could serve as indicators for alkanotrophy, when nucleic acid sequencing is not feasible, e.g. in very old samples and/or when DNA is degraded. Because of their chemical stability and longevity compared to nucleic acids, lipid-based biosignatures, i.e. "molecular fossils", may eventually become involved in the exploration of past or present extraterrestrial microbial life (Summons et al., 2022; Finkel et al., 2023). Extremophilic archaea are among the best candidates for extraterrestrial life, e.g. on Mars (Cavicchioli, 2002). With the first Martian soil samples scheduled to return to Earth in about 10 years (Grady, 2020), this is an exciting perspective.

## 5.4 Conclusion and outlook

In my PhD, I was able to enrich and study novel anaerobic thermophilic HC-degrading archaea and bacteria from GB sediment. This highlights once more the potential of this hydrothermal vent site as a well of anaerobic HC-degrading microorganisms, and invites to ponder upon which uncultured lineages with intriguing metabolisms are still waiting to be revealed. As the GB can be seen as a surface analogue for deeply situated heated petroleum reservoirs, the enriched microorganisms are potential key organisms in petroleum HC degradation in such reservoirs. Because these archaea and bacteria combine HC oxidation with sulfate reduction, they are more likely to occur in seawater-flooded than in pristine reservoirs. There, they potentially contribute to reservoir souring through sulfide formation (Tanji et al., 2014). Thermodesulfobacteria, the clade to which the partner SRB of the enriched mid-chain alkane oxidizers belong, are frequently detected in samples originating from petroleum reservoirs with temperatures ≥50 °C (Pannekens et al., 2019). This could imply that consortia of *Ca.* Alkanophaga and *Ca.* T. syntrophicum are viable and active in such reservoirs, but more studies are required to examine this possibility. Another process that these microorganisms may be involved in is carbonate formation in cap rocks, which is associated with HC oxidation and sulfate reduction and has been reported in various locations (Sassen et al., 1988; Aloisi et al., 2013; Caesar et al., 2019). It may be possible that these organisms can form syntrophic consortia with methanogenic archaea in the absence of sulfate, which would enable them to degrade HCs in pristine reservoirs, but this remains to be examined. The enriched archaea and bacteria grow at up to 70 °C, which adds to the small list of cultured microbes that are capable of HC degradation at temperatures close to the supposed sterilization temperature of reservoirs of 80 °C (Head et al., 2003). 70 °C could constitute a transition from moderately thermophilic to hyperthermophilic life, which requires membranes with very low permeability, indicated by a drastic switch in ML composition in cultures of ANKA and partner SRB. The study of the microbial community in subsurface reservoirs and the detailed processes microorganisms perform are still at its infancy. For economic reasons, samples for microbial analyses are mostly collected from the wellhead at the surface, which comes with a high chance of contamination (Magot et al., 2000; Marietou, 2021). Thus, interdisciplinary efforts between microbiologists, geochemists, and the petroleum industry are required to improve sampling strategies for a more reliable identification of the microbes inhabiting and thriving in this extreme habitat.

# Bibliography


Abbe, K., Takahashi, S., and Yamada, T. (1982). Involvement of oxygen-sensitive pyruvate formate-lyase in mixed-acid fermentation by *Streptococcus mutans* under strictly anaerobic conditions. *J. Bacteriol.* 152, 175–182. doi: 10.1128/jb.152.1.175-182.1982.

Abdelgadir, A., Chen, X., Liu, J., Xie, X., Zhang, J., Zhang, K., et al. (2014). Characteristics, Process Parameters, and Inner Components of Anaerobic Bioreactors. *Biomed Res. Int.* 2014, 841573. doi: 10.1155/2014/841573.

Abdullayev, N. R. (2020). Analysis of sedimentary thickness, volumes and geographic extent of the world sedimentary basins. *ANAS Trans. Earth Sci.*, 28–36. doi: 10.33677/ggianas20200100040.

Abraham, H. (1945). *Asphalts and allied substances: Their Occurrence, Modes of Production, Uses in the Arts and Methods of Testing*. D. van Nostrand company, inc.

Abraham, W.-R., Meyer, H., and Yakimov, M. (1998). Novel glycine containing glucolipids from the alkane using bacterium *Alcanivorax borkumensis*. *Biochim. Biophys. Acta - Lipids Lipid Metab.* 1393, 57–62. doi: https://doi.org/10.1016/S0005-2760(98)00058-7.

Abu Laban, N. (2010). Anaerobic benzene degradation by iron- and sulfate-reducing enrichment cultures. Available at: https://api.semanticscholar.org/CorpusID:90400401.

Abu Laban, N., Selesi, D., Rattei, T., Tischler, P., and Meckenstock, R. U. (2010). Identification of enzymes involved in anaerobic benzene degradation by a strictly anaerobic iron-reducing enrichment culture. *Environ. Microbiol.* 12, 2783–2796. doi: 10.1111/j.1462-2920.2010.02248.x.

Adam, P. S., Borrel, G., and Gribaldo, S. (2019). An archaeal origin of the Wood–Ljungdahl $H_4$MPT branch and the emergence of bacterial methylotrophy. *Nat. Microbiol.* 4, 2155–2163. doi: 10.1038/s41564-019-0534-2.

Aeckersberg, F., Bak, F., and Widdel, F. (1991). Anaerobic oxidation of saturated hydrocarbons to $CO_2$ by a new type of sulfate-reducing bacterium. *Arch. Microbiol.* 156, 5–14.

Aihara, J. (1992). Why Aromatic Compounds Are Stable. *Sci. Am.* 266, 62–69.

Aitken, C. M., Jones, D. M., and Larter, S. R. (2004). Anaerobic hydrocarbon biodegradation in deep subsurface oil reservoirs. *Nature* 431, 291–294. doi: 10.1038/nature02922.

Al-Hemoud, A., Al-Dousari, A., Misak, R., Al-Sudairawi, M., Naseeb, A., Al-Dashti, H., et al. (2019). Economic Impact and Risk Assessment of Sand and Dust Storms (SDS) on the Oil and Gas Industry in Kuwait. *Sustainability* 11. doi: 10.3390/su11010200.

Alamooti, A. M., and Malekabadi, F. K. (2018). "An Introduction to Enhanced Oil Recovery," in *Fundamentals of Enhanced Oil and Gas Recovery from Conventional and Unconventional Reservoirs*, ed. A. B. T.-F. of E. O. and G. R. from C. and U. R. Bahadori (Gulf Professional Publishing), 1–40. doi: https://doi.org/10.1016/B978-0-12-813027-8.00001-1.

Albers, S.-V., Van de Vossenberg, J. L. C. M., Driessen, A. J. M., and Konings, W. N. (2000). Adaptations of the archaeal cell membrane to heat stress. *Front. Biosci.* 5, 813–820.

Allmansberger, R., Bollschweiler, C., Konheiser, U., Müller, B., Muth, E., Pasti, G., et al. (1986). Arrangement and expression of methyl coenzyme M reductase genes in *Methanococcus voltae*. *Syst. Appl. Microbiol.* 7, 13–17. doi: https://doi.org/10.1016/S0723-2020(86)80117-5.

Aloisi, G., Baudrand, M., Lécuyer, C., Rouchy, J.-M., Pancost, R. D., Aref, M. A. M., et al. (2013). Biomarker and isotope evidence for microbially-mediated carbonate formation from gypsum and petroleum hydrocarbons. *Chem. Geol.* 347, 199–207. doi: https://doi.org/10.1016/j.chemgeo.2013.03.007.

Alonso-Alvarez, C., Munilla, I., López-Alonso, M., and Velando, A. (2007). Sublethal toxicity of the Prestige oil spill on yellow-legged gulls. *Environ. Int.* 33, 773–781. doi: https://doi.org/10.1016/j.envint.2007.02.012.

An, Y.-J. (2004). Toxicity of Benzene, Toluene, Ethylbenzene, and Xylene (BTEX) Mixtures to *Sorghum bicolor* and *Cucumis sativus*. *Bull. Environ. Contam. Toxicol.* 72, 1006–1011. doi: 10.1007/s00128-004-0343-y.

API Executive Committee on Standardization of Oilfield Equipment and Materials (1988). Glossary of Oilfield Production Terminology. Dallas.

Arakawa, K., Eguchi, T., and Kakinuma, K. (2001). 36-Membered Macrocyclic Diether Lipid is Advantageous for Archaea to Thrive under the Extreme Thermal Environments. *Bull. Chem. Soc. Jpn.* 74, 347–356. doi: 10.1246/bcsj.74.347.

Åström, E. K. L., Carroll, M. L., Ambrose Jr., W. G., Sen, A., Silyakova, A., and Carroll, J. (2018). Methane cold

seeps as biological oases in the high-Arctic deep sea. *Limnol. Oceanogr.* 63, S209–S231. doi: https://doi.org/10.1002/lno.10732.

Baquero, D. P., Cvirkaite-Krupovic, V., Hu, S. S., Fields, J. L., Liu, X., Rensing, C., et al. (2023). Extracellular cytochrome nanowires appear to be ubiquitous in prokaryotes. *Cell* 186, 2853-2864.e8. doi: 10.1016/j.cell.2023.05.012.

Bateman, J. N., Speer, B., Feduik, L., and Hartline, R. A. (1986). Naphthalene association and uptake in *Pseudomonas putida*. *J. Bacteriol.* 166, 155–161. doi: 10.1128/jb.166.1.155-161.1986.

Bauersachs, T., and Schwark, L. (2016). Glycerol monoalkanediol diethers: A novel series of archaeal lipids detected in hydrothermal environments. *Rapid Commun. Mass Spectrom.* 30, 54–60. doi: 10.1002/rcm.7417.

Bazylinski, D. A., Farrington, J. W., and Jannasch, H. W. (1988). Hydrocarbons in surface sediments from a Guaymas Basin hydrothermal vent site. *Org. Geochem.* 12, 547–558. doi: 10.1016/0146-6380(88)90146-5.

Beal, E. J., House, C. H., and Orphan, V. J. (2009). Manganese- and Iron-Dependent Marine Methane Oxidation. *Science* 325, 184–187. doi: 10.1126/science.1169984.

Becher, B., Müller, V., and Gottschalk, G. (1992). N5-methyl-tetrahydromethanopterin:coenzyme M methyltransferase of *Methanosarcina* strain Gö1 is an Na(+)-translocating membrane protein. *J. Bacteriol.* 174, 7656–7660. doi: 10.1128/jb.174.23.7656-7660.1992.

Belin, B. J., Busset, N., Giraud, E., Molinaro, A., Silipo, A., and Newman, D. K. (2018). Hopanoid lipids: from membranes to plant–bacteria interactions. *Nat. Rev. Microbiol.* 16, 304–315. doi: 10.1038/nrmicro.2017.173.

Beller, H. R., and Edwards, E. A. (2000). Anaerobic Toluene Activation by Benzylsuccinate Synthase in a Highly Enriched Methanogenic Culture. *Appl. Environ. Microbiol.* 66, 5503–5505. doi: 10.1128/AEM.66.12.5503-5505.2000.

Beller, H. R., Reinhard, M., and Grbić-Galić, D. (1992). Metabolic by-products of anaerobic toluene degradation by sulfate-reducing enrichment cultures. *Appl. Environ. Microbiol.* 58, 3192–3195. doi: 10.1128/aem.58.9.3192-3195.1992.

Benito Merino, D. (2023). Archaea and bacteria mediating anaerobic alkane degradation at its upper temperature limit. https://doi.org/10.26092/elib/2276

Benito Merino, D., Zehnle, H., Teske, A., and Wegener, G. (2022). Deep-branching ANME-1c archaea grow at the upper temperature limit of anaerobic oxidation of methane. *Front. Microbiol.* 13, 1–16. doi: 10.3389/fmicb.2022.988871.

Berdugo-Clavijo, C., and Gieg, L. M. (2014). Conversion of crude oil to methane by a microbial consortium enriched from oil reservoir production waters. *Front. Microbiol.* 5. doi: 10.3389/fmicb.2014.00197.

Berg, I. A., Kockelkorn, D., Ramos-Vera, W. H., Say, R. F., Zarzycki, J., Hügler, M., et al. (2010). Autotrophic carbon fixation in archaea. *Nat. Rev. Microbiol.* 8, 447–460. doi: 10.1038/nrmicro2365.

Berger, M., Picchioni, F., and Druetta, P. (2022). Simulation of Polymer Chemical Enhanced Oil Recovery in Ghawar Field. *Energies* 15. doi: 10.3390/en15197232.

Bergmann, F. D., Selesi, D., and Meckenstock, R. U. (2011). Identification of new enzymes potentially involved in anaerobic naphthalene degradation by the sulfate-reducing enrichment culture N47. *Arch. Microbiol.* 193, 241–250. doi: 10.1007/s00203-010-0667-4.

Birkeland, N.-K. (2004). "The microbial diversity of deep subsurface oil reservoirs," in *Petroleum Biotechnology*, eds. R. Vazquez-Duhalt and R. B. T.-S. in S. S. and C. Quintero-Ramirez (Elsevier), 385–403. doi: https://doi.org/10.1016/S0167-2991(04)80155-1.

Black, M. B., Lutz, R. A., and Vrijenhoek, R. C. (1994). Gene flow among vestimentiferan tube worm (*Riftia pachyptila*) populations from hydrothermal vents of the eastern Pacific. *Mar. Biol.* 120, 33–39. doi: 10.1007/BF00381939.

Boetius, A., Ravenschlag, K., Schubert, C. J., Rickert, D., Widdel, F., Gleseke, A., et al. (2000). A marine microbial consortium apparently mediating anaerobic oxidation of methane. *Nature* 407, 623–626. doi: 10.1038/35036572.

Boggs, S. J. (2006). *Principles of Sedimentology and Stratigraphy*. 4th ed. Pearson Prentice Hall.

Boll, M., Albracht, S. S. P., and Fuchs, G. (1997). Benzoyl-CoA reductase (dearomatizing), a key enzyme of anaerobic aromatic metabolism - A study of adenosinetriphosphatase activity, ATP stoichiometry of the reaction and EPR properties of the enzyme. *Eur. J. Biochem.* 244, 840–851. doi: 10.1111/j.1432-

1033.1997.00840.x.

Boll, M., Laempe, D., Eisenreich, W., Bacher, A., Mittelberger, T., Heinze, J., et al. (2000). Nonaromatic Products from Anoxic Conversion of Benzoyl-CoA with Benzoyl-CoA Reductase and Cyclohexa-1,5-diene-1-carbonyl-CoA Hydratase. *J. Biol. Chem.* 275, 21889–21895. doi: https://doi.org/10.1074/jbc.M001833200.

Bonch-Osmolovskaya, E. A., and Stetter, K. O. (1991). Interspecies Hydrogen Transfer in Cocultures of Thermophilic Archaea. *Syst. Appl. Microbiol.* 14, 205–208. doi: https://doi.org/10.1016/S0723-2020(11)80369-3.

Borowski, W. S., Paull, C. K., and Ussler, W. (1999). Global and local variations of interstitial sulfate gradients in deep-water, continental margin sediments: Sensitivity to underlying methane and gas hydrates. *Mar. Geol.* 159, 131–154. doi: https://doi.org/10.1016/S0025-3227(99)00004-3.

Borrel, G., Adam, P. S., McKay, L. J., Chen, L. X., Sierra-García, I. N., Sieber, C. M. K., et al. (2019). Wide diversity of methane and short-chain alkane metabolisms in uncultured archaea. *Nat. Microbiol.* 4, 603–613. doi: 10.1038/s41564-019-0363-3.

Boyd, J. A., Jungbluth, S. P., Leu, A. O., Evans, P. N., Woodcroft, B. J., Chadwick, G. L., et al. (2019). Divergent methyl-coenzyme M reductase genes in a deep-subseafloor Archaeoglobi. *ISME J.* 13, 1269–1279. doi: 10.1038/s41396-018-0343-2.

Brand, U., Morrison, J. O., and Campbell, I. T. (1998). "Diagenesis," in *Encyclopedia of Geochemistry* (Dordrecht: Springer Netherlands), 126–131. doi: 10.1007/1-4020-4496-8_76.

Breese, K., Boll, M., Alt-Mörbe, J., Schägger, H., and Fuchs, G. (1998). Genes coding for the benzoyl-CoA pathway of anaerobic aromatic metabolism in the bacterium *Thauera aromatica*. *Eur. J. Biochem.* 256, 148–154. doi: https://doi.org/10.1046/j.1432-1327.1998.2560148.x.

Brocks, J. J., Love, G. D., Summons, R. E., Knoll, A. H., Logan, G. A., and Bowden, S. A. (2005). Biomarker evidence for green and purple sulphur bacteria in a stratified Palaeoproterozoic sea. *Nature* 437, 866–870. doi: 10.1038/nature04068.

Bucher, K., and Frey, M. (1967). "Definition, Conditions and Types of Metamorphism," in *Petrogenesis of Metamorphic Rocks* (Springer Berlin Heidelberg), 3–15. doi: 10.1007/978-3-662-00866-9.

Budisa, N., and Schulze-Makuch, D. (2014). Supercritical Carbon Dioxide and Its Potential as a Life-Sustaining Solvent in a Planetary Environment. *Life* 4, 331–340. doi: 10.3390/life4030331.

Bugg, T., Foght, J. M., Pickard, M. A., and Gray, M. R. (2000). Uptake and Active Efflux of Polycyclic Aromatic Hydrocarbons by *Pseudomonas fluorescens* LP6a. *Appl. Environ. Microbiol.* 66, 5387–5392. doi: 10.1128/AEM.66.12.5387-5392.2000.

Caesar, K. H., Kyle, J. R., Lyons, T. W., Tripati, A., and Loyd, S. J. (2019). Carbonate formation in salt dome cap rocks by microbial anaerobic oxidation of methane. *Nat. Commun.* 10, 808. doi: 10.1038/s41467-019-08687-z.

Caineng, Z., Guangya, Z., Shizhen, T., Suyun, H., Xiaodi, L., Jianzhong, L., et al. (2010). Geological features, major discoveries and unconventional petroleum geology in the global petroleum exploration. *Pet. Explor. Dev.* 37, 129–145. doi: https://doi.org/10.1016/S1876-3804(10)60021-3.

Callaghan, A. (2013). Enzymes involved in the anaerobic oxidation of *n*-alkanes: from methane to long-chain paraffins. *Front. Microbiol.* 4. doi: 10.3389/fmicb.2013.00089.

Callaghan, A. Y., Gieg, L. M., Kropp, K. G., Suflita, J. M., and Young, L. Y. (2006). Comparison of Mechanisms of Alkane Metabolism under Sulfate-Reducing Conditions among Two Bacterial Isolates and a Bacterial Consortium. *Appl. Environ. Microbiol.* 72, 4274–4282. doi: 10.1128/AEM.02896-05.

Callaghan, A. V, Wawrik, B., Ní Chadhain, S. M., Young, L. Y., and Zylstra, G. J. (2008). Anaerobic alkane-degrading strain AK-01 contains two alkylsuccinate synthase genes. *Biochem. Biophys. Res. Commun.* 366, 142–148. doi: https://doi.org/10.1016/j.bbrc.2007.11.094.

Campbell, A. C., and Gieskes, J. M. (1984). Water column anomalies associated with hydrothermal activity in the Guaymas Basin, Gulf of California. *Earth Planet. Sci. Lett.* 68, 57–72. doi: https://doi.org/10.1016/0012-821X(84)90140-7.

Campbell, K. A. (2006). Hydrocarbon seep and hydrothermal vent paleoenvironments and paleontology: Past developments and future research directions. *Palaeogeogr. Palaeoclimatol. Palaeoecol.* 232, 362–407. doi: 10.1016/j.palaeo.2005.06.018.

Canadian American Seamount Expedition (1985). Hydrothermal vents on an axis seamount of the Juan de Fuca ridge. *Nature* 313, 212–214. doi: 10.1038/313212a0.

Carmona, M., Zamarro, M. T., Blázquez, B., Durante-Rodríguez, G., Juárez, J. F., Valderrama, J. A., et al. (2009). Anaerobic Catabolism of Aromatic Compounds: a Genetic and Genomic View. *Microbiol. Mol. Biol. Rev.* 73, 71–133. doi: 10.1128/mmbr.00021-08.

Cavicchioli, R. (2002). Extremophiles and the search for extraterrestrial life. *Astrobiology* 2, 281–292. doi: 10.1089/153110702762027862.

Ceramicola, S., Dupré, S., Somoza, L., and Woodside, J. (2018). "Cold Seep Systems," in *Submarine Geomorphology*, eds. A. Micallef, S. Krastel, and A. Savini (Springer International Publishing), 367–387. doi: 10.1007/978-3-319-57852-1_19.

Chadwick, G. L., Skennerton, C. T., Laso-Pérez, R., Leu, A. O., Speth, D. R., Yu, H., et al. (2022). Comparative genomics reveals electron transfer and syntrophic mechanisms differentiating methanotrophic and methanogenic archaea. *PLoS Biol.* 20, 1–71. doi: 10.1371/journal.pbio.3001508.

Chakraborty, R., and Coates, J. D. (2005). Hydroxylation and carboxylation - Two crucial steps of anaerobic benzene degradation by *Dechloromonas* strain RCB. *Appl. Environ. Microbiol.* 71, 5427–5432. doi: 10.1128/AEM.71.9.5427-5432.2005.

Charlesworth, J., Kimyon, O., Manefield, M., Beloe, C. J., and Burns, B. P. (2020). Archaea join the conversation: detection of AHL-like activity across a range of archaeal isolates. *FEMS Microbiol. Lett.* 367, fnaa123. doi: 10.1093/femsle/fnaa123.

Chen, J., Liu, Y.-F., Zhou, L., Irfan, M., Hou, Z.-W., Li, W., et al. (2020). Long-chain *n*-alkane biodegradation coupling to methane production in an enriched culture from production water of a high-temperature oil reservoir. *AMB Express* 10, 63. doi: 10.1186/s13568-020-00998-5.

Chen, S. C., Musat, N., Lechtenfeld, O. J., Paschke, H., Schmidt, M., Said, N., et al. (2019). Anaerobic oxidation of ethane by archaea from a marine hydrocarbon seep. *Nature* 568, 108–111. doi: 10.1038/s41586-019-1063-0.

Coates, J. D., Chakraborty, R., and McInerney, M. J. (2002). Anaerobic benzene biodegradation—a new era. *Res. Microbiol.* 153, 621–628. doi: https://doi.org/10.1016/S0923-2508(02)01378-5.

Coleman, G. A., Pancost, R. D., and Williams, T. A. (2018). Resolving the origins of membrane phospholipid biosynthesis genes using outgroupfree rooting. *bioRxiv*.

Comita, P. B., Gagosian, R. B., Pang, H., and Costello, C. E. (1984). Structural elucidation of a unique macrocyclic membrane lipid from a new, extremely thermophilic, deep-sea hydrothermal vent Archaebacterium, *Methanococcus jannaschii*. *J. Biol. Chem.* 259, 15234–15241. doi: 10.1016/s0021-9258(17)42540-3.

Cordes, E. E., Bergquist, D. C., and Fisher, C. R. (2009). Macro-Ecology of Gulf of Mexico Cold Seeps. *Ann. Rev. Mar. Sci.* 1, 143–168. doi: 10.1146/annurev.marine.010908.163912.

Cordes, E. E., Carney, S. L., Hourdez, S., Carney, R. S., Brooks, J. M., and Fisher, C. R. (2007). Cold seeps of the deep Gulf of Mexico: Community structure and biogeographic comparisons to Atlantic equatorial belt seep communities. *Deep Sea Res. Part I Oceanogr. Res. Pap.* 54, 637–653. doi: https://doi.org/10.1016/j.dsr.2007.01.001.

Crone, T. J., and Tolstoy, M. (2010). Magnitude of the 2010 Gulf of Mexico Oil Leak. *Science* 330, 634. doi: 10.1126/science.1195840.

Curray, J. R., Moore, D. G., Aguayo, J. E., Aubry, M. P., Einsele, G., Fornari, D. J., et al. (1982). Initial reports of the Deep Sea Drilling Project, Vol 64, Parts I and II. US Government Printing Office, Washington DC doi: 10.2973/dsdp.proc.64.1982.

D'Hondt, S., Inagaki, F., Zarikian, C. A., Abrams, L. J., Dubois, N., Engelhardt, T., et al. (2015). Presence of oxygen and aerobic communities from sea floor to basement in deep-sea sediments. *Nat. Geosci.* 8, 299–304. doi: 10.1038/ngeo2387.

D'Hondt, S., Rutherford, S., and Spivack, A. J. (2002). Metabolic Activity of Subsurface Life in Deep-Sea Sediments. *Science* 295, 2067–2070. doi: 10.1126/science.1064878.

Davidova, I. A., Marks, C. R., and Suflita, J. M. (2018). "Anaerobic Hydrocarbon-Degrading Deltaproteobacteria," in *Taxonomy, Genomics and Ecophysiology of Hydrocarbon-Degrading Microbes*, 1–38. doi: 10.1007/978-3-319-60053-6.

de Carvalho, C. C. C. R., Wick, L. Y., and Heipieper, H. J. (2009). Cell wall adaptations of planktonic and biofilm *Rhodococcus erythropolis* cells to growth on $C_5$ to $C_{16}$ *n*-alkane hydrocarbons. *Appl. Microbiol. Biotechnol.* 82, 311–320. doi: 10.1007/s00253-008-1809-3.

De la Lanza-Espino, G., and Soto, L. A. (1999). Sedimentary geochemistry of hydrothermal vents in Guaymas Basin, Gulf of California, Mexico. *Appl. Geochemistry* 14, 499–510. doi: https://doi.org/10.1016/S0883-2927(98)00064-X.

Deng, L., Ren, Y., Wei, C., and Wang, J. (2021). Biodegradation of pyrene by a novel strain of *Castellaniella* sp. under denitrifying condition. *J. Environ. Chem. Eng.* 9, 104970. doi: https://doi.org/10.1016/j.jece.2020.104970.

Deppenmeier, U., and Müller, V. (2008). "Life Close to the Thermodynamic Limit: How Methanogenic Archaea Conserve Energy," in *Bioenergetics: Energy Conservation and Conversion*, eds. G. Schäfer and H. S. Penefsky (Berlin, Heidelberg: Springer Berlin Heidelberg), 123–152. doi: 10.1007/400_2006_026.

Didyk, B. M., and Simoneit, B. R. T. (1989). Hydrothermal oil of Guaymas Basin and implications for petroleum formation mechanisms. *Nature* 342, 65–69. doi: 10.1038/342065a0.

Dombrowski, N., Donaho, J. A., Gutierrez, T., Seitz, K. W., Teske, A. P., and Baker, B. J. (2016). Reconstructing metabolic pathways of hydrocarbon-degrading bacteria from the Deepwater Horizon oil spill. *Nat. Microbiol.* 1, 16057. doi: 10.1038/nmicrobiol.2016.57.

Dombrowski, N., Teske, A. P., and Baker, B. J. (2018). Expansive microbial metabolic versatility and biodiversity in dynamic Guaymas Basin hydrothermal sediments. *Nat. Commun.* 9. doi: 10.1038/s41467-018-07418-0.

Dubilier, N., Bergin, C., and Lott, C. (2008). Symbiotic diversity in marine animals: the art of harnessing chemosynthesis. *Nat. Rev. Microbiol.* 6, 725–740. doi: 10.1038/nrmicro1992.

Dunne, J. P., Sarmiento, J. L., and Gnanadesikan, A. (2007). A synthesis of global particle export from the surface ocean and cycling through the ocean interior and on the seafloor. *Global Biogeochem. Cycles* 21. doi: 10.1029/2006GB002907.

Eberlein, C., Estelmann, S., Seifert, J., Von Bergen, M., Müller, M., Meckenstock, R. U., et al. (2013a). Identification and characterization of 2-naphthoyl-coenzyme A reductase, the prototype of a novel class of dearomatizing reductases. *Mol. Microbiol.* 88, 1032–1039. doi: 10.1111/mmi.12238.

Eberlein, C., Johannes, J., Mouttaki, H., Sadeghi, M., Golding, B. T., Boll, M., et al. (2013b). ATP-dependent/-independent enzymatic ring reductions involved in the anaerobic catabolism of naphthalene. *Environ. Microbiol.* 15, 1832–1841. doi: 10.1111/1462-2920.12076.

Edgcomb, V. P., Teske, A. P., and Mara, P. (2022). Microbial Hydrocarbon Degradation in Guaymas Basin—Exploring the Roles and Potential Interactions of Fungi and Sulfate-Reducing Bacteria. *Front. Microbiol.* 13, 1–16. doi: 10.3389/fmicb.2022.831828.

Edwards, E. A., and Grbić-Galić, D. (1992). Complete mineralization of benzene by aquifer microorganisms under strictly anaerobic conditions. *Appl. Environ. Microbiol.* 58, 2663–2666. doi: 10.1128/aem.58.8.2663-2666.1992.

Edwards, E. A., Wills, L. E., Reinhard, M., and Grbić-Galić, D. (1992). Anaerobic degradation of toluene and xylene by aquifer microorganisms under sulfate-reducing conditions. *Appl. Environ. Microbiol.* 58, 794–800. doi: 10.1128/aem.58.3.794-800.1992.

Ehrenreich, P., Behrends, A., Harder, J., and Widdel, F. (2000). Anaerobic oxidation of alkanes by newly isolated denitrifying bacteria. *Arch. Microbiol.* 173, 58–64. doi: 10.1007/s002030050008.

Einsele, G., Gieskes, J. M., Curray, J., Moore, D. M., Aguayo, E., Aubry, M. P., et al. (1980). Intrusion of basaltic sills into highly porous sediments, and resulting hydrothermal activity. *Nature* 283, 441–445. doi: 10.1038/283441a0.

Elferink, M. G. L., de Wit, J. G., Driessen, A. J. M., and Konings, W. N. (1994). Stability and proton-permeability of liposomes composed of archaeal tetraether lipids. *Biochim. Biophys. Acta - Biomembr.* 1193, 247–254. doi: https://doi.org/10.1016/0005-2736(94)90160-0.

Ellermann, J., Hedderich, R., Böcher, R., and Thauer, R. K. (1988). The final step in methane formation-investigations with highly purified methyl-CoM reductase (Component-C) from *Methanobacterium-thermoautotrophicum* (Strain Marburg). *Eur. J. Biochem.* 172, 669–677. doi: https://doi.org/10.1111/j.1432-1033.1988.tb13941.x.

Elsgaard, L., Isaksen, M. F., Jørgensen, B. B., Alayse, A. M., and Jannasch, H. W. (1994). Microbial sulfate

reduction in deep-sea sediments at the Guaymas Basin hydrothermal vent area: Influence of temperature and substrates. *Geochim. Cosmochim. Acta* 58, 3335–3343. doi: 10.1016/0016-7037(94)90089-2.

Erdoğmuş, S. F., Mutlu, B., Korcan, S. E., Güven, K., and Konuk, M. (2013). Aromatic hydrocarbon degradation by halophilic archaea isolated from Çamaltı Saltern, Turkey. *Water. Air. Soil Pollut.* 224, 1449. doi: 10.1007/s11270-013-1449-9.

Ermler, U., Grabarse, W., Shima, S., Goubeaud, M., and Thauer, R. K. (1997). Crystal structure of methyl-coenzyme M reductase: The key enzyme of biological methane formation. *Science* 278, 1457–1462. doi: 10.1126/science.278.5342.1457.

Estelmann, S., Blank, I., Feldmann, A., and Boll, M. (2015). Two distinct old yellow enzymes are involved in naphthyl ring reduction during anaerobic naphthalene degradation. *Mol. Microbiol.* 95, 162–172. doi: 10.1111/mmi.12875.

Evans, P. J., Ling, W., Goldschmidt, B., Ritter, E. R., and Young, L. Y. (1992). Metabolites formed during anaerobic transformation of toluene and o-xylene and their proposed relationship to the initial steps of toluene mineralization. *Appl. Environ. Microbiol.* 58, 496–501. doi: 10.1128/aem.58.2.496-501.1992.

Evans, P. N., Parks, D. H., Chadwick, G. L., Robbins, S. J., Orphan, V. J., Golding, S. D., et al. (2015). Methane metabolism in the archaeal phylum Bathyarchaeota revealed by genome-centric metagenomics. *Science* 350, 434–438. doi: 10.1126/science.aac7745.

Fatt, I. (1958). Pore Volume Compressibilities of Sandstone Reservoir Rocks. *J. Pet. Technol.* 10, 64–66. doi: 10.2118/970-G.

Fehler, S. W. G., and Light, R. J. (1970). Biosynthesis of hydrocarbons in *Anabaena variabilis*. Incorporation of [methyl-$^{14}$C] and [methyl-$^{2}H_2$] Methionine into 7- and 8-methyl-heptadecanes. *Biochemistry* 9, 418–422. doi: 10.1021/bi00804a032.

Felbeck, H. (1981). Chemoautotrophic potential of the hydrothermal vent tube worm, *Riftia pachyptila* Jones (Vestimentifera). *Science* 213, 336–338. doi: 10.1126/science.213.4505.336.

Fenchel, T., and Finlay, B. J. (1995). *Ecology and Evolution in Anoxic Worlds*. Oxford University Press Available at: https://books.google.de/books?id=VPi%5C_%5C_Ci2mBcC.

Fernandez, F., and Collins, M. D. (1987). Vitamin K composition of anaerobic gut bacteria. *FEMS Microbiol. Lett.* 41, 175–180. doi: 10.1111/j.1574-6968.1987.tb02191.x.

Finkel, P. L., Carrizo, D., Parro, V., and Sánchez-García, L. (2023). An Overview of Lipid Biomarkers in Terrestrial Extreme Environments with Relevance for Mars Exploration. *Astrobiology* 23, 563–604. doi: 10.1089/ast.2022.0083.

Firestone, M. K. (1982). "Biological Denitrification," in *Nitrogen in Agricultural Soils* Agronomy Monographs., 289–326. doi: https://doi.org/10.2134/agronmonogr22.c8.

Fisher, A. T., and Becker, K. (1991). Heat flow, hydrothermal circulation and basalt intrusions in the Guaymas Basin, Gulf of California. *Earth Planet. Sci. Lett.* 103, 84–99. doi: 10.1016/0012-821X(91)90152-8.

Flesher, J. W., and Myers, S. R. (1991). Methyl-substitution of benzene and toluene in preparations of human bone marrow. *Life Sci.* 48, 843–850. doi: https://doi.org/10.1016/0024-3205(91)90100-P.

Foster, J. W. (1962). Hydrocarbons as substrates for microorganisms. *Antonie Van Leeuwenhoek* 28.

Foucher, J. P., Westbrook, G. K., Boetius, A., Ceramicola, S., Dupré, S., Mascle, J., et al. (2009). Structure and Drivers of Cold Seep Ecosystems. *Oceanography* 22, 92–109.

Friedlingstein, P., Jones, M. W., O'Sullivan, M., Andrew, R. M., Hauck, J., Peters, G. P., et al. (2019). Global Carbon Budget 2019. *Earth Syst. Sci. Data* 11, 1783–1838. doi: 10.5194/essd-11-1783-2019.

Friedlingstein, P., O'Sullivan, M., Jones, M. W., Andrew, R. M., Hauck, J., Olsen, A., et al. (2020). Global Carbon Budget 2020. *Earth Syst. Sci. Data* 12, 3269–3340. doi: 10.5194/essd-12-3269-2020.

Fritsche, W., and Hofrichter, M. (2000). "Aerobic Degradation by Microorganisms," in *Biotechnology*, 144–167. doi: https://doi.org/10.1002/9783527620951.ch6.

Fuchsman, C. A., Collins, R. E., Rocap, G., and Brazelton, W. J. (2017). Effect of the environment on horizontal gene transfer between bacteria and archaea. *PeerJ* 5, e3865. doi: 10.7717/peerj.3865.

Galushko, A., Minz, D., Schink, B., and Widdel, F. (1999). Anaerobic degradation of naphthalene by a pure culture of a novel type of marine sulphate-reducing bacterium. *Environ. Microbiol.* 1, 415–420. doi: 10.1046/j.1462-

2920.1999.00051.x.

Gamo, T., Okamura, K., Hatanaka, H., Hasumoto, H., Komatsu, D., Chinen, M., et al. (2015). Hydrothermal plumes in the Gulf of Aden, as characterized by light transmission, Mn, Fe, $CH_4$ and $\delta^{13}C$–$CH_4$ anomalies. *Deep Sea Res. Part II Top. Stud. Oceanogr.* 121, 62–70. doi: https://doi.org/10.1016/j.dsr2.2015.06.004.

Gao, P., Tian, H., Li, G., Sun, H., and Ma, T. (2015). Microbial diversity and abundance in the Xinjiang Luliang long-term water-flooding petroleum reservoir. *Microbiologyopen* 4, 332–342. doi: https://doi.org/10.1002/mbo3.241.

Garcia, P. S., Gribaldo, S., and Borrel, G. (2022). Diversity and Evolution of Methane-Related Pathways in Archaea. *Annu. Rev. Microbiol.* 76, 727–755.

Gehman, H. M. J. (1962). Organic matter in limestones. *Geochim. Cosmochim. Acta* 26, 885–897. doi: https://doi.org/10.1016/0016-7037(62)90118-7.

Geilert, S., Hensen, C., Schmidt, M., Liebetrau, V., Scholz, F., Doll, M., et al. (2018). On the formation of hydrothermal vents and cold seeps in the Guaymas Basin, Gulf of California. *Biogeosciences* 15, 5715–5731. doi: 10.5194/bg-15-5715-2018.

Ghosal, D., Ghosh, S., Dutta, T. K., and Ahn, Y. (2016). Current state of knowledge in microbial degradation of polycyclic aromatic hydrocarbons (PAHs): A review. *Front. Microbiol.* 7. doi: 10.3389/fmicb.2016.01369.

Gieg, L. M., and Suflita, J. M. (2002). Detection of anaerobic metabolites of saturated and aromatic hydrocarbons in petroleum-contaminated aquifers. *Environ. Sci. Technol.* 36, 3755–3762. doi: 10.1021/es0205333.

Gill, C. O., and Ratledge, C. (1972a). Effect of *n*-alkanes on the transport of glucose in *Candida* sp. strain 107. *Biochem. J.* 127, 59P-60P. doi: 10.1042/bj1270059Pb.

Gill, C. O., and Ratledge, C. (1972b). Toxicity of *n*-Alkanes, *n*-Alk-1-enes, *n*-Alkan-1-ols and *n*-Alkyl-1-bromides towards Yeasts. *Microbiology* 72, 165–172. doi: https://doi.org/10.1099/00221287-72-1-165.

Gittel, A., Donhauser, J., Røy, H., Girguis, P. R., Jørgensen, B. B., and Kjeldsen, K. U. (2015). Ubiquitous Presence and Novel Diversity of Anaerobic Alkane Degraders in Cold Marine Sediments. *Front. Microbiol.* 6. doi: 10.3389/fmicb.2015.01414.

Glud, R. N. (2008). Oxygen dynamics of marine sediments. *Mar. Biol. Res.* 4, 243–289. doi: 10.1080/17451000801888726.

Goldfine, H. (1982). "Lipids of Prokaryotes–Structure and Distribution," in *Membrane Lipids of Prokaryotes*, eds. F. Bronner and A. B. T.-C. T. in M. and T. Kleinteller (Academic Press), 1–43. doi: https://doi.org/10.1016/S0070-2161(08)60307-X.

Golyshin, P. N., Chernikova, T. N., Abraham, W.-R., Lünsdorf, H., Timmis, K. N., and Yakimov, M. M. (2002). *Oleiphilaceae* fam. nov., to include *Oleiphilus messinensis* gen. nov., sp. nov., a novel marine bacterium that obligately utilizes hydrocarbons. *Int. J. Syst. Evol. Microbiol.* 52, 901–911. doi: https://doi.org/10.1099/00207713-52-3-901.

Grady, M. M. (2020). Exploring Mars with Returned Samples. *Space Sci. Rev.* 216, 51. doi: 10.1007/s11214-020-00676-9.

Grant, C., Deszcz, D., Wei, Y.-C., Martínez-Torres, R. J., Morris, P., Folliard, T., et al. (2014). Identification and use of an alkane transporter plug-in for applications in biocatalysis and whole-cell biosensing of alkanes. *Sci. Rep.* 4, 5844. doi: 10.1038/srep05844.

Gray, N. D., Sherry, A., Hubert, C., Dolfing, J., and Head, I. M. (2010). "Methanogenic Degradation of Petroleum Hydrocarbons in Subsurface Environments: Remediation, Heavy Oil Formation, and Energy Recovery," in *Advances in Applied Microbiology*, eds. A. I. Laskin, S. Sariaslani, and G. M. B. T.-A. in A. M. Gadd (Academic Press), 137–161. doi: https://doi.org/10.1016/S0065-2164(10)72005-0.

Green-Saxena, A., Dekas, A. E., Dalleska, N. F., and Orphan, V. J. (2014). Nitrate-based niche differentiation by distinct sulfate-reducing bacteria involved in the anaerobic oxidation of methane. *ISME J.* 8, 150–163. doi: 10.1038/ismej.2013.147.

Grunau, H. R. (1987). A Worldwide Look At the Cap-Rock Problem. *J. Pet. Geol.* 10, 245–265. doi: 10.1111/j.1747-5457.1987.tb00945.x.

Grundmann, O., Behrends, A., Rabus, R., Amann, J., Halder, T., Heider, J., et al. (2008). Genes encoding the candidate enzyme for anaerobic activation of *n*-alkanes in the denitrifying bacterium, strain HxN1. *Environ. Microbiol.* 10, 376–385. doi: https://doi.org/10.1111/j.1462-2920.2007.01458.x.

Gu, Y., Guberman-pfeffer, M. J., Srikanth, V., Shen, C., Giska, F., Gupta, K., et al. (2023). Structure of *Geobacter* cytochrome OmcZ identifies mechanism of nanowire assembly and conductivity. *Nat. Microbiol.* 8, 284–298. doi: 10.1038/s41564-022-01315-5.

Gundersen, J. K., Jørgensen, B. B., Larsen, E., and Jannasch, H. W. (1992). Mats of giant sulphur bacteria on deep-sea sediments due to fluctuating hydrothermal flow. *Nature* 360, 454–456.

Gunsalus, R. P., and Wolfe, R. S. (1980). Methyl coenzyme M reductase from *Methanobacterium thermoautotrophicum*. Resolution and properties of the components. *J. Biol. Chem.* 255, 1891–1895. doi: 10.1016/s0021-9258(19)85966-5.

Guo, X., Hu, D., Li, Y., Duan, J., Zhang, X., Fan, X., et al. (2019). Theoretical Progress and Key Technologies of Onshore Ultra-Deep Oil/Gas Exploration. *Engineering* 5, 458–470. doi: https://doi.org/10.1016/j.eng.2019.01.012.

Hahn, C. J., Laso-Pérez, R., Vulcano, F., Vaziourakis, K.-M., Stokke, R., Steen, I. H., et al. (2020). *Candidatus* Ethanoperedens, a Thermophilic Genus of Archaea Mediating the Anaerobic Oxidation of Ethane. *MBio* 11, e00600-20. doi: 10.1128/mBio.00600-20.

Hahn, C. J., Lemaire, O. N., Engilberge, S., Wegener, G., and Wagner, T. (2021). Crystal structure of a key enzyme for anaerobic ethane activation. *Science* 373, 118–121.

Halbouty, M. T., Meyerhoff, A. A., King, R. E., Dott Sr., R. H., Klemme, H. D., and Shabad, T. (1970). "Part I: Giant oil and gas fields," in *Geology of Giant Petroleum Fields*, ed. M. T. Halbouty (American Association of Petroleum Geologists), 0. doi: 10.1306/M14368C27.

Hallam, S. J., Girguis, P. R., Preston, C. M., Richardson, P. M., and DeLong, E. F. (2003). Identification of Methyl Coenzyme M Reductase A (*mcrA*) Genes Associated with Methane-Oxidizing Archaea. *Appl. Environ. Microbiol.* 69, 5483–5491. doi: 10.1128/AEM.69.9.5483-5491.2003.

Hallam, S. J., Putnam, N., Preston, C. M., Detter, J. C., Rokhsar, D., Richardson, P. H., et al. (2004). Reverse methanogenesis: Testing the hypothesis with environmental genomics. *Science* 305, 1457–1462. doi: 10.1126/science.1100025.

Hamilton-Brehm, S. D., Gibson, R. A., Green, S. J., Hopmans, E. C., Schouten, S., van der Meer, M. T. J., et al. (2013). *Thermodesulfobacterium geofontis* sp. nov., a hyperthermophilic, sulfate-reducing bacterium isolated from Obsidian Pool, Yellowstone National Park. *Extremophiles* 17, 251–263. doi: 10.1007/s00792-013-0512-1.

Haroon, M. F., Hu, S., Shi, Y., Imelfort, M., Keller, J., Hugenholtz, P., et al. (2013). Anaerobic oxidation of methane coupled to nitrate reduction in a novel archaeal lineage. *Nature* 500, 567–570. doi: 10.1038/nature12375.

Hawley, E. R., Malfatti, S. A., Pagani, I., Huntemann, M., Chen, A., Foster, B., et al. (2014a). Metagenomes from two microbial consortia associated with Santa Barbara seep oil. *Mar. Genomics* 18, 97–99. doi: https://doi.org/10.1016/j.margen.2014.06.003.

Hawley, E. R., Piao, H., Scott, N. M., Malfatti, S., Pagani, I., Huntemann, M., et al. (2014b). Metagenomic analysis of microbial consortium from natural crude oil that seeps into the marine ecosystem offshore Southern California. *Stand. Genomic Sci.* 9, 1259–1274. doi: 10.4056/sigs.5029016.

Head, I. M., Jones, D. M., and Larter, S. R. (2003). Biological activity in the deep subsurface and the origin of heavy oil. *Nature* 426, 344–352. doi: 10.1038/nature02134.

Head, I. M., Jones, D. M., and Röling, W. F. M. (2006). Marine microorganisms make a meal of oil. *Nat. Rev. Microbiol.* 4, 173–182. doi: 10.1038/nrmicro1348.

Heider, J. (2007). Adding handles to unhandy substrates: anaerobic hydrocarbon activation mechanisms. *Curr. Opin. Chem. Biol.* 11, 188–194. doi: 10.1016/j.cbpa.2007.02.027.

Heider, J., Spormann, A. M., Beller, H. R., and Widdel, F. (1998). Anaerobic bacterial metabolism of hydrocarbons. *FEMS Microbiol. Rev.* 22, 459–473. doi: 10.1016/S0168-6445(98)00025-4.

Heider, J., Szaleniec, M., Martins, B. M., Seyhan, D., Buckel, W., and Golding, B. T. (2016). Structure and Function of Benzylsuccinate Synthase and Related Fumarate-Adding Glycyl Radical Enzymes. *J. Mol. Microbiol. Biotechnol.* 26, 29–44. doi: 10.1159/000441656.

Heker, I., Haberhauer, G., and Meckenstock, R. U. (2023). Naphthalene Carboxylation in the Sulfate-Reducing Enrichment Culture N47 Is Proposed to Proceed via 1,3-Dipolar Cycloaddition to the Cofactor Prenylated Flavin Mononucleotide. *Appl. Environ. Microbiol.* 89, e01927-22. doi: 10.1128/aem.01927-22.

Henderson, P. J. F. (1971). Ion transport by energy-conserving biological membranes. *Annu. Rev. Microbiol.* 25, 393–428.

Himmelberg, A. M., Brüls, T., Farmani, Z., Weyrauch, P., Barthel, G., Schrader, W., et al. (2018). Anaerobic degradation of phenanthrene by a sulfate-reducing enrichment culture. *Environ. Microbiol.* 20, 3589–3600. doi: 10.1111/1462-2920.14335.

Hinrichs, K.-U., Hayes, J. M., Sylva, S. P., Brewer, P. G., and DeLong, E. F. (1999). Methane-consuming archaebacteria in marine sediments. *Nature* 398, 802–805. doi: 10.1038/19751.

Holler, T., Wegener, G., Niemann, H., Deusner, C., Ferdelman, T. G., Boetius, A., et al. (2011a). Carbon and sulfur back flux during anaerobic microbial oxidation of methane and coupled sulfate reduction. *Proc. Natl. Acad. Sci.* 108, E1484–E1490. doi: 10.1073/pnas.1106032108.

Holler, T., Widdel, F., Knittel, K., Amann, R., Kellermann, M. Y., Hinrichs, K. U., et al. (2011b). Thermophilic anaerobic oxidation of methane by marine microbial consortia. *ISME J.* 5, 1946–1956. doi: 10.1038/ismej.2011.77.

Holmes, D. E., Risso, C., Smith, J. A., and Lovley, D. R. (2011). Anaerobic oxidation of benzene by the hyperthermophilic archaeon *Ferroglobus placidus*. *Appl. Environ. Microbiol.* 77, 5926–5933. doi: 10.1128/AEM.05452-11.

Holze, H., Schrader, L., and Buellesbach, J. (2021). Advances in deciphering the genetic basis of insect cuticular hydrocarbon biosynthesis and variation. *Heredity (Edinb).* 126, 219–234. doi: 10.1038/s41437-020-00380-y.

Horsfield, B., Schulz, H.-M., Bernard, S., Mahlstedt, N., Han, Y., and Kuske, S. (2018). "Oil and Gas Shales," in *Hydrocarbons, Oils and Lipids: Diversity, Origin, Chemistry and Fate*, ed. H. Wilkes (Cham: Springer International Publishing), 1–34. doi: 10.1007/978-3-319-54529-5_18-1.

Hua, Z.-S., Wang, Y.-L., Evans, P. N., Qu, Y.-N., Goh, K. M., Rao, Y.-Z., et al. (2019). Insights into the ecological roles and evolution of methyl-coenzyme M reductase-containing hot spring Archaea. *Nat. Commun.* 10, 1–11. doi: 10.1038/s41467-019-12574-y.

Hubbert, M. K. (1966). History of Petroleum Geology and Its Bearing Upon Present and Future Exploration. *Am. Assoc. Pet. Geol. Bull.* 50, 2504–2518. doi: 10.1306/5D25B779-16C1-11D7-8645000102C1865D.

Hunt, J. M. (1975). Origin of gasoline range alkanes in the deep sea. *Nature* 254, 411–413. doi: 10.1038/254411a0.

Hunt, J. M. (1979). *Petroleum geochemistry and geology*. W.H. Freeman and Company, San Francisco.

Huwiler, S. G., Löffler, C., Anselmann, S. E. L., Stärk, H. J., Von Bergen, M., Flechsler, J., et al. (2019). One-megadalton metalloenzyme complex in *Geobacter metallireducens* involved in benzene ring reduction beyond the biological redox window. *Proc. Natl. Acad. Sci. U. S. A.* 116, 2259–2264. doi: 10.1073/pnas.1819636116.

Ishii, S., Kosaka, T., Hori, K., Hotta, Y., and Watanabe, K. (2005). Coaggregation facilitates interspecies hydrogen transfer between *Pelotomaculum thermopropionicum* and *Methanothermobacter thermautotrophicus*. *Appl. Environ. Microbiol.* 71, 7838–7845. doi: 10.1128/AEM.71.12.7838-7845.2005.

Israelachvili, J. N. (1974). The Nature of van der Waals Forces. *Contemp. Phys.* 15, 159–178. doi: 10.1080/00107517408210785.

Iversen, N., and Jørgensen, B. B. (1985). Anaerobic methane oxidation rates at the sulfate-methane transition in marine sediments from Kattegat and Skagerrak (Denmark)1. *Limnol. Oceanogr.* 30, 944–955. doi: https://doi.org/10.4319/lo.1985.30.5.0944.

Jackson, P. M., and Smith, L. K. (2014). Exploring the undulating plateau: the future of global oil supply. *Philos. Trans. R. Soc. A Math. Phys. Eng. Sci.* 372, 20120491. doi: 10.1098/rsta.2012.0491.

Jain, S., Caforio, A., and Driessen, A. J. M. (2014). Biosynthesis of archaeal membrane ether lipids. *Front. Microbiol.* 5, 1–16. doi: 10.3389/fmicb.2014.00641.

Jannasch, H. W., Nelson, D. C., and Wirsen, C. O. (1989). Massive natural occurrence of unusually large bacteria (*Beggiatoa* sp.) at a hydrothermal deep-sea vent site. *Nature* 342, 834–836. doi: 10.1038/342834a0.

Jeanthon, C., L'Haridon, S., Cueff, V., Banta, A., Reysenbach, A.-L., and Prieur, D. (2002). *Thermodesulfobacterium hydrogeniphilum* sp. nov., a thermophilic , chemolithoautotrophic, sulfate-reducing bacterium isolated from a deep-sea hydrothermal vent at Guaymas Basin, and emendation of the genus *Thermodesulfobacterium*. *Int. J. Syst. Evol. Microbiol.*, 765–772. doi: 10.1099/ijs.0.02025-0.The.

Jones, D. M., Head, I. M., Gray, N. D., Adams, J. J., Rowan, A. K., Aitken, C. M., et al. (2008). Crude-oil

biodegradation via methanogenesis in subsurface petroleum reservoirs. *Nature* 451, 176–180. doi: 10.1038/nature06484.

Joos, F., and Spahni, R. (2008). Rates of change in natural and anthropogenic radiative forcing over the past 20,000 years. *Proc. Natl. Acad. Sci.* 105, 1425–1430. doi: 10.1073/pnas.0707386105.

Jørgensen, B. B., and Boetius, A. (2007). Feast and famine - Microbial life in the deep-sea bed. *Nat. Rev. Microbiol.* 5, 770–781. doi: 10.1038/nrmicro1745.

Jørgensen, B. B., Wenzhöfer, F., Egger, M., and Glud, R. N. (2022). Sediment oxygen consumption: Role in the global marine carbon cycle. *Earth-Science Rev.* 228. doi: 10.1016/j.earscirev.2022.103987.

Joye, S. B., MacDonald, I. R., Leifer, I., and Asper, V. (2011). Magnitude and oxidation potential of hydrocarbon gases released from the BP oil well blowout. *Nat. Geosci.* 4, 160–164. doi: 10.1038/ngeo1067.

Kantzas, A., Chatzis, I., and Dullien, F. A. L. (1988). Enhanced Oil Recovery by Inert Gas Injection. *SPE Enhanc. Oil Recover. Symp.*, SPE-17379-MS. doi: 10.2118/17379-MS.

Karl, D. M., Taylor, G. T., Novitsky, J. A., Jannasch, H. W., Wirsen, C. O., Pace, N. R., et al. (1988). A microbiological study of Guaymas Basin high temperature hydrothermal vents. *Deep Sea Res. Part A. Oceanogr. Res. Pap.* 35, 777–791. doi: https://doi.org/10.1016/0198-0149(88)90030-1.

Khelifi, N., Amin Ali, O., Roche, P., Grossi, V., Brochier-Armanet, C., Valette, O., et al. (2014). Anaerobic oxidation of long-chain n-alkanes by the hyperthermophilic sulfate-reducing archaeon, *Archaeoglobus fulgidus*. *ISME J.* 8, 2153–2166. doi: 10.1038/ismej.2014.58.

Kim, I. S., Foght, J. M., and Gray, M. R. (2002). Selective transport and accumulation of alkanes by *Rhodococcus erythropolis* S+14He. *Biotechnol. Bioeng.* 80, 650–659. doi: 10.1002/bit.10421.

Kimes, N. E., Callaghan, A. V., Suflita, J. M., and Morris, P. J. (2014). Microbial transformation of the Deepwater Horizon oil spill - past, present, and future perspectives. *Front. Microbiol.* 5, 1–11. doi: 10.3389/fmicb.2014.00603.

Kinsara, R. A., and Demirbas, A. (2016). Upgrading of crude oil via distillation processes. *Pet. Sci. Technol.* 34, 1300–1306. doi: 10.1080/10916466.2016.1200080.

Kleindienst, S., and Joye, S. B. (2019). "Global Aerobic Degradation of Hydrocarbons in Aquatic Systems," in *Aerobic Utilization of Hydrocarbons, Oils, and Lipids.. Handbook of Hydrocarbon and Lipid Microbiology*, ed. F. Rojo (Cham: Springer, Cham.), 797–814. doi: 10.1007/978-3-319-50418-6_46.

Klug, M. J., and Markovetz, A. J. (1971). "Utilization of Aliphatic Hydrocarbons by Micro-organisms," in *Advances in Microbial Physiology*, eds. A. H. Rose and J. F. B. T.-A. in M. P. Wilkinson (Academic Press), 1–43. doi: https://doi.org/10.1016/S0065-2911(08)60404-X.

Kniemeyer, O., Musat, F., Sievert, S. M., Knittel, K., Wilkes, H., Blumenberg, M., et al. (2007). Anaerobic oxidation of short-chain hydrocarbons by marine sulphate-reducing bacteria. *Nature* 449, 898–901. doi: 10.1038/nature06200.

Knittel, K., and Boetius, A. (2009). Anaerobic Oxidation of Methane: Progress with an Unknown Process. *Annu. Rev. Microbiol.* 63, 311–334. doi: 10.1146/annurev.micro.61.080706.093130.

Knittel, K., Lösekann, T., Boetius, A., Kort, R., and Amann, R. (2005). Diversity and Distribution of Methanotrophic Archaea at Cold Seeps. *Appl. Environ. Microbiol.* 71, 467–479. doi: 10.1128/AEM.71.1.467-479.2005.

Koelschbach, J. S., Mouttaki, H., Merl-Pham, J., Arnold, M. E., and Meckenstock, R. U. (2019). Identification of naphthalene carboxylase subunits of the sulfate-reducing culture N47. *Biodegradation* 30, 147–160. doi: 10.1007/s10532-019-09872-z.

Koga, Y., Kyuragi, T., Nishihara, M., and Sone, N. (1998). Did archaeal and bacterial cells arise independently from noncellular precursors? A hypothesis stating that the advent of membrane phospholipid with enantiomeric glycerophosphate backbones caused the separation of the two lines of descent. *J. Mol. Evol.* 46, 54–63. doi: 10.1007/PL00006283.

Koga, Y., and Morii, H. (2007). Biosynthesis of Ether-Type Polar Lipids in Archaea and Evolutionary Considerations. *Microbiol. Mol. Biol. Rev.* 71, 97–120. doi: 10.1128/mmbr.00033-06.

Kohler, P., and Metcalf, W. (2012). Genetic manipulation of *Methanosarcina* spp. *Front. Microbiol.* 3. doi: 10.3389/fmicb.2012.00259.

Kondaveeti, S., Mohanakrishna, G., Lee, J. K., and Kalia, V. C. (2019). Methane as a Substrate for Energy

Generation Using Microbial Fuel Cells. *Indian J. Microbiol.* 59, 121–124. doi: 10.1007/s12088-018-0765-6.

Kraiselburd, I., Brüls, T., Heilmann, G., Kaschani, F., Kaiser, M., and Meckenstock, R. U. (2019). Metabolic reconstruction of the genome of candidate *Desulfatiglans* TRIP_1 and identification of key candidate enzymes for anaerobic phenanthrene degradation. *Environ. Microbiol.* 21, 1267–1286. doi: 10.1111/1462-2920.14527.

Kropp, K. G., Davidova, I. A., and Suflita, J. M. (2000). Anaerobic Oxidation of *n*-Dodecane by an Addition Reaction in a Sulfate-Reducing Bacterial Enrichment Culture. *Appl. Environ. Microbiol.* 66, 5393–5398. doi: 10.1128/AEM.66.12.5393-5398.2000.

Krukenberg, V., Harding, K., Richter, M., Glöckner, F. O., Gruber-Vodicka, H. R., Adam, B., et al. (2016). *Candidatus* Desulfofervidus auxilii, a hydrogenotrophic sulfate-reducing bacterium involved in the thermophilic anaerobic oxidation of methane. *Environ. Microbiol.* 18, 3073–3091. doi: 10.1111/1462-2920.13283.

Krukenberg, V., Riedel, D., Gruber-Vodicka, H. R., Buttigieg, P. L., Tegetmeyer, H. E., Boetius, A., et al. (2018). Gene expression and ultrastructure of meso- and thermophilic methanotrophic consortia. *Environ. Microbiol.* 20, 1651–1666. doi: 10.1111/1462-2920.14077.

Krumholz, L. R., Bradstock, P., Sheik, C. S., Diao, Y., Gazioglu, O., Gorby, Y., et al. (2015). Syntrophic growth of *Desulfovibrio alaskensis* requires genes for $H_2$ and formate metabolism as well as those for flagellum and biofilm formation. *Appl. Environ. Microbiol.* 81, 2339–2348. doi: 10.1128/AEM.03358-14.

Kube, M., Heider, J., Amann, J., Hufnagel, P., Kühner, S., Beck, A., et al. (2004). Genes involved in the anaerobic degradation of toluene in a denitrifying bacterium, strain EbN1. *Arch. Microbiol.* 181, 182–194. doi: 10.1007/s00203-003-0627-3.

Kümmel, S., Herbst, F. A., Bahr, A., Duarte, M., Pieper, D. H., Jehmlich, N., et al. (2015). Anaerobic naphthalene degradation by sulfate-reducing *Desulfobacteraceae* from various anoxic aquifers. *FEMS Microbiol. Ecol.* 91, 1–13. doi: 10.1093/femsec/fiv006.

Kuypers, M. M. M., Blokker, P., Erbacher, J., Kinkel, H., Pancost, R. D., Schouten, S., et al. (2001). Massive expansion of marine archaea during a mid-Cretaceous oceanic anoxic event. *Science* 293, 92–94. doi: 10.1126/science.1058424.

Kvenvolden, K. A., and Cooper, C. K. (2003). Natural seepage of crude oil into the marine environment. *Geo-Marine Lett.* 23, 140–146. doi: 10.1007/s00367-003-0135-0.

Kvenvolden, K. A., Rapp, J. B., Hostettler, F. D., David King, J., and Claypool, G. E. (1988). Organic geothermometry of petroleum from Escanaba Trough, offshore northern California. *Org. Geochem.* 13, 351–355. doi: https://doi.org/10.1016/0146-6380(88)90055-1.

L'Haridon, S., Reysenbacht, A.-L., Glénat, P., Prieur, D., and Jeanthon, C. (1995). Hot subterranean biosphere in a continental oil reservoir. *Nature* 377, 223–224. doi: 10.1038/377223a0.

Lamendella, R., Strutt, S., Borglin, S., Chakraborty, R., Tas, N., Mason, O., et al. (2014). Assessment of the Deepwater Horizon oil spill impact on Gulf coast microbial communities. *Front. Microbiol.* 5. doi: 10.3389/fmicb.2014.00130.

Lamparter, L., and Galic, M. (2020). Cellular Membranes, a Versatile Adaptive Composite Material. *Front. Cell Dev. Biol.* 8. doi: 10.3389/fcell.2020.00684.

Laso-Pérez, R. (2018). A novel mechanism for the anaerobic degradation of non-methane hydrocarbons in archaea. http://nbn-resolving.de/urn:nbn:de:gbv:46-00107156-15.

Laso-Pérez, R., Hahn, C., van Vliet, D. M., Tegetmeyer, H. E., Schubotz, F., Smit, N. T., et al. (2019). Anaerobic Degradation of Non-Methane Alkanes by "*Candidatus* Methanoliparia" in Hydrocarbon Seeps of the Gulf of Mexico. *MBio* 10, e01814-19. doi: 10.1128/mBio.01814-19.

Laso-Pérez, R., Wegener, G., Knittel, K., Widdel, F., Harding, K. J., Krukenberg, V., et al. (2016). Thermophilic archaea activate butane via alkyl-coenzyme M formation. *Nature* 539, 396–401. doi: 10.1038/nature20152.

Lawver, L. A., Williams, D. L., and Von Herzen, R. P. (1975). A major geothermal anomaly in the Gulf of California. *Nature* 257, 23–28. doi: 10.1038/257023a0.

Le Bris, N., Arnaud-Haond, S., Beaulieu, S., Cordes, E., Hilario, A., Rogers, A., et al. (2016). Hydrothermal Vents and Cold Seeps.

Lelieveld, J., Crutzen, P. J., and Dentener, F. J. (1998). Changing concentration, lifetime and climate forcing of atmospheric methane. *Tellus B* 50, 128–150. doi: https://doi.org/10.1034/j.1600-0889.1998.t01-1-00002.x.

Lemaire, O. N., and Wagner, T. (2022). A Structural View of Alkyl-Coenzyme M Reductases, the First Step of Alkane Anaerobic Oxidation Catalyzed by Archaea. *Biochemistry* 61, 805–821. doi: 10.1021/acs.biochem.2c00135.

Li, G. (2011). *World atlas of oil and gas basins*. Wiley-Blackwell.

Li, W., Wang, L.-Y., Duan, R.-Y., Liu, J.-F., Gu, J.-D., and Mu, B.-Z. (2012). Microbial community characteristics of petroleum reservoir production water amended with n-alkanes and incubated under nitrate-, sulfate-reducing and methanogenic conditions. *Int. Biodeterior. Biodegradation* 69, 87–96. doi: https://doi.org/10.1016/j.ibiod.2012.01.005.

Li, X.-X., Mbadinga, S. M., Liu, J.-F., Zhou, L., Yang, S.-Z., Gu, J.-D., et al. (2017). Microbiota and their affiliation with physiochemical characteristics of different subsurface petroleum reservoirs. *Int. Biodeterior. Biodegradation* 120, 170–185. doi: https://doi.org/10.1016/j.ibiod.2017.02.005.

Lin, J., Hao, B., Cao, G., Wang, J., Feng, Y., Tan, X., et al. (2014). A study on the microbial community structure in oil reservoirs developed by water flooding. *J. Pet. Sci. Eng.* 122, 354–359. doi: https://doi.org/10.1016/j.petrol.2014.07.030.

Link, W. K. (1952). Significance of Oil and Gas Seeps in World Oil Exploration. *Am. Assoc. Pet. Geol. Bull.* 36, 1505–1540. doi: 10.1306/5CEADB3F-16BB-11D7-8645000102C1865D.

Liu, C., and Shao, Z. (2005). *Alcanivorax dieselolei* sp. nov., a novel alkane-degrading bacterium isolated from sea water and deep-sea sediment. *Int. J. Syst. Evol. Microbiol.* 55, 1181–1186. doi: https://doi.org/10.1099/ijs.0.63443-0.

Liu, J.-F., Mbadinga, S. M., Sun, X.-B., Yang, G.-C., Yang, S.-Z., Gu, J.-D., et al. (2016). Microbial communities responsible for fixation of $CO_2$ revealed by using *mcrA*, *cbbM*, *cbbL*, *fthfs*, *fefe-hydrogenase* genes as molecular biomarkers in petroleum reservoirs of different temperatures. *Int. Biodeterior. Biodegradation* 114, 164–175. doi: https://doi.org/10.1016/j.ibiod.2016.06.019.

Liu, X., Holmes, D. E., Walker, D. J. F., Li, Y., Meier, D., Pinches, S., et al. (2022). Cytochrome OmcS Is Not Essential for Extracellular Electron Transport via Conductive Pili in *Geobacter sulfurreducens* Strain KN400. *Appl. Environ. Microbiol.* 88, e01622-21. doi: 10.1128/AEM.01622-21.

Liu, X. L., Summons, R. E., and Hinrichs, K. U. (2012). Extending the known range of glycerol ether lipids in the environment: Structural assignments based on tandem mass spectral fragmentation patterns. *Rapid Commun. Mass Spectrom.* 26, 2295–2302. doi: 10.1002/rcm.6355.

Liu, Y.-Q., Liu, Y., and Tay, J.-H. (2004). The effects of extracellular polymeric substances on the formation and stability of biogranules. *Appl. Microbiol. Biotechnol.* 65, 143–148. doi: 10.1007/s00253-004-1657-8.

Lloyd, C. T., Iwig, D. F., Wang, B., Cossu, M., Metcalf, W. W., Boal, A. K., et al. (2022). Discovery, structure and mechanism of a tetraether lipid synthase. *Nature* 609, 197–203. doi: 10.1038/s41586-022-05120-2.

Lombard, J., López-García, P., and Moreira, D. (2012). The early evolution of lipid membranes and the three domains of life. *Nat. Rev. Microbiol.* 10, 507–515. doi: 10.1038/nrmicro2815.

Lonsdale, P. (1985). Transform Continental Margin Rich in Hydrocarbons, Gulf of California. *Am. Assoc. Pet. Geol. Bull.* 69, 1160–1180. doi: 10.1306/ad462ba0-16f7-11d7-8645000102c1865d.

Lonsdale, P., and Becker, K. (1985). Hydrothermal plumes, hot springs, and conductive heat flow in the Southern Trough of Guaymas Basin. *Earth Planet. Sci. Lett.* 73, 211–225. doi: 10.1016/0012-821X(85)90070-6.

Lonsdale, P., and Lawver, L. A. (1980). Immature plate boundary zones studied with a submersible in the Gulf of California. *GSA Bull.* 91, 555–569. doi: 10.1130/0016-7606(1980)91<555:IPBZSW>2.0.CO;2.

López Barragán, M. J., Carmona, M., Zamarro, M. T., Thiele, B., Boll, M., Fuchs, G., et al. (2004). The *bzd* Gene Cluster, Coding for Anaerobic Benzoate Catabolism, in *Azoarcus* sp. Strain CIB. *J. Bacteriol.* 186, 5762–5774. doi: 10.1128/JB.186.17.5762-5774.2004.

Lorenzen, W., Ahrendt, T., Bozhüyük, K. A. J., and Bode, H. B. (2014). A multifunctional enzyme is involved in bacterial ether lipid biosynthesis. *Nat. Chem. Biol.* 10, 425–427. doi: 10.1038/nchembio.1526.

Lösekann, T., Knittel, K., Nadalig, T., Fuchs, B., Niemann, H., Boetius, A., et al. (2007). Diversity and Abundance of Aerobic and Anaerobic Methane Oxidizers at the Haakon Mosby Mud Volcano, Barents Sea. *Appl. Environ. Microbiol.* 73, 3348–3362. doi: 10.1128/AEM.00016-07.

Luo, F., Gitiafroz, R., Devine, C. E., Gong, Y., Hug, L. A., Raskin, L., et al. (2014). Metatranscriptome of an anaerobic benzene-degrading, nitrate-reducing enrichment culture reveals involvement of carboxylation in

benzene ring activation. *Appl. Environ. Microbiol.* 80, 4095–4107. doi: 10.1128/AEM.00717-14.

Maeng, J. H., Sakai, Y., Tani, Y., and Kato, N. (1996). Isolation and characterization of a novel oxygenase that catalyzes the first step of *n*-alkane oxidation in *Acinetobacter* sp. strain M-1. *J. Bacteriol.* 178, 3695–3700. doi: 10.1128/jb.178.13.3695-3700.1996.

Magot, M. (2014). Indigenous Microbial Communities in Oil Fields. *Pet. Microbiol.*, 21–33. doi: 10.1128/9781555817589.ch2.

Magot, M., Ollivier, B., and Patel, B. K. C. (2000). Microbiology of petroleum reservoirs. *Antonie Van Leeuwenhoek* 77, 103–116. doi: 10.1023/A:1002434330514.

Malik, S., Kishore, S., Dhasmana, A., Kumari, P., Mitra, T., Chaudhary, V., et al. (2023). A Perspective Review on Microbial Fuel Cells in Treatment and Product Recovery from Wastewater. *Water* 15. doi: 10.3390/w15020316.

Mardanov, A. V., Ravin, N. V., Svetlitchnyi, V. A., Beletsky, A. V., Miroshnichenko, M. L., Bonch-Osmolovskaya, E. A., et al. (2009). Metabolic Versatility and Indigenous Origin of the Archaeon *Thermococcus sibiricus*, Isolated from a Siberian Oil Reservoir, as Revealed by Genome Analysis. *Appl. Environ. Microbiol.* 75, 4580–4588. doi: 10.1128/AEM.00718-09.

Marietou, A. (2021). "Sulfate reducing microorganisms in high temperature oil reservoirs," in *Advances in Applied Microbiology*, eds. G. M. Gadd and S. Sariaslani (Elsevier Inc.), 99–131. doi: 10.1016/bs.aambs.2021.03.004.

Marshall, S. A., Payne, K. A. P., and Leys, D. (2017). The UbiX-UbiD system: The biosynthesis and use of prenylated flavin (prFMN). *Arch. Biochem. Biophys.* 632, 209–221. doi: https://doi.org/10.1016/j.abb.2017.07.014.

Martin, W. F., and Sousa, F. L. (2016). Early microbial evolution: The age of anaerobes. *Cold Spring Harb. Perspect. Biol.* 8, 1–18. doi: 10.1101/cshperspect.a018127.

Mbadinga, S. M., Li, K.-P., Zhou, L., Wang, L.-Y., Yang, S.-Z., Liu, J.-F., et al. (2012). Analysis of alkane-dependent methanogenic community derived from production water of a high-temperature petroleum reservoir. *Appl. Microbiol. Biotechnol.* 96, 531–542. doi: 10.1007/s00253-011-3828-8.

Mbadinga, S. M., Wang, L. Y., Zhou, L., Liu, J. F., Gu, J. D., and Mu, B. Z. (2011). Microbial communities involved in anaerobic degradation of alkanes. *Int. Biodeterior. Biodegrad.* 65, 1–13. doi: 10.1016/j.ibiod.2010.11.009.

McCarthy, K., Rojas, K., Niemann, M., Palrnowski, D., Peters, K., and Stankiewicz, A. (2011). Basic petroleum geochemistry for source rock evaluation. *Oilf. Rev.* 23, 32–43.

McCune, C. C. (1982). Seawater Injection Experience An Overview. *J. Pet. Technol.* 34, 2265–2270. doi: 10.2118/9630-PA.

McIntosh, T. J., Simon, S. A., and MacDonald, R. C. (1980). The organization of *n*-alkanes in lipid bilayers. *Biochim. Biophys. Acta - Biomembr.* 597, 445–463. doi: https://doi.org/10.1016/0005-2736(80)90219-9.

McKay, L. J., MacGregor, B. J., Biddle, J. F., Albert, D. B., Mendlovitz, H. P., Hoer, D. R., et al. (2012). Spatial heterogeneity and underlying geochemistry of phylogenetically diverse orange and white *Beggiatoa* mats in Guaymas Basin hydrothermal sediments. *Deep. Res. Part I Oceanogr. Res. Pap.* 67, 21–31. doi: 10.1016/j.dsr.2012.04.011.

McKay, L., Klokman, V. W., Mendlovitz, H. P., Larowe, D. E., Hoer, D. R., Albert, D., et al. (2016). Thermal and geochemical influences on microbial biogeography in the hydrothermal sediments of Guaymas Basin, Gulf of California. *Environ. Microbiol. Rep.* 8, 150–161. doi: 10.1111/1758-2229.12365.

McLatchie, A. S., Hemstock, R. A., and Young, J. W. (1958). The Effective Compressibility of Reservoir Rock and Its Effects on Permeability. *J. Pet. Technol.* 10, 49–51. doi: 10.2118/894-G.

McMillen, D. F., and Golden, D. M. (1982). Hydrocarbon Bond Dissociation Energies. *Annu. Rev. Phys. Chem.* 33, 493–532. doi: 10.1146/annurev.pc.33.100182.002425.

McNally, T. (2011). "1 - Introduction to polymer modified bitumen (PmB)," in *Polymer Modified Bitumen - Properties and Characterisation*, ed. T. B. T.-P. M. B. McNally (Woodhead Publishing), 1–21. doi: https://doi.org/10.1533/9780857093721.1.

Meckenstock, R. U., Annweiler, E., Michaelis, W., Richnow, H. H., and Schink, B. (2000). Anaerobic Naphthalene Degradation by a Sulfate-Reducing Enrichment Culture. *Appl. Environ. Microbiol.* 66, 2743–2747. doi: 10.1128/AEM.66.7.2743-2747.2000.

Meckenstock, R. U., Boll, M., Mouttaki, H., Koelschbach, J. S., Cunha Tarouco, P., Weyrauch, P., et al. (2016).

Anaerobic degradation of benzene and polycyclic aromatic hydrocarbons. *J. Mol. Microbiol. Biotechnol.* 26, 92–118. doi: 10.1159/000441358.

Megonigal, J. P., Hines, M. E., and Visscher, P. T. (2004). "Anaerobic Metabolism: Linkages to Trace Gases and Aerobic Processes," in *Biogeochemistry*, 317–424. Available at: https://repository.si.edu/bitstream/handle/10088/15579/Megonigal_Hines_Visscher_2004.pdf?sequence=1&isAllowed=y.

Meinschein, W. G. (1969). "Hydrocarbons — Saturated, Unsaturated and Aromatic," in *Organic Geochemistry*, eds. G. Eglinton and M. T. J. Murphy (Springer, Berlin, Heidelberg), 330–356. doi: 10.1007/978-3-642-87734-6_15.

Merewether, R., Olsson, M. S., and Lonsdale, P. (1985). Acoustically detected hydrocarbon plumes rising from 2-km depths in Guaymas Basin, Gulf of California. *J. Geophys. Res.* 90, 3075. doi: 10.1029/jb090ib04p03075.

Merkel, S. M., Eberhard, A. E., Gibson, J., and Harwood, C. S. (1989). Involvement of coenzyme A thioesters in anaerobic metabolism of 4-hydroxybenzoate by *Rhodopseudomonas palustris*. *J. Bacteriol.* 171, 1–7. doi: 10.1128/jb.171.1.1-7.1989.

Meyer, R. F. (1987). Exploration for Heavy Crude Oil and Natural Bitumen. American Association of Petroleum Geologists doi: 10/1306/St25468.

Meyerdierks, A., Kube, M., Kostadinov, I., Teeling, H., Glöckner, F. O., Reinhardt, R., et al. (2010). Metagenome and mRNA expression analyses of anaerobic methanotrophic archaea of the ANME-1 group. *Environ. Microbiol.* 12, 422–439. doi: 10.1111/j.1462-2920.2009.02083.x.

Moore, D. G. (1973). Plate-Edge Deformation and Crustal Growth, Gulf of California Structural Province. *GSA Bull.* 84, 1883–1906. doi: 10.1130/0016-7606(1973)84<1883:PDACGG>2.0.CO;2.

Moore, S. J., and Warren, M. J. (2012). The anaerobic biosynthesis of vitamin B12. *Biochem. Soc. Trans.* 40, 581–586. doi: 10.1042/BST20120066.

Morrison, R. T., and Boyd, R. N. (1992). *Organic Chemistry*. 6th ed. Englewood Cliffs, NJ: Prentice Hall.

Musat, F., Galushko, A., Jacob, J., Widdel, F., Kube, M., Reinhardt, R., et al. (2009). Anaerobic degradation of naphthalene and 2-methylnaphthalene by strains of marine sulfate-reducing bacteria. *Environ. Microbiol.* 11, 209–219. doi: 10.1111/j.1462-2920.2008.01756.x.

Musat, F., and Widdel, F. (2008). Anaerobic degradation of benzene by a marine sulfate-reducing enrichment culture, and cell hybridization of the dominant phylotype. *Environ. Microbiol.* 10, 10–19. doi: 10.1111/j.1462-2920.2007.01425.x.

Naether, D. J., Slawtschew, S., Stasik, S., Engel, M., Olzog, M., Wick, L. Y., et al. (2013). Adaptation of the Hydrocarbonoclastic Bacterium *Alcanivorax borkumensis* SK2 to Alkanes and Toxic Organic Compounds: a Physiological and Transcriptomic Approach. *Appl. Environ. Microbiol.* 79, 4282–4293. doi: 10.1128/AEM.00694-13.

NAS (1975). Petroleum in the Marine Environment. Washington, D.C.

Nayfach, S., Roux, S., Seshadri, R., Udwary, D., Varghese, N., Schulz, F., et al. (2021). A genomic catalog of Earth's microbiomes. *Nat. Biotechnol.* 39, 499–509. doi: 10.1038/s41587-020-0718-6.

Nelson, D. C., and Jannasch, H. W. (1983). Chemoautotrophic growth of a marine *Beggiatoa* in sulfide-gradient cultures. *Arch. Microbiol.* 136, 262–269. doi: 10.1007/BF00425214.

Nelson, D. C., Wirsen, C. O., and Jannasch, H. W. (1989). Characterization of Large, Autotrophic *Beggiatoa* spp. Abundant at Hydrothermal Vents of the Guaymas Basin. *Appl. Environ. Microbiol.* 55, 2909–2917. doi: 10.1128/aem.55.11.2909-2917.1989.

Niemann, H., and Elvert, M. (2008). Diagnostic lipid biomarker and stable carbon isotope signatures of microbial communities mediating the anaerobic oxidation of methane with sulphate. *Org. Geochem.* 39, 1668–1677. doi: https://doi.org/10.1016/j.orggeochem.2007.11.003.

Niemann, H., Losekann, T., de Beer, D., Elvert, M., Nadalig, T., Knittel, K., et al. (2006). Novel microbial communities of the Haakon Mosby mud volcano and their role as a methane sink. *Nature* 443, 854–858.

Norman J. Hyne (2013). Nontechnical guide to petroleum geology, exploration, drilling, and production. *J. Chem. Inf. Model.* 53, 1689–1699.

Onajite, E. (2014). Sedimentation and Oil/Gas Formation. *Seism. Data Anal. Tech. Hydrocarb. Explor.*, 3–16. doi: 10.1016/b978-0-12-420023-4.00001-0.

Orcutt, B. N., Joye, S. B., Kleindienst, S., Knittel, K., Ramette, A., Reitz, A., et al. (2010). Impact of natural oil and higher hydrocarbons on microbial diversity, distribution, and activity in Gulf of Mexico cold-seep sediments. *Deep Sea Res. Part II Top. Stud. Oceanogr.* 57, 2008–2021. doi: https://doi.org/10.1016/j.dsr2.2010.05.014.

Orphan, V. J., Hinrichs, K.-U., Ussler, W., Paull, C. K., Taylor, L. T., Sylva, S. P., et al. (2001a). Comparative Analysis of Methane-Oxidizing Archaea and Sulfate-Reducing Bacteria in Anoxic Marine Sediments. *Appl. Environ. Microbiol.* 67, 1922–1934. doi: 10.1128/AEM.67.4.1922-1934.2001.

Orphan, V. J., House, C. H., Hinrichs, K. U., McKeegan, K. D., and DeLong, E. F. (2001b). Methane-consuming archaea revealed by directly coupled isotopic and phylogenetic analysis. *Science* 293, 484–487. doi: 10.1126/science.1061338.

Paduan, J. B., Zierenberg, R. A., Clague, D. A., Spelz, R. M., Caress, D. W., Troni, G., et al. (2018). Discovery of Hydrothermal Vent Fields on Alarcón Rise and in Southern Pescadero Basin, Gulf of California. *Geochemistry, Geophys. Geosystems* 19, 4788–4819. doi: https://doi.org/10.1029/2018GC007771.

Pannekens, M., Kroll, L., Müller, H., Mbow, F. T., and Meckenstock, R. U. (2019). Oil reservoirs, an exceptional habitat for microorganisms. *N. Biotechnol.* 49, 1–9. doi: 10.1016/j.nbt.2018.11.006.

Park, C., and Park, W. (2018). Survival and energy producing strategies of Alkane degraders under extreme conditions and their biotechnological potential. *Front. Microbiol.* 9, 1–15. doi: 10.3389/fmicb.2018.01081.

Parks, D. H., Chuvochina, M., Rinke, C., Mussig, A. J., Chaumeil, P. A., and Hugenholtz, P. (2022). GTDB: An ongoing census of bacterial and archaeal diversity through a phylogenetically consistent, rank normalized and complete genome-based taxonomy. *Nucleic Acids Res.* 50, D785–D794. doi: 10.1093/nar/gkab776.

Paul, J. H., Hollander, D., Coble, P., Daly, K. L., Murasko, S., English, D., et al. (2013). Toxicity and Mutagenicity of Gulf of Mexico Waters During and After the Deepwater Horizon Oil Spill. *Environ. Sci. Technol.* 47, 9651–9659. doi: 10.1021/es401761h.

Pavkov-Keller, T., Steiner, K., Faber, M., Tengg, M., Schwab, H., Gruber-Khadjawi, M., et al. (2017). Crystal Structure and Catalytic Mechanism of CouO, a Versatile C-Methyltransferase from *Streptomyces rishiriensis*. *PLoS One* 12, e0171056. Available at: https://doi.org/10.1371/journal.pone.0171056.

Pepper, A., and Santiago, C. (2001). Impact of biodegradation on petroleum exploration and production, Observations and outstanding problems. *Earth Syst. Process.*

Pester, M., Schleper, C., and Wagner, M. (2011). The Thaumarchaeota: an emerging view of their phylogeny and ecophysiology. *Curr. Opin. Microbiol.* 14, 300–306. doi: https://doi.org/10.1016/j.mib.2011.04.007.

Peter, J. M., Simoneit, B. R. T., Kawka, O. E., and Scott, S. D. (1990). Liquid hydrocarbon-bearing inclusions in modern hydrothermal chimmeys and mounds from the southern trough of Guaymas Basin, Gulf of California. *Appl. Geochemistry* 5. doi: 10.1016/0883-2927(90)90035-4.

Pevneva, G. S., Fursenko, E. A., Voronetskaya, N. G., Mozhayskaya, M. V., Golovko, A. K., Nesterov, I. I., et al. (2017). Hydrocarbon composition and structural parameters of resins and asphaltenes of naphthenic oils of northern West Siberia. *Russ. Geol. Geophys.* 58, 425–433. doi: 10.1016/j.rgg.2016.09.018.

Phelps, C. D., Kazumi, J., and Young, L. Y. (1996). Anaerobic degradation of benzene in BTX mixtures dependent on sulfate reduction. *FEMS Microbiol. Lett.* 145, 433–437. doi: 10.1016/S0378-1097(96)00446-6.

Phelps, C. D., Kerkhof, L. J., and Young, L. Y. (1998). Molecular characterization of a sulfate-reducing consortium which mineralizes benzene. *FEMS Microbiol. Ecol.* 27, 269–279. doi: 10.1016/S0168-6496(98)00073-7.

Porter, A. W., and Young, L. Y. (2014). "Benzoyl-CoA, a Universal Biomarker for Anaerobic Degradation of Aromatic Compounds," in *Advances in Applied Microbiology* (Elsevier Inc.), 167–203. doi: 10.1016/B978-0-12-800260-5.00005-X.

Rabus, R., Boll, M., Heider, J., Meckenstock, R. U., Buckel, W., Einsle, O., et al. (2016). Anaerobic Microbial Degradation of Hydrocarbons: From Enzymatic Reactions to the Environment. *Microb. Physiol.* 26, 5–28. doi: 10.1159/000443997.

Rabus, R., Hansen, T. A., and Widdel, F. (2013). "Dissimilatory Sulfate- and Sulfur-Reducing Prokaryotes," in *The Prokaryotes: Prokaryotic Physiology and Biochemistry*, eds. E. Rosenberg, E. F. DeLong, S. Lory, E. Stackebrandt, and F. Thompson (Berlin Heidelberg: Springer Berlin Heidelberg), 309–404. doi: 10.1007/978-3-642-30141-4_70.

Rabus, R., Wilkes, H., Behrends, A., Armstroff, A., Fischer, T., Pierik, A. J., et al. (2001). Anaerobic Initial Reaction of *n*-Alkanes in a Denitrifying Bacterium: Evidence for (1-Methylpentyl)succinate as Initial Product and for Involvement of an Organic Radical in *n*-Hexane Metabolism. *J. Bacteriol.* 183, 1707–1715. doi:

10.1128/jb.183.5.1707-1715.2001.

Raghoebarsing, A. A., Pol, A., van de Pas-Schoonen, K. T., Smolders, A. J. P., Ettwig, K. F., Rijpstra, W. I. C., et al. (2006). A microbial consortium couples anaerobic methane oxidation to denitrification. *Nature* 440, 918–921. doi: 10.1038/nature04617.

Ramírez, G. A., Mara, P., Sehein, T., Wegener, G., Chambers, C. R., Joye, S. B., et al. (2021). Environmental factors shaping bacterial, archaeal and fungal community structure in hydrothermal sediments of Guaymas Basin, Gulf of California. *PLoS One* 16, 1–31. doi: 10.1371/journal.pone.0256321.

Rapp, P., and Gabriel-Jürgens, L. H. E. (2003). Degradation of alkanes and highly chlorinated benzenes, and production of biosurfactants, by a psychrophilic *Rhodococcus* sp. and genetic characterization of its chlorobenzene dioxygenase. *Microbiology* 149, 2879–2890. doi: https://doi.org/10.1099/mic.0.26188-0.

Redelius, P., and Soenen, H. (2015). Relation between bitumen chemistry and performance. *Fuel* 140, 34–43. doi: https://doi.org/10.1016/j.fuel.2014.09.044.

Reeburgh, W. S. (1996). ""Soft Spots" in the Global Methane Budget," in *Microbial Growth on C1 Compounds: Proceedings of the 8th International Symposium on Microbial Growth on C1 Compounds, held in San Diego, U.S.A., 27 August -- 1 September 1995*, eds. M. E. Lidstrom and F. R. Tabita (Dordrecht: Springer Netherlands), 334–342. doi: 10.1007/978-94-009-0213-8_44.

Reeburgh, W. S. (2007). Oceanic Methane Biogeochemistry. *Chem. Rev.* 107, 486–513. doi: 10.1021/cr050362v.

Regnier, P., Friedlingstein, P., Ciais, P., Mackenzie, F. T., Gruber, N., Janssens, I. A., et al. (2013). Anthropogenic perturbation of the carbon fluxes from land to ocean. *Nat. Geosci.* 6, 597–607. doi: 10.1038/ngeo1830.

Reguera, G., McCarthy, K. D., Mehta, T., Nicoll, J. S., Tuominen, M. T., and Lovley, D. R. (2005). Extracellular electron transfer via microbial nanowires. *Nature* 435, 1098–1101. doi: 10.1038/nature03661.

Rinke, C., Chuvochina, M., Mussig, A. J., Chaumeil, P. A., Davín, A. A., Waite, D. W., et al. (2021). A standardized archaeal taxonomy for the Genome Taxonomy Database. *Nat. Microbiol.* 6, 946–959. doi: 10.1038/s41564-021-00918-8.

Rospert, S., Linder, D., Ellermann, J., and Thauer, R. K. (1990). Two genetically distinct methyl-coenzyme M reductases in *Methanobacterium thermoautotrophicum* strain Marburg and ΔH. *Eur. J. Biochem.* 194, 871–877. doi: https://doi.org/10.1111/j.1432-1033.1990.tb19481.x.

Rossel, P. E., Lipp, J. S., Fredricks, H. F., Arnds, J., Boetius, A., Elvert, M., et al. (2008). Intact polar lipids of anaerobic methanotrophic archaea and associated bacteria. *Org. Geochem.* 39, 992–999. doi: 10.1016/j.orggeochem.2008.02.021.

Rouse, J. D., Sabatini, D. A., Suflita, J. M., and Harwell, J. H. (1994). Influence of surfactants on microbial degradation of organic compounds. *Crit. Rev. Environ. Sci. Technol.* 24, 325–370. doi: 10.1080/10643389409388471.

Rueter, P., Rabus, R., Wilkest, H., Aeckersberg, F., Rainey, F. A., Jannasch, H. W., et al. (1994). Anaerobic oxidation of hydrocarbons in crude oil by new types of sulphate-reducing bacteria. *Nature* 372, 455–458. doi: 10.1038/372455a0.

Ruff, S. E., Kuhfuss, H., Wegener, G., Lott, C., Ramette, A., Wiedling, J., et al. (2016). Methane seep in shallow-water permeable sediment harbors high diversity of anaerobic methanotrophic communities, Elba, Italy. *Front. Microbiol.* 7, 1–20. doi: 10.3389/fmicb.2016.00374.

Rullkötter, J., von der Dick, H., and Welte, D. H. (1982). Organic Petrography and Extractable Hydrocarbons of Sediments from the Gulf of California, Deep Sea Drilling Project Leg 64. *Initial Reports Deep Sea Drill. Proj. 64*. doi: 10.2973/dsdp.proc.64.128.1982.

Safinowski, M., and Meckenstock, R. U. (2006). Methylation is the initial reaction in anaerobic naphthalene degradation by a sulfate-reducing enrichment culture. *Environ. Microbiol.* 8, 347–352. doi: https://doi.org/10.1111/j.1462-2920.2005.00900.x.

Sahonero-Canavesi, D. X., Siliakus, M. F., Asbun, A. A., Koenen, M., Von Meijenfeldt, F. A. B., Boeren, S., et al. (2022). Disentangling the lipid divide: Identification of key enzymes for the biosynthesis of membrane-spanning and ether lipids in Bacteria. *Sci. Adv.* 8, 1–16. doi: 10.1126/sciadv.abq8652.

Sakai, Y., Maeng, J. H., Kubota, S., Tani, A., Tani, Y., and Kato, N. (1996). A non-conventional dissimilation pathway for long chain *n*-alkanes in *Acinetobacter* sp. M-1 that starts with a dioxygenase reaction. *J. Ferment. Bioeng.* 81, 286–291. doi: https://doi.org/10.1016/0922-338X(96)80578-2.

Samiullah, Y. (1985). Biological effects of marine oil pollution. *Oil Petrochemical Pollut.* 2, 235–264. doi: 10.1016/S0143-7127(85)90233-9.

Sassen, R., Chinn, E. W., and McCabe, C. (1988). Recent hydrocarbon alteration, sulfate reduction and formation of elemental sulfur and metal sulfides in salt dome cap rock. *Chem. Geol.* 74, 57–66. doi: https://doi.org/10.1016/0009-2541(88)90146-5.

Scheller, S. (2018). Microbial interconversion of alkanes to electricity. *Front. Energy Res.* 6. doi: 10.3389/fenrg.2018.00117.

Scheller, S., Goenrich, M., Boecher, R., Thauer, R. K., and Jaun, B. (2010). The key nickel enzyme of methanogenesis catalyses the anaerobic oxidation of methane. *Nature* 465, 606–608. doi: 10.1038/nature09015.

Scheller, S., Goenrich, M., Thauer, R. K., and Jaun, B. (2013). Methyl-Coenzyme M Reductase from Methanogenic Archaea: Isotope Effects on the Formation and Anaerobic Oxidation of Methane. *J. Am. Chem. Soc.* 135, 14975–14984.

Scheller, S., Yu, H., Chadwick, G. L., Mcglynn, S. E., and Orphan, V. J. (2016). Artificial electron acceptors decouple archaeal methane oxidation from sulfate reduction. *Science* 351, 703–707.

Schink, B. (1997). Energetics of syntrophic cooperation in methanogenic degradation. *Microbiol. Mol. Biol. Rev.* 61, 262–280. doi: 10.1128/mmbr.61.2.262-280.1997.

Schlesinger, W. H. (1997). *Biogeochemistry: an Analysis of Global Change*. Academic Press, San Diego.

Schmeling, S., Narmandak, A., Schmitt, O., Gad'on, N., Schühle, K., Fuchs, G., et al. (2004). Phenylphosphate Synthase: a New Phosphotransferase Catalyzing the First Step in Anaerobic Phenol Metabolism in *Thauera aromatica*. *J. Bacteriol.* 186, 8044–8057. doi: 10.1128/jb.186.23.8044-8057.2004.

Schobert, H. H. (2013). "Formation of fossil fuels," in *Chemistry of Fossil Fuels and Biofuels* (Cambridge University Press), 13–131. Available at: https://app.knovel.com/web/view/khtml/show.v/rcid:kpCFFB0001/cid:kt00C83XR1/viewerType:khtml//root_slug:8-formation-of-fossil-fuels/url_slug:formation-fossil-fuels?b-toc-cid=kpCFFB0001&b-toc-root-slug=&b-toc-url-slug=formation-fossil-fuels&b-toc-title=Che.

Schreiber, L., Holler, T., Knittel, K., Meyerdierks, A., and Amann, R. (2010). Identification of the dominant sulfate-reducing bacterial partner of anaerobic methanotrophs of the ANME-2 clade. *Environ. Microbiol.* 12, 2327–2340. doi: https://doi.org/10.1111/j.1462-2920.2010.02275.x.

Schühle, K., and Fuchs, G. (2004). Phenylphosphate Carboxylase: a New C-C Lyase Involved in Anaerobic Phenol Metabolism in *Thauera aromatica*. *J. Bacteriol.* 186, 4556–4567. doi: 10.1128/JB.186.14.4556-4567.2004.

Seewald, J. S. (2003). Organic–inorganic interactions in petroleum-producing sedimentary basins. *Nature* 426, 327–333. doi: 10.1038/nature02132.

Seitz, K. W., Dombrowski, N., Eme, L., Spang, A., Lombard, J., Sieber, J. R., et al. (2019). Asgard archaea capable of anaerobic hydrocarbon cycling. *Nat. Commun.* 10, 1822. doi: 10.1038/s41467-019-09364-x.

Selesi, D., Jehmlich, N., Von Bergen, M., Schmidt, F., Rattei, T., Tischler, P., et al. (2010). Combined genomic and proteomic approaches identify gene clusters involved in anaerobic 2-methylnaphthalene degradation in the sulfate-reducing enrichment culture N47. *J. Bacteriol.* 192, 295–306. doi: 10.1128/JB.00874-09.

Selley, R. C., and Sonnenberg, S. A. (2015). "Chapter 8 - Sedimentary Basins and Petroleum Systems," in, eds. R. C. Selley and S. A. B. T.-E. of P. G. (Third E. Sonnenberg (Boston: Academic Press), 377–426. doi: https://doi.org/10.1016/B978-0-12-386031-6.00008-4.

Shen, A., Zheng, J., Chen, Y., Ni, X., and Huang, L. (2016). Characteristics, origin and distribution of dolomite reservoirs in Lower-Middle Cambrian, Tarim Basin, NW China. *Pet. Explor. Dev.* 43, 375–385. doi: https://doi.org/10.1016/S1876-3804(16)30044-1.

Shibuya, T., and Takai, K. (2022). Liquid and supercritical $CO_2$ as an organic solvent in Hadean seafloor hydrothermal systems: implications for prebiotic chemical evolution. *Prog. Earth Planet. Sci.* 9, 60. doi: 10.1186/s40645-022-00510-6.

Shima, S., Krueger, M., Weinert, T., Demmer, U., Kahnt, J., Thauer, R. K., et al. (2012). Structure of a methyl-coenzyme M reductase from Black Sea mats that oxidize methane anaerobically. *Nature* 481, 98–101. doi: 10.1038/nature10663.

Shimoyama, T., Kato, S., Ishii, S., and Watanabe, K. (2009). Flagellum mediates symbiosis. *Science* 323, 1574. doi:

10.1126/science.1170086.

Sieber, J. R., McInerney, M. J., and Gunsalus, R. P. (2012). Genomic Insights into Syntrophy: The Paradigm for Anaerobic Metabolic Cooperation. *Annu. Rev. Microbiol.* 66, 429–452. doi: 10.1146/annurev-micro-090110-102844.

Sierra-Garcia, I. N., and Oliveira, V. M. (2013). "Microbial Hydrocarbon Degradation: Efforts to Understand Biodegradation in Petroleum Reservoirs," in *Biodegradation - Engineering and Technology*, 47–72. Available at: http://www.intechopen.com/books/biodegradation-engineering-and-technology/microbial-hydrocarbon-degradation-efforts-to-understand-biodegradation-in-petroleum-reservoirs.

Sikkema, J., De Bont, J. A. M., and Poolman, B. (1995). Mechanisms of membrane toxicity of hydrocarbons. *Microbiol. Rev.* 59, 201–222. doi: 10.1128/mmbr.59.2.201-222.1995.

Siliakus, M. F., van der Oost, J., and Kengen, S. W. M. (2017). Adaptations of archaeal and bacterial membranes to variations in temperature, pH and pressure. *Extremophiles* 21, 651–670. doi: 10.1007/s00792-017-0939-x.

Simoneit, B. R. T. (1983). "Effects of Hydrothermal Activity on Sedimentary Organic Matter: Guaymas Basin, Gulf of California — Petroleum Genesis and Proto-Kerogen Degradation," in *Hydrothermal Processes at Seafloor Spreading Centers*, eds. P. A. Rona, K. Boström, L. Laubier, and K. L. Smith (Springer New York, NY), 451–471. doi: https://doi.org/10.1007/978-1-4899-0402-7.

Simoneit, B. R. T. (1984). Hydrothermal effects on organic matter-high vs low temperature components. *Org. Geochem.* 6, 857–864. doi: 10.1016/0146-6380(84)90108-6.

Simoneit, B. R. T. (1990). Petroleum generation, an easy and widespread process in hydrothermal systems: an overview. *Appl. Geochemistry* 5, 3–15. doi: 10.1016/0883-2927(90)90031-Y.

Simoneit, B. R. T. (1993). "Hydrothermal Activity and its Effects on Sedimentary Organic Matter," in *Bitumens in Ore Deposits*, eds. J. Parnell, H. Kucha, and P. Landais (Springer Berlin, Heidelberg), 81–95. doi: 10.1007/978-3-642-85806-2_6.

Simoneit, B. R. T. (2018). "Hydrothermal petroleum: composition and utility as a biogenic carbon source," in *Hydrocarbons, Oils and Lipids: Diversity, Origin, Chemistry and Fate*, ed. H. Wilkes (Springer, Cham.), 49–56.

Simoneit, B. R. T., and Galimov, E. M. (1984). Geochemistry of interstitial gases in Quaternary sediments of the Gulf of California. *Chem. Geol.* 43, 151–166. doi: https://doi.org/10.1016/0009-2541(84)90145-1.

Simoneit, B. R. T., Goodfellow, W. D., and Franklin, J. M. (1992). Hydrothermal petroleum at the seafloor and organic matter alteration in sediments of Middle Valley, Northern Juan de Fuca Ridge. *Appl. Geochemistry* 7, 257–264. doi: https://doi.org/10.1016/0883-2927(92)90041-Z.

Simoneit, B. R. T., Grimalt, J. O., Hayes, J. M., and Hartman, H. (1987). Low temperature hydrothermal maturation of organic matter in sediments from the Atlantis II Deep, Red Sea. *Geochim. Cosmochim. Acta* 51, 879–894. doi: https://doi.org/10.1016/0016-7037(87)90101-3.

Simoneit, B. R. T., Kawka, O. E., and Brault, M. (1988). Origin of gases and condensates in the Guaymas Basin hydrothermal system (Gulf of California). *Chem. Geol.* 71, 169–182. doi: https://doi.org/10.1016/0009-2541(88)90113-1.

Simoneit, B. R. T., and Lonsdale, P. F. (1982). Hydrothermal petroleum mineralised mounds at the seabed at Guaymas Basin. *Nature* 295, 198–202.

Simoneit, B. R. T., Summerhayes, C. P., and Meyers, P. A. (1986). Sources and hydrothermal alteration of organic matter in Quaternary sediments: A synthesis of studies from the Central Gulf of California. *Mar. Pet. Geol.* 3, 282–297. doi: 10.1016/0264-8172(86)90033-4.

Simoneit, B. T. R., and Bode, G. R. (1982). Carbon/Carbonate and Nitrogen Analyses, Leg 64, Gulf of California. *Initial Reports Deep Sea Drill. Proj. 64*, 1303–1305. doi: 10.2973/dsdp.proc.64.app2.1982.

Singh, R., Guzman, M. S., and Bose, A. (2017). Anaerobic oxidation of ethane, propane, and butane by marine microbes: A mini review. *Front. Microbiol.* 8, 1–8. doi: 10.3389/fmicb.2017.02056.

Sinninghe Damsté, J. S., Schouten, S., Hopmans, E. C., van Duin, A. C. T., and Geenevasen, J. A. J. (2002). Crenarchaeol. *J. Lipid Res.* 43, 1641–1651. doi: 10.1194/jlr.M200148-JLR200.

So, C. M., and Young, L. Y. (1999a). Initial Reactions in Anaerobic Alkane Degradation by a Sulfate Reducer, Strain AK-01. *Appl. Environ. Microbiol.* 65, 5532–5540. doi: 10.1128/AEM.65.12.5532-5540.1999.

So, C. M., and Young, L. Y. (1999b). Isolation and Characterization of a Sulfate-Reducing Bacterium That

Anaerobically Degrades Alkanes. *Appl. Environ. Microbiol.* 65, 2969–2976. doi: 10.1128/AEM.65.7.2969-2976.1999.

So, C. M., and Young, L. Y. (2001). Anaerobic biodegradation of alkanes by enriched consortia under four different reducing conditions. *Environ. Toxicol. Chem.* 20, 473–478. doi: https://doi.org/10.1002/etc.5620200303.

Sofia, H. J., Chen, G., Hetzler, B. G., Reyes-Spindola, J. F., and Miller, N. E. (2001). Radical SAM, a novel protein superfamily linking unresolved steps in familiar biosynthetic pathways with radical mechanisms: functional characterization using new analysis and information visualization methods. *Nucleic Acids Res.* 29, 1097–1106. doi: 10.1093/nar/29.5.1097.

Sohlenkamp, C., and Geiger, O. (2016). Bacterial membrane lipids: diversity in structures and pathways. *FEMS Microbiol. Rev.* 40, 133–159. doi: 10.1093/femsre/fuv008.

Sojo, V. (2019). Why the Lipid Divide? Membrane Proteins as Drivers of the Split between the Lipids of the Three Domains of Life. *BioEssays* 41, 1–6. doi: 10.1002/bies.201800251.

Sojo, V., Pomiankowski, A., and Lane, N. (2014). A Bioenergetic Basis for Membrane Divergence in Archaea and Bacteria. *PLOS Biol.* 12, e1001926. Available at: https://doi.org/10.1371/journal.pbio.1001926.

Sollich, M., Yoshinaga, M. Y., Häusler, S., Price, R. E., Hinrichs, K. U., and Bühring, S. I. (2017). Heat stress dictates microbial lipid composition along a thermal gradient in marine sediments. *Front. Microbiol.* 8, 1–19. doi: 10.3389/fmicb.2017.01550.

Solomon, S. (2007). Carbon Dioxide Storage: Geological Security and Environmental Issues-Case Study on the Sleipner Gas field in Norway. *Bellona Rep.* 1986, 128.

Solomon, S., Plattner, G. K., Knutti, R., and Friedlingstein, P. (2009). Irreversible climate change due to carbon dioxide emissions. *Proc. Natl. Acad. Sci. U. S. A.* 106, 1704–1709. doi: 10.1073/pnas.0812721106.

Song, B., and Ward, B. B. (2005). Genetic diversity of benzoyl coenzyme a reductase genes detected in denitrifying isolates and estuarine sediment communities. *Appl. Environ. Microbiol.* 71, 2036–2045. doi: 10.1128/AEM.71.4.2036-2045.2005.

Song, M. (2020). Gaseous hydrocarbon cycling and lipid biogeochemistry in cold and hot seep sediments. *PhD thesis*. doi: https://doi.org/10.26092/elib/215.

Spakowicz, D. J., and Strobel, S. A. (2015). Biosynthesis of hydrocarbons and volatile organic compounds by fungi: bioengineering potential. *Appl. Microbiol. Biotechnol.* 99, 4943–4951. doi: 10.1007/s00253-015-6641-y.

Speight, J. G. (2011). "Sources of Hydrocarbons," in *Handbook of Industrial Hydrocarbon Processes*, 43–83. doi: 10.1016/b978-0-7506-8632-7.10002-7.

Stagars, M. H., Emil Ruff, S., Amann, R., and Knittel, K. (2016). High diversity of anaerobic alkane-degrading microbial communities in marine seep sediments based on (1-methylalkyl)succinate synthase genes. *Front. Microbiol.* 6, 1–17. doi: 10.3389/fmicb.2015.01511.

Stokke, R., Roalkvam, I., Lanzen, A., Haflidason, H., and Steen, I. H. (2012). Integrated metagenomic and metaproteomic analyses of an ANME-1-dominated community in marine cold seep sediments. *Environ. Microbiol.* 14, 1333–1346. doi: https://doi.org/10.1111/j.1462-2920.2012.02716.x.

Sturt, H. F., Summons, R. E., Smith, K., Elvert, M., and Hinrichs, K. U. (2004). Intact polar membrane lipids in prokaryotes and sediments deciphered by high-performance liquid chromatography/electrospray ionization multistage mass spectrometry - New biomarkers for biogeochemistry and microbial ecology. *Rapid Commun. Mass Spectrom.* 18, 617–628. doi: 10.1002/rcm.1378.

Summons, R. E., Welander, P. V., and Gold, D. A. (2022). Lipid biomarkers: molecular tools for illuminating the history of microbial life. *Nat. Rev. Microbiol.* 20, 174–185. doi: 10.1038/s41579-021-00636-2.

Suzuki, M., Hayakawa, T., Shaw, J. P., Rekik, M., and Harayama, S. (1991). Primary structure of xylene monooxygenase: similarities to and differences from the alkane hydroxylation system. *J. Bacteriol.* 173, 1690–1695. doi: 10.1128/jb.173.5.1690-1695.1991.

Syutsubo, K., Kishira, H., and Harayama, S. (2001). Development of specific oligonucleotide probes for the identification and in situ detection of hydrocarbon-degrading *Alcanivorax* strains. *Environ. Microbiol.* 3, 371–379. doi: https://doi.org/10.1046/j.1462-2920.2001.00204.x.

Takeda, K., and Akira, S. (2004). Microbial recognition by Toll-like receptors. *J. Dermatol. Sci.* 34, 73–82. doi: 10.1016/j.jdermsci.2003.10.002.

Tanji, Y., Toyama, K., Hasegawa, R., and Miyanaga, K. (2014). Biological souring of crude oil under anaerobic

conditions. *Biochem. Eng. J.* 90, 114–120. doi: 10.1016/j.bej.2014.05.023.

Tapilatu, Y. H., Grossi, V., Acquaviva, M., Militon, C., Bertrand, J.-C., and Cuny, P. (2010). Isolation of hydrocarbon-degrading extremely halophilic archaea from an uncontaminated hypersaline pond (Camargue, France). *Extremophiles* 14, 225–231. doi: 10.1007/s00792-010-0301-z.

Tengg, M., Stecher, H., Remler, P., Eiteljörg, I., Schwab, H., and Gruber-Khadjawi, M. (2012). Molecular characterization of the C-methyltransferase NovO of *Streptomyces spheroides*, a valuable enzyme for performing Friedel–Crafts alkylation. *J. Mol. Catal. B Enzym.* 84, 2–8. doi: https://doi.org/10.1016/j.molcatb.2012.03.016.

Teske, A. (2019). "Hydrocarbon-Degrading Microbial Communities in Natural Oil Seeps," in *Microbial Communities Utilizing Hydrocarbons and Lipids: Members, Metagenomics and Ecophysiology*, ed. T. McGenity (Springer, Cham.), 81–111. doi: 10.1007/978-3-319-60063-5_3-1.

Teske, A. (2020). "Guaymas Basin, a Hydrothermal Hydrocarbon Seep Ecosystem," in *Marine Hydrocarbon Seeps: Microbiology and Biogeochemistry of a Global Marine Habitat*, eds. A. Teske and V. Carvalho (Cham: Springer International Publishing), 43–68. doi: 10.1007/978-3-030-34827-4_3.

Teske, A., Callaghan, A. V., and LaRowe, D. E. (2014). Biosphere frontiers of subsurface life in the sedimented hydrothermal system of Guaymas Basin. *Front. Microbiol.* 5. doi: 10.3389/fmicb.2014.00362.

Teske, A., and Carvalho, V. (2020). *Marine Hydrocarbon Seeps: Microbiology and Biogeochemistry of a Global Marine Habitat*. Available at: http://link.springer.com/10.1007/978-3-030-34827-4.

Teske, A., De Beer, D., McKay, L. J., Tivey, M. K., Biddle, J. F., Hoer, D., et al. (2016). The Guaymas Basin hiking guide to hydrothermal mounds, chimneys, and microbial mats: Complex seafloor expressions of subsurface hydrothermal circulation. *Front. Microbiol.* 7, 1–23. doi: 10.3389/fmicb.2016.00075.

Teske, A., and Joye, S. B. (2020). "The Gulf of Mexico: An Introductory Survey of a Seep-Dominated Seafloor Landscape," in *Marine Hydrocarbon Seeps: Microbiology and Biogeochemistry of a Global Marine Habitat*, eds. A. Teske and V. Carvalho (Cham: Springer International Publishing), 69–100. doi: 10.1007/978-3-030-34827-4_4.

Teske, A., McKay, L. J., Ravelo, A. C., Aiello, I., Mortera, C., Núñez-Useche, F., et al. (2019). Characteristics and Evolution of sill-driven off-axis hydrothermalism in Guaymas Basin – the Ringvent site. *Sci. Rep.* 9, 1–16. doi: 10.1038/s41598-019-50200-5.

Thauer, R. K. (2019). Methyl (Alkyl)-Coenzyme M Reductases: Nickel F-430-Containing Enzymes Involved in Anaerobic Methane Formation and in Anaerobic Oxidation of Methane or of Short Chain Alkanes. *Biochemistry* 58, 5198–5220. doi: 10.1021/acs.biochem.9b00164.

The Editors of Encyclopædia Britannica (2023). gas reservoir. *Encycl. Br.* Available at: https://www.britannica.com/science/gas-reservoir.

Timmers, P. H. A., Welte, C. U., Koehorst, J. J., Plugge, C. M., Jetten, M. S. M., and Stams, A. J. M. (2017). Reverse Methanogenesis and Respiration in Methanotrophic Archaea. *Archaea* 2017. doi: 10.1155/2017/1654237.

Tissot, B., Durand, B., Espitalié, J., and Combaz, A. (1974). Influence of Nature and Diagenesis of Organic Matter in Formation of Petroleum1. *Am. Assoc. Pet. Geol. Bull.* 58, 499–506. doi: 10.1306/83D91425-16C7-11D7-8645000102C1865D.

Tissot, B. P., and Welte, D. H. (1984). Diagenesis, catagenesis, and metagenesis of organic matter. doi: 10.1007/978-3-642-96446-6_6.

Tomei, M. C., Braguglia, C. M., Cento, G., and Mininni, G. (2009). Modeling of Anaerobic Digestion of Sludge. *Crit. Rev. Environ. Sci. Technol.* 39, 1003–1051. doi: 10.1080/10643380801977818.

Tourte, M., Schaeffer, P., Grossi, V., and Oger, P. M. (2022). Membrane adaptation in the hyperthermophilic archaeon *Pyrococcus furiosus* relies upon a novel strategy involving glycerol monoalkyl glycerol tetraether lipids. *Environ. Microbiol.* 24, 2029–2046. doi: 10.1111/1462-2920.15923.

Tsuneda, S., Aikawa, H., Hayashi, H., Yuasa, A., and Hirata, A. (2003). Extracellular polymeric substances responsible for bacterial adhesion onto solid surface. *FEMS Microbiol. Lett.* 223, 287–292. doi: 10.1016/S0378-1097(03)00399-9.

Tveit, M. R., Khalifeh, M., Nordam, T., and Saasen, A. (2021). The fate of hydrocarbon leaks from plugged and abandoned wells by means of natural seepages. *J. Pet. Sci. Eng.* 196, 108004. doi: 10.1016/j.petrol.2020.108004.

Ulrich, A. C., Beller, H. R., and Edwards, E. A. (2005). Metabolites Detected during Biodegradation of $^{13}C_6$-Benzene in Nitrate-Reducing and Methanogenic Enrichment Cultures. *Environ. Sci. Technol.* 39, 6681–6691. doi: 10.1021/es050294u.

Valentine, D. L. (2001). "Thermodynamic Ecology of Hydrogen-Based Syntrophy," in *Symbiosis: Mechanisms and Model Systems*, ed. J. Seckbach (Dordrecht: Springer Netherlands), 147–161. doi: 10.1007/0-306-48173-1_9.

Valentine, D. L. (2007). Adaptations to energy stress dictate the ecology and evolution of the Archaea. *Nat. Rev. Microbiol.* 5, 316–323. doi: 10.1038/nrmicro1619.

Van de Vossenberg, J. L. C. M., Driessen, A. J. M., and Konings, W. N. (1998). The essence of being extremophilic: The role of the unique archaeal membrane lipids. *Extremophiles* 2, 163–170. doi: 10.1007/s007920050056.

Van Mooy, B. A. S., Rocap, G., Fredricks, H. F., Evans, C. T., and Devol, A. H. (2006). Sulfolipids dramatically decrease phosphorus demand by picocyanobacteria in oligotrophic marine environments. *Proc. Natl. Acad. Sci.* 103, 8607–8612. doi: 10.1073/pnas.0600540103.

Vandenbroucke, M., and Largeau, C. (2007). Kerogen origin, evolution and structure. *Org. Geochem.* 38, 719–833. doi: https://doi.org/10.1016/j.orggeochem.2007.01.001.

Vanwonterghem, I., Evans, P. N., Parks, D. H., Jensen, P. D., Woodcroft, B. J., Hugenholtz, P., et al. (2016). Methylotrophic methanogenesis discovered in the archaeal phylum Verstraetearchaeota. *Nat. Microbiol.* 1, 16170. doi: 10.1038/nmicrobiol.2016.170.

Vences-Guzmán, M. Á., Geiger, O., and Sohlenkamp, C. (2012). Ornithine lipids and their structural modifications: from A to E and beyond. *FEMS Microbiol. Lett.* 335, 1–10. doi: 10.1111/j.1574-6968.2012.02623.x.

Vogt, C., Kleinsteuber, S., and Richnow, H. H. (2011). Anaerobic benzene degradation by bacteria. *Microb. Biotechnol.* 4, 710–724. doi: 10.1111/j.1751-7915.2011.00260.x.

Von Damm, K. L., Edmond, J. M., Measures, C. I., and Grant, B. (1985). Chemistry of submarine hydrothermal solutions at Guaymas Basin, Gulf of California. *Geochim. Cosmochim. Acta* 49, 2221–2237. doi: 10.1016/0016-7037(85)90223-6.

Wackett, L. P., and Wilmot, C. M. (2015). "Chapter 2 - Hydrocarbon Biosynthesis in Microorganisms," in *Direct Microbial Conversion of Biomass to Advanced Biofuels*, ed. M. E. B. T.-D. M. C. of B. to A. B. Himmel (Amsterdam: Elsevier), 13–31. doi: https://doi.org/10.1016/B978-0-444-59592-8.00002-6.

Wagner, T., Wegner, C.-E., Kahnt, J., Ermler, U., and Shima, S. (2017). Phylogenetic and Structural Comparisons of the Three Types of Methyl Coenzyme M Reductase from Methanococcales and Methanobacteriales. *J. Bacteriol.* 199, 10.1128/jb.00197-17. doi: 10.1128/jb.00197-17.

Wang, W., and Shao, Z. (2014). The long-chain alkane metabolism network of *Alcanivorax dieselolei*. *Nat. Commun.* 5, 5755. doi: 10.1038/ncomms6755.

Wang, Y., Feng, X., Natarajan, V. P., Xiao, X., and Wang, F. (2019a). Diverse anaerobic methane- and multi-carbon alkane-metabolizing archaea coexist and show activity in Guaymas Basin hydrothermal sediment. *Environ. Microbiol.* 21, 1344–1355. doi: 10.1111/1462-2920.14568.

Wang, Y., Wegener, G., Hou, J., Wang, F., and Xiao, X. (2019b). Expanding anaerobic alkane metabolism in the domain of Archaea. *Nat. Microbiol.* 4, 595–602. doi: 10.1038/s41564-019-0364-2.

Wang, Y., Wegener, G., Ruff, S. E., and Wang, F. (2020). Methyl/alkyl-coenzyme M reductase-based anaerobic alkane oxidation in archaea. *Environ. Microbiol.* 00. doi: 10.1111/1462-2920.15057.

Wang, Y., Wegener, G., Williams, T. A., Xie, R., Hou, J., Wang, F., et al. (2021). A methylotrophic origin of methanogenesis and early divergence of anaerobic multicarbon alkane metabolism. *Sci. Adv.* 7. doi: 10.1126/sciadv.abh1051.

Wang, Y., Yu, M., Austin, B., and Zhang, X.-H. (2012). *Oleispira lenta* sp. nov., a novel marine bacterium isolated from Yellow sea coastal seawater in Qingdao, China. *Antonie Van Leeuwenhoek* 101, 787–794. doi: 10.1007/s10482-011-9693-8.

Wardlaw, N. C. (1996). "Factors affecting oil recovery from carbonate reservoirs and prediction of recovery," in *Carbonate Reservoir Characterization: A Geologic - Engineering Analysis*, eds. G. V Chilingarian, S. J. Mazzullo, and H. H. B. T.-D. in P. S. Rieke (Elsevier), 867–903. doi: https://doi.org/10.1016/S0376-7361(96)80032-X.

Warren, J. K. (2016). "Hydrocarbons and Evaporites," in *Evaporites: A Geological Compendium*, ed. J. K. Warren (Cham: Springer International Publishing), 959–1079. doi: 10.1007/978-3-319-13512-0_10.

Weber, A., and Jørgensen, B. B. (2002). Bacterial sulfate reduction in hydrothermal sediments of the Guaymas Basin, Gulf of California, Mexico. *Deep. Res. Part I Oceanogr. Res. Pap.* 49, 827–841. doi: 10.1016/S0967-0637(01)00079-6.

Wegener, G., Krukenberg, V., Riedel, D., Tegetmeyer, H. E., and Boetius, A. (2015). Intercellular wiring enables electron transfer between methanotrophic archaea and bacteria. *Nature* 526, 587–590. doi: 10.1038/nature15733.

Wegener, G., Krukenberg, V., Ruff, S. E., Kellermann, M. Y., and Knittel, K. (2016). Metabolic capabilities of microorganisms involved in and associated with the anaerobic oxidation of methane. *Front. Microbiol.* 7, 1–16. doi: 10.3389/fmicb.2016.00046.

Wei, L., Yu, H., Hou, L., and Zhao, J. (2014). The design and development of integrity database management platform for crude oil storage tank. 32, 9097–9104.

White, D. C., Davis, W. M., Nickels, J. S., King, J. D., and Bobbie, R. J. (1979). Determination of the sedimentary microbial biomass by extractible lipid phosphate. *Oecologia* 40, 51–62. doi: 10.1007/BF00388810.

Whiticar, M. J., and Suess, E. (1990). Hydrothermal hydrocarbon gases in the sediments of the King George Basin, Bransfield Strait, Antarctica. *Appl. Geochemistry* 5, 135–147. doi: https://doi.org/10.1016/0883-2927(90)90044-6.

Whitman, W. B., Coleman, D. C., and Wiebe, W. J. (1998). Prokaryotes: The unseen majority. *Proc. Natl. Acad. Sci.* 95, 6578–6583. doi: 10.1073/pnas.95.12.6578.

Widdel, F., Knittel, K., and Galushko, A. (2010). "Anaerobic Hydrocarbon-Degrading Microorganisms: An Overview," in *Handbook of Hydrocarbon and Lipid Microbiology*, ed. K. N. Timmis (Springer-Verlag Berlin Heidelberg), 1997–2021. doi: 10.1007/978-3-540-77587-4.

Wilhelms, A., Larter, S. R., Head, I., Farrimond, P., di-Primio, R., and Zwach, C. (2001). Biodegradation of oil in uplifted basins prevented by deep-burial sterilization. *Nature* 411, 1034–1037. doi: 10.1038/35082535.

Wilkes, H. (2020). *Hydrocarbons, Oils and Lipids: Diversity, Origin, Chemistry and Fate*. , eds. K. N. Timmis, M. Boll, O. Geiger, H. Goldfine, T. Krell, S. Yup, et al. Springer, Cham. doi: 10.1007/978-3-319-90569-3.

Wilkes, H., Rabus, R., Fischer, T., Armstroff, A., Behrends, A., and Widdel, F. (2002). Anaerobic degradation of n-hexane in a denitrifying bacterium: Further degradation of the initial intermediate (1-methylpentyl)succinate via C-skeleton rearrangement. *Arch. Microbiol.* 177, 235–243. doi: 10.1007/s00203-001-0381-3.

Wilkes, H., and Schwarzbauer, J. (2010). "Hydrocarbons: An Introduction to Structure, Physico-Chemical Properties and Natural Occurrence," in *Handbook of Hydrocarbon and Lipid Microbiology*, ed. K. N. Timmis (Springer, Berlin, Heidelberg), 1–48. doi: 10.1007/978-3-540-77587-4_1.

Williams, D. L., Becker, K., Lawver, L. A., and Von Herzen, R. P. (1979). Heat flow at the spreading centers of the Guaymas Basin, Gulf of California. *J. Geophys. Res. Solid Earth* 84, 6757–6769. doi: https://doi.org/10.1029/JB084iB12p06757.

Wischgoll, S., Heintz, D., Peters, F., Erxleben, A., Sarnighausen, E., Reski, R., et al. (2005). Gene clusters involved in anaerobic benzoate degradation of *Geobacter metallireducens*. *Mol. Microbiol.* 58, 1238–1252. doi: https://doi.org/10.1111/j.1365-2958.2005.04909.x.

Witholt, B., de Smet, M. J., Kingma, J., van Beilen, J. B., Kok, M., Lageveen, R. G., et al. (1990). Bioconversions of aliphatic compounds by *Pseudomonas oleovorans* in multiphase bioreactors: background and economic potential. *Trends Biotechnol.* 8, 46–52. doi: 10.1016/0167-7799(90)90133-I.

Wolfe, A., Shimer, G. H. J., and Meehan, T. (1987). Polycyclic Aromatic Hydrocarbons Physically Intercalate into Duplex Regions of Denatured DNA. *Biochemistry* 26, 6392–6396.

Würf, J., Pokorny, T., Wittbrodt, J., Millar, J. G., and Ruther, J. (2020). Cuticular Hydrocarbons as Contact Sex Pheromone in the Parasitoid Wasp *Urolepis rufipes*. *Front. Ecol. Evol.* 8. doi: 10.3389/fevo.2020.00180.

Xiao, R., and Zheng, Y. (2016). Overview of microalgal extracellular polymeric substances (EPS) and their applications. *Biotechnol. Adv.* 34, 1225–1244. doi: https://doi.org/10.1016/j.biotechadv.2016.08.004.

Xu, Q., Qiao, Q., Gao, Y., Hou, J., Hu, M., Du, Y., et al. (2021). Gut Microbiota and Their Role in Health and Metabolic Disease of Dairy Cow. *Front. Nutr.* 8. doi: 10.3389/fnut.2021.701511.

Yakimov, M. M., Giuliano, L., Gentile, G., Crisafi, E., Chernikova, T. N., Abraham, W.-R., et al. (2003). *Oleispira antarctica* gen. nov., sp. nov., a novel hydrocarbonoclastic marine bacterium isolated from Antarctic coastal sea water. *Int. J. Syst. Evol. Microbiol.* 53, 779–785. doi: https://doi.org/10.1099/ijs.0.02366-0.

Yakimov, M. M., Golyshin, P. N., Lang, S., Moore, E. R. B., Abraham, W.-R., Lünsdorf, H., et al. (1998). *Alcanivorax borkumensis* gen. nov., sp. nov., a new, hydrocarbon-degrading and surfactant-producing marine bacterium. *Int. J. Syst. Evol. Microbiol.* 48, 339–348. doi: https://doi.org/10.1099/00207713-48-2-339.

Yakimov, M. M., Timmis, K. N., and Golyshin, P. N. (2007). Obligate oil-degrading marine bacteria. *Curr. Opin. Biotechnol.* 18, 257–266. doi: https://doi.org/10.1016/j.copbio.2007.04.006.

Yamauchi, K., Doi, K., Yoshida, Y., and Kinoshita, M. (1993). Archaebacterial lipids: highly proton-impermeable membranes from 1,2-diphytanyl-*sn*-glycero-3-phosphocoline. *Biochim. Biophys. Acta - Biomembr.* 1146, 178–182. doi: https://doi.org/10.1016/0005-2736(93)90353-2.

Yan, Z., Zhang, Y., Wu, H., Yang, M., Zhang, H., Hao, Z., et al. (2017). Isolation and characterization of a bacterial strain: *Hydrogenophaga* sp. PYR1 for anaerobic pyrene and benzo [a] pyrene biodegradation. *RSC Adv.* 7, 46690–46698. doi: 10.1039/c7ra09274a.

Yang, X., Ye, J., Lyu, L., Wu, Q., and Zhang, R. (2013). Anaerobic Biodegradation of Pyrene by *Paracoccus denitrificans* Under Various Nitrate/Nitrite-Reducing Conditions. *Water, Air, Soil Pollut.* 224, 1578. doi: 10.1007/s11270-013-1578-1.

Yang, Y.-L., Yang, F.-L., Jao, S.-C., Chen, M.-Y., Tsay, S.-S., Zou, W., et al. (2006). Structural elucidation of phosphoglycolipids from strains of the bacterial thermophiles *Thermus* and *Meiothermus*. *J. Lipid Res.* 47, 1823–1832. doi: https://doi.org/10.1194/jlr.M600034-JLR200.

Yee, M. O., and Rotaru, A.-E. (2020). Extracellular electron uptake in Methanosarcinales is independent of multiheme c-type cytochromes. *Sci. Rep.* 10, 1–12. doi: 10.1038/s41598-019-57206-z.

Yoshinaga, M. Y., Kellermann, M. Y., Valentine, D. L., and Valentine, R. C. (2016). Phospholipids and glycolipids mediate proton containment and circulation along the surface of energy-transducing membranes. *Prog. Lipid Res.* 64, 1–15. doi: https://doi.org/10.1016/j.plipres.2016.07.001.

Zeng, Z., Chen, H., Yang, H., Chen, Y., Yang, W., Feng, X., et al. (2022). Identification of a protein responsible for the synthesis of archaeal membrane-spanning GDGT lipids. *Nat. Commun.* 13. doi: 10.1038/s41467-022-29264-x.

Zengler, K., Richnow, H. H., Rosselló-Mora, R., Michaelis, W., and Widdel, F. (1999). Methane formation from long-chain alkanes by anaerobic microorganisms. *Nature* 401, 266–269. doi: 10.1038/45777.

Zhang, G., Zhang, F., Ding, G., Li, J., Guo, X., Zhu, J., et al. (2012). Acyl homoserine lactone-based quorum sensing in a methanogenic archaeon. *ISME J.* 6, 1336–1344. doi: 10.1038/ismej.2011.203.

Zhang, T., Tremblay, P. L., Chaurasia, A. K., Smith, J. A., Bain, T. S., and Lovley, D. R. (2013). Anaerobic benzene oxidation via phenol in *Geobacter metallireducens*. *Appl. Environ. Microbiol.* 79, 7800–7806. doi: 10.1128/AEM.03134-13.

Zhang, X., Sullivan, E. R., and Young, L. Y. (2000). Evidence for aromatic ring reduction in the biodegradation pathwayof carboxylated naphthalene by a sulfate reducing consortium. *Biodegradation* 11, 117–124. doi: 10.1023/A:1011128109670.

Zhang, Z., Guo, H., Sun, J., Gong, X., Wang, C., and Wang, H. (2021a). Anaerobic phenanthrene biodegradation by a newly isolated sulfate-reducer, strain PheS1, and exploration of the biotransformation pathway. *Sci. Total Environ.* 797, 149148. doi: https://doi.org/10.1016/j.scitotenv.2021.149148.

Zhang, Z., Sun, J., Guo, H., Gong, X., Wang, C., and Wang, H. (2021b). Investigation of anaerobic biodegradation of phenanthrene by a sulfate-dependent *Geobacter sulfurreducens* strain PheS2. *J. Hazard. Mater.* 409, 124522. doi: https://doi.org/10.1016/j.jhazmat.2020.124522.

Zhou, Z., Zhang, C., Liu, P., Fu, L., Laso-Pérez, R., Yang, L., et al. (2022). Non-syntrophic methanogenic hydrocarbon degradation by an archaeal species. *Nature* 601, 257–262. doi: 10.1038/s41586-021-04235-2.

## Acknowledgments

While I had some doubts for most of these four (and a little…) years that I would actually make it to this point, somehow, here I am, and I have some people to thank for that.

First of all, I want to thank my biology teacher from high school, who got me intrigued about the intricacy and beauty of nature: **Herr Schuon**, even though you told us not to become biologists, DNA replication and transcription was just too fascinating. Maybe you have more luck with the next students! Thank you so much for everything you've taught me, you are what a teacher should be.

Thank you so much **Antje** and **Gunter**, for investing in me, even though I did not come from a marine microbiology background, and needed some time to adapt. I appreciate a lot that you supported me going on a cruise, which was an incredible experience. **Gunter**, thank you also for your fast and helpful feedback on any texts and manuscript parts. Thank you to **Rafa**, **Andreas**, and **Florence** for being part of my thesis committee and sharing your knowledge and experience. **Florence**, thank you also so much for introducing me to the world of lipids, it was fun and very motivating to work with you, and thank you for the nice teas in your office.

A huge thanks also to the Organic Geochemistry group at MARUM, for sharing their lab spaces and for the nice cooperation. **Charlotte**, thank you for giving me the best introduction to lipid extractions. **Julius**, thank you for not giving up on finding the right settings for the precious samples. **Heidi**, thank you for your amazing sample analysis and for caring about the data afterwards.

Thank you to the **captain and crew** of *RV Meteor* cruise M167. I'm very glad I got to be on that cruise with you, to experience the dolphin's feast, beautiful sunsets, playing ping pong in rocky seas, and learning how to make the best vegan chocolate cake. I'm very happy I could learn the challenges and magic of ship life with you.

I want to thank everyone from the Habitat group for the nice work environment. **Eddie**, and **Rafa**, we did not have a lot of time together, but you made me feel welcome from the beginning. **Rafa**, thank you for your help with bioinformatics and sharing your amazing scripts and knowledge with me. **Cedric**, thank you for sharing your CARD-FISH experience and for always being nice and having an open ear. **Christina**, thank you for your entertaining lunch stories and for making intense MarMic practical weeks fun. **Matthias**, I'm sorry we never realized our Kohlfahrt reign, I hope the next Kohlfahrt will be epic. **Susanne** and **Martina**, thank you so much for organizing the lab, despite the struggles, taking the best care of cultures and samples. **Anja**, thank you for sharing the joys and struggles of preparing buffers. **Shareen**, thanks for philosophical lunch times and coffees and for sharing your enthusiasm about large environments replicated in small containers. **Stian**, **Raïssa**, **Verena**, it was a pleasure sharing a corridor with you and meeting you in the kitchen for little chats. **Valeria** and **Farooq**, I'm glad we got to exchange some treats and spend some lunch times, Kaffee & Kuchen, and catsitting

together. **Mikayla** and **Carolin**, thank you so much for deciding to do a lab rotation with me and doing amazing work.

**Batu**, **Lewen**, and **David**, I'm very grateful that we could spend that time together in the best office of the MPI. We had crazy fun and helped each other getting through the hard parts with snacks and music. **Lewen**, you need to come back. **Batu**, thanks for many conversations about space, rockets, politics, and football, and for showing me Wet Leg. **David**, I can't even express how grateful I am to have been on this journey with you, I could not have done it without your company, processing CARD-FISH struggles and cultivation issues together, and just being there on the good days and the bad. Thank you for supporting me with cake, always providing some sarcasm and tea, being another parent to my plants, and judging me in Spanish in the best way. I promise someday I will stop chewing your ear off about capybaras, but today is not that day.

I want to thank the Lübeck people, **Marie**, **Lina**, **Kerstin**, **Verena**, **Anna-Lena** for keeping up to date with our lives, and accompanying us along the way, be it far or close. I'm always looking forward to our next catch-up Zoom, endless brunches and Matratzenlager.

Tantas gracias a mis amigues de Würzburg, **Marc**, **Daniel**, **Gemma**, **Matze**, **Anki**! It's nice to feel like having another home, and to be able to return to it. I'm happy we got to see each other more again this year.

Thank you to the best cousin crew, **Nikolai**, **Matthias**, **Kilian**, **Teresa**, **Janine**, rooftop will always be there, and I'm excited to have our next reunion.

**Mama**, **Papa**, **Volker** and **Thomas**, thank you for supporting me on my way here.

**Mati**, no puedo agradecerte suficientemente por acompañarme tanto en este viaje, y darme esperanza en los momentos en que me faltó. Los últimos meses te bancaste mucho de mi, y siempre me hiciste sentir que no estoy sola en este viaje. Muchas gracias por tu paciencia y empatía. Te quiero muchísimo!

# List of manuscripts and declaration of contributions

## Manuscript 1 (Chapter 2)

| | |
|---|---|
| Title: | *Candidatus* Alkanophaga archaea from Guaymas Basin hydrothermal vent sediment oxidize petroleum alkanes |
| Authors: | Hanna Zehnle, Rafael Laso-Pérez, Julius Lipp, Dietmar Riedel, David Benito Merino, Andreas Teske, Gunter Wegener |
| Journal: | *Nature Microbiology* (2023)<br>doi: 10.1038/s41564-023-01400-3 |

Contribution of the candidate in % of the total work load

| | |
|---|---|
| Experimental concept and design | 60 % |
| Experimental work and/or acquisition of data | 80 % |
| Data analysis and interpretation | 90 % |
| Preparation of Figures and Tables | 90 % |
| Drafting of the manuscript | 90 % |

## Manuscript 2 (Chapter 3)

| | |
|---|---|
| Title: | Anaerobic oxidation of benzene and naphthalene by thermophilic microorganisms from the Guaymas Basin |
| Authors: | Hanna Zehnle, Carolin Otersen, David Benito Merino, Gunter Wegener |
| Journal | Submitted to *Frontiers in Microbiology* |

Contribution of the candidate in % of the total work load

| | |
|---|---|
| Experimental concept and design | 100 % |
| Experimental work and/or acquisition of data | 100 % |
| Data analysis and interpretation | 80 % |
| Preparation of Figures and Tables | 100 % |
| Drafting of the manuscript | 90 % |

## Manuscript 3 (Chapter 4)

| | |
|---|---|
| Title: | The core lipidome of anaerobic alkane-oxidizing archaea and their sulfate-reducing partner bacteria |
| Authors: | Hanna Zehnle, Christopher Klaembt, Qing-Zeng Zhu, Gunter Wegener, Florence Schubotz |
| Journal | To be decided, manuscript in preparation |

Contribution of the candidate in % of the total work load

| | |
|---|---|
| Experimental concept and design | 40 % |
| Experimental work and/or acquisition of data | 20 % |
| Data analysis and interpretation | 30 % |
| Preparation of Figures and Tables | 90 % |
| Drafting of the manuscript | 90 % |

## Versicherung an Eides Statt / *Affirmation in lieu of an oath*

**gem. § 5 Abs. 5 der Promotionsordnung vom 18.06.2018 /**
***according to § 5 (5) of the Doctoral Degree Rules and Regulations of 18 June, 2018***

Ich / *I*, _____
(Vorname / *First Name*, Name / *Name*, Anschrift / *Address*, ggf. Matr.-Nr. / *student ID no., if applicable*)

versichere an Eides Statt durch meine Unterschrift, dass ich die vorliegende Dissertation selbständig und ohne fremde Hilfe angefertigt und alle Stellen, die ich wörtlich dem Sinne nach aus Veröffentlichungen entnommen habe, als solche kenntlich gemacht habe, mich auch keiner anderen als der angegebenen Literatur oder sonstiger Hilfsmittel bedient habe und die zu Prüfungszwecken beigelegte elektronische Version (PDF) der Dissertation mit der abgegebenen gedruckten Version identisch ist. / *With my signature I affirm in lieu of an oath that I prepared the submitted dissertation independently and without illicit assistance from third parties, that I appropriately referenced any text or content from other sources, that I used only literature and resources listed in the dissertation, and that the electronic (PDF) and printed versions of the dissertation are identical*.

Ich versichere an Eides Statt, dass ich die vorgenannten Angaben nach bestem Wissen und Gewissen gemacht habe und dass die Angaben der Wahrheit entsprechen und ich nichts verschwiegen habe. / *I affirm in lieu of an oath that the information provided herein to the best of my knowledge is true and complete*.

Die Strafbarkeit einer falschen eidesstattlichen Versicherung ist mir bekannt, namentlich die Strafandrohung gemäß § 156 StGB bis zu drei Jahren Freiheitsstrafe oder Geldstrafe bei vorsätzlicher Begehung der Tat bzw. gemäß § 161 Abs. 1 StGB bis zu einem Jahr Freiheitsstrafe oder Geldstrafe bei fahrlässiger Begehung. / *I am aware that a false affidavit is a criminal offence which is punishable by law in accordance with § 156 of the German Criminal Code (StGB) with up to three years imprisonment or a fine in case of intention, or in accordance with § 161 (1) of the German Criminal Code with up to one year imprisonment or a fine in case of negligence.*

_____ _____

Ort / *Place*, Datum / *Date* Unterschrift / *Signature*